UNIVERSIDADE FEDERAL DE PERNAMBUCO
CENTRO DE CIÊNCIAS EXATAS E DA NATUREZA
PROGRAMA DE PÓS-GRADUAÇÃO EM QUÍMICA

CARLA JASMINE OLIVEIRA E SILVA

Synthesis of thio-derivatives conjugated to glycero-carbohydrates and their potential as anti-tuberculosis agents

Recife
2024

CARLA JASMINE OLIVEIRA E SILVA

Synthesis of thio-derivatives conjugated to glycero-carbohydrates and their potential as anti-tuberculosis agents

Dissertation presented to the Graduate Program in Chemistry at the Federal University of Pernambuco, as a requirement for obtaining a master's degree in Chemistry. Area of concentration: Organic Chemistry.

Advisor: Prof. PhD. Ronaldo Nascimento de Oliveira

Co-advisor: Prof. PhD. Arnaud Tatibouët

Recife

2024

Catalogação na fonte
Bibliotecário Josias Machado da Silva Junior, CRB4-1690

S586s Silva, Carla Jasmine Oliveira e
Synthesis of thio-derivatives conjugated to glycero-carbohydrates and their potential as anti-tuberculosis agents / Carla Jasmine Oliveira e Silva. – 2024.
149 f.: il., fig., tab., abrev. e sigls.

Orientador: Ronaldo Nascimento de Oliveira
Coorientador: Arnaud Tatibouët
Dissertação (Mestrado) – Universidade Federal de Pernambuco. CCEN, Química, Recife, 2024.
Inclui referências e apêndices.

1. Glicoconjugados. 2. Glicerol. 3. Fenilsulfoniletilideno (PSE) acetal. 4. oxazolidinationa. 5. Tiazolidinationa. 6. Oxazol. I. Oliveira, Ronaldo Nascimento de (orientador). II. Tatibouët, Arnaud. III. Título.

543 CDD (23. ed.) UFPE-CCEN 2024 - 32

CARLA JASMINE OLIVEIRA E SILVA

Synthesis of thio-derivatives conjugated to glycero-carbohydrates and their potential as anti-tuberculosis agents

Dissertação apresentada ao Programa de Pós-Graduação no Departamento de Química Fundamental da Universidade Federal de Pernambuco, como requisito parcial para a obtenção do título de Mestre em Química.

Aprovada em: 30/01/2024

BANCA EXAMINADORA

_____

Prof. Ronaldo Nascimento de Oliveira (Orientador)
Universidade Federal Rural de Pernambuco

_____

Prof. Arnaud Tatibouët (Coorientador)
Université d'Orléans

_____

Prof. Celso de Amorim Câmara
Universidade Federal Rural de Pernambuco

_____

Profª. Patrícia Lopes Barros de Araújo
Universidade Federal de Pernambuco

I dedicate this work to the person who dedicated almost her entire life to taking care of me, and who still does in the big and small details, my beloved mother, Hosana.

ACKNOWLEDGMENTS

I would like to thank my supervisors, Prof. PhD. Ronaldo Nascimento de Oliveira and Prof. PhD. Arnaud Tatibouët, for the opportunity to carry out this research, for all the knowledge they have passed on, and for the trust they have placed in me.

Thanks to my colleagues in the LSCB laboratory, Pedro Ramos, Adiel Soares, and Bruna Martins, for all their help and moments of fun, especially to Bruna for all her teachings and conversations. She has always welcomed me since my undergraduate studies and this continued throughout my master's degree.

I would like to thank the professors at the Federal University of Pernambuco (UFPE) for their contributions to my academic and professional formation.

Thanks to the support agencies CNPq, FACEPE, and CAPES for their financial support in carrying out this research, and especially FACEPE for awarding me the grant.

I would also like to thank the Multiuser Analysis Laboratory of the Chemistry Department - UFRPE, the Analytical Center of the Fundamental Chemistry Department - UFPE and the Multiuser Characterization and Analysis Laboratory - UFPB, especially the technical Evandro, for his promptness in carrying out the requested analyses.

Slow down, you crazy child
You're so ambitious for a juvenile
But then if you're so smart
Tell me why are you still so afraid?
Where's the fire?
What's the hurry about?
You better cool it off before you burn it out
You got so much to do and only so many hours in a day

(Billy Joel. **Vienna**. Nova York: Columbia, 1977)

ABSTRACT

Tuberculosis is a disease that still brings risks to global health since resistance to existing drugs promotes the search for new treatments. The aim of this study was therefore to synthesize new glycero-carbohydrates conjugated to thio-heterocycles and evaluate its biological profile against tuberculosis. We first synthesized glycerol derivatives: glycerol carbonate **1** (96%), tosylated glycerol carbonate **2** (65%), glycerol iodo-carbonate **3** (80%) and glycerol thio-carbonate **4** (85%). The (*R*) azido-alcohol **7a** was previously prepared by our research group, as was the mixture of diastereoisomers of the 2,3-unsaturated *O*-glycosides **6a**/**6b** which was used to prepare the keto-azide **8**, with a yield of 88%. In another synthetic strategy, we protected tri-*O*-acetyl-*D*-glucal **5** with (Z)-1,2-bis(phenylsulfonyl)ethylene (BPSE) **9** to obtain PSE-glucal **10** (77%). The double bond epoxidation reaction of PSE-glucal **10** with *m*-CPBA stereoselectively provided the unprecedented *α*-mannopyranoside **11** in 52% yield, and after acetylation under acidic conditions (K-10) we obtained *α*-mannopyranoside **12** (77%). The aglycone portion of α-mannopyranoside **12** was also replaced by the glycerol carbonate ring, and the unprecedented *R*/*S* mixture of *β*-mannopyranoside **13** was obtained in 64% yield. In the glycosylation reaction under Ferrier conditions between PSE-glucal **10** and glycerol carbonate **1**, was observed the formation of a complex mixture **14a** and the mixture *R*/*S* of the new α-2-deoxy-*O*-glucoside isomer **14b** with yields of 33% and 42%, as a result of a Michael addition reaction. The new heterocycles 1,3-oxazolidine-2-thione **16a** and 1,3-thiazolidine-2-thione **16b** were synthesized from (*R*) azido-alcohol **7a** using CS_2 and PPh_3, with yields of 22% and 39%, respectively. 2-mercapto-oxazole **17** (59%) was prepared from the reaction of keto-azide **8** in the presence of CS_2 and PPh_3 as well. Finally, in the biological study, thio-derivatives **16a**, **16b** and **17** didn't show any activity against tuberculosis, however, they weren't considered toxic to the cells tested.

Keywords: glycoconjugates; glycerol; phenylsulfonylethylidene (PSE) acetal; oxazolidinethione; thiazolidinethione; oxazole.

RESUMO

A tuberculose é uma doença que ainda traz riscos à saúde global, uma vez que a resistência aos medicamentos já existentes impulsiona a busca pelo desenvolvimento de novos tratamentos. Dessa forma, o objetivo do presente trabalho foi sintetizar novos glicero-carboidratos conjugados com tio-heterociclos e avaliar seu perfil biológico contra a tuberculose. Num primeiro momento, realizamos a síntese dos derivados do glicerol: carbonato de glicerol **1** (96%), carbonato de glicerol tosilado **2** (65%), iodo-carbonato de glicerol **3** (80%) e tio-carbonato de glicerol **4** (85%). O (*R*) azido-álcool **7a** foi previamente preparado pelo nosso grupo de pesquisa, bem como a mistura de diastereoisômeros dos *O*-glicosídeos 2,3-insaturados **6a**/**6b** que foi utilizada para preparar a ceto-azida **8**, com rendimento de 88%. Em outra estratégia sintética, realizamos a proteção do tri-*O*-acetil-*D*-glucal **5** com o (Z)-1,2-bis(fenilsulfonil)etileno (BPSE) **9** para obter o PSE-glical **10** (77%). A reação de epoxidação na dupla ligação do PSE-glical **10** com o *m*-CPBA forneceu estereosseletivamente o *α*-manopiranosídeo **11** inédito com 52% de rendimento, e após reação de acetilação em condições ácidas (k-10) obtivemos o *α*-manopiranosídeo **12** (77%). Também foi realizada a substituição da porção aglicona *α*-manopiranosídeo **12** pelo anel do carbonato de glicerol, a mistura *R*/*S* do novo *β*-manopiranosídeo **13** foi obtida com rendimento de 64%. Na reação de glicosilação sob condições de Ferrier entre o PSE-glical **10** e o carbonato de glicerol **1**, observamos a formação de uma mistura complexa **14a** e da mistura *R*/*S* do novo isômero *α*-2-desoxi-*O*-glicosídeo **14b** com rendimentos de 33% e 42%, como resultado de uma reação de adição de Michael. Posteriormente, realizou-se a síntese dos novos heterociclos 1,3-oxazolidina-2-tiona **16a** e 1,3-tiazolidina-2-tiona **16b** a partir do (*R*) azido-álcool **7a** com CS_2 e PPh_3, com rendimentos de 22% e 39%, respectivamente. O 2-mercapto-oxazol **17** (59%) foi preparado a partir da reação da ceto-azida **8** na presença de CS_2 e PPh_3 também. Por fim, no que diz respeito ao estudo biológico, os tio-derivados **16a**, **16b**, e **17** não apresentaram atividade contra tuberculose, no entanto, não foram considerados tóxicos para as células testadas.

Palavras-chave: glicoconjugados; glicerol; fenilsulfoniletilideno (PSE) acetal; oxazolidinationa; tiazolidinationa; oxazol.

LIST OF FIGURES

Figure 41 - Cytotoxicity graph of thio-derivatives 16a, 16b and 17. 106

LIST OF SCHEMES

LIST OF TABLES

LIST OF ABBREVIATIONS AND ACRONYMS

AcOH	Acetic acid
ap.	Apparent
br.	Broad
$CDCl_3$	Deuterated chloroform
DMF	Dimethylformamide
DCM	Dichloromethane
DMSO	Dimethyl sulfoxide
DMSO-d_6	Deuterated dimethyl sulfoxide
dd	Double duplet
ddd	Double of doublets
dt	Double triplet
eq.	Equivalent
EtOAc	Ethyl acetate
Hex	Hexane
IR	Infrared
J	Coupling constant
m	Multiplet
M.W.	Microwave
NMR	Nuclear Magnetic Resonance
PPh_3	Triphenylphosphine
PSE	Phenylsulfonylethylidene
ppm	Parts per million
s	Singlet
t	Triplet
TLC	Thin-Layer Chromatography
TMSOTf	Trimethylsilyl trifluoromethanesulfonate

CONTENTS

1 INTRODUCTION

Covid-19 has raised the alarm about the imminence of new pandemics caused mainly by biological agents (viruses, bacteria, or fungi). However, some already-known diseases are still major public health problem, such as tuberculosis, declared a global emergency by the World Health Organization (WHO) in 1993. According to the WHO, "Tuberculosis (TB) is a serious but preventable global health problem; an estimated 10.6 million people developed tuberculosis in 2022 and 1.3 million people died worldwide, making it the 13th leading cause of death and the second leading cause of death by infection after Covid-19 (above HIV/AIDS)" (WHO, 2023).

Tuberculosis is an infectious disease, caused by a bacterium (*Mycobacterium tuberculosis*), which mainly affects the lungs, but can affect various organs and manifest clinically in numerous ways (Kozakevich; Silva, 2015). It's estimated that around a quarter of the global population has been infected with the tuberculosis bacterium, which is transmitted through the air when active people cough, sneeze, or spit. However, people who are infected but have not yet developed the disease cannot transmit it (WHO, 2023). Furthermore, people with compromised immune systems, such as HIV, malnutrition, diabetes, or smokers, are at greater risk of falling ill.

In response to this global health threat, the WHO approved the End TB Strategy at the 2014 World Health Assembly. This strategy defined targets (for 2020 and 2025), such as a 35% reduction in the number of deaths from tuberculosis and a 20% reduction in the tuberculosis incidence rate, and goals (for 2030 and 2035), such as a 90% reduction in the number of deaths from tuberculosis and an 80% reduction in the tuberculosis incidence rate compared to 2015 levels (WHO, 2023). In addition, ending the tuberculosis epidemic by 2030 is also among the health targets of the United Nations Sustainable Development Goals (SDGs).

The main objective of TB treatment is to cure patients and rapidly interrupt the transmission of the disease. Currently, the therapeutic regimen is standardized with the use of four drugs (rifampicin, isoniazid, pyrazinamide, and ethambutol) (Figure 1) in a single pill with a fixed combined dose for two months, and two drugs (isoniazid and rifampicin) for another four months, totaling six months of treatment (Arbex *et al*., 2010). However, according to the authors, rifampicin, isoniazid, and pyrazinamide can produce undesirable drug interactions between themselves or with other drugs being

used by the patient, which can cause drug hepatitis. Besides, the early interruption of therapeutic treatment and the use of inadequate doses, mistakenly or irregularly, has led to the development of drug resistance in bacteria.

Figure 1 - Structures of first-line drugs: rifampicin, isoniazid, pyrazinamide, and ethambutol.

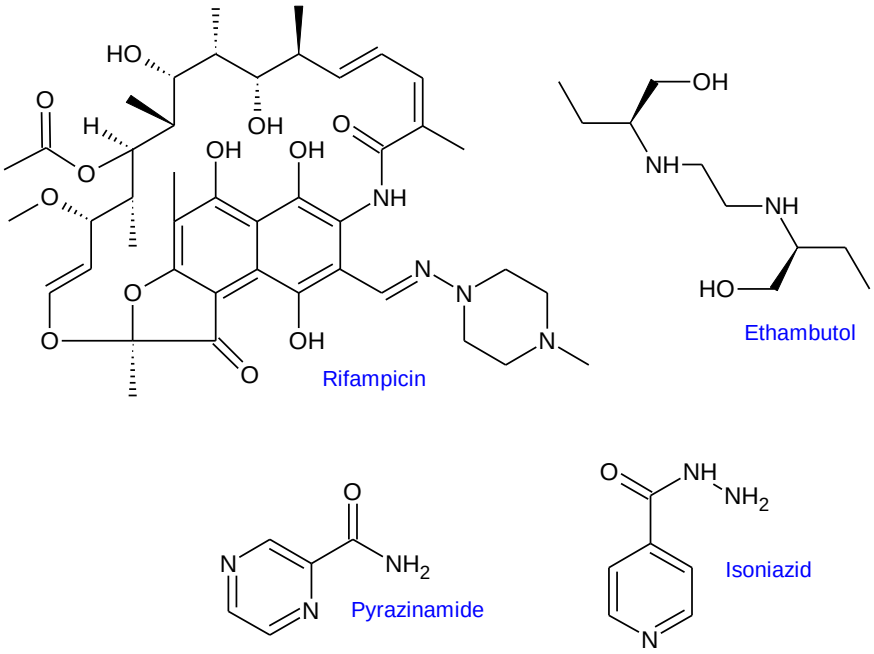

Source: The author (2024).

Multidrug-resistant tuberculosis (MDR-TB) is a form of tuberculosis caused by bacteria that do not respond to the treatment of first-line drugs, however, it is curable and treatable with the use of second-line drugs, which can include more extensive, expensive, and toxic treatments (WHO, 2023). Second-line drugs are classified as fluoroquinolones (Group A), aminoglycosides (Group B), other important agents (Group C), and additional agents (Group D) (Massabni; Bonini, 2019). The WHO suggests using a 6-month treatment regimen consisting of bedaquiline (Group D), pretomanid (Group B), linezolid (Group C), and moxifloxacin (Group A) for rifampicin-resistant tuberculosis (RR-TB) and fluoroquinolone-resistant tuberculosis (pre-XDR-TB), for people who have had no previous exposure to bedaquiline and linezolid or who have been exposed for less than 1 month (WHO, 2022). Other second-line drugs are also used and the treatment regimen can also be extended from 9 to 18 months, for example.

Figure 2 - Structures of second-line drugs: bedaquiline, pretomanide, linezolid, and moxifloxacin.

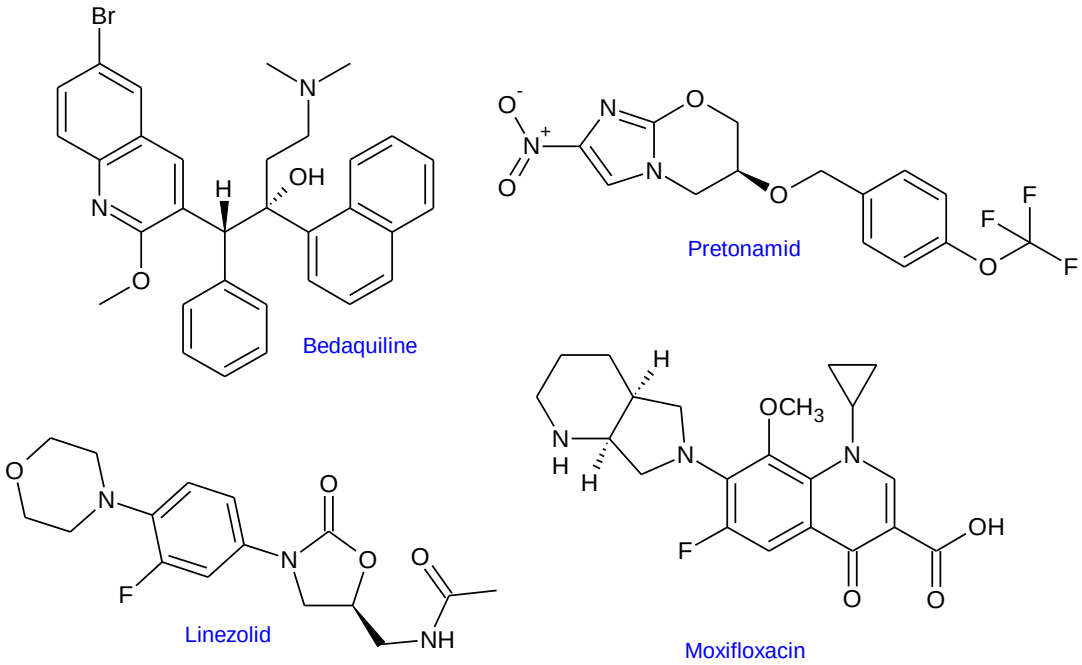

Source: The author (2024)

Heterocycles with nitrogen and oxygen atoms in their structure, such as the oxazolidine, oxazoline, and oxazole moieties, have often been used as building blocks for the discovery of new drugs against tuberculosis. The oxazolidine nucleus has a five-membered ring with nitrogen and oxygen in positions 1 and 3. Gonçalves and collaborators (2012) synthesized new mefloquine-oxazolidine derivatives and evaluated their *in vitro* activity against *Mycobacterium tuberculosis* (*MTb*), including the multidrug-resistant tuberculosis strain T113. It was observed that compounds **A** and **B** (MICs = 11.9 and 12.1 µM, respectively) were around 2.7 times more active than mefloquine alone (MIC = 33 µM), with better activity compared to the first-choice agent ethambutol (MIC = 15.9 µM), and even with the same MICs for the MDR-TB T113 strain.

The other two rings, oxazoline and oxazole, have similar structures to the oxazolidine ring, with the difference being the presence of a double bond. Moraski, Franzblau, and Miller (2010a) discovered by coincidence that the **C** intermediate containing the 2-oxazoline ring (Figure 3), which is a precursor in the synthesis of mycobactins, exhibited remarkable anti-tuberculosis activity (MIC H37Rv = 7.7 µM). In another study by Moraski *et al*. (2010b), the authors explored the conversion of active oxazoline analogs to the corresponding oxazoles, which were tested for inhibition of

MTb (H37Rv) in two different culture media, GAS and GAST, using rifampicin as a positive control. In particular, the oxazole derivative **D** showed submicromolar MICs against *MTb* (H37Rv), MIC = 0.47 µM (GAS) and MIC = 0.49 µM (GAST).

Figure 3 - Examples of oxazolidine, oxazoline, and oxazole derivatives with anti-tuberculosis activity.

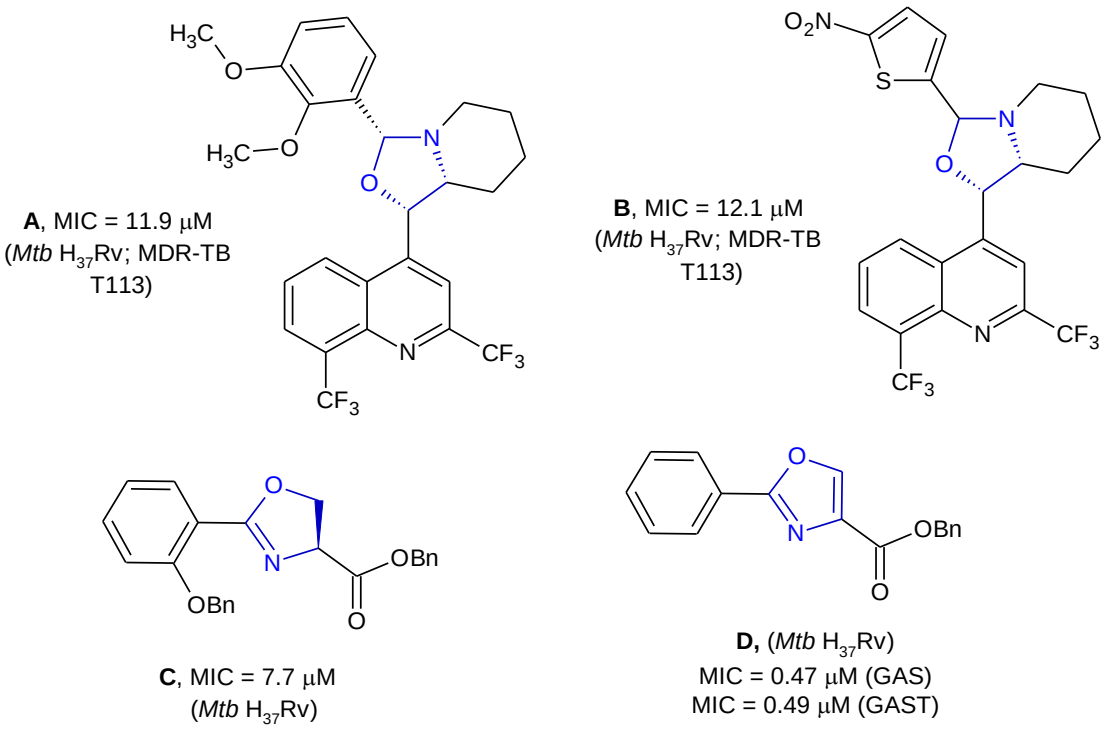

Source: The author (2024).

Oxazolidinones are considered a new class of synthetic antibacterial agents active against a broad spectrum of multidrug-resistant Gram-positive bacteria (GPB), including *vancomycin-resistant Enterococcus* (VRE), *methicillin-resistant Staphylococcus aureus* (MRSA) and *Mycobacterium tuberculosis* (*MTb*). Linezolid (LNZ) was the first oxazolidinone approved for clinical use by the FDA (Food and Drug Administration) in 2000 (Michalska *et al*., 2013). LNZ is widely used to treat infections caused by GPB, and is also effective for surgical infections, in the treatment of drug-resistant lung infections and multidrug-resistant tuberculosis (MDR-TB) infections (Foti *et al.*, 2021). Sutezolid (STD) is an antibacterial candidate developed by Pfizer and Sequella for the treatment of *MTb* infections, which is currently in clinical trials but is already showing promising results, and its structure is similar to LNZ, replacing oxygen with sulfur in the morpholine ring, seen figure 4 (Yuan *et al*., 2023).

Figure 4 - Linezolid and Sutezolid drug structures.

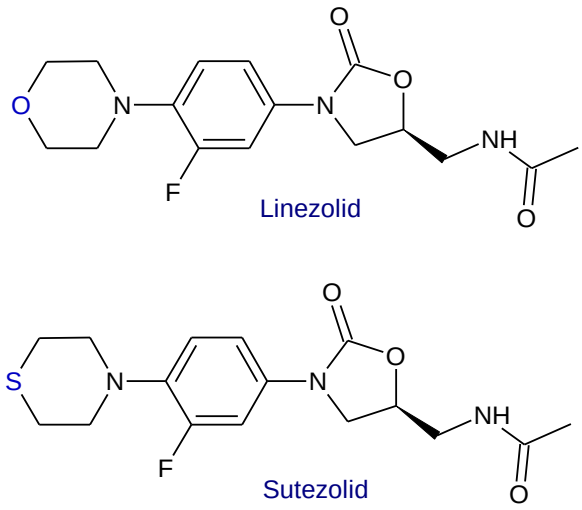

Source: The author (2024).

1.1 OBJECTIVES

The general aim of this dissertation is to synthesize thio-derivative hybrids conjugated with glycero-carbohydrates in search of applications against *Mycobacterium tuberculosis*.

1.1.1 Specific objectives

- Obtain the synthetic precursors tri-*O*-acetyl-*D*-glucal **5**, glycerol carbonate **1**, glycerol thio-carbonate **4,** and PSE-glucal **10**;
- Prepare azido-alcohols and keto-azido-carbohydrates;
- Synthesis of glycero-carbohydrates from PSE-glucal **10**;
- Synthesis of the thio-derivatives of the oxazolidinethione, thiazolidinethione, and oxazolinethione/oxazole moieties;
- Evaluate the cytotoxic activity in mammalian cell lines and the spectrum of antibacterial activity of the compounds oxazolidinethione **16a**, thiazolidinethione **16b**, and oxazole **17**.

1.2 ORGANIZATION OF THE DISSERTATION

This dissertation is structured as follows. This first topic provides an introduction with an overview of the problem of tuberculosis, the drugs that have been used to treat this disease, and the compounds that have been studied and tested against the bacterium. The second topic is dedicated to presenting the fundamentals of our work, such as the role that glycerol has acquired in organic synthesis, a recap of the theory behind glycosylation reactions, the protecting groups in carbohydrate chemistry, and the heterocycles that contain nitrogen, oxygen, and sulfur in their structure. In the third topic, we present our experimental procedures and the structural description of the compounds synthesized and biological studies. Then, in the fourth topic, we describe and discuss the experimental results obtained. Finally, in the fifth and sixth topics, we present the conclusions of our work and suggest future prospects. We also present all the spectra obtained from the synthesized compounds in Annex A.

2 BACKGROUND: STATE OF THE ART

In this topic, we present the fundamental concepts that support this research. Firstly, we discuss an overview of glycerol production and how it has gained relevance in organic chemistry. We also analyze the most important points in a glycosylation reaction, the well-known Ferrier reaction for preparing 2,3-unsaturated *O*-glycosides, and the methods for preparing *S*-glycosides. We also discuss the role of protecting groups in carbohydrate chemistry, in particular the acetal protection of hydroxyl group. Finally, we discuss some of the heterocycle compounds that contain nitrogen, oxygen, and sulfur in their structure: oxazolidinethione, thiazolidinethione, and oxazolinethione/oxazole.

2.1 USE OF GLYCEROL IN ORGANIC SYNTHESIS

Biodiesel is a biodegradable fuel obtained from clean and renewable sources, which when compared to fossil fuels from oil (a finite and non-renewable source), has offered advantages such as reducing the emission of dangerous chemicals and greenhouse gases into the environment (Kaur *et al*., 2020). According to the authors, it can be considered a mixture of esters obtained through the transesterification process of triglycerides (vegetable oils, tallow/fats, waste cooking oils, edible plants, biomass, and microalgae). In this process, the main by-product formed is glycerol (Figure 5), which represents 10% of biodiesel production, meaning that for every 10 kg of triglycerides consumed, 9 kg of biodiesel and 1 kg of glycerol are generated (Checa *et al*., 2020).

According to Kaur *et al*. (2020), 66% of the world's glycerol comes from only the biodiesel industry, and so a huge production of glycerol could cause a threat to the economy. In this context, the sustainable use of glycerol as a raw material is extremely important, not only because of its large production but also because it's a non-toxic, edible, biosustainable, and biodegradable compound (Gade; Saptal; Bhanage, 2022). Glycerol, also known as 1,2,3-propanetriol or glycerin, is used in the food, pharmaceutical, cosmetics, textile industries, etc. (Lima *et al*., 2022). It also has several applications in medicine: pure glycerol is used to treat ulcers, cuts, bites, rashes, burns, and nitroglycerin is used to treat cardiovascular diseases (Singh *et al*., 2020).

Figure 5 - 3D Molecular structure of glycerol.

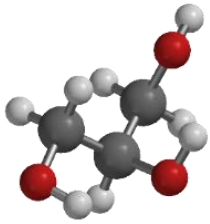

Source: The author (2024).

It has three hydroxyls that make it an ideal candidate for conversion into high value-added chemicals through reactions such as hydrogenolysis, dehydration, esterification, etherification, pyrolysis, carboxylation, oligomerization, and polymerization (Houache; Hughes; Baranova, 2019). Among the chemical compounds that can be prepared from glycerol, glycerol carbonate has stood out as a biodegradable material with potential as a reagent or building block in organic chemistry (Vilkauskaite *et al*., 2013). Glycerol carbonate (GC) or 4-hydroxymethyl-2-oxo-1,3-dioxolane has functional groups such as hydroxyl, carbonyl, and C-O bonds that provide broad reactivity due to the presence of nucleophilic and electrophilic sites, as can be seen in figure 6 (Gade; Saptal; Bhanage, 2022).

Figure 6 - Active centers of glycerol carbonate.

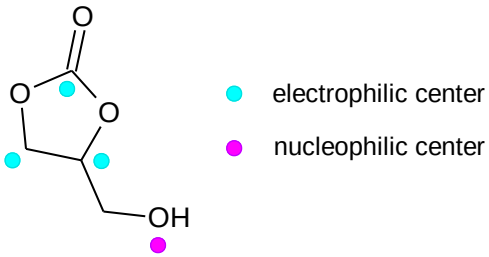

Source: Adapted from Gade; Saptal; Bhanage (2022).

Several methods and reagents exist for the synthesis of glycerol carbonate, such as direct and indirect carbonation using phosgene ($COCl_2$), CO/O_2, CO_2, $KHCO_3/K_2CO_3$, and transesterification using cyclic/acyclic carbonates and urea (Gade; Saptal; Bhanage, 2022). According to the authors, transesterification with dimethyl carbonate (DMC) is the most efficient and sustainable methodology, since the only by-product formed is methanol, which has a low boiling point and is easily separated from the reaction mixture, and can also be reused for the synthesis of DMC from CO_2.

Scheme 1 - Synthesis of GC from glycerol and DMC.

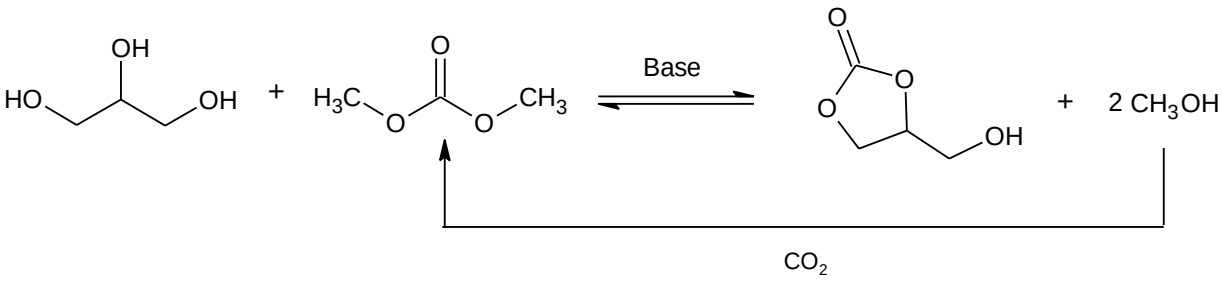

Source: Adapted from Gade; Saptal; Bhanage (2022).

2.2 GLYCOSYLATION REACTION

Carbohydrates are one of the most relevant classes of biomolecules in nature, they play an important role in maintaining life by regulating numerous processes of cell communication and recognition, such as cell adhesion, inflammation, immune response, and cell growth (Kafle; Liu; Cui, 2016). The simplest carbohydrates are found in the form of monosaccharides, while more complex carbohydrates (oligosaccharides and polysaccharides) are the result of glycosidic bonds between monosaccharides. However, they can also be found conjugated with a variety of other biomolecules, such as proteins, lipids, alkaloids, and flavonoids.

The structure of glycoconjugates is based on the covalent bond between a glycone (sugar portion) and an aglycone (non-saccharide portion), where this bond can be of the *O*-, *C*-, *N*-, and *S*-glycosidic type. The basic reaction for the synthesis of glycoconjugates is glycosylation, which has undergone extensive development since it was first reported in 1879 by Michael, followed by Fischer in 1891 (Mukherjee; Ghosh; Hanover, 2022). There is no universal glycosylation method, but in general, a glycosyl donor is activated by a catalyst to give rise to an electrophilic species capable of reacting with a nucleophilic acceptor species, resulting in the glycosidic bond (Souza Neto *et al*., 2021).

The activation of the glycosyl donor can lead to the formation of oxocarbenium ions (less stable and more reactive), and these can be associated with the counter-ion providing contact ion pairs (CIPs), or they can be separated from the counter-ion in solvent-separated ion pairs (SSIPs) (Van der Vorm *et al*., 2017). These intermediates can be attacked by the nucleophilic acceptor species and the stereochemistry of the

covalent species formed can be different depending on the mechanism followed (S_N1 or S_N2) (Scheme 2). However, many factors can affect the stereoselectivity of glycosylation reactions, such as the structures of the glycosyl donors and acceptors, conformational constraints, promoters, as well as the reaction medium, solvent, and temperature (Mukherjee; Ghosh; Hanover, 2022).

Two anomers can be formed in the glycosylation process: the α and β glycosides. For glucose, since the α-isomer is favored thermodynamically due to the anomeric effect, the *α*-glucoside is formed as the majority product at high temperatures, while the *β*-glucoside is favored kinetically and prevails at low temperatures (Souza Neto *et al*., 2021). As seen in scheme 2, intermediate species with charges are present during glycosylation reactions and the stabilization of these species can be affected by the solvent used. According to Kafle, Liu, and Cui (2016), there are two hypotheses to explain the participation of the solvent in the glycosylation reaction: solvent coordination and distribution of conformers and counter-ions.

Scheme 2 - The different routes of intermediates during glycosylation reactions.

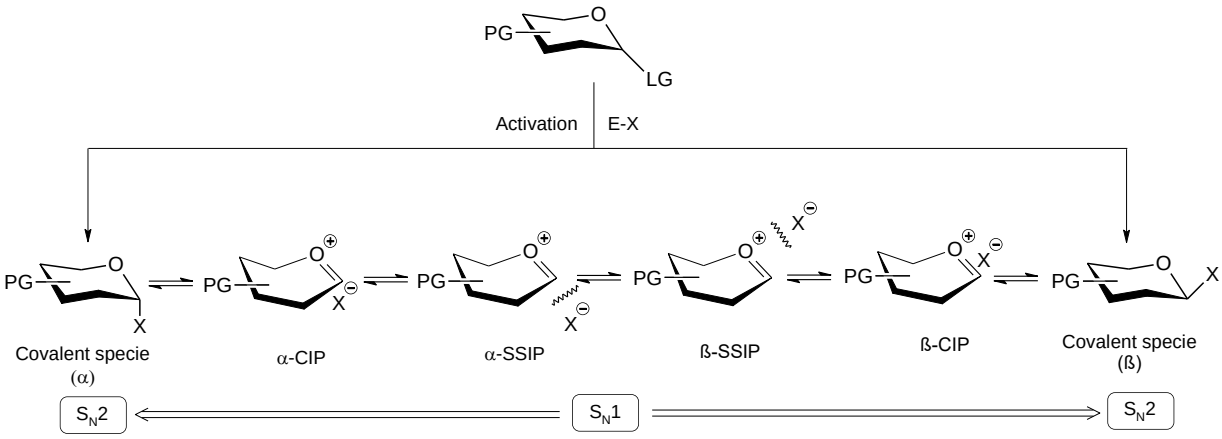

Source: Adapted from Vorm *et al*. (2017).

In the first hypothesis, the solvent binds preferentially to one of the faces of the oxocarbenium ion and the nucleophile only has the opposite face to attack; in the case of acetonitrile, the α-glycopyranosyl acetonitrile ion was isolated, proving the preferential formation of the β-glycoside in the presence of this solvent (Kafle; Liu; Cui, 2016). Solvents such as ethyl ether or tetrahydrofuran (THF) generate an intermediate in the equatorial position, leading to the formation of the α-glycosidic bond (Souza Neto *et al*., 2021). On the other hand, in the second hypothesis of the distribution of conformers and counter-ions, the oxocarbenium ion can assume different

conformations depending on the nature of the solvent used, and in this way, the counter-ion can approach and block one of the faces (Kafle; Liu; Cui, 2016).

The effect of the solvent does not work in the presence of protective groups such as *O*-acetyl (OAc), *O*-benzoyl (OBz), and *N*-phthalimide (NPhth) in the C-2 position of the glycosyl donor, another effect ends up occurring: the anchimeric assistance of the neighboring group (Mukherjee; Ghosh; Hanover, 2022). The attack of the acyl-C2 group on the anomeric carbon of the oxocarbenium ion leads to the formation of an intermediate dioxolenium ion (Scheme 3), and in this way, one of the faces of the ring is blocked leading to the exclusive formation of 1,2-trans-β-glucoside (Volbeda; Van Der Marel; Codée, 2018). Nevertheless, acyl groups located at more distant positions can provide remote anchimeric assistance if there is no participating group at C-2, for example, acyl groups located at *O*-3, *O*-4, and *O*-6 can favor 1,2-cis-*α* selectivity (Komarova *et al*., 2013).

Scheme 3 - Anchimeric assistance of acyl groups at C-2 and remote anchimeric assistance of acyl groups at *O*-3, *O*-4, and *O*-6.

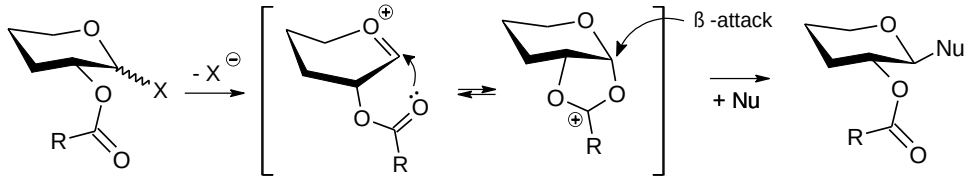

a) Synthesis of 1,2-trans-glucoside via vicinal anchimeric assistance.

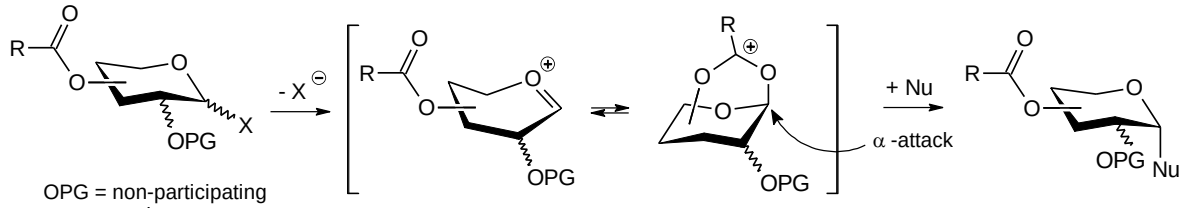

b) Possible mechanism for the formation of α-glycosides from donors bearing non-vicinal acyl groups with ß-face protection.

Source: Adapted from Komarova; Tsvetkov; Nifantiev (2013).

The nature of the nucleophilic acceptor species can also influence the stereoselectivity of the glycosylation reaction. Xiang *et al*. (2015) observed in their studies that stronger nucleophiles stereoselectively provided products with a β-glycosidic bond, while the use of weaker nucleophiles led to the formation of products with an α-glycosidic bond. About glycosylation reaction promoters, transition metals

have been used since the first Koenigs-Knorr procedures, however, they present a problem with waste generation, and as an alternative boron trifluoride etherate ($BF_3 \cdot Et_2O$) and trimethylsilyl trifluoromethanesulfonate (TMSOTf) are commonly used as promoters in glycosylation reactions (Souza Neto *et al*., 2021).

2.2.1 2,3-unsaturated *O*-glycosides: Ferrier reaction

2,3-unsaturated *O*-glycosides are considered chiral building blocks in the synthesis of bioactive molecules and have been used as intermediates to obtain glycopeptides, oligosaccharides, and modified carbohydrates (Zhang; Liu, 2007). Among the synthetic transformations of 2,3-unsaturated *O*-glycosides, we can mention hydrogenation, hydroxylation, oxidation, azidation, and epoxidation reactions, among others, with high stereoselectivity (Moura *et al*., 2018). In addition, unsaturation provides greater reactivity at the anomeric carbon (C-1) and the hydroxyl group (C-4), allowing new routes for nucleophilic functionalization.

One of the methods for preparing 2,3-unsaturated *O*-glycosides is the rearrangement of glycals catalyzed by a Lewis acid in the presence of alcohols. This method was initially developed by Ferrier using $BF_3.Et_2O$ and became known as the Ferrier reaction or rearrangement (Procopio *et al*., 2007). However, several Lewis acids have been described in the literature to the present day, such as Montmorillonite K-10, $SnCl_4$, 2,3-dichloro-5,6-dicyano-1,4-quinone (DDQ), $K_5CoW_{12}O_{40}.3H_2O$, $InCl_3$, $BiCl_3$, $Dy(OTf)_3$, $CeCl_3.7H_2O$, $ZnCl_2$, $ZrCl_4$, $FeCl_3$, *N*-iodosuccinimide (NIS), $Sc(OTf)_3$, I_2, $HClO_4$-SiO_2, ceric ammonium nitrate (CAN), $Bi(NO_3)_3.5H_2O$, $Fe(NO_3)_3.9H_2O$, and $NbCl_5$ (Zhang; Liu, 2007). The Ferrier rearrangement generally involves the formation of a cyclic allylic oxocarbenium intermediate by displacing the C-3 substituent in glycal derivatives containing acyloxy groups (Scheme 4, intermediate **B**) (Procopio *et al*., 2007).

According to Melo *et al*. (2015), the *α*-isomer is often predominant in *O*-glycosylation reactions. These authors proposed a mechanistic route for the formation of alkynyl *O*-glycosides using Montmorillonite K-10/$FeCl_3.6H_2O$ as a catalyst (Scheme 4). The use of Montmorillonite K-10 doped with iron (III) chloride results in a synergistic effect, and the first step of the proposed mechanism is the complexation of the Lewis acid (xM^{n+}) with the acetyl group located at C-3 to form complex **A**, which then

undergoes elimination and produces an allylic oxocarbenium ion (intermediate **B**) (Melo *et al*., 2015). According to the authors, intermediate **C** can be formed with the help of the neighboring acetyl group at C-4, however; the *α*-stereoselectivity was explain by the steric hindrance of the *β*-face of the **D**/**D'** transition states via anchimeric assistance of the acetoxymethyl group at the C-5 position.

Scheme 4 - Proposed mechanistic route to alkynyl *O*-glycosides with MK-10/$FeCl_3.6H_2O$.

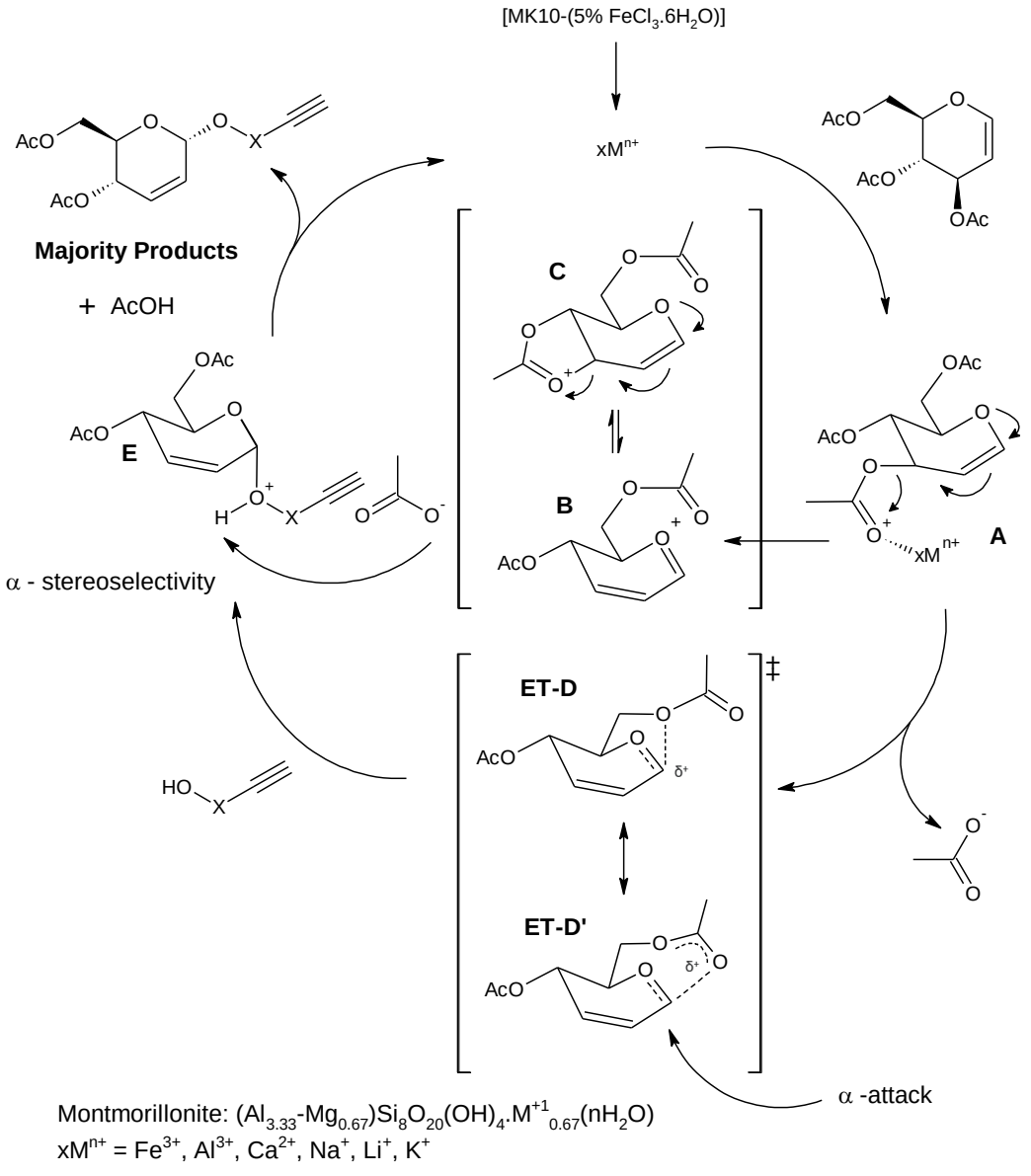

Source: Adapted from Melo *et al*. (2015).

In another study carried out by the same research group (Da Costa *et al*., 2016), the Ferrier reaction was performed between glycerol carbonate and tri-*O*-acetyl-*D*-glucal, using $BF_3.Et_2O$ or MK-10 doped with iron (III) chloride as catalysts, to obtain a

mixture of diastereoisomers whose spontaneous crystallization provided the pure diastereoisomer with the *S* configuration in 28% yield.

Scheme 5 - Ferrier rearrangement of tri-*O*-acetyl-*D*-glucal and (±)-GC.

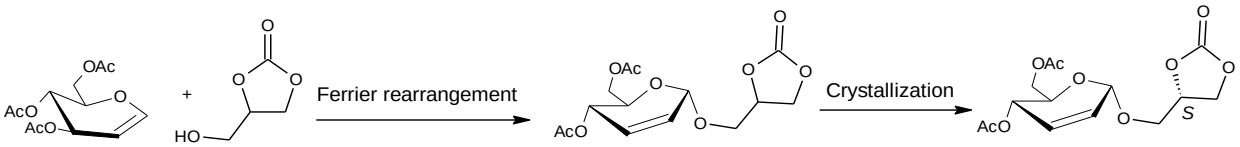

Source: Adapted from Da Costa *et al*. (2016).

2.2.2 *S*-glycosides

S-glycosides are known for their high stability to various reaction conditions, in fact, the same modification of protective groups that occurs in common carbohydrates makes it possible to prepare highly functionalized thioglycoside donors (De Oliveira *et al*., 2021). Sulfur-containing sugars are more stable to chemical/enzymatic hydrolysis compared to *O*-glycosides and their conjugates, and since sulfur is the bioisostere of oxygen in medicinal chemistry, thiosugars can play important roles in drug discovery (Xiong *et al*., 2022). Among the biological activities of *S*-glycosides, we can highlight anticancer, antimicrobial, anti-inflammatory, antioxidant, antitumor, antiviral, and others (De Oliveira *et al*., 2021).

1-thioglycosides rarely occur naturally, most of which belong to the class of glucosinolates, *O*-sulfated thiohydroximates of 1-thio-*β*-*D*-glucopyranosides obtained mainly from Brassicales plants (Lian; Zhang; Yu, 2015). 1-thio-sugars are the most common and important glycosyl donors used in the synthesis of *O*-glycosides, *N*-glycosides, *C*-glycosides, oligosaccharides, and polysaccharides (Xiong *et al*., 2022). The main procedures for obtaining thioglycosides are the direct introduction of a mercaptan (thiol) through the displacement reaction of an anomeric leaving group, sometimes assisted by a promoter, in a way similar to an *O*-glycosylation reaction (Scheme 6) (Oscarson, 2008).

Scheme 6 - *S*-glycosylation.

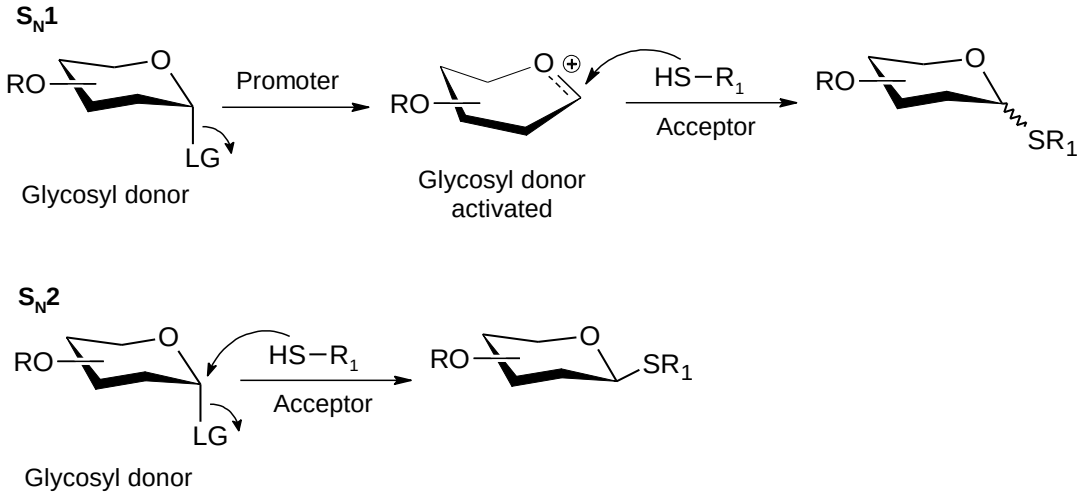

Source: Adapted from Oscarson (2008).

According to Agnihotri, Tiwari, and Misra (2005), a widely used method for the synthesis of thioglycosides is the treatment of per-*O*-acetylated sugars with alkyl/arylthiols or alkyl/aryl thiotrimethyl silanes in the presence of a Lewis acid. More specifically, reactions of glycals with thiols catalyzed by a Lewis acid can involve allylic displacement and the formation of the Ferrier rearrangement product, 2,3-didesoxy-1-thioglycoside. However, some reaction conditions can prevent the formation of the intermediate allylic cation and the dominant reaction is a direct addition to the double bond to provide 2-deoxy thioglycosides (Oscarson, 2008).

In summary, there are different methodologies for obtaining *S*-glycosides in the literature. De Oliveira and collaborators (2021) summarized in six proposals, which can be seen in scheme 7: 1) *S*-glycosylation promoted by acid on the anomeric carbon, using glycosyl donors; 2) *S*-glycosylation via S_N2 reaction of 1-thiosugars; 3) *S*-glycosylation via S_N2 reaction of thiolate ion; 4) *S*-glycosylation via Michael addition of 1-thiosugars to an *α*,*β*-unsaturated system; 5) enzymatic *S*-glycosylation; 6) *S*-glycosylation via Ferrier rearrangement.

Scheme 7 - Some routes for the synthesis of *S*-glycosides.

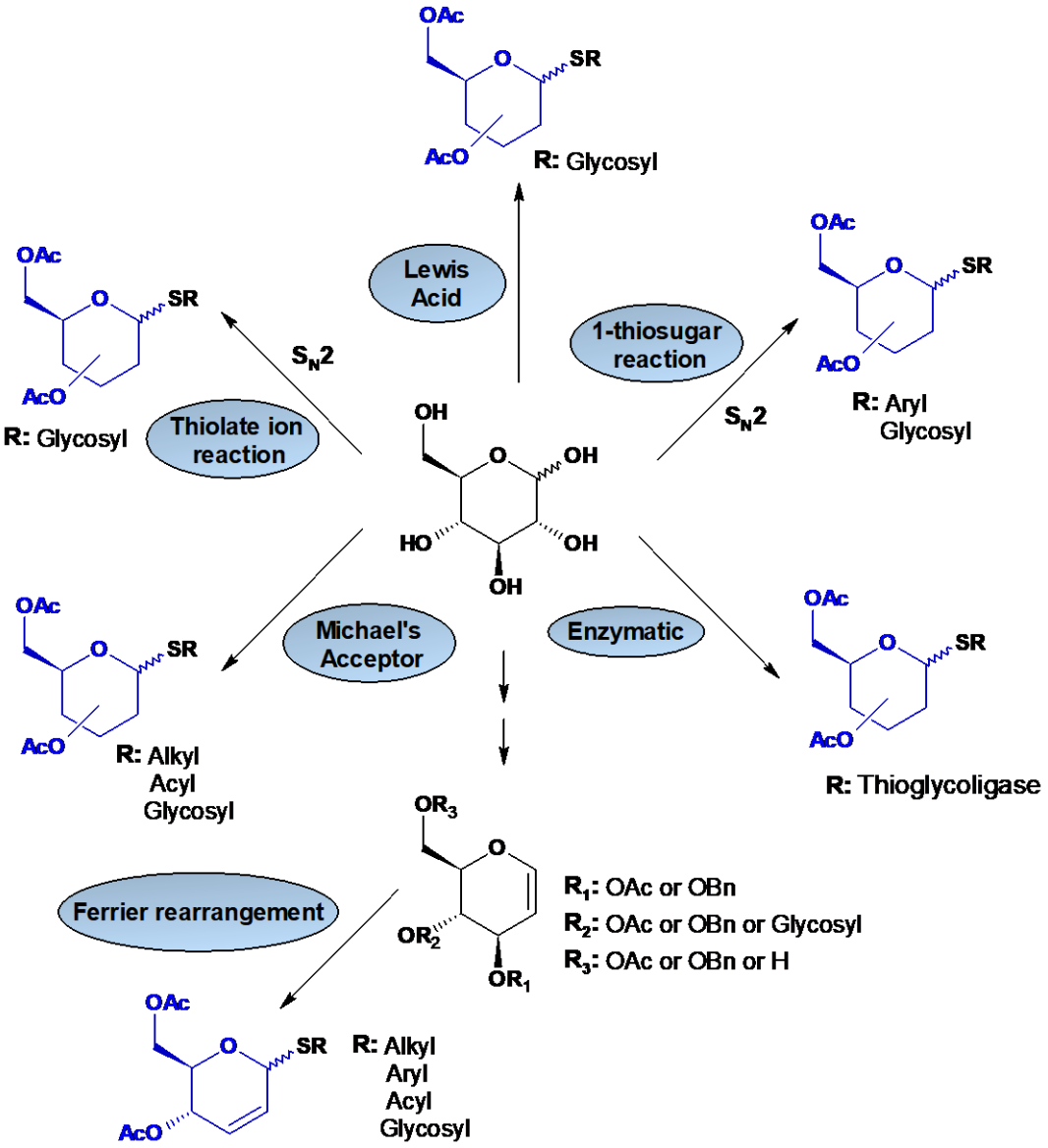

Source: De Oliveira *et al*. (2021).

2.3 PROTECTIVE GROUPS IN CARBOHYDRATE CHEMISTRY

Protective groups are commonly used in organic synthesis to mask a functional group to avoid temporary its reactivity with some reagents. In carbohydrate chemistry, protective groups can also increase or decrease reactivity and participate in reactions, thus affecting the stereochemistry of glycosylation reactions (Guo; Ye, 2010). Carbohydrates contain multiple hydroxyls and their protection help to increase the

solubility of these compounds in organic solvents, besides facilitating compounds purification and elucidation of structures (Hung; Wang, 2016).

The ester group is widely used as a temporary protecting group for sugar hydroxyls since they are sensitive to bases and easy to attach and remove (Hung; Wang, 2016). As discussed in section 2.2, the stereoselectivity of glycosylation reactions is profoundly influenced by protecting groups. For example, an ester-type protecting group at C-2 provides anchimeric assistance in the glycosylation reaction leading to the formation of 1,2-trans glycosides, whereas the ether-type group, such as 2-*O*-benzyl in a glucopyranoside scaffold, does not participate in the reaction and allows the predominant formation of the 1,2-cis bond due to the influence of the anomeric effect (Ghosh; Kulkarni, 2020).

Another strategy used in carbohydrate chemistry is acetal protection of hydroxyls, where protection at positions 4 and 6 in a hexapyranose is common, forming a stable 6-membered cyclic acetal (Figure 7) (Pétursson, 1997). Cyclic acetal protecting groups are known for their stability under basic conditions and their ability to be removed under acid-catalyzed hydrolysis (Fernandes *et al*., 2008). According to Codée *et al*. (2011), benzylidene acetals are widely used to selectively protect alcohols in the C-4 and C-6 positions, isopropylidene ketals are used to block two neighboring cis hydroxyls, and butane-2,3-bis acetals to protect vicinal diequatorial diols. In this work, we will focus on a less known and used cyclic protecting group, the phenylsulfonylethylidene (PSE) acetal.

Figure 7 - Generic structure of a cyclic acetal as a protecting group in a hexapyranose.

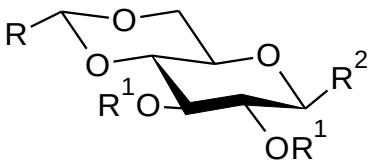

Source: The author (2024).

2.3.1 Phenylsulfonylethylidene (PSE) acetal

1,2-Bis(phenylsulfonyl)ethylene [(*Z*)- and (*E*)- BPSE] has often been used as a dienophile in Diels-Alder cycloaddition reactions, although, recently its strong electrophilic character has been explored in Michael double additions, leading to the

synthesis of arylsulfonyl acetals as carbohydrate protecting groups (De Lucchi *et al*., 2005). According to the authors, (*Z*)-BPSE can be prepared by oxidizing (*Z*)-1,2-bis(thiophenyl)ethylene, obtained from (*Z*)-1,2-dichloroethylene or a mixture of (*Z*)- and (*E*)-1,2-dichloroethylenes, however, the (*E*) isomer is not reactive under these conditions. The (*E*)-1,2-bis(phenylsulfonyl)ethylene isomer can be obtained by the thermal process known as isomerization of (*Z*)-1,2-bis(thiophenyl)ethylene followed by oxidation, but it can also be prepared by the sunlight-iodine catalyzed isomerization of the (*Z*)-1,2-bis(phenylsulfonyl)ethylene isomer (De Lucchi *et al*., 1984).

Scheme 8 - Synthesis of (*Z*)- and (*E*)-1,2-Bis(phenylsulfonyl)ethylene.

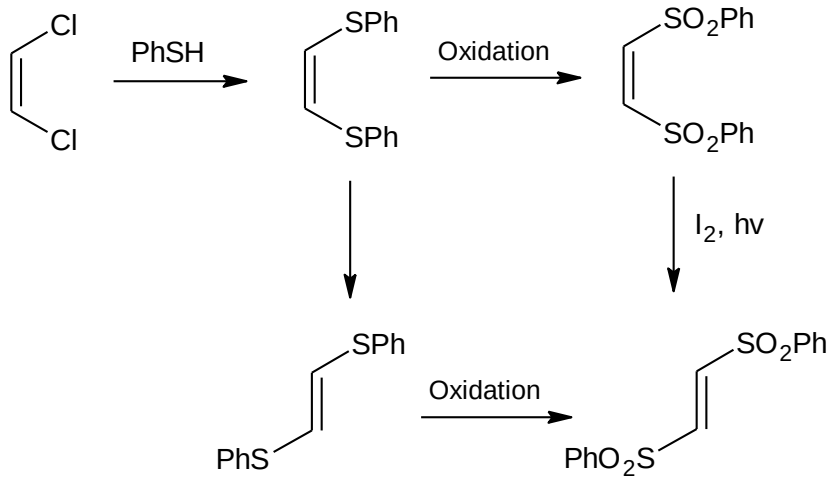

Source: Adapted from De Lucchi *et al*. (1984).

Phenylsulfonylethylidene (PSE) acetals are easily prepared from carbohydrates following a double Michael addition pathway, in which (*Z*)- or (*E*)-1,2-bis(phenylsulfonyl) ethylenes can react with various *α* and *β* diols in THF using NaH as a base and Bu_4NBr as a phase transfer catalyst at room temperature (Chéry *et al*., 2001). Similarly, saccharide polyols react in DMF using *t*-BuOK as a base. As can be seen in scheme 9, the initial addition of an alkoxide ion is followed by the elimination of a sulfinate ion, and in this way, the resulting alkoxy vinyl sulfone is then attacked by a second alkoxide ion to form phenylsulfonylethylidene (PSE) acetal (Chéry *et al*., 2001).

Scheme 9 - Synthesis of PSE acetal.

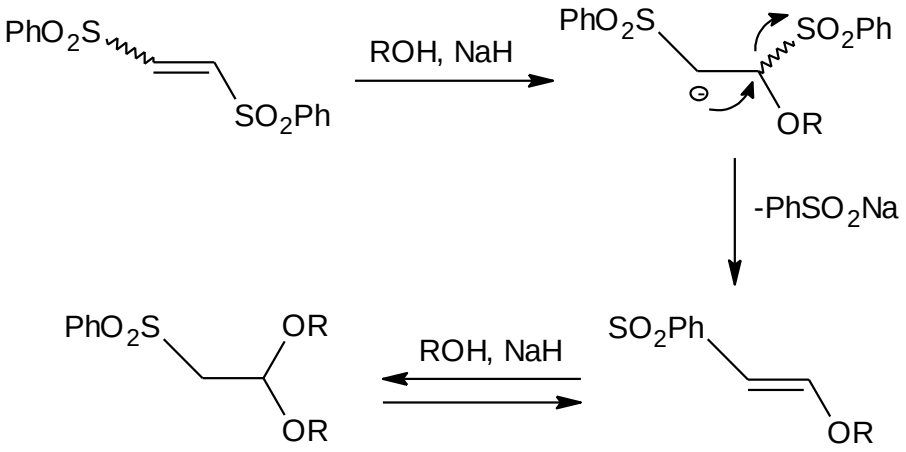

Source: Adapted from Chéry *et al*. (2001).

Chéry and collaborators (2000) investigated the deprotection conditions for PSE acetal in their work and noticed that this protecting group has an unusual behavior compared to other cyclic acetal protecting groups: a strong reluctance to cleave under standard conditions of acid hydrolysis or alcoholysis (CH_3COOH 80%, H_2SO_4 0.7 N, $BF_3.Et_2O/CH_2Cl_2$/MeOH or TFA:H_2O). According to the authors, this behavior can be explained by the presence of the sulfonyl group which makes both acetal oxygens harder and therefore more difficult to protonate. On the other side, PSE acetals can be easily removed under basic conditions ($CsCO_3$/EtOH) or strongly reducing conditions ($LiAlH_4$), as well as being stable under oxidizing conditions (DDQ) or in the presence of strong Lewis acids (Fernandes *et al*., 2008).

The total removal of PSE acetal follows a retro-Michael type reaction; however, this process can be controlled to produce alkoxyvinyl sulfones. The formation of a regioisomeric (1:1) mixture of alkoxyvinyl sulfones with exclusive *E* configuration in the double bond has been observed, where the weak regioselectivity observed between the primary (*O*-6) and secondary (*O*-4) positions may be the result of an equilibrium established between the cyclic acetal and open-chain anionic species (Chéry *et al*., 2012). The authors proposed a mechanism (Scheme 10), in which the first equivalent of *n*-BuLi removes the α proton from the sulfonyl group, and then cleavage of the cyclic acetal **A** occurs to produce the vinyl sulfones **B** or **C**.

In contrast, the second equivalent of *n*-BuLi removes the more reactive α-vinyl proton to form the stabilized carbanion **D** or **E**, which in the end attacks electrophilic species and stereoselectively provides *E*-alkoxyvinyl sulfones. Attempts were also

made to *O*-alkylate the **D** or **E** carbanions, however, even with an excess of any electrophile, no *O*-alkylation was observed by the authors, but rather selective *C*-alkylation at the *α* position of the *β*-alkoxyvinyl sulfones.

Scheme 10 - Intermediates in the base-induced ring cleavage of a PSE acetal.

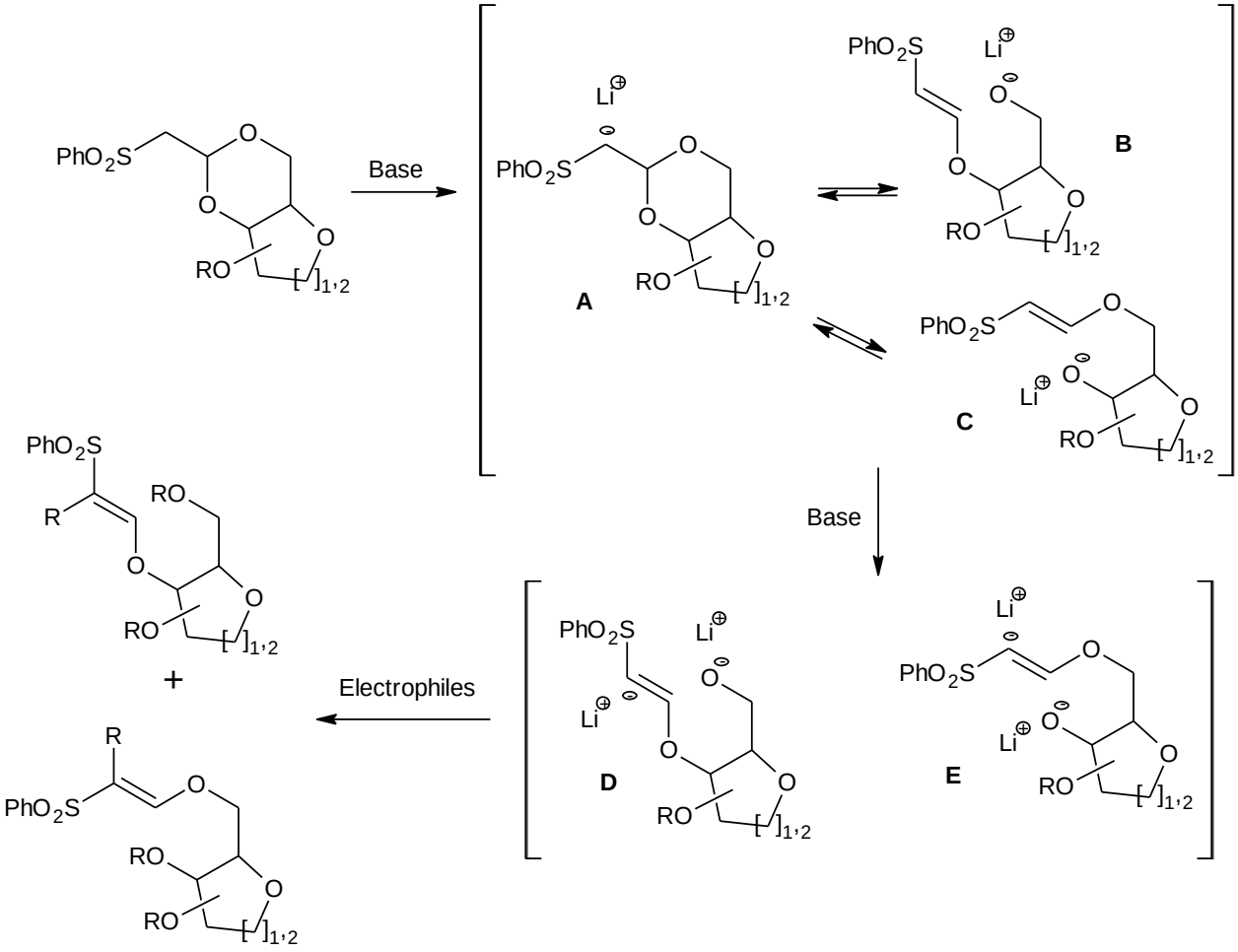

Source: Adapted from Chéry *et al*. (2012).

2.4 HETEROCYCLIC COMPOUNDS

Heterocyclic compounds are cyclic rings containing at least one atom other than carbon (heteroatom), the most common are nitrogen, oxygen, and sulfur; however, rings including heteroatoms such as phosphorus, iron, magnesium, selenium, etc. are common (Kabir; Uzzaman, 2022). They can be aromatic or non-aromatic, the most common are five- and six-membered rings, and the best known with basic structure are pyridine, pyrrole, furan, and thiophene (Arora *et al*., 2012).

Figure 8 - Examples of simpler heterocyclics.

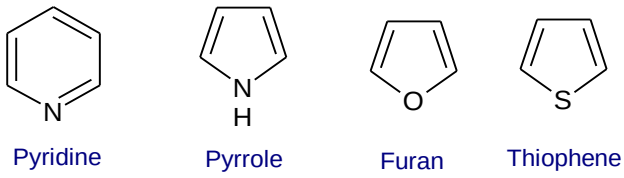

Source: The author (2024).

Heterocycles have a wide range of applications, such as fungicides, herbicides, anticorrosive agents, photo stabilizers, agrochemicals, dyes, copolymers, photographic developers, flavoring agents, etc. (Dua *et al*., 2011). However, one of the greatest application interests for heterocyclic is in medicinal chemistry, since they are found in biomolecules such as enzymes, vitamins, natural products, and biologically active compounds (Al-Mulla, 2017). Can be highlighted some of the biological activities involving these compounds, such as antifungal, antimycobacterial, trypanocidal, anti-HIV, antileishmanial, genotoxic, antitubercular, antimalarial, analgesic, anti-inflammatory, muscle relaxant, anticonvulsant, anticancer, lipid peroxidation inhibitor, hypnotic, antidepressant, antitumor, and anthelmintic agents (Dua *et al*., 2011).

Heterocycles play an important role in organic chemistry, since they can be involved in various types of reactions, and behaving as acids or bases according to the pH of the medium, thus forming anions or cations (Dua *et al*., 2011). Therefore, they can interact with electrophilic or nucleophilic reagents, can be easily oxidized and resistant to reduction, as well as being easily hydrogenated but stable to the action of oxidizing agents. In this work, we will discuss some heterocycles containing nitrogen, oxygen, and sulfur atoms.

2.4.1 1,3-oxazolidine-2-thione and 1,3-thiazolidine-2-thione

Oxazolidinones are heterocycles with a five-membered ring that has the structure of an oxazolidine with a ketone between nitrogen and oxygen, as can be seen in figure 9 (Pandit; Singla; Shrivastava, 2012). As mentioned earlier, Linezolid was the first oxazolidinone approved for clinical use by the FDA. Gandhi *et al*. (2004) decided to study the effect of replacing the carbonyl group of the oxazolidinone ring (C=O) with a thiocarbonyl group (C=S) in Linezolid against GPB bacteria (*Enterococcus faecium*, *E. faecalis*, *Bacillus cereus*, *B. subtilis*, *Staphylococcus epidermidis*, *S. aureus*, and *B.*

pumilus). According to the authors, replacing oxygen with sulfur can lead to improved efficacy, pharmacokinetics, and lower toxicity of the drug candidate. Nevertheless, the thio-analogues of LNZ did not exhibit inhibition, and to investigate this result, molecular modeling studies were carried out, where they observed that the formation of the structure necessary for enzyme inhibition did not occur.

Figure 9 - Structures of the oxazoline and oxazolidinone rings, the drug Linezolid, and its thio-analogues prepared by Gandhi *et al*. (2004).

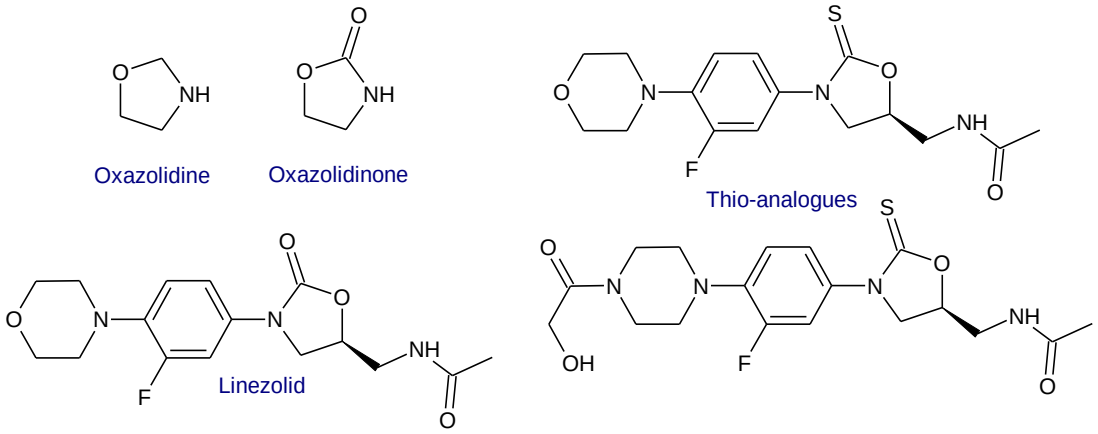

Source: The author (2024).

Saygili, Özalp, and Yildorim (2014) analyzed five new compounds containing the oxazolidinethione nucleus for antimicrobial activity and observed minimum inhibitory concentration values against *Staphylococcus aureus*, *Enterococcus faecalis*, *Escherichia coli*, and *Pseudomonas aeruginosa*. Therefore, the formation of sulfur analogs of oxazolidinone has been studied, since rings such as oxazolidinethiones and thiazolidinethiones present a variety of biological activities, such as inhibitors of the D-fructose transporter, antithyroid, antifertility, antibacterial and insecticidal (Mishra; Agrahari; Tiwari, 2017). The 1,3-oxazolidine-2-thiones have a five-membered ring with a thiocarbonyl (C=S) attached to the O and N atoms, while the 1,3-thiazolidine-2-thiones have S and N atoms attached to the thiocarbonyl (Figure 10).

Figure 10 - Structures of the oxazolidinethione and thiazolidinethione rings.

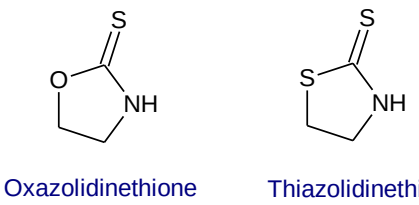

Source: The author (2024).

Oxazolidinethiones (OZTs) and thiazolidinethiones (TZTs) can be obtained from the condensation of the same amino alcohols with thiophosgene or carbon disulfide by changing the reaction conditions (Morales-Nava; Fernández-Zertuche; Ordóñez, 2011). In a low alkaline medium with a stoichiometric amount of carbon disulfide during a limited reaction time, oxazolidinethione can be obtained almost exclusively (Shamszad; Crimmins, 2012).

According to the authors, in this process, the carbon disulfide reacts mainly with the amino group, leading to the dithiocarbamate intermediate **A**, which is in equilibrium with intermediate **B** (Scheme 11). Finally, following path III, an intramolecular nucleophilic attack occurs on the thiocarbonyl group to produce oxazolidinethione. According to Shamszad and Crimmins (2012), under more drastic conditions with a very alkaline medium, a large amount of carbon disulfide, and a longer reaction time, the hydroxyl group of intermediate **A** undergoes nucleophilic addition of the carbon disulfide, leading to intermediate **C** (path IV). At this point, intermediate **C** can no longer produce oxazolidinethione, and so thiazolidinethione is formed through intramolecular cyclization (pathway V).

Scheme 11 - Mechanistic pathways for generating oxazolidinethiones and thiazolidinethiones.

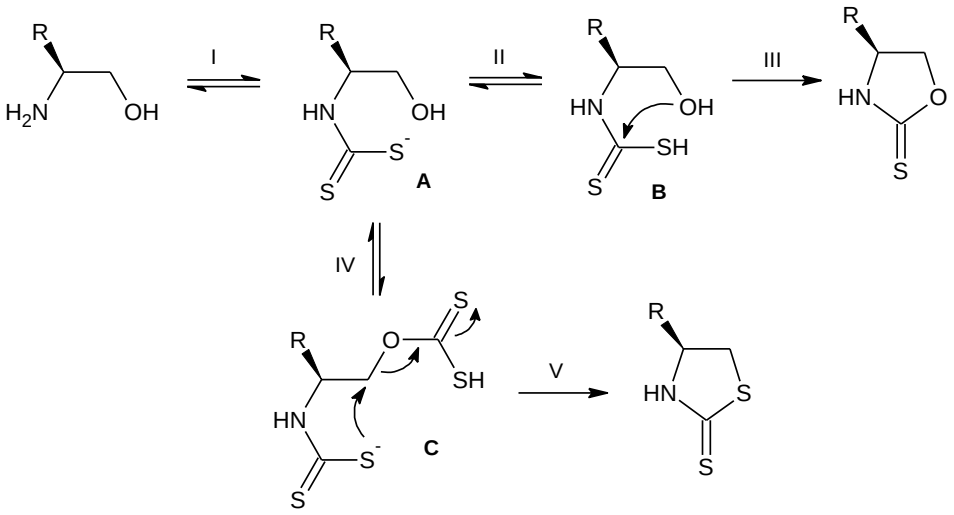

Source: Adapted from Shamszad; Crimmins (2012).

Mishra, Agrahari, and Tiwari (2017) reported the synthesis of oxazolidine-2-thiones and thiazolidine-2-thiones from azido-glycosyl alcohols (Scheme 12), which are easier to prepare compared to amino alcohols, as well as being known for their excellent reactivity with triphenylphosphine.

Scheme 12 - Synthesis of 1,3-oxazolidine-2-thiones and 1,3-thiazolidine-2-thiones from azido-glycosyl alcohols.

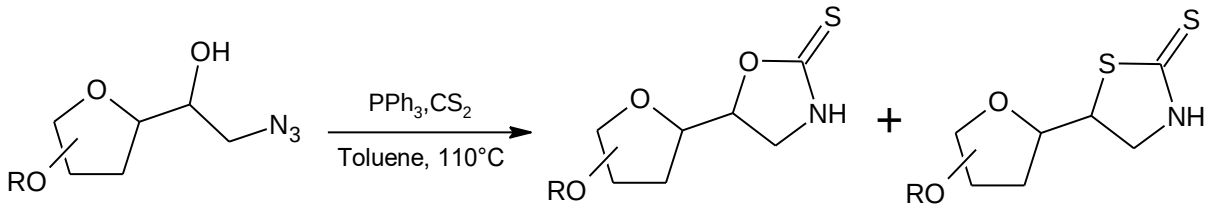

Source: Adapted from Mishra; Agrahari; Tiwari (2017).

In recent years, OZTs and TZTs have become popular chiral auxiliaries in asymmetric synthesis (Morales-Nava; Fernández-Zertuche; Ordóñez, 2011). Kederienė *et al*. (2022) carried out chemoselective *S*-arylation using copper iodide and dimethylethylenediamine (DMEDA) as the best ligand under basic conditions from OZTs linked to the carbohydrates *D*-arabinofuranose, *D*-xylofuranose and *D*-ribofuranose (Scheme 13).

Scheme 13 - C-S coupling reaction model with OZTs linked to *D*-xylo, *D*-ribo, and *D*-arabino carbohydrates.

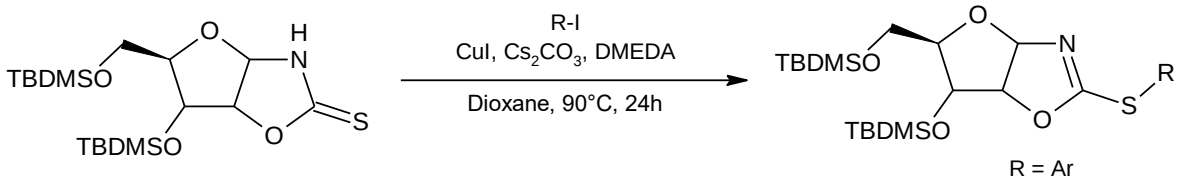

Source: Adapted from Kederienė *et al*. (2022).

2.4.2 1,3-oxazoline-2-thione or 2-mercapto-1,3-oxazole

Unlike the 1,3-oxazolidine-2-thiones (OZTs), few studies have looked at the 1,3-oxazoline-2-thiones (OXTs), although both rings are considered to be parent heterocycles (Silva *et al*., 2008b). Oxazolines have a five-membered ring containing nitrogen, oxygen, and a double bond, in which this unsaturation can be located in different positions allowing the existence of three oxazoline rings (Figure 11) (Bansal; Halve, 2014). In the case of oxazolinethiones, the double bond is located in position 4, and there is the presence of a thiocarbonyl between the oxygen and nitrogen atoms, as can be seen in Figure 11.

Figure 11 - Oxazoline and oxazolinethione rings.

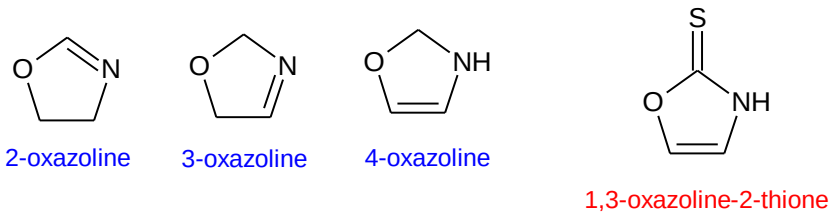

Source: Adapted from Bansal; Halve (2014).

The first synthetic approach to OXTs was carried out in 1956 by Gompper, through a thionation of substituted 1,3-oxazolin-2-ones using phosphorus pentasulfide, the results of which were reasonable in only a few cases (Sansinenea; Rollin; Silva, 2017).

Scheme 14 - Gompper Thionation (a); Willems and Vandenbergue Method (b).

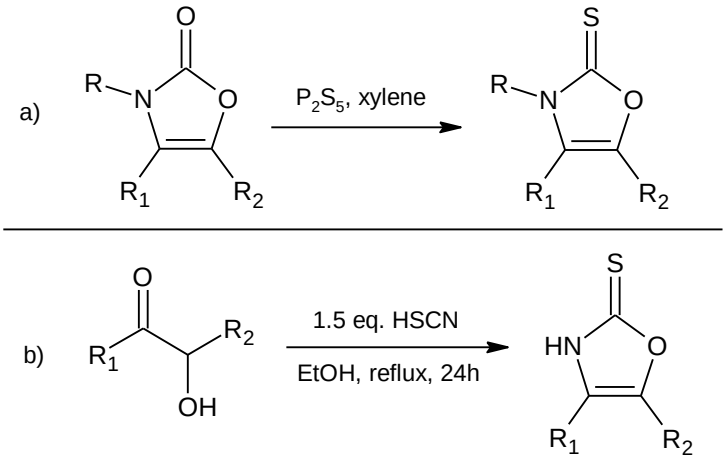

Source: Adapted from Sansinenea; Rollin; Silva (2017).

Willems and Vandenbergue then developed a new method in 1961 to obtain the same substituted 1,3-oxazoline-2-thiones by condensing α-hydroxyketones with thiocyanic acid or its salts (Scheme 14). Willems and Vandenbergue (1961) observed an important infrared behavior of these compounds that followed the prediction made by Gompper: the possibility of the existence of two isomers.

Indeed, there is a tautomeric thione-thiol equilibrium between the 1,3-oxazoline-2-thiones and 2-mercapto-1,3-oxazoles (Scheme 15), and several authors have observed in the spectroscopic data of this class of compounds the presence of this equilibrium and the prevalence of the thione form (Sansinenea; Rollin; Silva, 2017). This is a feature that arouses interest in this class of molecules since it makes it

possible to explore the reactivity of the two nucleophilic sites, the nitrogen and sulfur atoms.

Scheme 15 - Thione-thiol tautomerism in 1,3-oxazoline-2-thiones.

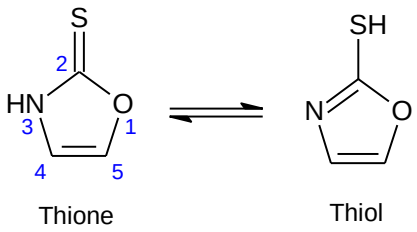

Source: Sansinenea; Rollin; Silva (2017).

Leconte *et al*. (2005) also carried out the condensation of hydroxyketones with thiocyanic acid to form bis-OZTs and OXTs. In addition, the authors investigated the selective S-functionalization of OXTs using electrophiles such as benzyl bromide or bromoacetophenone (Scheme 16). However, in the *N*-functionalization reaction with acrylonitrile or phenylvinylsulfone, the unexpected formation of *N*- and *S*-alkylated derivatives was observed, only with 1,2-bis-phenylsulfonylethylene (BPSE) a complete *N*-selectivity was achieved.

Scheme 16 - Selective reactions of *N*- and *S*-functionalization in OXTs.

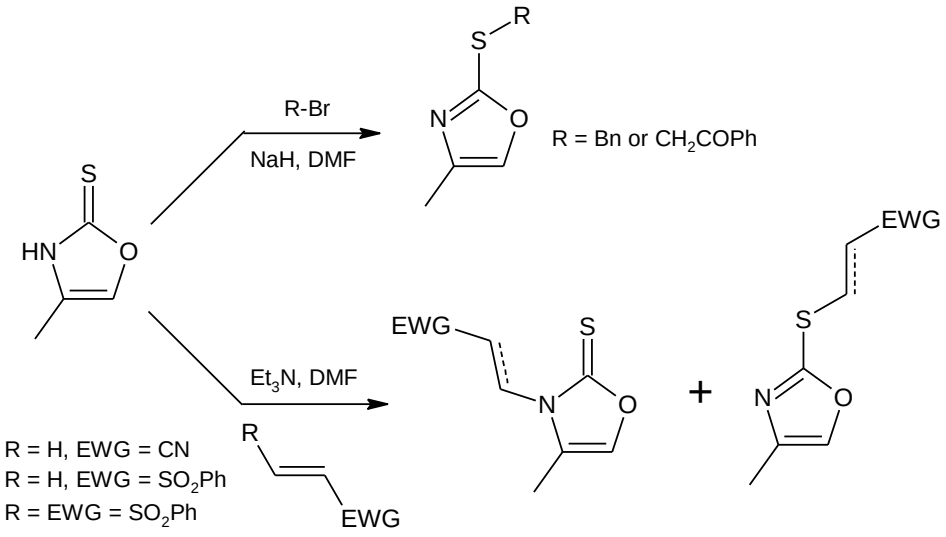

Source: Leconte *et al*. (2005).

Besides the nucleophilic reactivity observed, OXTs are used as substrates in various carbon-carbon cross-coupling processes. Silva *et al.* (2008a) developed a new Sonogashira cross-coupling method using OXTs and OZTs as substrates for the first

time (Scheme 17). In this work, the authors observed a cooperative effect of two different copper (I) species for the reaction to take place: CuI and CuTc.

Scheme 17 - Sonogashira cross-coupling with OXTs and OZTs.

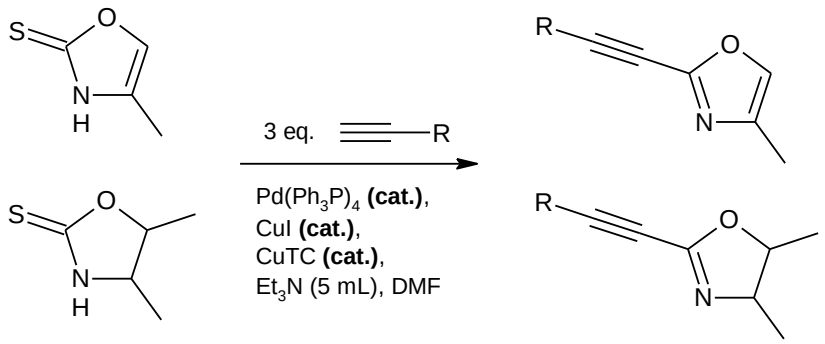

Source: Silva *et al*. (2008a).

In another work by Silva *et al*. (2008b), Suzuki and Stille cross-coupling reactions were carried out with OXTs and OZTs in microwaves to produce 2-aryloxazolines and 2-aryloxazoles (Scheme 18). The direct cross-coupling of OZTs did not obtain satisfactory results and for this reason, a selective *S*-alkylation of the OZTs was carried out as an activation protocol for the cross-coupling. On the other hand, the two-step procedure (*S*-alkylation and cross-coupling) was not efficient for OXTs. In this case, no coupling was observed, so the best protocol for OXTs is direct coupling in a single step due to the thione-thiol equilibrium.

Exploring other methodologies for preparing OXTs, Reddy *et al*. (1984) condensed an amino-alcohol with carbon disulfide in the presence of potassium hydroxide to obtain 2-mercapto-oxazole and subsequently carried out S-alkylations. These compounds were tested for antibacterial activity and showed potential against Bacillus pumilus, B. mugaterium, and Proteus vulgaris. In more recent work, Oka, Yabuuchi, and Sekiguchi (2013) synthesized 2-mercapto-oxazoles through the reaction of a *β*-ketoazide with carbon disulfide and triphenylphosphine (TPP) mediated by an iminophosphorane intermediate according to the mechanism proposed by the authors (Scheme 19).

Scheme 18 - Suzuki and Stille cross-coupling with OXTs and OZTs.

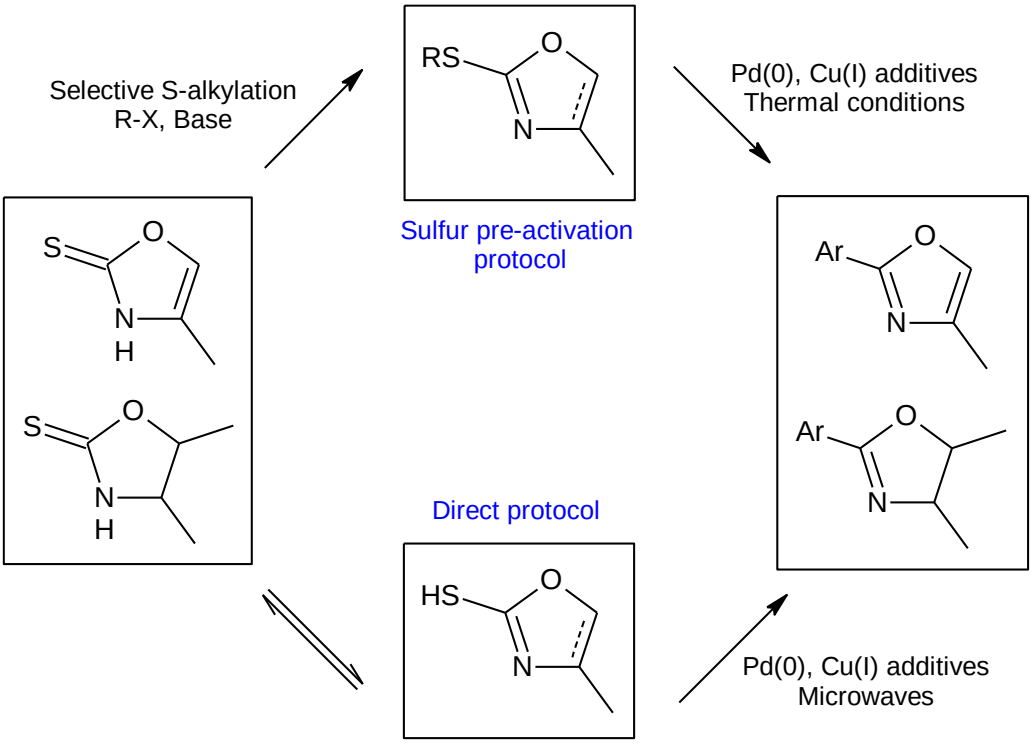

Source: Silva *et al*. (2008b).

Scheme 19 - Possible mechanism of 2-mercapto-oxazole formation mediated by the iminophosphorane intermediate.

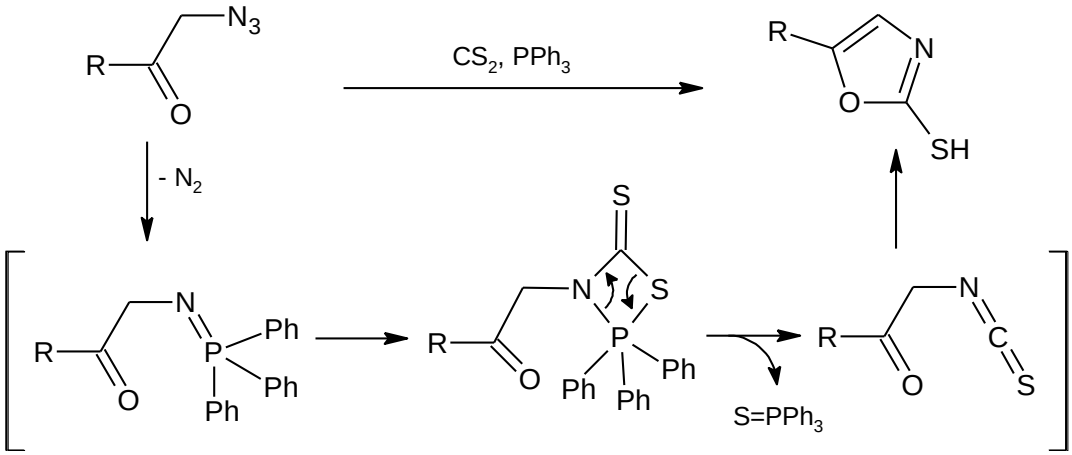

Source: Oka; Yabuuchi; Sekiguchi (2013).

3 METHODOLOGY

In this topic, we present a description of the methods used to synthesize all the compounds and to realize the biological studies. The compounds were characterized according to physical properties such as melting point and specific rotation, as well as spectroscopic properties such as infrared (IR) and Nuclear Magnetic Resonance (NMR).

3.1 MATERIALS

The reagents used were purchased commercially by Sigma-Aldrich and Dinâmica. The dimethylformamide (DMF) solvent was distilled with the drying agent calcium hydride (CaH_2), and the molecular sieve (4Å) was added after activation in the muffle at a temperature of 300°C. In other solvents or reagents that required an anhydrous condition, the molecular sieve (4Å) was also added for drying. The products were purified by column chromatography using 60 µm silica gel and an elution system with different proportions of solvents. The reactions were accompanied by thin-layer chromatography (TLC), where revelation was carried out under ultraviolet light at 365 nm or by immersion in previously prepared solutions, such as 10% or 5% (v/v) sulfuric acid/ethanol. The azido-alcohol **7a** and diastereoisomeric mixture **6a**/**6b** were provided by our research group for use in this work.

3.2 EQUIPMENTS

The specific rotations were carried out on the ANTON-PAAR benchtop digital polarimeter, model MCP200, and concentration in g/100mL (Bioactive Compounds Synthesis Laboratory (LSCB)-UFRPE). Melting points were measured using the Melting Point Meter - PFM-II (Bioactive Compounds Synthesis Laboratory (LSCB)-UFRPE). The microwave reactions were carried out in the Discover SP-D CEM microwave reactor (Multiuser Chemical Analysis Laboratory (LABMAQ)-UFRPE). The infrared spectra were carried out on the Shimadzu IRTracer apparatus (Multiuser Chemical Analysis Laboratory (LABMAQ)-UFRPE) and the Shimadzu IRSpirit apparatus (Analytical Center (CA/DQF)-UFPE). The NMR spectra were carried out

using the Varian Mercury 400 MHz apparatus for hydrogen (^{1}H) and 100 MHz for carbon (^{13}C) (Analytical Center (CA/DQF)-UFPE) and the Bruker 500 MHz apparatus for hydrogen (^{1}H) and 125 MHz for carbon (^{13}C) (Laboratory of Multiuser Characterization and Analysis (LMCA)-UFPB), using $CDCl_3$ or DMSO-d_6 as solvents, the chemical shifts (δ) were expressed in parts per million (ppm), and the coupling constants (*J*) in hertz (Hz), the multiplicities were indicated according to conventions: s (singlet), d (duplet), dd (double duplet), ddd (double of doublets), t (triplet), dt (double triplet), m (multiplet), ap s (apparent singlet), br s (broad singlet).

3.3 SYNTHETIC METHODS

3.3.1 Synthesis of 4-(hydroxymethyl)-1,3-dioxolan-2-one (1) [CAS Reg. N°. 931-40-8]

In a round-bottomed flask, 10 g (84.68 mmol) of glycerol and 26 mL (260 mmol, 3 eq.) of dimethyl carbonate were added. The flask was attached to a Dean Stark and the reaction mixture was stirred and heated. When the system reached 60°C, 0.45 g (3.26 mmol, 10% m/m) of K_2CO_3 was added. The reaction remained at 78°C for 5 hours. After this, the reaction was concentrated under reduced pressure and washed with acetone to precipitate the K_2CO_3. Filtration was carried out and a colorless oil was obtained after removing the solvent under reduced pressure (Adapted from Rokicki *et al*., 2005).

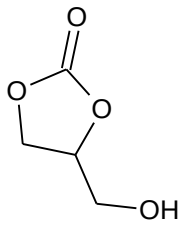

Yield 96%; colorless oil; R_f = 0.47 (EtOAc). **IR (ATR) v/cm^{-1}:** 3363, 2935, 2879, 1770, 1402, 1176, 1045. **NMR**: Data matches with literature values (Rokicki *et al*., 2005).

3.3.2 Synthesis of (2-oxo-1,3-dioxolan-4-yl)methyl 4-methylbenzenesulfonate (2) [CAS Reg. N°. 949895-84-5]

In a round-bottomed flask, 3.54 g (30 mmol) of glycerol carbonate **1** solubilized in 7.5 mL of pre-dried DCM was added. Next, a solution of 7.5 g (39.33 mmol, 1.3 eq.) of tosyl chloride in 7.5 mL of pre-dried DCM was added drop by drop under an argon atmosphere and ice bath. Then 7.5 mL of Et_3N was added and the reaction mixture was stirred for 16 hours at room temperature. Work up: the reaction mixture was diluted with 50 mL of DCM and washed with distilled water (3 x 50 mL) and a 0.2 M HCl solution (1 x 10 mL). Work up: extraction was carried out with DCM (3 x 50 mL), the organic phase was dried with Na_2SO_4, and the solvent was removed under reduced pressure. A white solid was obtained after precipitation with hexane, washing with EtOAc, and filtration (Simão *et al*., 2006).

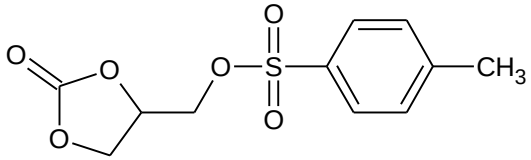

Yield 65%; white solid; R_f = 0.5 (Hex/EtOAc, 1:1); Mp = 114-115°C; Lit. (Giardi *et al*., 2010): MP = 108°C. **IR (KBr) v/cm^{-1}:** 1795, 1595, 1361, 1159, 1095, 1044, 742, 663, 551. **NMR**: Data matches with literature values (Giardi *et al*., 2010).

3.3.3 Synthesis of 4-(iodomethyl)-1,3-dioxolan-2-one (3) [CAS Reg. No. 78947-99-6]

In a round-bottomed flask, 5 g (18.63 mmol) of glycerol carbonate tosylated **2** was added to 40 mL of acetone. Then 11.16 g (74.52 mmol, 4 eq.) of NaI was added and the reaction mixture was refluxed at 56°C for 5 hours. After dilution with EtOAc, it was washed with saturated $Na_2S_2O_3$ solution and saturated NaCl solution. Work up: extraction was then carried out with EtOAc (3 x 50 mL), the organic phase was dried with Na_2SO_4, and the solvent was removed under reduced pressure. A chromatographic column was performed (Hex/EtOAc, 7:3, 6:4, 1:1), and colorless crystals were obtained (Adapted from Rousseau *et al*., 2009).

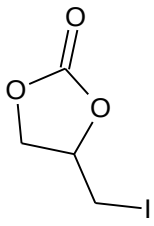

Yield 80%; colorless crystal; R_f = 0.4 (Hex/EtOAc, 6:4); Mp = 67-69 °C; lit. (Rousseau *et al*., 2009): Mp = 67-69°C. **IR (KBr) v/cm^{-1}:** 3022, 2982, 2929, 1777, 1480, 1393, 1175, 1066, 607. **^{1}H NMR (400 MHz, $CDCl_3$):** δ 4.85-4.78 (m, 1H, H-5), 4.60 (t, 1H, $J_{4a,4b}$ = 8.8 Hz, H-4a), 4.23 (dd, 1H, $J_{4b,4a}$ = 8.8 Hz, $J_{4b,5}$ = 6 Hz, H-4b), 3.43 (dd, 1H, $J_{6a,6b}$ = 10.8 Hz; $J_{6a,5}$ = 4.4 Hz, H-6a), 3.33 (dd, 1H, $J_{6b,6a}$ = 10.8 Hz; $J_{6b,5}$ = 8.4 Hz, H-6b). **^{13}C NMR (100 MHz, $CDCl_3$):** δ 154.1, 74.7, 69.8, 3.6.

3.3.4 Synthesis of 4-(mercaptomethyl)-1,3-dioxolan-2-one (4) [CAS Reg. No. 1193191-64-8]

In a round-bottomed flask, 2.7 g (11.84 mmol) of glycerol carbonate iodide **3** was added to 72 mL of DMF. Then 2.7 g (35.53 mmol, 3 eq.) of thiourea was added. The reaction mixture was stirred at 70°C for 3 hours. After this, the solvent was removed under reduced pressure and the residue was solubilized in 96 mL of distilled water and 22.50 g of $Na_2S_2O_5$ was added. The final mixture was refluxed for 10 min. After dilution with EtOAc, it was washed with saturated NaCl solution and extracted with EtOAc (3 x 50 mL), the organic phase was dried with Na_2SO_4, and the solvent was removed under reduced pressure to obtain a white solid.

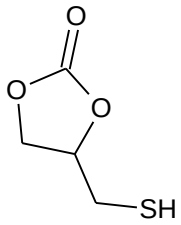

Yield 85%; white solid; R_f = 0.5 (EtOAc/MeOH, 9:1); Mp = 156-158°C; **^{1}H NMR (400 MHz, $CDCl_3$):** δ 4.85-4.78 (m, 1H, H-5), 4.60 (t, 1H, $J_{4a,4b}$ = 9.0 Hz, H-4a), 4.23 (dd, 1H, $J_{4b,4a}$ = 9.0 HZ; $J_{4b,5}$ = 6.2 Hz, H-4b), 3.43 (dd, 1H, $J_{6a,6b}$ = 10.6 Hz; $J_{6a,5}$ = 3.9 Hz, H-6a), 3.32 (dd, 1H, $J_{6b,6a}$ = 10.6 Hz; $J_{6b,5}$ = 8.2 Hz, H-6b) , 1.26 (s, 1H, SH). **^{13}C NMR (100 MHz, $CDCl_3$):** δ 159.4, 74.7, 69.8, 36.5.

3.3.5 Synthesis of 3,4,6-Tri-*O*-Acetyl-*D*-Glucal (5) [CAS Reg. No. 2873-29-2]

In a round-bottomed flask, 10 g (55.5 mmol) of *D*-glucose and 36.7 mL of acetic anhydride (7 eq.) were added, ending with the addition of a 31% HBr/AcOH solution

(1.25 mL of the solution, containing 0.25 mL of 48% HBr in 1.0 mL of acetic acid). This mixture was kept stirring for 1 hour and then cooled to 10°C, before slowly adding more of the 31% HBr/AcOH solution (150 mL of the solution, containing 30 mL of 48% HBr in 120 mL of acetic anhydride), which had been prepared at 0°C. Once the HBr/AcOH solution had been added, the reaction mixture was stirred for 12 hours, gradually returning to room temperature. Next, 20g of anhydrous sodium acetate (24 mol) was added under vigorous stirring for 30 minutes, and then a suspension containing 3.15g of $CuSO_4.5H_2O$ (12.6 mmol), 126g of zinc (2 mols) in 100 mL of water and 150 mL of acetic acid with 94.5g of sodium acetate (1.15 mol) was added, leaving it under vigorous stirring for 2 hours. The reaction mixture was then filtered to remove the solid residue, washed with ethyl acetate (100 mL), and then water (100 mL). The organic phase was also washed with a saturated $NaHCO_3$ solution and a saturated NaCl solution, and dried with Na_2SO_4. The final product was purified in a chromatographic column with hexane/ethyl acetate (9:1), obtaining a white solid (Shull; Wu; Koreeda; 1996).

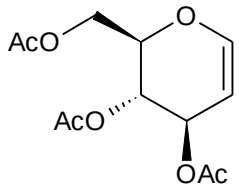

Yield 49%; white solid; R_f = 0.48 (Hex/EtOAc, 6:4); Mp = 50-51°C; Lit. (Zhao *et al*., 2011): Mp = 50-51°C. **IR (ATR) v/cm^{-1}:** 2958, 1732, 1647, 1369, 1211, 1024. **NMR**: Data matches with literature values (Zhao *et al*., 2011).

3.3.6 Synthesis of 1'-*O*-(4,6-di-*O*-acetyl-2,3-dideoxy-α-*D*-erythro-hex-2-enopyranosyl)-(3'-azido-3'-deoxy)-sn-glycerol (7a/7b)

2.5g of the solid diastereoisomeric mixture **6a**/**6b** (7.67 mmol) solubilized in 25 mL DMF:DMSO (1:1) was added to a round-bottom flask, followed by 0.99 g of sodium azide (15.35 mmol, 2 eq.) and the mixture was stirred at 100°C for 5 hours, protected from light. The mixture was then extracted with EtOAc (3x 50 mL), the organic phase was dried with Na_2SO_4, and the solvent was removed under reduced pressure. The residue was purified on a chromatographic column (Hex/EtOAc, 1:1) to obtain a yellowish oil.

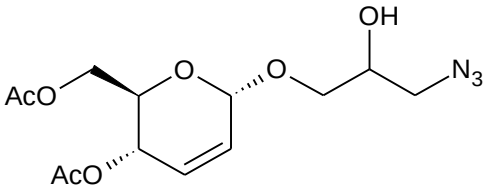

Yield 52%; yellowish oil; R_f = 0.62 (Hex/EtOAc, 3:7); $[\alpha]_D^{25}$ = + 71 (c = 0.1, CH_2Cl_2). **IR (KBr) v/cm^{-1}:** 3482, 2927, 2099, 1737, 1595, 1367, 1225, 1036.

3.3.7 Synthesis of 1'-*O*-(4,6-di-*O*-acetyl-2,3-dideoxy-α-*D*-erythro-hex-2-enopyranosyl)-(3'-azido-3'-deoxy)-propan-2'-one (8)

In a round-bottomed flask, 0.658 g of the diastereoisomeric mixture **7a**/**7b** (2 mmol) solubilized in 4 mL DCM pre-dried in $CaCl_2$ was added, then 0.672 g of $NaHCO_3$ (8 mmol, 4 eq.), and the reaction mixture was stirred for 30 minutes at room temperature. Then 1.272 g of Dess-Martin Periodinane (DMP) was added, and the reaction mixture was stirred for 1 hour at room temperature. After this, the reaction mixture was diluted in 4 mL of DCM and a mixture containing a saturated solution of sodium thiosulfate, a saturated solution of sodium bicarbonate, and distilled water (1:1:1) was slowly added. This mixture was kept under vigorous stirring for 1 hour, resulting in a two-phase separation. Work up: extraction was carried out with DCM (3x 50 mL), the organic phases were collected and dried with Na_2SO_4, the solvent was removed under reduced pressure. The residue was purified on a chromatographic column (DCM/EtOAc, 9:1) to obtain a yellowish oil (Oliveira, 2020. Thesis).

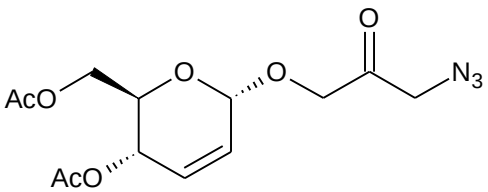

Yield 88%; yellowish oil; R_f = 0.60 (DCM/EtOAc, 9:1); $[\alpha]_D^{25}$ = + 80 (c = 0.1, $CHCl_3$). **IR (KBr) v/cm^{-1}:** 2914, 2104, 1796, 1733, 1597, 1368, 1225, 1038, 963. **^{1}H NMR (500 MHz, $CDCl_3$):** δ 5.96 (d, 1H, $J_{3,2}$ = 10.25 Hz, H-3), 5.87 (dd, 1H, $J_{2,3}$ = 10.2; $J_{2,1}$ = 1.85 Hz, H-2), 5.31 (d, 1H, $J_{4,5}$ = 9.6 Hz, H-4), 5.06 (s, 1H, H-1), 4.40 (dd, 1H, $J_{7a,7b}$ = 17.1 Hz; J = 0.9 Hz, H-7a), 4.50 (d, 1H, $J_{7b,7a}$ = 17.16 Hz, H-7b), 4.23-4,18 (m, 2H, H-6a, H-6b), 4.15 (s, 1H, H-8a, H-8b), 4.11-4.08 (m, 1H, H-5), 2.10 (s, 3H, CH_3C=O), 2.09 (s,

3H, $CH_3C=O$). **^{13}C NMR (125 MHz, $CDCl_3$):** δ 201.7, 170.1, 170.1, 130.3, 126.4, 94.8, 71.8, 67.5, 65.0, 62.7, 55.5, 20.9, 20.7.

3.3.8 Synthesis of (Z)-1,2-Bis(phenylsulfonyl)ethene (9) [CAS Reg. No. 963-15-5]

The synthesis of the BPSE protecting group was divided into two steps. In the first step, a solution of 5 mL (64.5 mmol) of 1,2-dichloroethene in 50 mL of ethanol was added to a solution of 7.5 g (133.7 mmol, 2 eq.) of KOH and 8 mL (78.4 mmol, 1.2 eq.) of PhSH in 100 mL of ethanol. The resulting solution was heated at 90°C for 17h, after which the solvent was removed under reduced pressure and the residue was washed with distilled water (3 x 30 mL) and extracted with EtOAc (3 x 30 mL). Finally, the organic phase was dried with Na_2SO_4 and the solvent was removed under reduced pressure (Adapted from Parham; Heberling, 1954). In the second step, the alkene obtained in the first step (40.8 mmol) was solubilized in 177 mL of acetic acid and then 38.5 mL (40 eq.) of H_2O_2 was added drop by drop. Finally, a few drops of sulfuric acid were added. After 7 days and monitoring by TLC plate, neutralization was carried out with a saturated $NaHCO_3$ solution and extraction with EtOAc, the organic phase was dried with Na_2SO_4, and the solvent was removed under reduced pressure. A white solid was obtained and washed with hexane (Adapted from Truce; Mcmanimie, 1954).

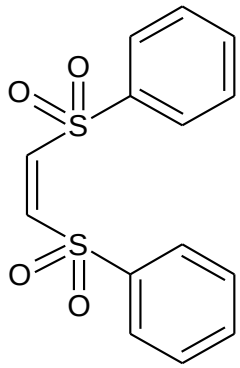

Yield 56%; white solid; R_f = 0.53 (Hex/EtOAc, 1:1); Mp = 82-84°C; Lit. (Truce; Mcmanimie, 1954): Mp = 101°C. **IR (KBr) v/cm^{-1}:** 3026, 1581, 1448, 1325, 1305, 1141, 1078, 986, 725. **^{1}H NMR (400 MHz, $CDCl_3$):** δ 8.07 (d, 4H, *J* = 7.8 Hz, H-2, H-6, H-16, H-20), 7.71 (t, 2H, *J* = 7.44 Hz, H-4, H-18), 7.60 (t, 4H, *J* = 7.8 Hz, H-3, H-5, H-17, H-

19), 6.83 (s, 2H, H-10, H-11). **^{13}C NMR (100 MHz, $CDCl_3$):** δ 140.5, 139.4, 134.5, 129.4, 128.7.

3.3.9 Synthesis of 4,6-*O*-(2-phenylsulfonyl)ethylidene-1,5-anhydro-*D*-arabino-hex-1-enitol (10) [CAS Reg. No. 330151-23-0]

In the first transesterification step, tri-*O*-acetyl-*D*-glucal **5** (1.83 mmol) was added to a solution of metallic sodium (0.11 mmol) in 5 mL of MeOH. The reaction was stirred under an argon atmosphere at room temperature. After 30 min, amberlite IR 120 was added and filtered through celite. Without purification, *D*-glucal (1.83 mmol) was solubilized in 5 mL of DMF, then 0.616 g (5.49 mmol, 3 eq.) of potassium tert-butoxide was added. After 15 minutes, 1.128 g (3.66 mmol, 2 eq.) of BPSE **9** and a few crystals of Bu_4NBr were added. The reaction mixture was stirred at room temperature and under an argon atmosphere for 48 hours. Then, the solvent was removed under reduced pressure and a chromatographic column was run (Hex/EtOAc, 7:3, 6:4, 1:1) (Adapted from Chéry *et al*., 2000).

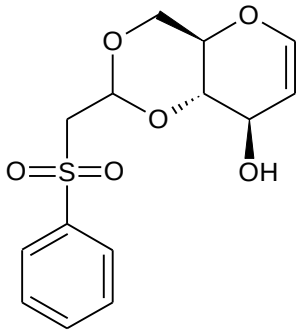

Yield 77%; yellowish solid; R_f = 0.3 (Hex/EtOAc, 1:1); Mp = 107-109°C; $[\alpha]_D^{25}$ = + 20 (c = 0.1, CH_2Cl_2); Lit. (Chéry *et al*., 2000): $[\alpha]_D^{25}$ = + 18 (c = 1.4, $CHCl_3$). **IR (KBr) v/cm^{-1}:** 3504, 3067, 2918, 1633, 1584, 1447, 1324, 1306, 1130, 1078, 1013, 749, 686. **^{1}H NMR (400 MHz, $CDCl_3$):** δ 7.95-7.93 (m, 2H, H-*o*), 7.70-7.66 (m, 2H, H-*m*), 7.61-7.57 (m, 1H, H-*p*), 6.25 (dd, 1H, $J_{1,2}$ = 6.28 Hz; $J_{1,3}$ = 1.56 Hz, H-1), 5.09 (t, 1H, *J* = 5.08 Hz, H-7), 4.70 (dd, 1H, $J_{2,1}$ = 5.88 Hz; $J_{2,3}$ = 1.96 Hz, H-2), 4.22 (ddd, 1H, $J_{3,4}$ = 7.84 Hz; $J_{3,2}$ = 1.56 Hz; $J_{3,1}$ = 1.56 Hz, H-3), 4.13 (dd, 1H, $J_{6a,6b}$ = 10.2 Hz; $J_{6a,5}$ = 4.72 Hz, H-6a), 3.64 (dd, 1H, $J_{6b,6a}$ = 10.16 Hz; $J_{6b,5}$ = 4.76 Hz, H-6b), 3.60-3.49 (m, 4H, H-4, H-5, H-

8a, H-8b), 2.22 (br s, 1H, OH). **^{13}C NMR (100 MHz, $CDCl_3$):** δ 143.9, 139.7, 133.9, 129.1, 128.3, 103.4, 96.8, 80.4, 67.9, 67.7, 66.2, 59.8.

3.3.10 Synthesis of 1-*O*-(*m*-chlorobenzoyl)-4,6-*O*-phenylsulfonylethylidene-α-*D*-mannopyranose (11)

In a microwave tube, 0.3 g (0.96 mmol) of PSE-glucal **10** and 20 mL of dichloromethane pre-dried in $CaCl_2$ were added. Subsequently, 0.331 g (1.92 mmol, 2 eq.) of *m*-CPBA was added. The reaction was carried out in the microwave (150W) at room temperature for 10 minutes. After the end of the reaction, the solvent was removed under reduced pressure and a chromatographic column was performed (EtOAc/Hex, 6:4, 7:3, 8:2) (Adapted from Marín *et al*., 2011).

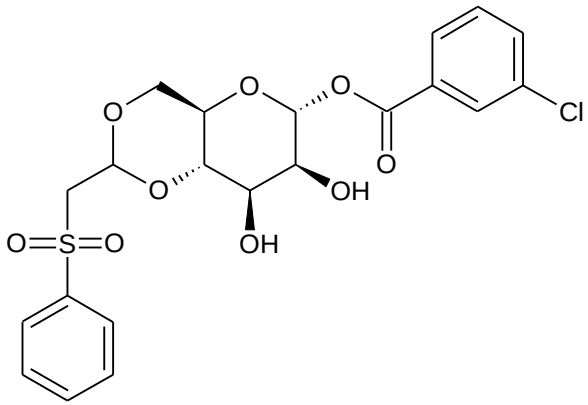

Yield 52%; white solid; R_f = 0.46 (Hex/EtOAc, 2:8); $[\alpha]_D^{25}$ = + 45 (c = 0.1, $CHCl_3$). **IR (ATR) v/cm^{-1}:** 3483, 1728, 1575, 1305, 1251, 1147, 1112, 1078, 964, 742, 686. **^{1}H NMR (400 MHz, DMSO-*d*$_6$):** δ 7.98-7.92 (m, 4H, H-*o*), 7.78-7.70 (m, 2H, H-*p*), 7.64-7.56 (m, 3H, H-*m*), 6.05 (d, 1H, *J* = 1.16 Hz, H-1), 5.60 (d, 1H, *J* = 4. 68 Hz; OH), 5.02 (t, 1H, *J* = 5.12 Hz, H-7), 4.96 (d, 1H, *J* = 6.68 Hz, OH), 3.90-3.82 (m, 3H, H-2, H-3, H-6a), 3.77 (t, 1H, *J* = 9.4 Hz, H-6b), 3.67-3.60 (m, 3H, H-4, H-8a, H-8b), 3.51 (t, 1H, *J* = 10.2 Hz, H-5). **^{13}C NMR (100 MHz, DMSO-*d*$_6$):** δ 162.7, 139.6, 133.8, 133.7, 133.6, 131.0, 130.9, 129.1, 129.0, 128.3, 128.2, 96.8, 95.2, 77.8, 69.8, 67.2, 67.1, 65.8, 59.0.

3.3.11 Synthesis of 2,3-di-*O*-acetyl-1-*O*-(*m*-chlorobenzoyl)-4,6-*O*-phenylsulfonylethylidene-α-*D*-mannopyranose (12)

In a round-bottomed flask, 0.05 g (0.103 mmol) of mannopyranoside **11** solubilized in 1 mL of acetic anhydride was added, followed by 0.1 g (200% w/w of **11**) of montmorillonite K-10. The reaction was stirred for 1 hour, after which the solvent was removed under reduced pressure and a chromatographic column (Hex/EtOAc, 7:3) was performed.

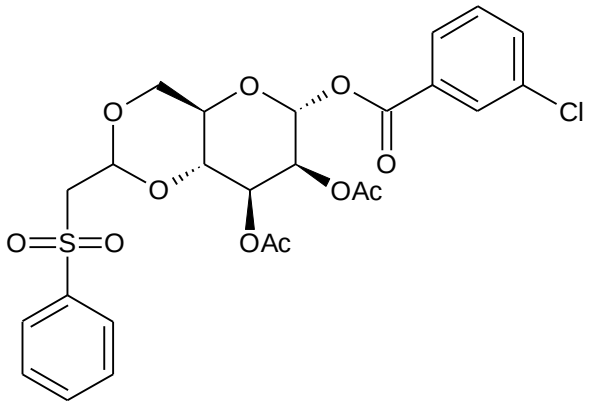

Yield 77%; colorless oil; R_f = 0.65 (Hex/AcOEt, 1:1); $[\alpha]_D^{25}$ = + 46.6 (c = 0.1, $CHCl_3$). **IR (KBr) v/cm^{-1}:** 2917, 2848, 1742, 1574, 1309, 1227, 1150, 1081, 962, 745, 686. **^{1}H NMR (500 MHz, $CDCl_3$):** δ 7.99 (s, 1H, H-*o*-Cl), 7.91 (t, 3H, *J* = 8.1 Hz, H-*o*), 7.65 (t, 1H, *J* = 4.3 Hz, H-*p*), 7.61-7.53 (m, 4H, H-*m*), 7.43 (t, 1H, *J* = 7.8 Hz, H-*p*-Cl), 6.21 (s, 1H, H-1), 5.44 (d, 1H, *J* = 1.36 Hz, H-2), 5.38 (dd, 1H, *J* = 10.4 Hz; 3.5 Hz, H-3), 5.18 (t, 1H, *J* = 5 Hz, H-7), 4.07 (dd, 1H, $J_{6a,6b}$ = 10.55 Hz; $J_{6a,5}$ = 4.9 Hz, H-6a), 3.99 (t, 1H, $J_{4,5}$ = 9.95 Hz, H-4), 3.87-3.82 (m, 1H, H-5), 3.63 (t, 1H, $J_{6b,\ 6a}$ = 10.35 Hz, H-6b), 3.49 (t, 2H, *J* = 5.35 Hz, H-8a, H-8b), 2.21 (s, 3H, CH_3C=O), 2.08 (s, 3H, CH_3C=O). **^{13}C NMR (125 MHz, $CDCl_3$):** δ 169.9, 169.5, 162.7, 139.9, 134.9, 134.1, 133.9, 130.2, 130.0, 129.9, 129.0, 128.1, 97.2, 92.1, 75.4, 68.6, 67.6, 65.7, 60.4, 59.7, 21.0, 20.8, 20.7, 14.2.

3.3.12 Synthesis of (2-oxo-1,3-dioxolan-4-yl)methyl 2,3-di-*O*-acetyl-4,6-*O*-phenylsulfonylethylidene-*β*-*D*-mannopyranoside (13)

In a round-bottomed flask, 0.1 g (0.175 mmol) of mannopyranoside **12** solubilized in 2 mL of DCM pre-dried in $CaCl_2$ was added, then 3Å molecular sieve (0.2 g) was added. The reaction mixture was cooled to 0°C, and 41.5 mg of glycerol carbonate **1** (0.35 mmol, 2 eq.), followed by 32 μL of TMSOTf (0.175 mmol, 1 eq.). The

reaction was stirred for 4 hours, after which the solvent was removed under reduced pressure. Work up: Extraction was carried out with EtOAc (3x 15 mL) and washed with a saturated NaCl solution (15 mL). The organic phase was dried with Na_2SO_4 and the solvent was removed under reduced pressure. The residue was purified on a chromatographic column (Hex/AcOEt, 3:7) to obtain the mannopyranoside **13**.

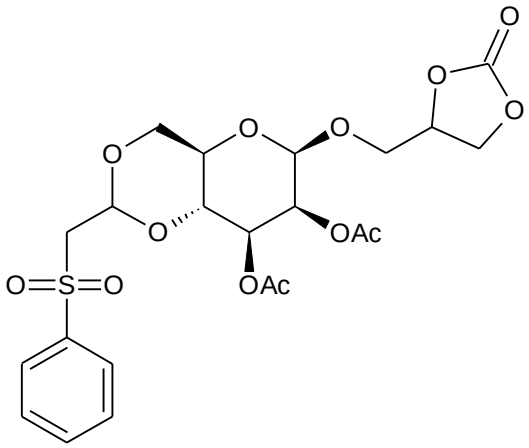

Yield 64%; colorless oil; R_f = 0.18 (Hex/AcOEt, 3:7); $[\alpha]_D^{25}$ = + 23 (c = 0.1, CH_2Cl_2). **IR (KBr) v/cm^{-1}:** 2924, 1788, 1743, 1371, 1307, 1240, 1136, 1045, 896, 752, 688. **^{1}H NMR (400 MHz, $CDCl_3$):** δ 7.91-7.89 (m, 2H, H-*o*), 7.68-7.94 (m, 1H, H-*p*), 7.55 (t, 2H, *J* = 7.92 Hz, H-*m*), 5.28 (ddd, 1H, $J_{2,1}$ = 8.04 Hz, $J_{2,3}$ = 3.52 Hz; $J_{2,4}$ = 1.6 Hz, H-2), 5.20-5.13 (m, 2H, H-3, H-7), 4.88-4.82 (m, 1H, H-4'), 4.78 (dd, 1H, $J_{1,2}$ = 7.32 Hz; $J_{1,3}$ = 1.48 Hz, H-1), 4.54 (dt, 1H, $J_{5a',5b'}$ = 8.56 Hz; $J_{5a',4'}$ = 3.4 Hz, H-5a'), 4.29 (ddd, 1H, *J* = 15.04 Hz; $J_{5b',5a'}$ = 8.68 Hz; $J_{5b',4'}$ = 6.36 Hz, H-5b'), 4.06 (dd, 1H, $J_{6a,6b}$ = 10.04 Hz; $J_{6a,5}$ = 4.4 Hz, H-6a), 3.92-3.81 (m, 2H, H-4, H-6a'), 3.71-3.67 (m, 2H, H-5, H-6b'), 3.62 (dd, 1H, $J_{6b,6a}$ = 10.16 Hz; $J_{6b,5}$ = 4.64 Hz, H-6b), 3.47 (dd, 2H, *J* = 4.88 Hz; *J* = 2.2 Hz, H8a, H8b), 2.16 (s, 3H, CH_3C=O), 2.04 (s, 3H, CH_3C=O). **^{13}C NMR (100 MHz, $CDCl_3$):** δ 169.8, 169.7 169.7, 154.2, 140.0, 133.9, 129.1, 128.1, 99.0, 99.0, 97.1, 75.8, 75.7, 74.3, 74.2, 69.4, 64.3, 68.0, 67.6, 67.5, 67.4, 67.4, 66.1, 65.8, 64.0, 63.9, 59.8, 53.4, 20.8, 20.7, 20.7.

3.3.13 Synthesis of (2-oxo-1,3-dioxolan-4-yl)methyl 2-deoxy-4,6-*O*-phenylsulfonylethylidene-α-*D*-mannopyranoside (14a/14b)

In a round-bottomed flask, 0.1 g of PSE-glucal **10** (0.32 mmol) solubilized in 4 mL of DCM pre-dried in $CaCl_2$ was added, then 3Å molecular sieve (0.2 g) was added,

followed by 0.189 g of glycerol carbonate **1** (1.60 mmol, 5 eq.). The reaction mixture was cooled to 0°C and stirred for 1 hour under an argon atmosphere. Then, 0.07 mL of TMSOTf (0.98 mmol, 1.2 eq.) was added, and the reaction mixture was gradually returned to room temperature and stirred for 30 minutes. Work up: Extraction was carried out with EtOAc (3x 15 mL) and washed with a saturated NaCl solution (15 mL). The organic phase was dried with Na_2SO_4 and the solvent was removed under reduced pressure (Fernandes *et al*., 2008). The residue was purified on a chromatographic column (DCM/Acetone, 9:1) to obtain the alpha (R/S) isomer.

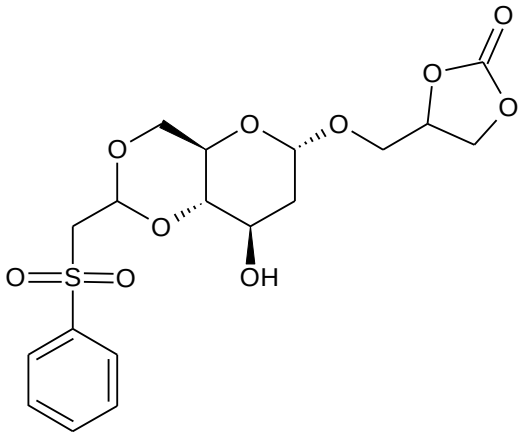

Yield 42%; colorless oil; Rf = 0.22 (DCM/Acetone, 9:1); $[\alpha]_D^{25}$ = +43 (c = 0.1, $CHCl_3$). **IR (KBr) v/cm^{-1}:** 3506, 2933, 1788, 1305, 1128, 1062, 1006, 752, 688. **^{1}H NMR (500 MHz, $CDCl_3$):** δ 7.92 (d, 2H, *J* = 7.8 Hz, H-*o*), 7.69-7.66 (m, 1H, H-*p*), 7.58 (t, 2H, *J* = 7.5 Hz, H-*m*), 5.05 (t, 1H, *J* = 4.4 Hz, H-7), 4.88 (d, 1H, *J* = 3.5 Hz, H-1), 4.85-4.80 (m, 1H, H-4'), 4.50 (t, 1H, *J* = 8.4 Hz, H-5a'), 4.33-4.29 (m, 1H, H-5b'), 4.01 (d, 1H, J = 5.5 Hz, H-6a), 3.88 (dd, 1H, $J_{6b,6a}$ = 14.65 Hz; $J_{6b,5}$ = 3.05 Hz, H-6b), 3.92-3.81 (m, 1H, H-3), 3.67 (ddd, 1H, *J* = 15.1 Hz, $J_{6a',6b'}$ = 11.6 Hz; $J_{6a',4'}$ = 3.35 Hz, H-6a'), 3.57-3.45 (m, 4H, H-5, H-8a, H-8b, H-6b'), 3.19 (dd, 1H, *J* = 18.65 Hz; *J* = 9.35 Hz, H-4), 2.24 (s, 1H, OH), 2.18-2.14 (m, 1H, H-2a), 1.72-1.66 (m, 1H, H-2b). **^{13}C NMR (125 MHz, $CDCl_3$):** δ 154.7, 154.7, 139.7, 139.6, 134.0, 133.9, 129.1, 129.1, 128.2, 98.6, 98.2, 96.9, 96.8, 83.1, 83.0, 74.5, 74.5, 68.4, 68.3, 66.8, 66.4, 66.0, 65.9, 65.1, 65.0, 62.7, 62.5, 59.7,36.8, 29.2.

3.3.14 Synthesis of the thioderivatives oxazolidinethione and thiazolidinethione

In a round-bottomed flask, 0.115 g of azido-alcohol **7a** (0.35 mmol) was added, followed by 4 mL of a CS_2/Toluene (1:1) mixture (33.08 mmol, 94 eq.), and lastly 0.110 g of PPh_3 (0.42 mmol, 1.2 eq.). The mixture was refluxed at 110°C for 6 hours (Mishra; Agrahari; Tiwari, 2017). After this, the solvent was removed under reduced pressure and the residue was purified on a chromatographic column (Hex/EtOAc, 7:3, 6:4, 1:1, 4:6) to obtain the compounds **16a** and **16b** as greenish oils.

(2-sulfanylidene-1,3-oxazolidin-5-yl)methyl 4,6-di-O-acetyl-2,3-dideoxy-α-D-erythro-hex-2-enopyranoside (**16a**)

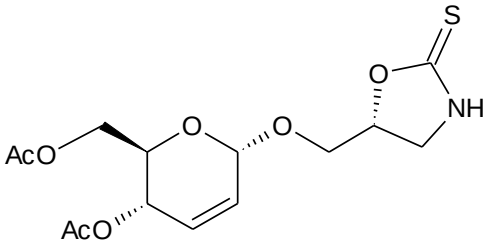

Yield 22%; greenish oil; R_f = 0.43 (EtOAc/Hex, 6:4); $[\alpha]_D^{25}$ = + 74.2 (c = 0.1, $CHCl_3$). **IR (ATR) v/cm^{-1}:** 3275, 2918, 2848, 1734, 1537, 1481, 1369, 1224, 1037, 910. **^{1}H NMR (500 MHz, $CDCl_3$):** δ 7.88 (br s, 1H, NH), 5.93 (d, 1H, $J_{3,2}$ = 10.2 Hz, H-3), 5.82 (d, 1H, $J_{2,3}$ = 10.25 Hz, H-2), 5.29 (d, 1H, $J_{4,5}$ = 10.85 Hz, H-4), 5.07 (s, 1H, H-1), 4.51-4.45 (m, 1H, H-4'), 4.22 (d, 2H, J = 2.9 Hz, H-6a, H-6b), 4.08-4.06 (m, 1H, H-5), 3.90 (t, 1H, $J_{7a,7b}$ = 9.8 Hz, H-7a), 3.70 (dd, 1H, $J_{7b,7a}$ = 10 Hz; $J_{7b,4'}$ = 4.55 Hz, H-7b), 3.64 (dd, 1H, $J_{5a',5b'}$ = 11 Hz; $J_{5a',4'}$ = 8.55 Hz, H-5a'), 3.31 (dd, 1H, $J_{5b',5a'}$ = 11.3 Hz; $J_{5b',4'}$ = 6.55 Hz, H-5b'), 2.12 (s, 3H, CH_3C=O), 2.10 (s, 3H, CH_3C=O). **^{13}C NMR (125 MHz, $CDCl_3$):** δ 201.2, 170.8, 170.3, 130.0, 126.7, 94.9, 69.2, 67.6, 65.1, 63.0, 35.1, 21.0, 20.9.

(2-sulfanylidene-1,3-thiazolidin-5-yl)methyl 4,6-di-O-acetyl-2,3-dideoxy-α-D-erythro-hex-2-enopyranoside (**16b**)

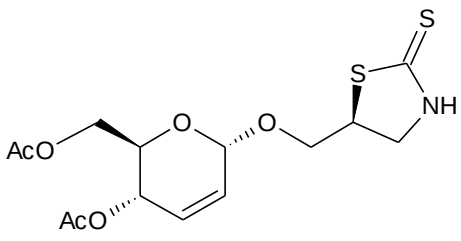

Yield 39%; greenish oil; R_f = 0.33 (AcOEt/Hex, 6:4); $[\alpha]_D^{25}$ = + 89.1 (c = 0.1, $CHCl_3$). **IR (ATR) v/cm^{-1}:** 3277, 2924, 1734, 1500, 1456, 1369, 1222, 1028, 966. **^{1}H NMR (500 MHz, $CDCl_3$):** δ 7.98 (br s, 1H, NH), 5.91 (d, 1H, $J_{3,2}$ = 9.95 Hz, H-3), 5.81 (d, 1H, $J_{2,3}$ = 9.45 Hz, H-2), 5.28 (d, 1H, $J_{4,5}$ = 9 Hz, H-4), 5.06 (s, 1H, H-1), 4.19 (ap. s, 3H, H-4', H-6a, H-6b), 4.05 (d, 2H, *J* = 9.8 Hz, H-5, H-5a'), 3.93-3.87 (m, 2H, H-5b', H-7a), 3.75 (t, 1H, *J* = 8.85 Hz, H-7b), 2.10, 2.09 (s, 6H, 2x CH_3C=O). **^{13}C NMR (125 MHz, $CDCl_3$):** δ 200.7, 170.9, 170.4, 130.0, 127.1, 95.2, 69.8, 67.5, 65.3, 63.2, 53.3, 49.0, 21.2, 21.1.

(2-hydroxy-3-isothiocyanate)methyl 4,6-di-O-acetyl-2,3-dideoxy-α-D-erythro-hex-2-enopyranoside (**16c**)

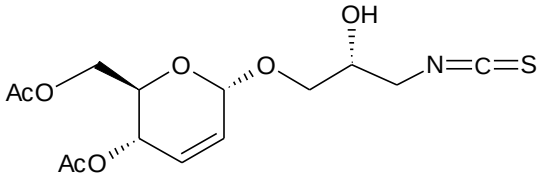

Yield 25%; white solid; R_f = 0.16 (AcOEt/Hex, 6:4); Mp = 112-114°C; $[\alpha]_D^{25}$ = + 47.85 (c = 0.1, $CHCl_3$). **IR (ATR) v/cm^{-1}**: 3433, 2927, 2362, 1737, 1519, 1373, 1311, 1219, 1035, 1014, 977. **^{1}H NMR (500 MHz, $CDCl_3$):** δ 9.90 (s, 1H, SH), 5.92-5.86 (m, 2H, H-2, H-3), 5.20 (d, 1H, $J_{4,5}$ = 9.75 Hz, H-4), 5.13 (s, 1H, H-1), 5.09-5.04 (m, 1H,H-4'), 4.17-4.10 (m, 2H, H-6a, H-6b), 4.00-3.97 (m, 1H, H-5), 3.85 (dd, 1H, $J_{5a',5b'}$ = 11.45 Hz, $J_{5a',4}$ = 3.2 Hz, H-5a'), 3.74 (t, 1H, $J_{7a,7b}$ = 9.95 Hz, H-7a), 3.70 (dd, 1H, $J_{5b',5a'}$ = 11.6 Hz; $J_{5b',4'}$ = 5.55 Hz, H-5b'), 3.42 (dd, 1H, $J_{7b,7a}$ = 9.8 Hz; $J_{7b,4'}$ = 7.65 Hz, H-7b), 2.05 (s, 3H, CH_3C=O), 2.03 (s, 3H, CH_3C=O). **^{13}C NMR (125 MHz, $CDCl_3$):** δ 187.9, 170.1, 169.9, 129.0, 127.8, 93.9, 80.5, 66.3, 66.5, 64.6, 62.5, 45.3, 20.7, 20.5.

3.3.15 Synthesis of (2-sulfanyl-1,3-oxazol-5-yl) methyl 4,6-di-*O*-acetyl-2,3-dideoxy-α-*D*-erythro-hex-2-enopyranoside (17)

In a round-bottomed flask, 0.1g of keto-azide **8** (0.31 mmol) solubilized in 1.5 mL of 1,4-dioxane was added, followed by 0.122 g of PPh_3 (0.47 mmol, 1.5 eq.) and 0056 mL of CS_2 (0.93 mmol, 3 eq.). The mixture was stirred for 30 minutes at room temperature and then refluxed at 100°C for 4 hours (Oka; Yabuuchi; Sekiguchi, 2013). After this, the solvent was removed under reduced pressure and the residue was

purified on a chromatographic column (Hex/EtOAc, 4:6) to obtain the compound **17** as a yellowish oil.

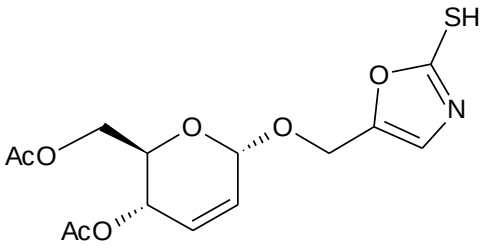

Yield 59%; yellowish oil; R_f = 0.5 (EtOAc/Hex, 7:3); $[\alpha]_D^{25}$ = + 54 (c = 0.1, $CHCl_3$). **IR (KBr) v/cm^{-1}:** 3138, 2929, 1736, 1480, 1368, 1225, 1148, 1024, 963. **^{1}H NMR (500 MHz, $CDCl_3$):** δ 11.20 (br s, 1H, SH), 6.90 (s, 1H, H-5'), 5.95 (d, 1H, $J_{3,2}$ = 10.25 Hz, H-3), 5.83 (dt, 1H, $J_{2,3}$ = 10.25; $J_{2,1}$ = 4.47 Hz; $J_{2,4}$ = 2.3 Hz, H-2), 5.34 (dd, 1H, $J_{4,5}$ = 9.65 Hz; $J_{4,2}$ = 1.1 Hz, H-4), 5.14 (s, 1H, H-1), 4.62 (d, 1H, $J_{7a,7b}$ = 13.6 Hz, H-7a), 4.50 (d, 1H, $J_{7b,7a}$ = 13.6 Hz, H-7b), 4.26 (t, 2H, J = 4.75 Hz, H-6a, H-6b), 4.14-4.10 (m, 1H, H-5), 2.13 (s, 3H, CH_3C=O), 2.11 (s, 3H, CH_3C=O). **^{13}C NMR (125 MHz, $CDCl_3$):** δ 179.4, 170.9, 170.3, 146.5, 130.0, 126.8, 114.4, 93.8, 67.3, 65.1, 62.8, 59.3, 21.0, 20.9.

3.4 BIOLOGICAL METHODS

This study was carried out by the student Luanna De Ângelis at the Instituto Aggeu Magalhães Institute (Fiocruz-PE), under the supervision of Professor PhD Lílian Pimentel.

3.4.1 Determination of cytotoxicity (CC_{50})

For the cytotoxicity test, the MTT test (3-(4,5-dimethylthiazol-2-yl)-2,5-diphenyltetrazolium bromide) was carried out in a 96-well plate according to Mosmann (1983) and modifications. The J774A.1 strains (ATCC TIB-67), corresponding to murine macrophages, were cultured in DMEM medium enriched with 10% fetal bovine serum (FBS) and 1% antibiotics (streptomycin - 100 µg/mL and penicillin - 100 µg/mL). The culture was maintained at 37ºC in an atmosphere containing 5% of CO_2 until cell confluence was reached.

The cells were recovered, resuspended in the appropriate medium and an aliquot was quantified using Trypan blue in a Neubauer chamber. The medium was then adjusted so that 1 x 10^5 cells were seeded per well and incubated for 24 hours under the same initial culture conditions to allow cell adhesion. The compounds **16a**, **16b**, and **17** were serially diluted (128 to 0.5 µg/mL) in the appropriate medium for the cell line and these solutions were transferred to the plate containing the cells and reincubated for a further 24 hours. Control wells were used with only cells and culture medium, as well as the DMSO control in medium (5%).

After 24 hours of exposure, 100 µL of MTT solution in PBS (5 mg/mL) was added. The plates were reincubated for three hours, protected from direct light, under the same environmental and temperature conditions. After this period, the medium was aspirated and 100 µL of DMSO was added to dissolve the formazan crystals resulting from the reduction of MTT in viable cells. The absorbance of each well was measured through the 540 nm filter in a plate reader.

3.4.2 Determination of *in vitro* antimycobacterial activity

Mycobacterium tuberculosis H37Ra (ATCC 25177) was used in this study as a reference strain from the American Type Culture Collection, classified as sensitive to all first-line drugs (isoniazid, rifampicin, ethambutol and pyrazinamide). The mycobacterium was grown in Middlebrook 7H9 broth supplemented with 10% OADC (oleic acid, albumin, dextrose and catalase), 0.2% glycerol and 0.05% Tween 80. The incubation time was 21 to 28 days for *Mtb*. The ATCC reference strain was obtained from the Collection of Reference Microorganisms in Health Surveillance - CMRVS, FIOCRUZ-INCQS, Rio de Janeiro, RJ.

The antimycobacterial activity of the compounds **16a**, **16b**, and **17** was determined through the Minimum Inhibitory Concentration using the colorimetric microdilution method in 96-well plates, described by Palomino *et al*. (2002).

In order to avoid evaporation of the culture medium system and diluted compounds due to the long incubation period, 200 µL of distilled water was added to the wells on the outer perimeter of the microplate. Then 100 µL of 7H9 broth supplemented with 10% OADC and 0.2% glycerol was poured into the remaining wells.

Serial dilutions of 1:2 of the compounds were made directly on the microplate, with concentrations ranging from 128 µg/mL to 0.5 µg/mL. Rifampicin was used as a positive control for antimycobacterial activity, with concentrations ranging from 16 to 0.5 µg/mL. Positive control wells for growth of the inoculum and sterility control of the culture medium were included in all the plates.

The *Mtb* H37Ra culture, in logarithmic growth phase, was transferred to a conical tube containing glass beads and PBS with 0.05% Tween 80 and shaken in a vortex for two minutes. It was then placed in a vertical resting position for fifteen minutes to allow lumps to settle and reduce aerosolization. The supernatant was aspirated into another tube and standardized using Mc Farland scale n° 01. Subsequently, a 1:20 (v/v) dilution was made and 100 µL of this suspension (~ 1.5 x 10^7 CFU/mL) added to the appropriate wells. The plates were wrapped in plastic wrap and incubated at 37ºC in a normal atmosphere for 7 days.

After the incubation period, 30 µL of a sterile solution of resazurin (Sigma Aldrich) at 0.01% was added to all wells and reincubated overnight, under the same temperature and atmosphere conditions. The MIC was defined as the lowest concentration of the drug that prevented the color from changing from blue (oxidized state) to pink (reduced state).

4 RESULTS AND DISCUSSION

This part was divided into six sections: the first one describes the reactions of the glycerol derivatives; the second shows the synthesis of the *O*-glycosides from tri-*O*-acetyl-*D*-glucal; the third section is related to *O*-glycosylation reactions on PSE-glucal; the fourth section describes the *S*-glycosylation reactions; the fifty section is on the preparation of the oxazolidinethione, thiazolidinethione, and oxazole derivatives; and finally, the last one about the discussion of biological studies. We also provide a detailed description of the ^{1}H and ^{13}C NMR spectra that confirm the structures of the synthesized compounds.

4.1 SYNTHESIS OF GLYCEROL DERIVATIVES

To obtain glycerol carbonate (GC) **1**, the transesterification protocol developed by Rokicki *et al*. (2005) was applied onto glycerol with an excess (3 eq.) of dimethyl carbonate (DMC) and K_2CO_3 as a catalyst (Scheme 20). The reaction remained at reflux for 5 hours and using a Dean Stark glassware to collect the methanol formed as a by-product. glycerol carbonate was obtained in 96% yield.

Scheme 20 - Synthesis of glycerol carbonate (GC) **1**.

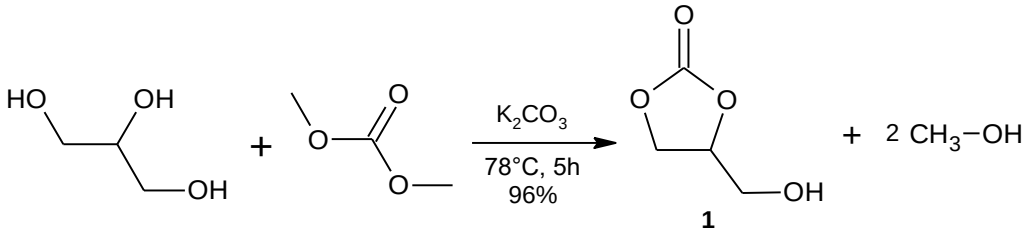

Source: The author (2024).

According to Gade, Saptal, and Bhanage (2022), the hydroxyl from glycerol carbonate can be activated by tosylation, to improving its selectivity and reactivity. The tosylation reaction was carried out under basic conditions (Scheme 21) following the methodology described by Simão *et al*. (2006). Tosyl chloride, triethylamine, and dichloromethane were reacted with CG **1**, and after 16 hours furnished glycerol carbonate tosylated (GCT) **2** with 65% of yield. CG **1** and GCT **2** were characterized using infrared spectroscopy.

Scheme 21 - Synthesis of glycerol carbonate tosylated (GCT) **2**.

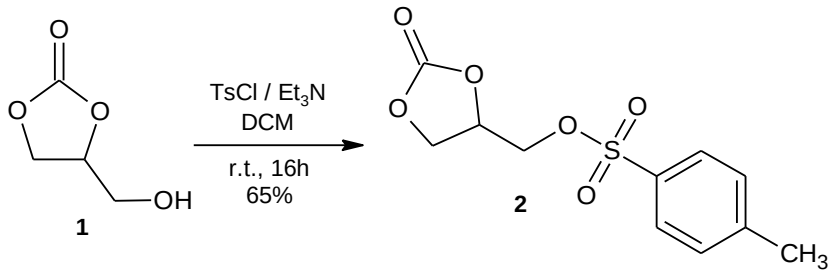

Source: The author (2024).

With the formation of the tosyl group, the primary carbon of the GCT behaves like an electrophilic center, enabling reactions with various nucleophiles. Then, following the protocol described by Rousseau *et al*. (2009), we carried out the reaction of GCT **2** with sodium iodide at reflux for 4 hours (Scheme 22). Initially using 2 equivalents of NaI, however, no total consumption of GCT **2** was observed, and afforded glycerol carbonate iodide (GCI) **3** in moderate yield of 52%. With this result, we decided to double the amount of sodium iodide (4 equiv.), and after 4 hours of reaction compound **3** was obtained in 80% of yield.

Scheme 22 - Synthesis of glycerol carbonate iodide (GCI) **3**.

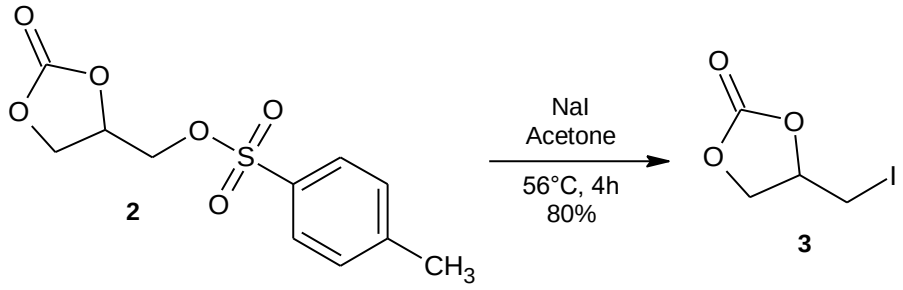

Source: The author (2024).

Figure 12 shows the ^{1}H NMR spectrum of GCI **3**. Between δ 4.85 and δ 4.78 ppm, was found a multiplet referring to hydrogen 5. At δ 4.60 ppm was noticed an apparent triplet referring to the diastereotopic hydrogen H-4a, in fact this signal was a double duplet that didn't unfold, and have equal coupling constant $J_{4a,4b} = J_{4a,5} = 8.8$ Hz. At δ 4.23 ppm was observed the diastereotopic hydrogen H-4b with geminal coupling constants $J_{4b,4a} = 8.8$ Hz and vicinal $J_{4b,5} = 6$ Hz. At δ 3.43 ppm was noticed the diastereotopic hydrogen H-6a with geminal coupling constants $J_{6a,6b} = 10.8$ Hz and vicinal $J_{6a,5} = 4.4$ Hz. At δ 3.33 ppm a double duplet related to the diastereotopic

hydrogen H-6b with geminal and vicinal coupling constants, $J_{6b,6a}$ = 10.8 Hz and $J_{6b,5}$ = 8.4 Hz.

Figure 12 - ^{1}H NMR spectrum and expansions (400 MHz, $CDCl_3$) of GCI **3**.

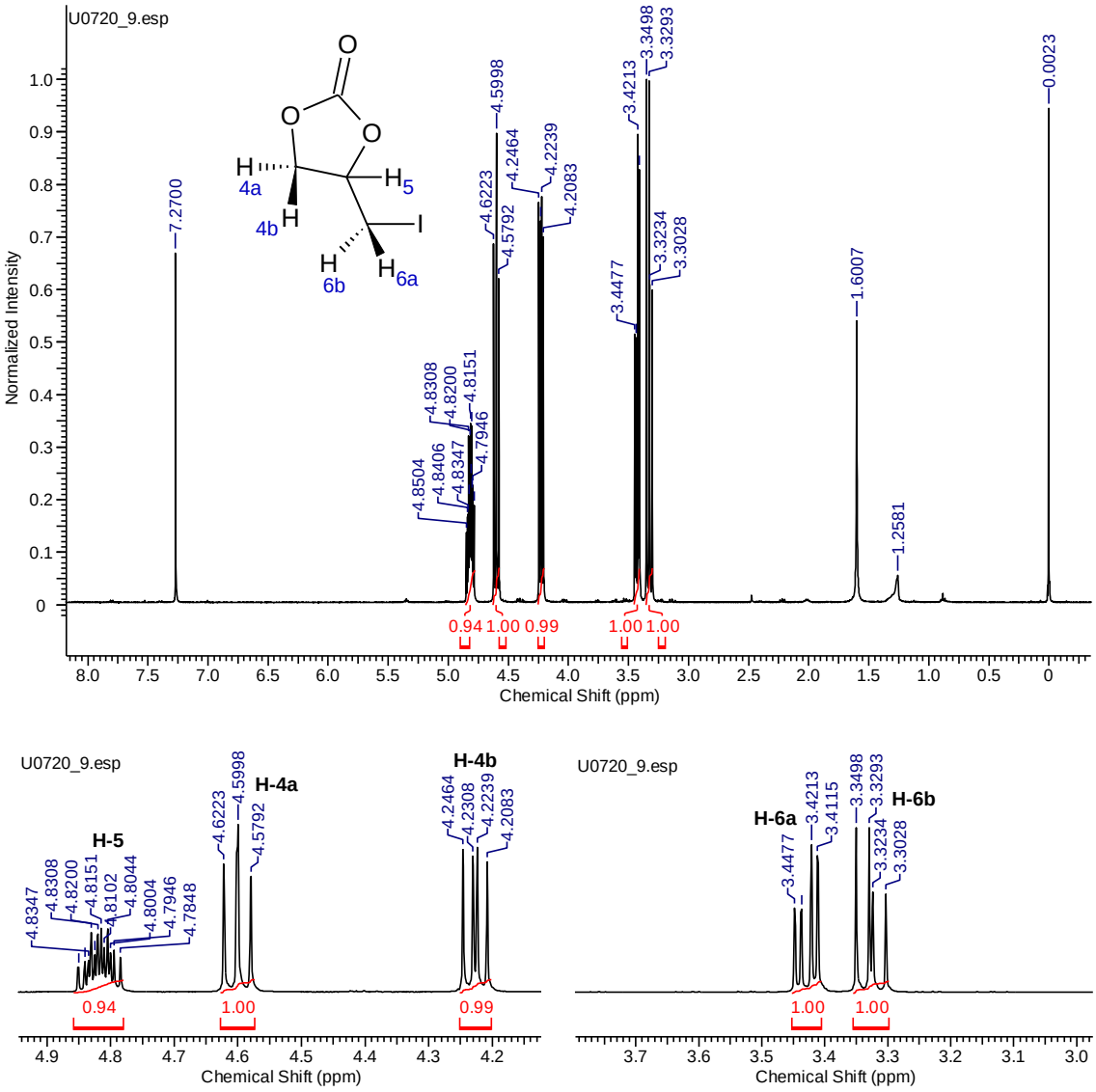

Source: The author (2024).

The ^{13}C NMR spectrum at 100 MHz of GCI **3** is shown in figure 13. At δ 154.1 ppm was noticed the signal for the carbonyl, and at δ 74.7 and δ 69.8 ppm were observed the signals for C-4 and C-5 respectively. Finally, we found the C-6 signal at δ 3.6 ppm, because of the direct effect of iodine in ^{13}C with a very strong shielding.

Figure 13 - ^{13}C NMR spectrum (100 MHz, $CDCl_3$) of GCI **3**.

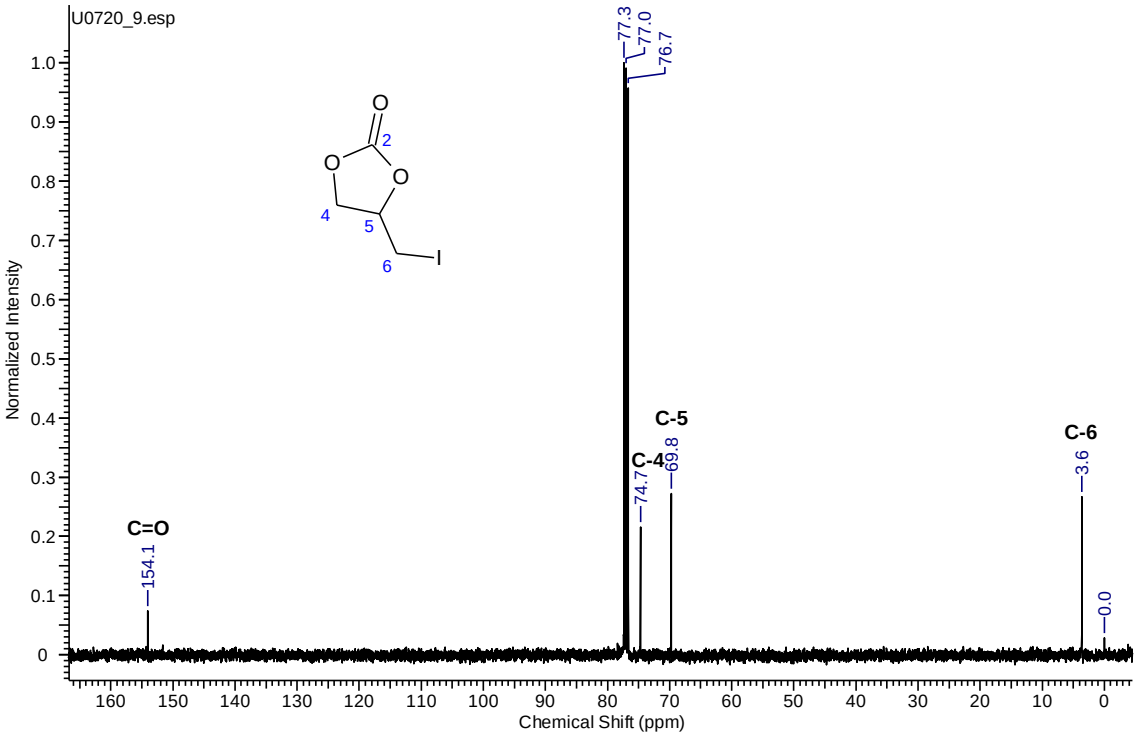

Source: The author (2024).

In the next step, GCI **3** was used to prepare glycerol thio-carbonate **4**, which will be used later in *S*-glycosylation reactions in this work. Rousseau *et al*. (2009) showed in their work that GCT **2** does not react directly with thiourea, and because of this, compound **3** was first prepared as a precursor in the synthesis of thio-GC **4**. In this way, GCI **3** reacted with thiourea to form the isothiouronium salt (Scheme 23), and then hydrolysis was carried out under reductive conditions on the crude salt, which gave thio-GC **4** in 85% yield.

Scheme 23 - Synthesis of glycerol thio-carbonate (thio-GC) **4**.

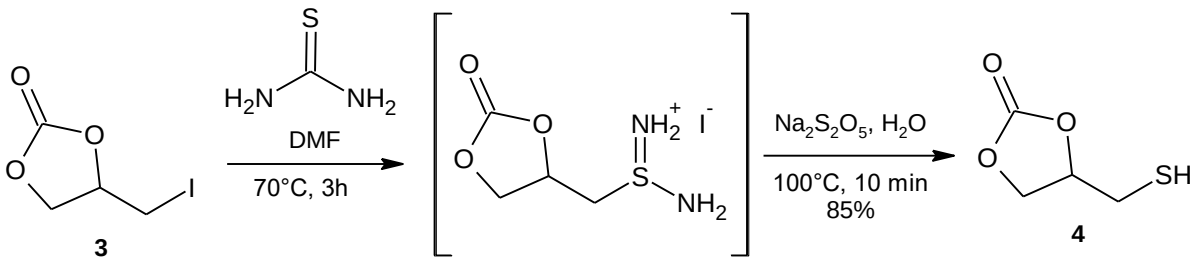

Source: The author (2024).

Rousseau *et al*. (2009) noted that thio-GC **4** can undergo spontaneous and rapid oxidation to dimeric disulfide, so we attempted to carry out NMR analysis of thio-

GC **4** shortly after its synthesis. In the ^{1}H NMR spectrum at 400 MHz of thio-GC **4**, it was possible to observe the presence of peaks of solvent DMF (δ 8.01, 2.96, and 2.88 ppm) (Figure 14).

Figure 14 - ^{1}H NMR spectrum and expansions (400 MHz, $CDCl_3$) of thio-GC **4**.

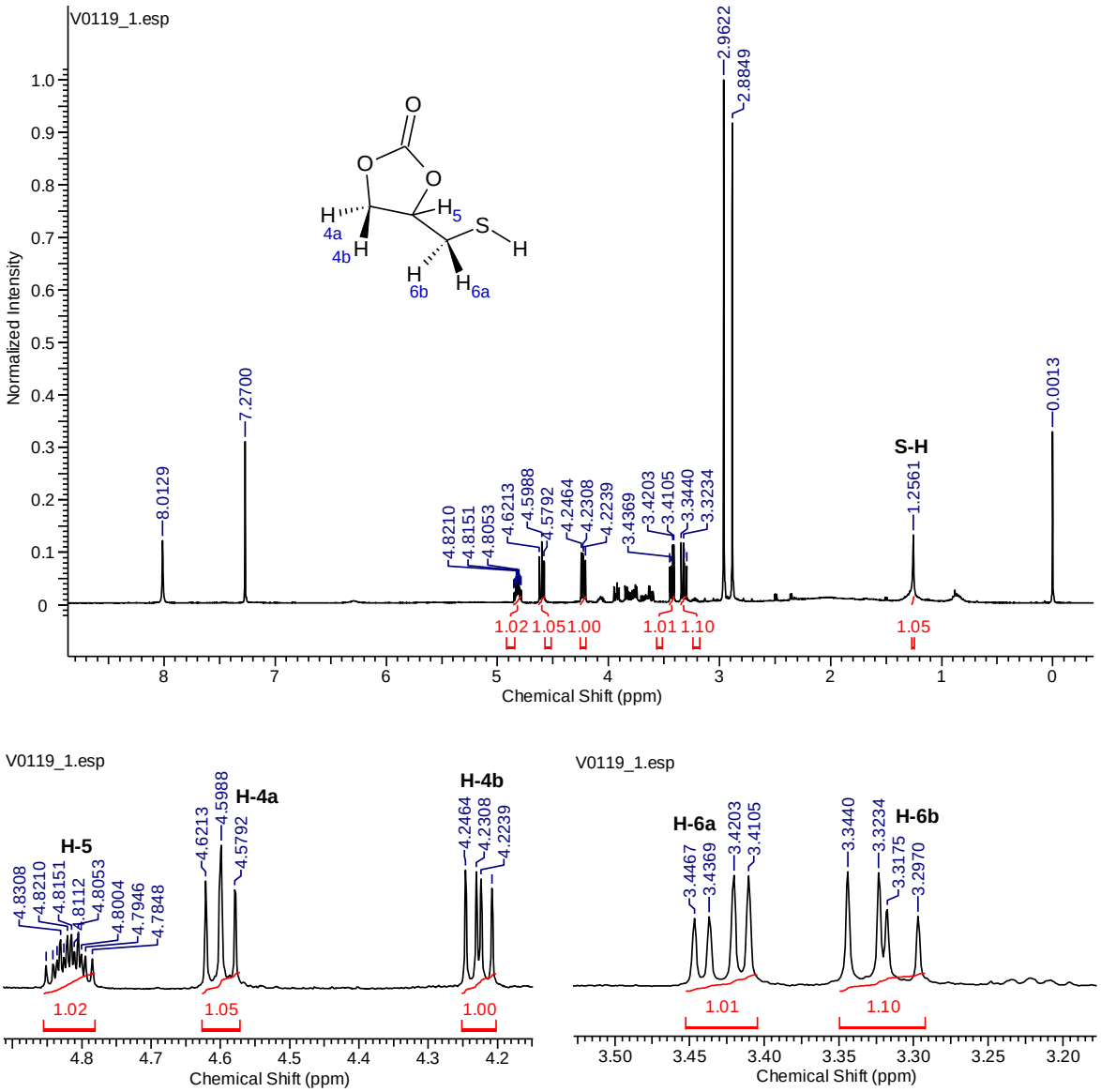

Source: The author (2024).

Despite that, it is possible to observe signals that confirm the structure of thio-GC **4**, which is very similar to the spectrum of GCI **3**. Between δ 4.85 and δ 4.78 ppm was found a multiplet referring to H-5. At δ 4.60 ppm was observed an apparent triplet, which is a double duplet that didn't unfold, referring to the diastereotopic hydrogen H-4a with constants $J_{4a,4b}$ = $J_{4a,5}$ = 9.0 Hz. At δ 4.23 ppm was found the diastereotopic hydrogen H-4b with geminal and vicinal coupling constants, $J_{4b,4a}$ = 9.0 Hz and $J_{4b,5}$ =

6.2 Hz. At δ 3.43 ppm was observed the other diastereotopic hydrogen H-6a with geminal and vicinal coupling constants, $J_{6a,6b}$ = 10.6 Hz and $J_{6a,5}$ = 3.9 Hz. At δ 3.32 ppm a double duplet referring to the diastereotopic hydrogen H-6b with geminal and vicinal coupling constants, $J_{6b,6a}$ = 10.6 Hz and $J_{6b,5}$ = 8.2 Hz was observed. Finally, at δ 1.26 ppm was found a singlet, which can refer to SH, although the authors (Rousseau *et al*., 2009) observed a triplet to this hydrogen.

4.2 SYNTHESIS OF *O*-GLYCOSIDES FROM TRI-*O*-ACETYL-*D*-GLUCAL

The Ferrier reaction between glycerol carbonate **1** and tri-*O*-acetyl-*D*-glucal **5**, using $BF_3.Et_2O$ or Montmorillonite K-10 doped with iron (III) chloride as catalysts provides the mixture of diastereoisomers **6a** and **6b** (Scheme 24), with yields of 81% and 94% respectively (Da Costa *et al*., 2016). According to the authors, spontaneous crystallization of the diastereoisomeric mixture in ethyl acetate/hexane provides the pure diastereoisomer **6a** with yields of 28% ($BF_3.Et_2O$) and 31% (K-10/$FeCl_3$). The X-ray crystallographic study confirmed that glycoside **6a** has an *S* configuration and *α* orientation.

Scheme 24 - Synthesis of azido-alcohol **7a**.

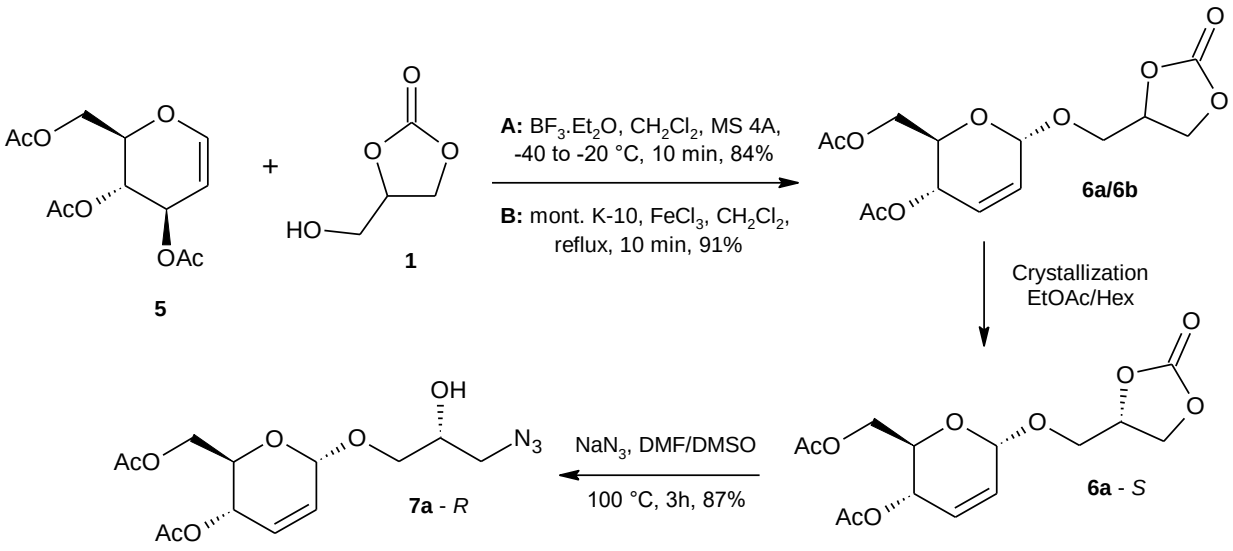

Source: The author (2024).

According to the literature (Rousseau *et al*., 2009; Simão *et al*., 2006; Vilkauskaité *et al*., 2013), the reactivity of the glycerol carbonate ring can be explored in the presence of different nucleophiles. In this perspective, Da Costa *et al*. (2016)

explored various conditions for opening the carbonate ring with sodium azide and concluded that the use of the DMF/DMSO solvent mixture (1:1) for 3h at 100°C was most successful in the synthesis of azido-alcohol **7a** (Scheme 24) with a yield of 87%, since DMSO helps in the solvation and stabilization of the carbonate ion during the decarboxylation process. The azido-alcohol **7a** was provided by our research group for use in this work.

After the spontaneous crystallization of diastereoisomer **6a**, the resulting mixture, which contains more of the diastereoisomer *R* (**6b**) and only traces of the diastereoisomer *S* (**6a**), was used in the next step. The mixture **6a**/**6b** was also made available by our research group. Then, the mixture (**6b** >>> **6a**) with sodium azide were used in the reaction (Scheme 25) following the same parameters used with the pure diastereoisomer **6a** described by Da Costa *et al*. (2016). However, when performing the reaction with 2.3 g of the mixture, we observed that the starting material was not consumed after 3 hours of reaction. The mixture of azido-alcohols **7a**/**7b** was obtained with a yield of 52% after 5h, and was then used in the oxidation process using Dess-Martin Periodinane (DMP). The oxidation reaction followed the conditions described in the work by Oliveira (2020, Thesis), and keto-azide **8** was obtained in 88% yield.

Scheme 25 - Synthesis of keto-azide **8**.

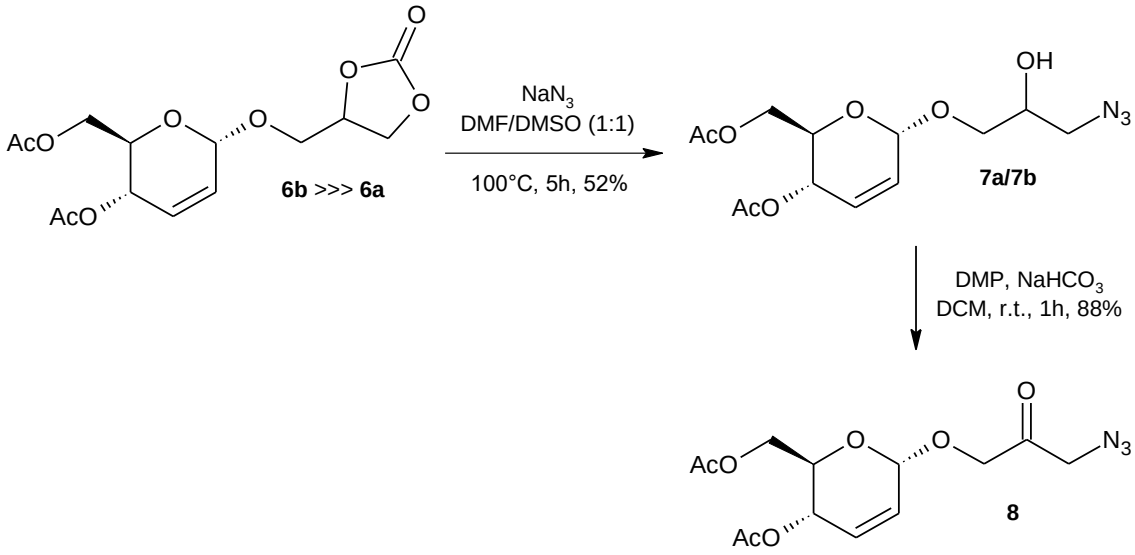

Source: The author (2024).

Figure 15 - ^{1}H NMR spectrum and expansion (500 MHz, $CDCl_3$) of keto-azide **8**.

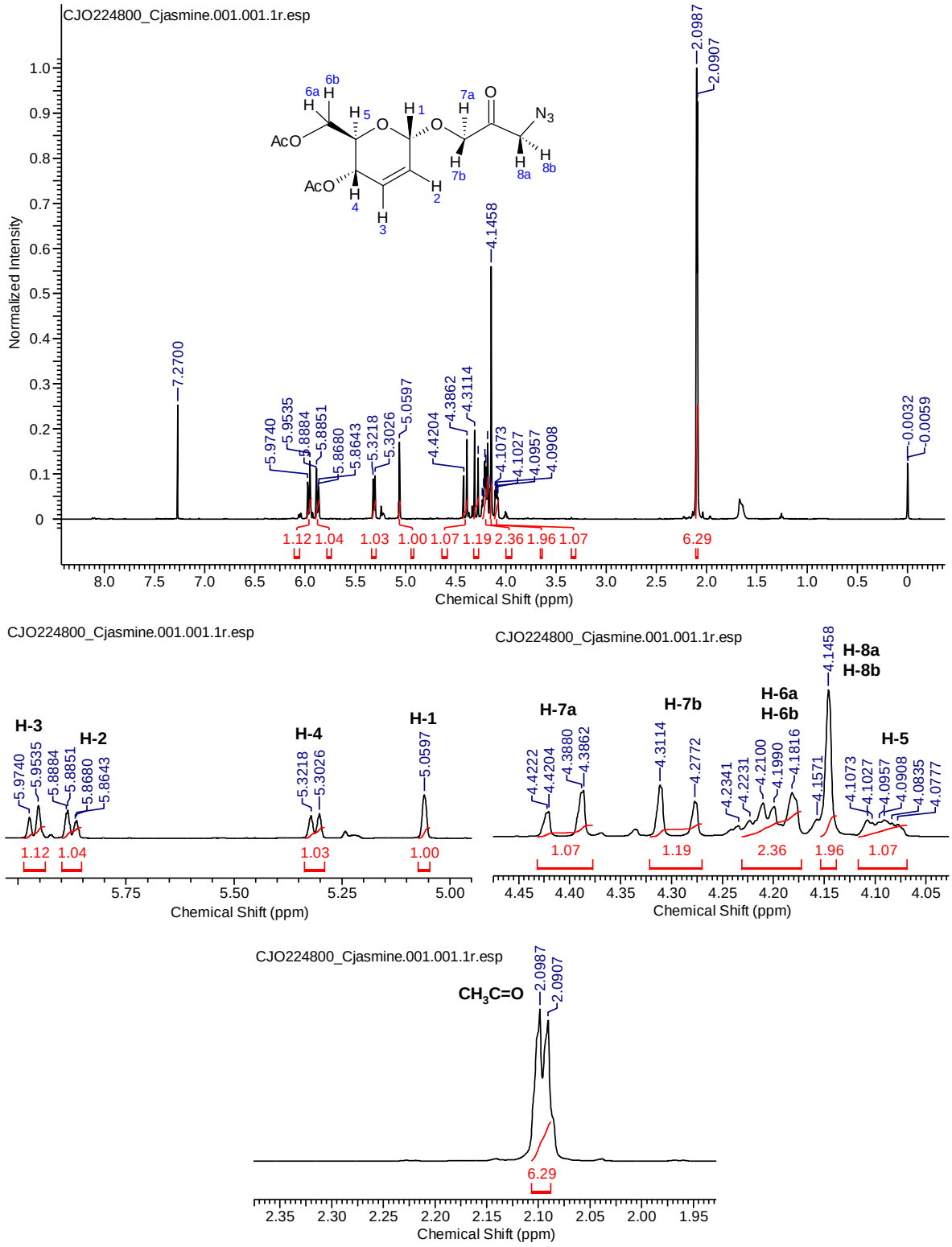

Source: The author (2024).

Figure 15 shows the ^{1}H NMR spectrum of keto-azide **8**. At δ 5.96 ppm was found a duplet referring to H-3 with $J_{3,2}$ = 10.25 Hz, while at δ 5.87 ppm another duplet for H-2 with $J_{2\text{-}3}$ = 10.2 Hz. A duplet was observed at δ 5.31 ppm referring to H-4 with $J_{4,5}$ =

9.6 Hz and a simplet at δ 5.06 ppm referring to H-1. At δ 4.40 ppm was noticed a doble duplet with $J_{7a,7b}$ = 17.1 Hz and *J* = 0.9 Hz from H-7a, while at δ 4.50 ppm a duplet with $J_{7b,7a}$ = 17.1 Hz referring to H-7b. Ranged from δ 4.23-4.18 ppm was observed a multiplet referring to H-6a and H-6b, while at δ 4.15 ppm was noticed a simplet referring to H-8a and H-8b. Finally, between δ 4.11-4.08 ppm was found a multiplet referring to H-5, and the two methyls from the acetyl groups at δ 2.10 and δ 2.09 ppm.

4.3 SYNTHESIS OF *O*-GLYCOSIDES FROM PSE-GLUCAL

Initially, we reacted the (*Z*)- and (*E*)-1,2-dichloroethylene mixture with thiophenol under basic conditions at 90°C for 17h to obtain (*Z*)-1,2-bis(thiophenyl)ethylene (Scheme 26), following the method described by Parham and Heberling (1954). According to De Lucchi *et al*. (2005), the E isomer is not reactive under these conditions, so only (*Z*)-1,2-bis(thiophenyl)ethylene was obtained. Without purification, the crude material obtained was submitted to the oxidation reaction described by Truce and Mcmanimie (1954). In this second stage, we used hydrogen peroxide as the oxidizing agent to obtain (*Z*)-1,2-bis(phenylsulfonyl)ethylene (BPSE) **9**. The reaction was stirred for 7 days and monitored using a CDD plate until complete consumption of the (*Z*)-1,2-bis(thiophenyl)ethylene. BPSE **9** was obtained with an overall yield of 56% from 1,2-dichloroethylene mixture.

Scheme 26 - Synthesis of (*Z*)-1,2-bis(phenylsulfonyl)ethylene (BPSE) **9**.

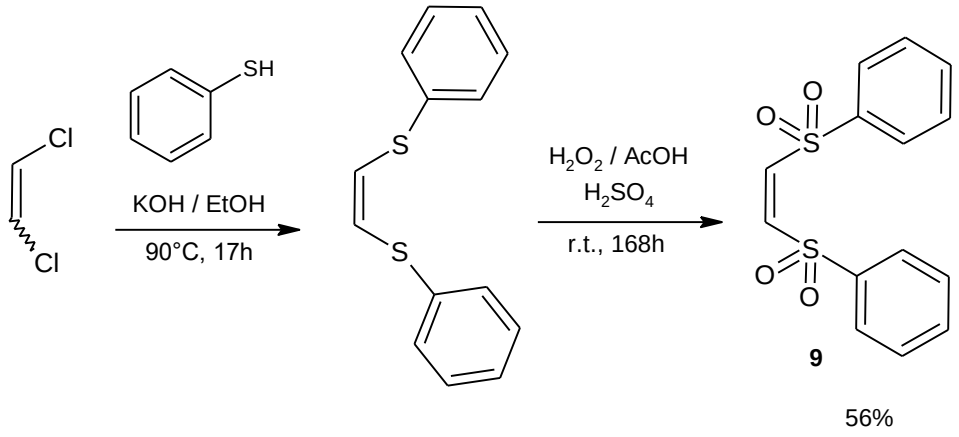

Source: The author (2024).

Figure 16 shows the ^{1}H NMR spectrum of BPSE **9**. We observe a duplet at δ 8.07 ppm referring to the *ortho* hydrogens (H-2, H-6, H-16, and H-20) with a coupling constant of 7.8 Hz. At δ 7.71 ppm was observed another triplet referring to the *para* hydrogens (H-4 and H-18) with a coupling constant of 7.44 Hz. At δ 7.60 ppm a triplet referring to the *meta* hydrogens (H-3, H-5, H-17, and H-19) with a coupling constant of 7.8 Hz was observed. Finally, as the molecule has a symmetrical plane, H-10 and H-11 of the cis double bond appeared as a single singlet at δ 6.83 ppm.

Figure 16 - ^{1}H NMR spectrum and expansion (400 MHz, $CDCl_3$) of BPSE **9**.

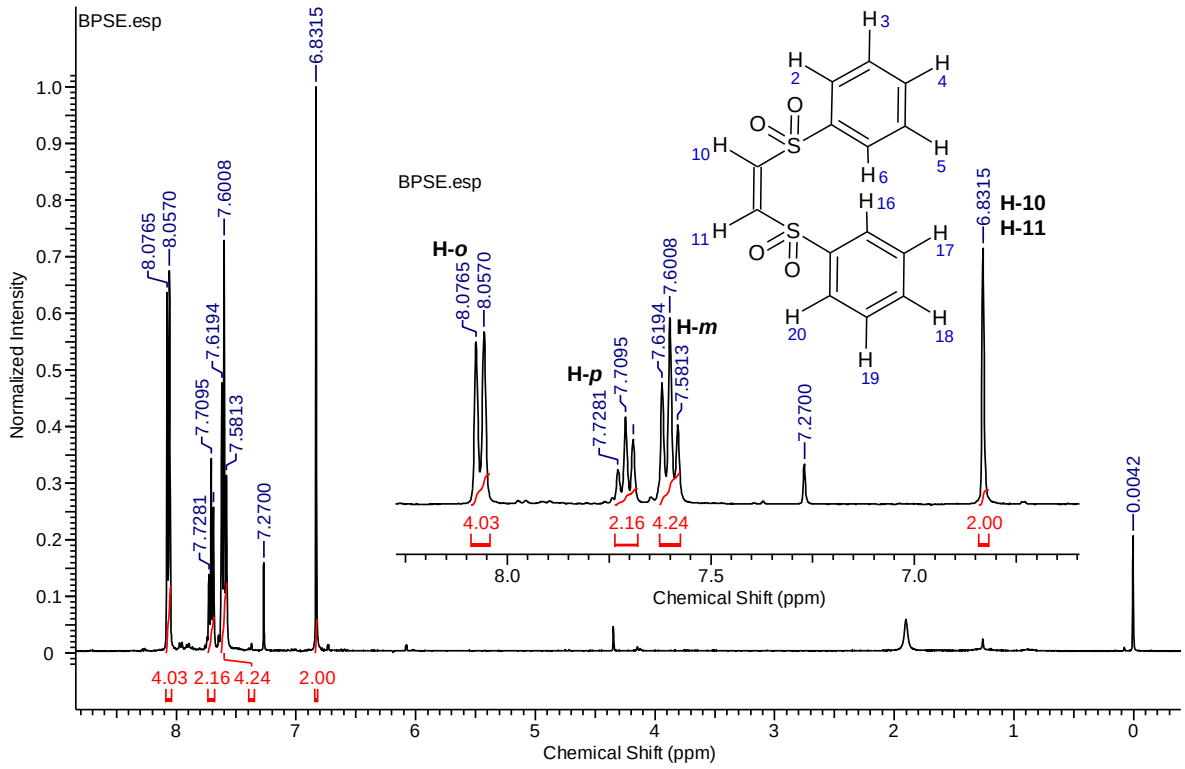

Source: The author (2024).

Next, the protection 4,6-position of *D*-glucal with BPSE **9** was realized to obtain phenylsulfonylethylidene (PSE)-glucal **10** (Scheme 27). In the first step, we carried out the transesterification reaction of tri-*O*-acetyl-*D*-glucal **5** with MeOH/NaOMe base generated *in situ* by using metallic sodium in HPLC-grade methanol. The reaction was stirred for 30 minutes, after that the cationic resin amberlite IR 120 was added to neutralized the solution.

Scheme 27 - Synthesis of PSE-glucal **10**.

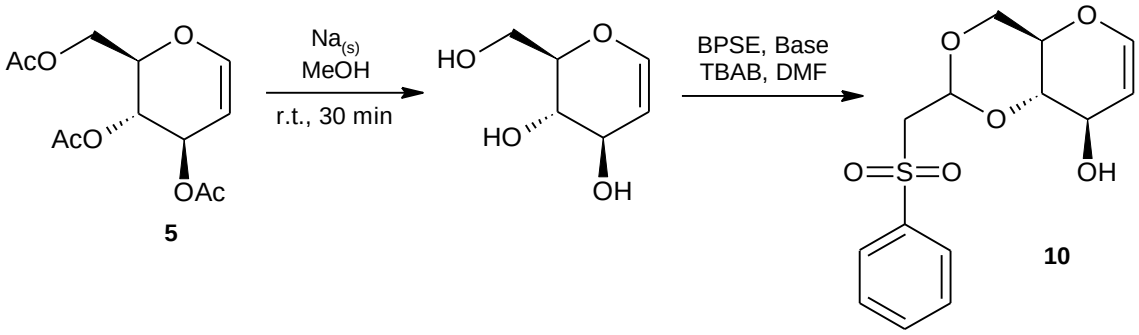

Source: The author (2024).

Chéry *et al*. (2001) described the reaction to protect *D*-glucal (a polyol) using 2 equivalents of the *t*-BuOK base and 1 equivalent of BPSE with a reaction time of 12 hours and with 70% of yield. However, when we reproduced this methodology (entry 1, Table 1), the yield obtained was much lower than expected (24%), then was made some modifications in the methodology (Table 1). In the second entry, the reaction was stirred for 68 hours and we obtained a yield of 34%, which was still not satisfactory. We decided to test another base (NaH) used by the authors for diols. However, even after 65 hours of reaction, the yield obtained was 31%. Then, we opted to increase the equivalence of the *t*-BuOK base to 2.5 and BPSE to 1.2 (in entry 4). The reaction remained stirring for 17 hours, but the yield obtained was only 32%. Finally, we increased the quantify of *t*-BuOK base to 3 equivalents and BPSE to 2 equivalents and after 48 hours the yield obtained was 77% (entry 5).

Table 1 - Optimizations carried out in the synthesis of PSE-glucal **10**.

Entry	Base	Eq. Base	Eq. BPSE	Time	Yield
1	*t*-BuOK	2	1	12h	24%
2	*t*-BuOK	2	1	68h	34%
3	NaH	2	1	65h	31%
4	*t*-BuOK	2.5	1.2	17h	32%
5	*t*-BuOK	3	2	48h	77%

Source: The author (2024).

Figure 17 shows the ^{1}H NMR spectrum of PSE-glucal **10**. Ranged from δ 7.95-7.93 ppm was found a multiplet referring to the two aromatic *ortho* H, while between δ 7.70-7.66 ppm, was observed another multiplet referring to the aromatic *para* H, and

at δ 7.61-7.57 ppm we noticed a multiplet referring to the two aromatic *meta* H. We found a double duplet referring to H-1 at δ 6.25 ppm with $J_{1,2}$ = 6.28 Hz, and $J_{1,3}$ = 1.96 Hz. At δ 5.09 ppm corresponding to the triplet of H-7 with J = 5.08 Hz.

Figure 17 - ^{1}H NMR spectrum and expansions (400 MHz, $CDCl_3$) of PSE-glucal **10**.

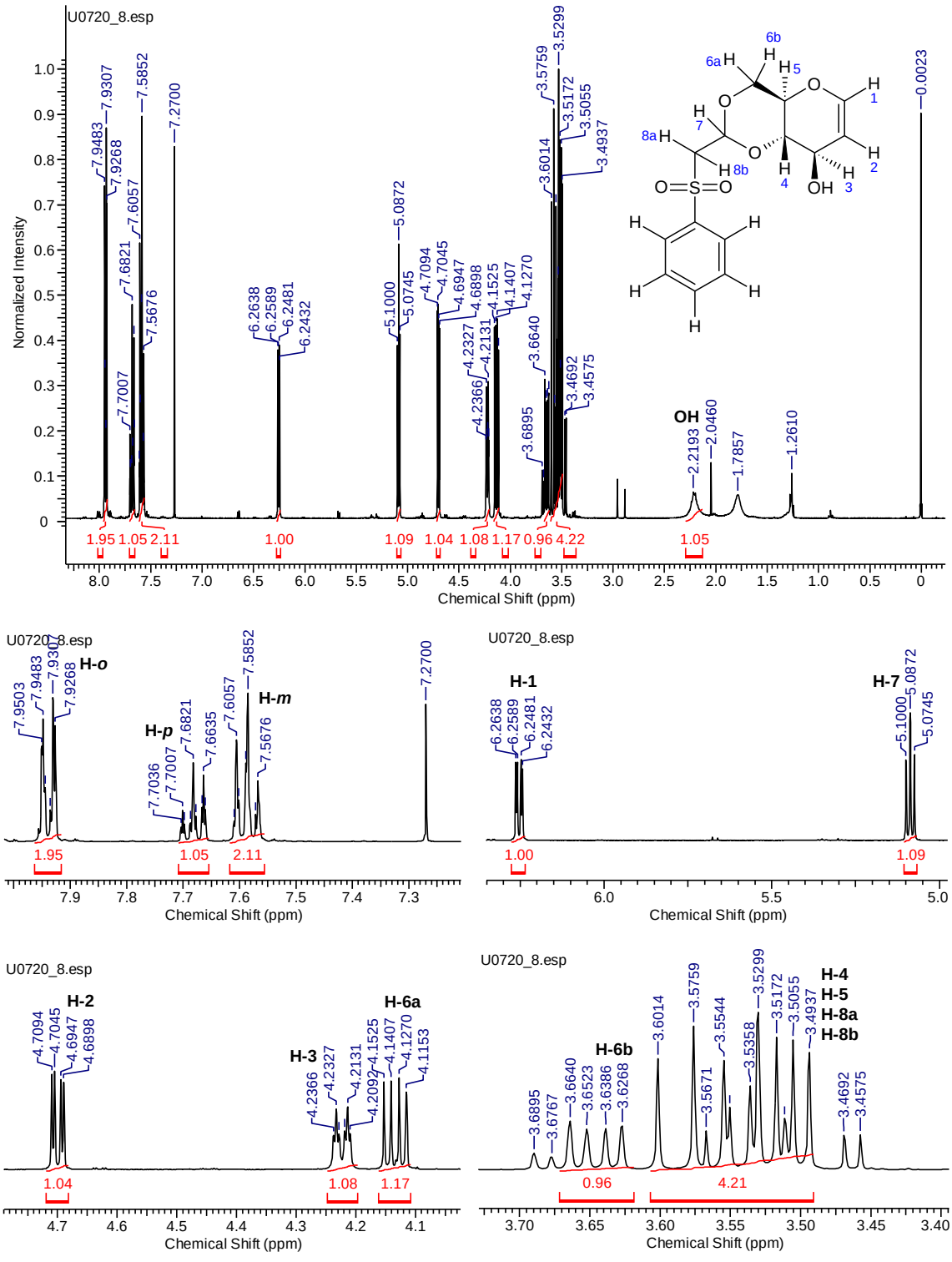

Source: The author (2024).

A double duplet for H-2 with $J_{2,1}$ = 5.88 Hz, and $J_{2,3}$ = 1.56 Hz was found at δ 4.70 ppm. At δ 4.22 ppm was observed an apparent dt which correspond to a double of doublets (ddd) with last *J* equal: $J_{3,4}$ = 7.84 Hz, $J_{3,2}$ = 1.56 Hz, and $J_{3,1}$ = 1.56 Hz referring to H-3. At δ 4.13 and δ 3.64 ppm, were observed two double duplets referring to H-6a and H-6b respectively. The proton H-6a showed coupling constant $J_{6a,6b}$ = 10.2 Hz, $J_{6a,5}$ = 4.72 Hz; H-6b showed $J_{6b,6a}$ = 10.16 Hz, and $J_{6b,5}$ = 4.76 Hz, corroborating a cyclical and more rigid structure. At δ 3.60-3.49 ppm was noticed a multiplet referring to H-4, H-5, H-8a, H-8b. Finally, at δ 2.22 was found a broad singlet which could be the OH.

Glycals have a wide application as building blocks in the synthesis of various glycoconjugates, such as 2,3-unsaturated *O*-glycosides and *S*-glycosides. The double bond of glycals can be activated through the epoxidation reaction allowing access to 1,2-anhydrosugars, which can be used as glycosyl donors or as precursors to more stable glycosyl donors (Marín *et al*., 2011). The authors carried out a study of the glycosylation/epoxidation of glycals with *m*-CPBA to obtain glycopyranosides and manopyrannosides, they observed that when the partially protected *D*-glucal with a more rigid system reacted with *m*-CPBA the mannopyranoside derivative was obtained almost exclusively.

Therefore, we decided to study the behavior of the phenylsulfonylethylidene protecting group of PSE-glucal **10** under epoxidation conditions. PSE acetals is a rigid system and an acid-resistant protecting group. The reaction of PSE-glucal **10** with *meta*-chloroperbenzoic acid (*m*-CPBA) was carried out at room temperature for 3 hours and *α*-mannopyranoside **11** was obtained in 42% yield. On the other hand, when the reaction was performed under focused microwave irradiation, the reaction time was reduced to 10 min with 52% of yield (Scheme 28). The preparation of *α*-mannopyranoside **11** involves the *in situ* formation of the intermediate *β*-epoxide. The presence of the PSE protecting group on carbons 4 and 6 makes the glycal structure more rigid and probably facilitates the transition state (Figure 18) between PSE-glucal and *m*-CPBA. In this way, the nucleophilic attack of the benzoate ion occurs exclusively on the *α* face, opposite the epoxide, leading to the stereoselective formation of α-mannopyranoside **11**.

Scheme 28 - Synthesis of *α*-mannopyranoside **11**.

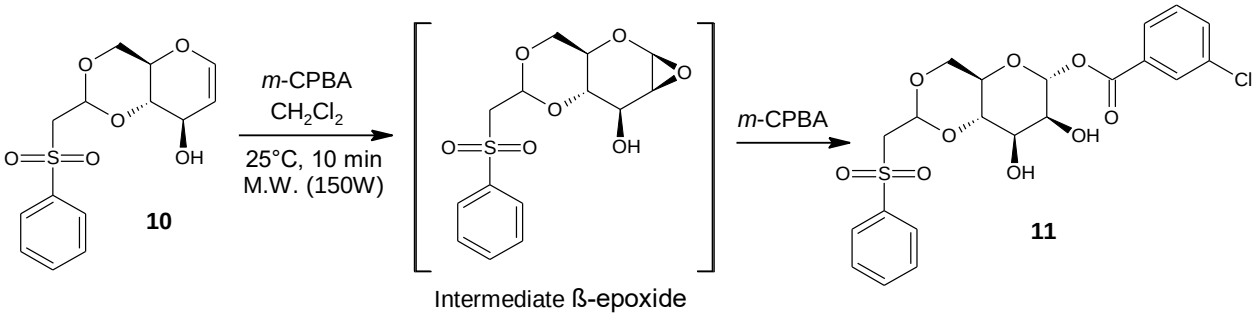

Source: The author (2024).

Figure 18 - Transition state between glycals and *m*-CPBA.

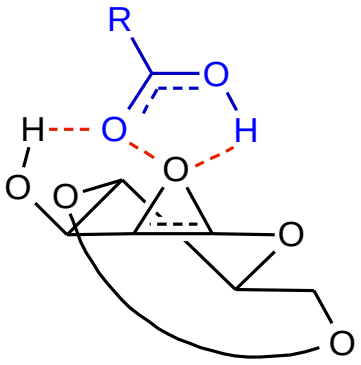

Source: Adapted from Marín *et al*. (2011).

Figure 19 shows ^{1}H NMR spectrum of *α*-mannopyranoside **11**. In the region between δ 8.0 and δ 7.5 ppm there are signals from the aromatic rings of the PSE protecting group and of the *m*-chloro-benzoate (the aglycone portion). A multiplet was found at δ 7.98-7.92 ppm referring to the four H-*o*, while between δ 7.78-7.70 ppm was observed another multiplet referring to the two H-*p*, and at δ 7.64-7.56 ppm was noticed a multiplet referring to the three H-*m*. Regarding the sugar portion, at δ 6.05 ppm was found a duplet corresponding to H-1 with *J* = 1.16 Hz and at δ 5.02 ppm was observed a triplet referring to H-7 with *J* = 5.12 Hz. In δ 5.60 and δ 4.96 was found two duplets referring to the hydroxyl's groups with *J* = 4.68 and 6.68 Hz respectively. A multiplet referring to H-2, H-3, and H-6a was noticed at δ 3.90-3.82 ppm, while at δ 3.77 ppm was found a triplet with *J* = 9.4 Hz corresponding to H-6b. Another multiplet was observed at δ 3.67-3.60 ppm referring to H-4, H-8a, and H-8b. Finally, was found a triplet at δ 3.51 ppm referring to H-5 with *J* = 10.2 Hz.

Figure 19 - ^{1}H NMR spectrum and expansions (400 MHz, DMSO-d_6) of α-mannopyranoside **11**.

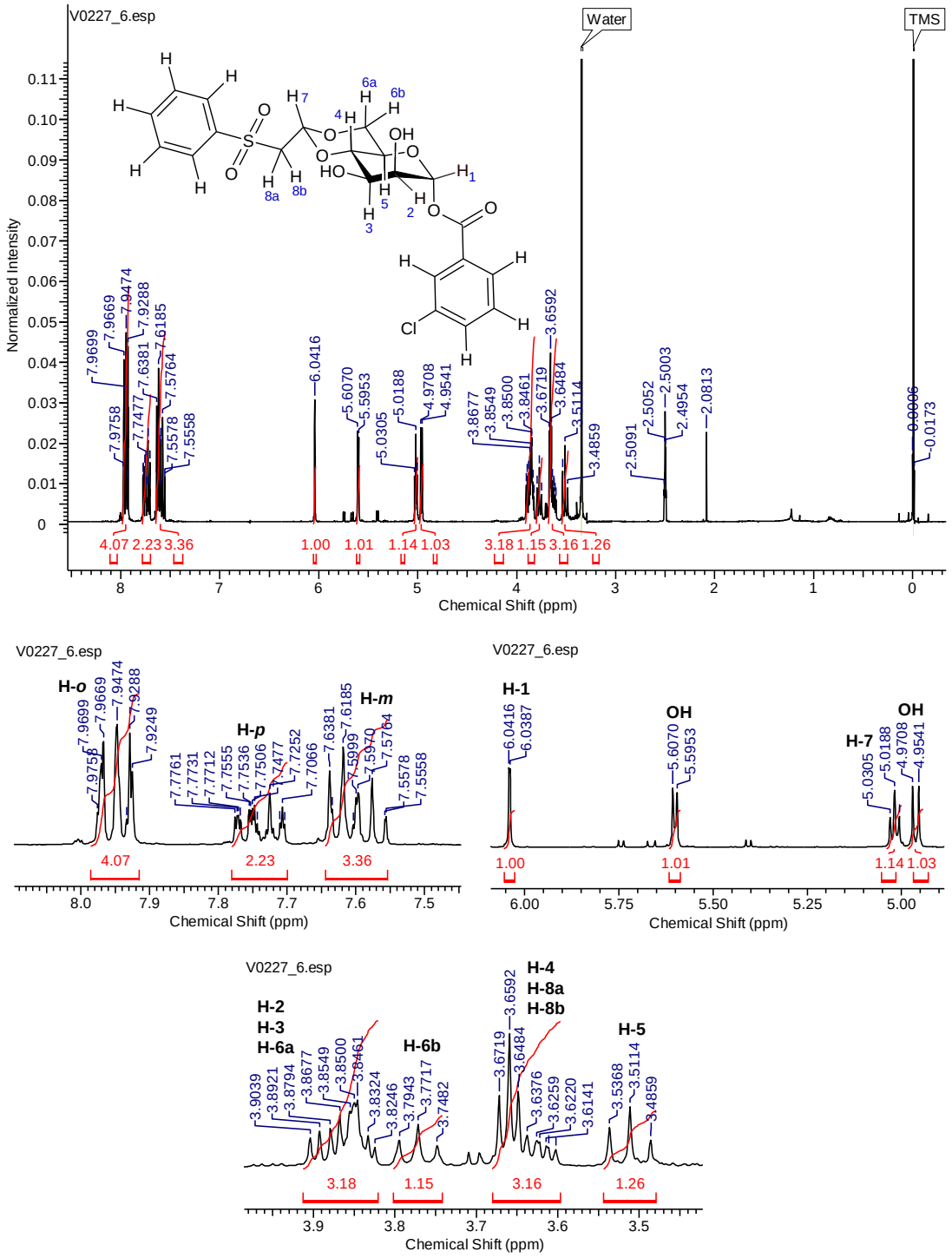

Source: The author (2024).

The confirmation that the two duplets at δ 5.60 and δ 4.96 ppm correspond to the OH groups can be seen in the expansion of the 2D HSQC NMR spectrum (Figure 20), where they are the only signals that do not couple with any carbon.

Figure 20 - Expansion of the 2D HSQC NMR spectrum of *α*-mannopyranoside **11** (Full spectrum in attachments).

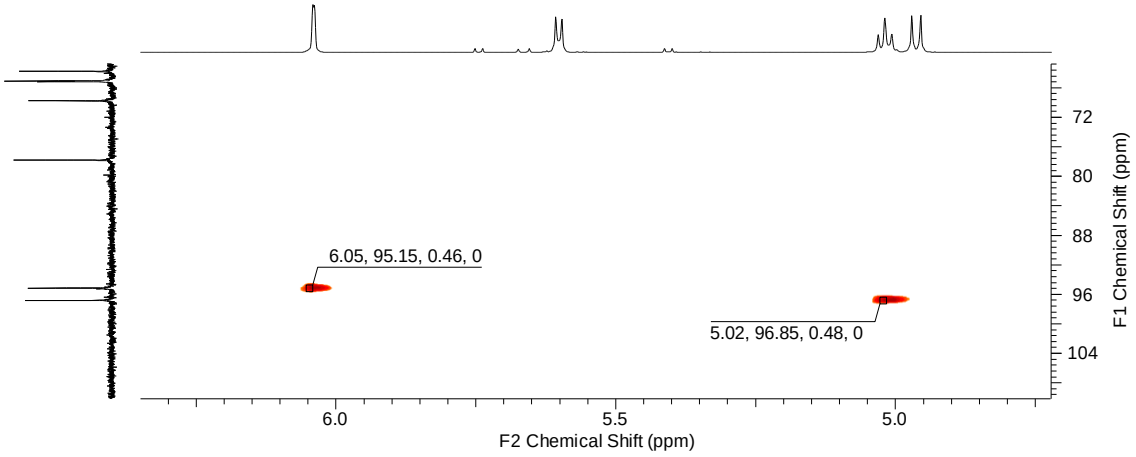

Source: The author (2024).

Figure 21 - ^{13}C NMR spectrum and expansions (100 MHz, DMSO-d_6) of *α*-mannopyranoside **11**.

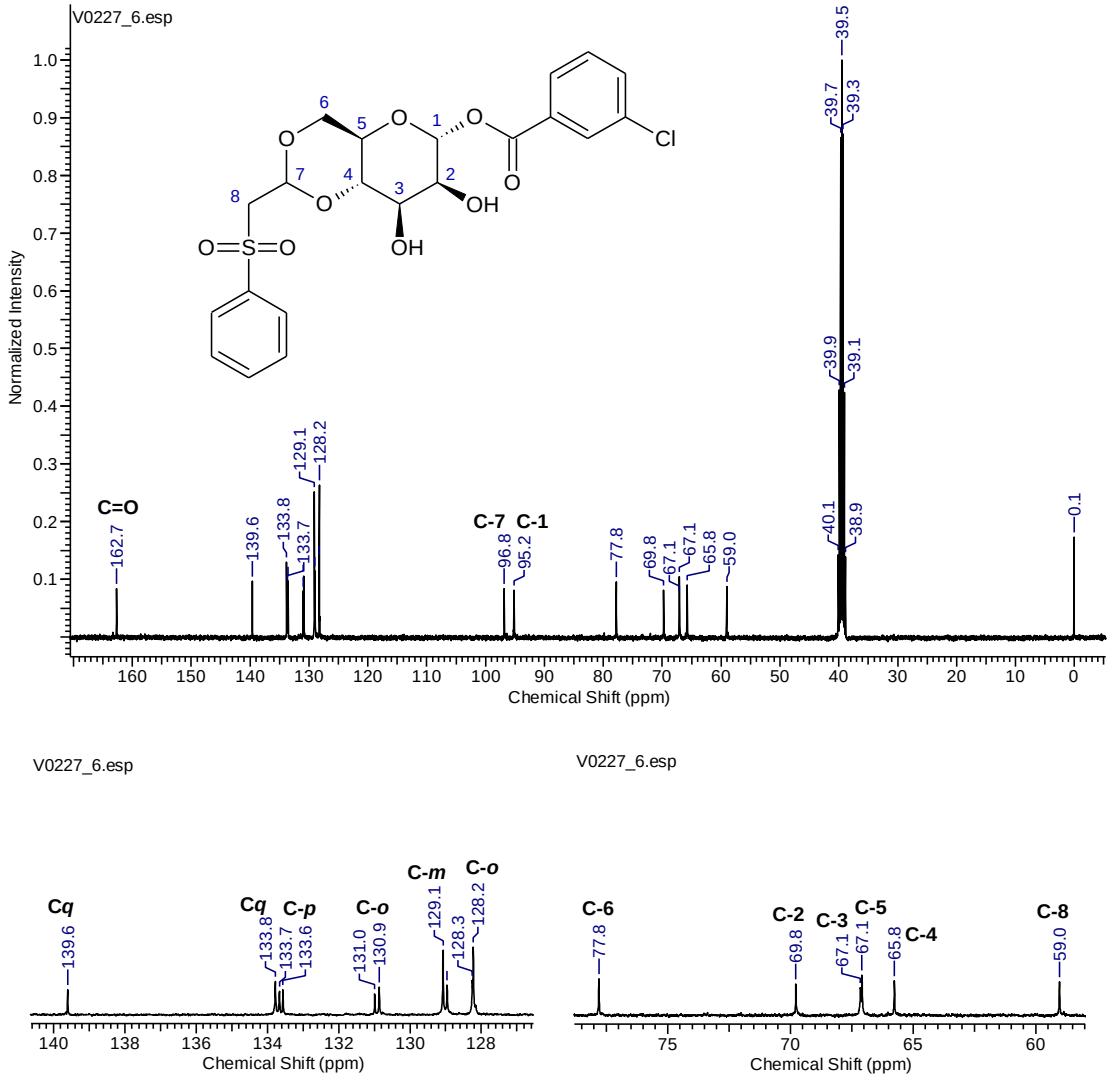

Source: The author (2024).

In the ^{13}C NMR spectrum of *α*-mannopyranoside **11** (Figure 21), at δ 162.7 ppm was observed the carbonyl signal, while at δ 139.6 ppm was found the quaternary carbon signal from the protecting group ring. The other quaternary carbon signal from the *m*-chloro-benzoate was noticed ring at δ 133.8 ppm. We observed the C-*p* signals at δ 133.7 and δ 133.6 ppm, and at δ 131.0 and δ 130.9 ppm, was found two signals for the C-*o* of the *m*-chloro-benzoate ring. We noticed the C-*m* signals at δ 129.1 and δ 129.0 ppm, and was observed the C-*o* at δ 128.3 and δ 128.2 ppm. At δ 96.8 ppm we noticed the C-7 signal, while at δ 95.2 ppm we found the C-1 signal. At δ 77.8 we observed the C-6 signal, while at δ 69.8, δ 67.1, δ 67.1, and δ 65.8 ppm we found the C-2, C-3, C-5, and C-4 signals respectively. Finally, we noticed C-8 at δ 59.0 ppm.

The acetylation reaction of *α*-mannopyranoside **11** was carried out using montmorillonite K-10 (200% w/w of **11**) and acetic anhydride (Scheme 29). The reaction was stirred for 1 hour and the acetylated *α*-mannopyranoside **12** was obtained in 77% yield.

Scheme 29 - Acetylation reaction to obtain acetylated *α*-mannopyranoside **12**.

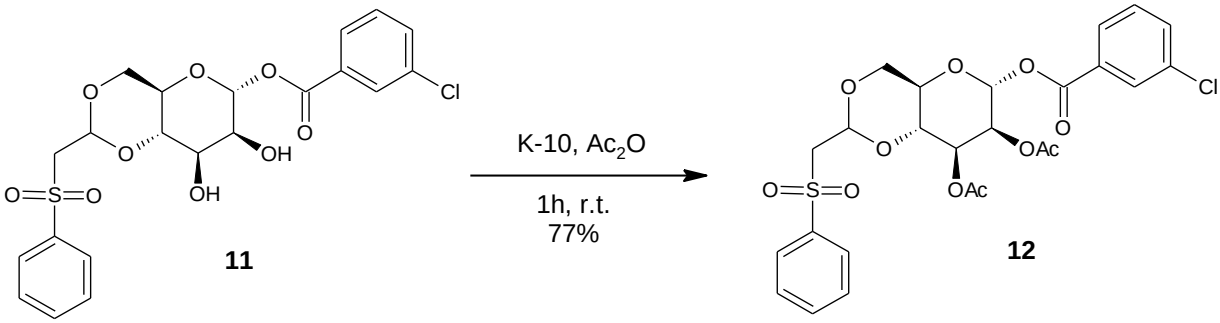

Source: The author (2024).

The signs of the aromatic rings unfolded differently in the ^{1}H NMR spectrum of acetylated *α*-mannopyranoside **12** (Figure 22). The H-*o* next to the chlorine atom of the *m*-chloro-benzoate ring was noticed at δ 7.99 ppm as a singlet. At δ 7.91 ppm was found a triplet referring to the other three H-*o* with *J* = 8.1 Hz, and at δ 7.65 ppm was observed another triplet referring to the H-*p* of the ring's protecting group with *J* = 4.3 Hz. Finally, between δ 7.61-7.53 ppm was found a multiplet referring to the three H-*m*, and at δ 7.43 ppm was observed a triplet referring to the H-*p* of the *m*-chloro-benzoate ring with *J* = 7.8 Hz. At δ 6.21 ppm we found a singlet referring to H-1, and with the acetyl protection of the hydroxyls at C-2 and C-3, the signals of H-2 and H-3 shifted

to δ 5.44 ppm as a duplet with *J* = 1.36 Hz, and at δ 5.38 ppm as a double duplet with *J* = 10.4 and 3.5 Hz, respectively.

Figure 22 - ^{1}H NMR spectrum and expansions (500 MHz, $CDCl_3$) of acetylated *α*-mannopyranoside **12**.

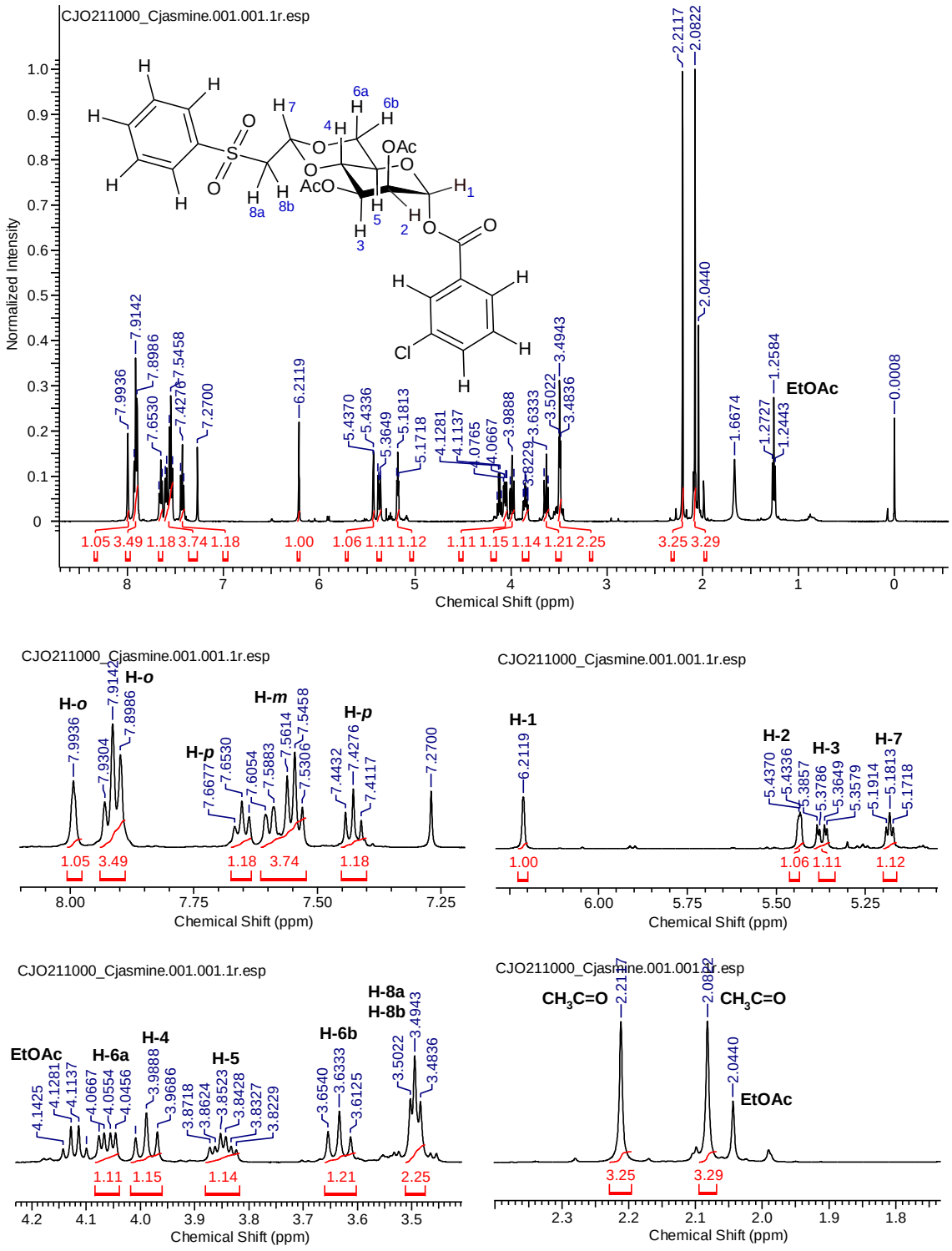

Source: The author (2024).

At δ 5.18 ppm we found a triplet with J = 5.0 Hz corresponding to H-7. A double duplet was observed at δ 4.07 ppm referring to H-6a with $J_{6a,6b}$ = 10.55 Hz, $J_{6a,5}$ = 4.9 Hz, and at δ 3.99 ppm was noticed a triplet with $J_{4,5}$ = 9.95 Hz which refers to H-4. Between δ 3.87-3.82 ppm, was found a multiplet referring to H-5, and at δ 3.63 and δ 3.49 ppm we found two triplets, the first referring to H-6b with $J_{6b,6a}$ = 10.35 Hz, and the second referring to H-8a and H-8b with J = 5.35 Hz. At δ 2.21 and δ 2.08 ppm, two singlets are referring to the methyls of the acetyl groups. It was also possible to observe a quartet at δ 4.12 ppm, a singlet at δ 2.04 ppm, and a triplet at δ 1.26 ppm corresponding to the ethyl acetate solvent.

Attempts were made to use the *α*-mannopyranoside **12** as a glycosyl donor and replace the aglycone moiety (Scheme 30), with glycerol carbonate as a nucleophile for the formation of glycero-carbohydrates. Boron trifluoride etherate ($BF_3.Et_2O$, 1 eq.) was used as a Lewis acid with mannopyranoside **12**, and after 24h no change was observed on the TLC plate. When we carried out tests with TMSOTf (1 eq.), the formation of β-mannopyranoside **13**, was observed after 4h with yield of 64%.

Scheme 30 - Substitution of the aglycone portion in α-mannopyranoside **12**.

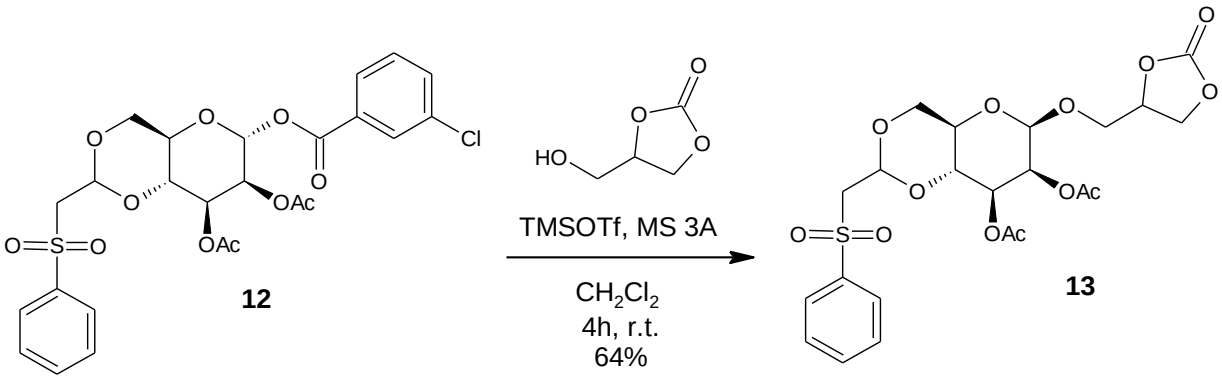

Source: The author (2024).

Figure 23 shows ^{1}H NMR spectrum of β-mannopyranoside **13**. In the aromatic region between δ 8.0 and δ 7.5 ppm, was observed the characteristic signals of the PSE protector group and was no longer observed the signals of the *m*-chloro-benzoate ring. At δ 4.78 ppm was found a doublet of doublets referring to H-2 with $J_{2,1}$ = 8.04 Hz, $J_{2,3}$ = 3.52 Hz, and $J_{2,4}$ = 1.56 Hz, while between δ 5.20-5.13 ppm was noticed a multiplet referring to H-3 and H-7. Another multiplet was observed ranged δ 4.88 from δ 4.82 ppm referring to H-4', while a double duplet at δ 4.78 ppm with $J_{1,2}$ = 7.32 Hz

and $J_{1,3}$ = 1.48 Hz concerning to H-1, the high value of the constant is an indication that this may be the beta isomer.

Figure 23 - ^{1}H NMR spectrum and expansions (400 MHz, $CDCl_3$) of *β*-mannopyranoside **13**.

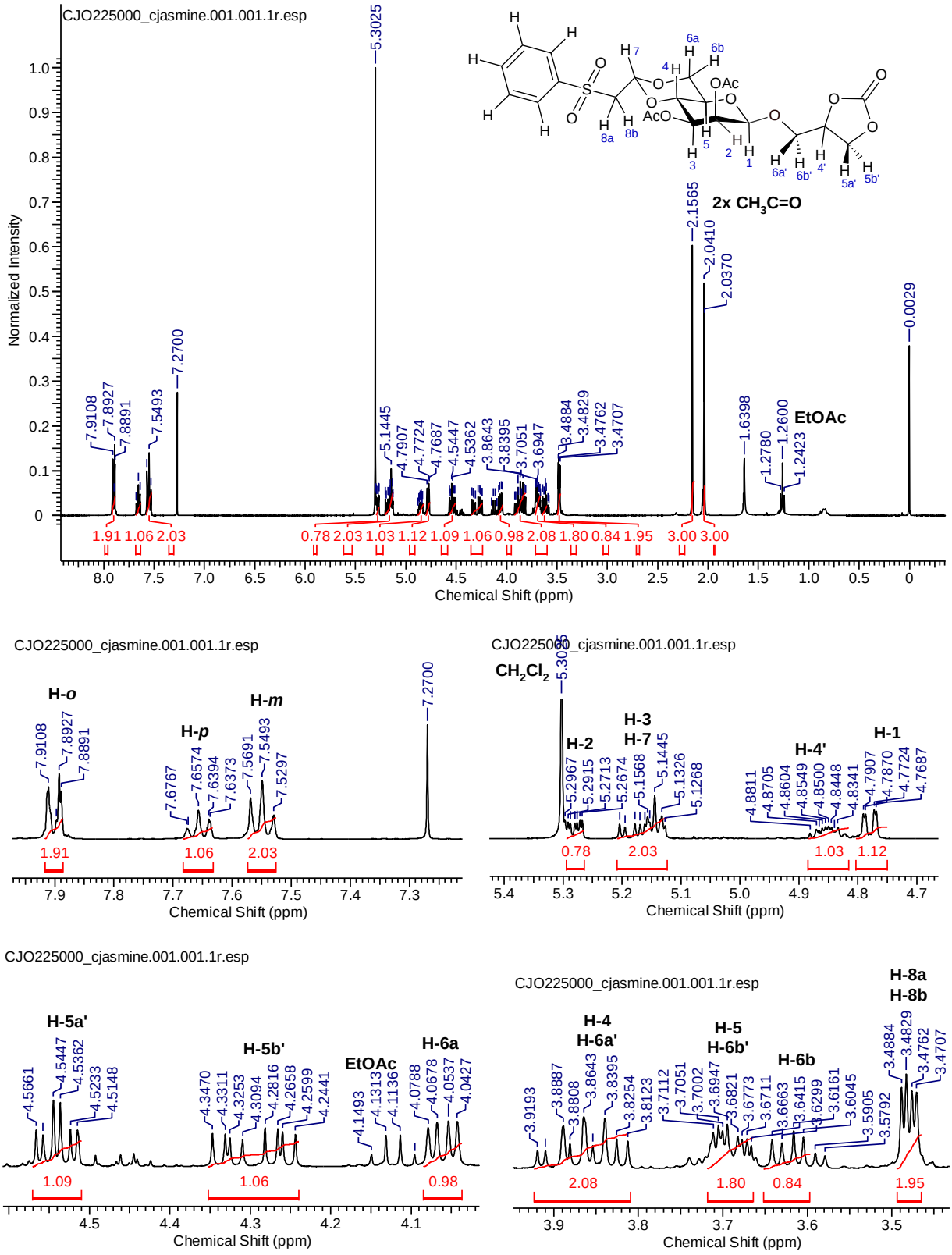

Source: The author (2024).

A double triplet was found at δ 4.54 ppm referring to H-5a' with $J_{5a',5b'}$ = 8.56 Hz, and $J_{5a',4'}$ = 3.4 Hz, and a doublet of doublets of duplets referring to H-5b' with J = 15.08 Hz, $J_{5b',5a'}$ = 8.68 Hz, and $J_{5b',4'}$ = 6.36 Hz at δ 4.29 ppm. Referring to H-6a was found a double duplet at δ 4.06 ppm with $J_{6a,6b}$ = 10.04 Hz and $J_{6a,5}$ = 4.4 Hz. A multiplet was observed between δ 3.92-3.81 ppm referring to H-4 and H-6a'; and δ 3.71-.67 ppm related to H-5 and H-6b'. At δ 3.62 ppm was noticed a double duplet with $J_{6b,6a}$ ppm= 10.16 Hz and $J_{6b,5}$ = 4.64 Hz concerning to H-6b, while at δ 3.47 ppm another double duplet concerning to H-8a and H-8b with *J* = 4.88 and 2.2 Hz. Finally, two singlets related to the methyls of the acetyl groups at δ 2.16 and δ 2.04 ppm. It was also possible to observe the signals corresponding to the ethyl acetate and dichloromethane solvents. An important point noted in the ^{13}C NMR spectrum of β-mannopyranoside **13**, were the duplicated signals of the carbons, which indicates the presence of the R/S mixture.

In the figure below we can see that H-1 and H-2 have an equatorial/equatorial coupling in *α*-mannopyranoside **12**, so a lower coupling constant is expected. In *β*-mannopyranoside **13,** is observed an axial/equatorial coupling between H-1 and H-2, and due to their proximity we would expect a higher constant, such as the one found, 7.32 Hz.

Figure 24 - Coupling between H-1 and H-2 of mannopyranosides **12** and **13**.

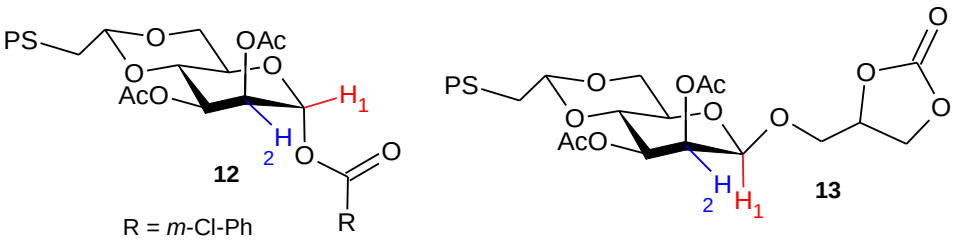

Source: The author (2024).

A possible mechanism that explains the formation of the beta isomer is shown in the scheme 31. Following path A, there is an attack by the carbonyl of the *m*-Cl-benzoate group on the Si atom of TMSOTf, and the attack of the acetyl group of C-2 forms the intermediate dioxolenium ion. The OTf ion can then attack the intermediate dioxolenium ion from the alpha face. The OTf group is an excellent leaving group and nucleophilic substitution occurs with glycerol carbonate to form *β*-mannopyranoside **13**. Following path B, which also passes through the formation of the intermediate

dioxolenium ion, however, the electron pair of the ring oxygen can form the oxocarbenium ion. The OTf ion can block the alpha face leading to attack on the beta face by glycerol carbonate and the formation of *β*-mannopyranoside **13**, but the OTf ion can also block the beta face leading to the *α*-mannopyranoside, which wasn't observed.

Scheme 31 - Proposed mechanism for the formation of *β*-mannopyranoside **13**.

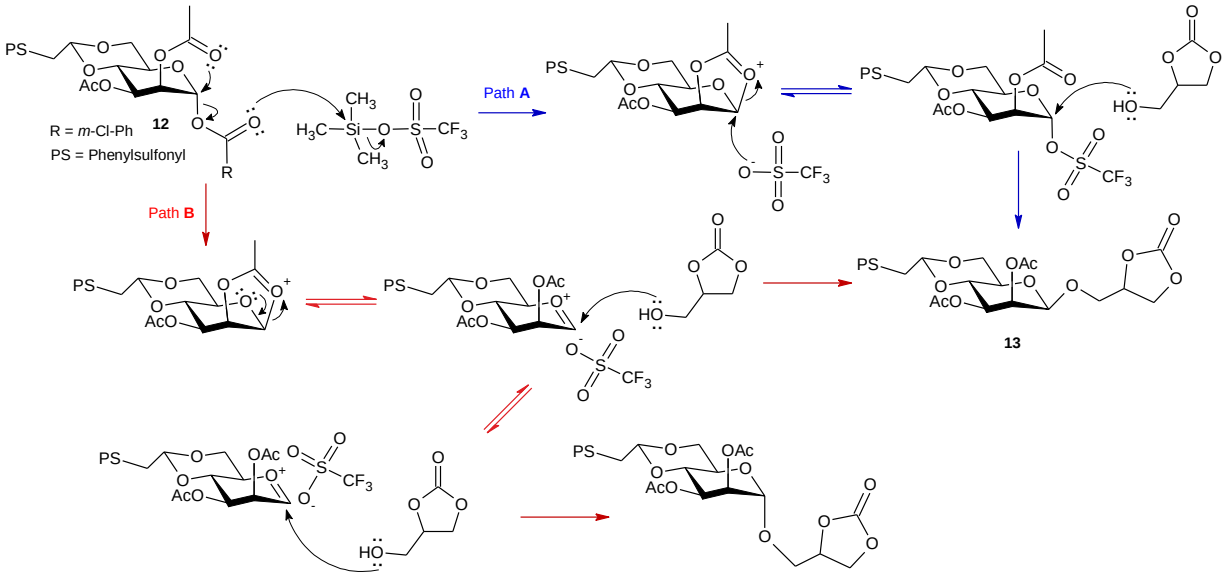

Source: The author (2024).

Still looking to take advantage of the stability of the PSE-glucal protecting group under acidic conditions, Fernandes *et al*. (2008) investigated the allylic rearrangement of acetylated glycals, known as the Ferrier reaction. Some Lewis acids were tested, such as $BF_3.Et_2O$, TMSOTf, and $Bi(OTf)_3$, moreover methanol was used as the nucleophile. However, an unexpected behavior was observed, under Ferrier reaction conditions, the acetylated and non-protected PSE-glucals mainly followed a simple addition process. Initially, Fernandes *et al*. (2008) thought that the presence of the protective group could cause a certain rigidity to the ring and that this could affect the course of the reaction; however, after a radio-crystallographic analysis of the PSE-glucal, a standard half-chair conformation was revealed. Another proposition was then presented: during the transition state of the allyloxycarbenium, the sulfonyl group could exert a complexation effect on the Lewis acid, which would lead to the addition process; however, further investigations still need to be more done.

In the addition process, the authors noted some important points, such as the increased reactivity when a stoichiometric amount of Lewis acid was used and the improved selectivity when trimethylsilyl trifluoromethanesulfonate (TMSOTf) was used. We therefore decided to test the reaction of PSE-glucal **10** with glycerol carbonate **1** using 1.2 equivalents of TMSOTf (Scheme 32).

Scheme 32 - Synthesis of 2-deoxy-*O*-glucoside **14a/b**.

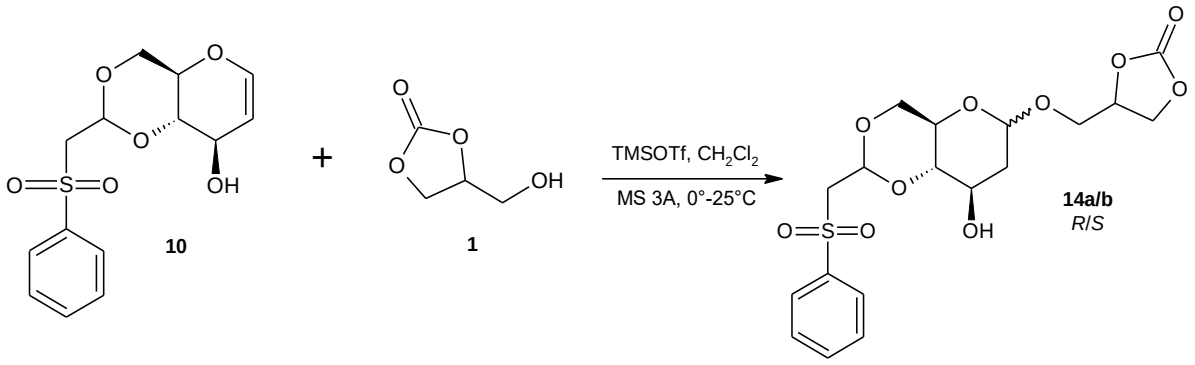

Source: The author (2024).

We tested different equivalents of GC **1** at different reaction times (Table 2), and the best result was obtained when an excess of GC **1** (5 equivalents) for 30 min was employed (Entry 3). In addition, we observed the separation of two spots on the TLC plate when dichloromethane/acetone (9:1) was used as eluent system (Figure 25), likely α and β isomers of 2-deoxy-*O*-glucoside **14a/b**. Separation was attempted on the chromatographic column, and even using the DCM/acetone (9:1) system, the two points were still very close, and eventually mixing occurred during the chromatographic column. The yields obtained can be seen in Table 2.

Table 2 - Attempts to optimize and obtain 2-deoxy-*O*-glucoside **14a/b**.

Entry	Eq. CG	Time	1p	Majority mixture 1p	2p	Majority mixture 2p	Total yield
1	1.2	30 min	33%	-	11%	24%	68%
2	1.2	1h	43%	-	14%	8%	65%
3	5	30 min	33%	5%	42%	11%	91%

Source: The author (2024).

Figure 25 - TLC plate revealed in 5% (v/v) sulfuric acid/ethanol of 2-deoxy-*O*-glucoside **14a**/**14b** in DCM/acetone (9:1).

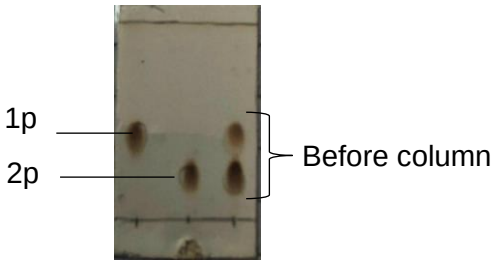

Source: The author (2024).

When we carried out the ^{1}H NMR, we realized that 1p (**14a**) was an isomeric mixture with a complex ^{1}H NMR that was difficult to identify (Figure 26). On the other hand, the ^{1}H NMR of 2p (**14b**) allowed us to identify the signs of the α-2-deoxy-*O*-glucoside **14b** (Figure 27).

Figure 26 - ^{1}H NMR spectrum and expansion (500 MHz, $CDCl_3$) of compound **14a**.

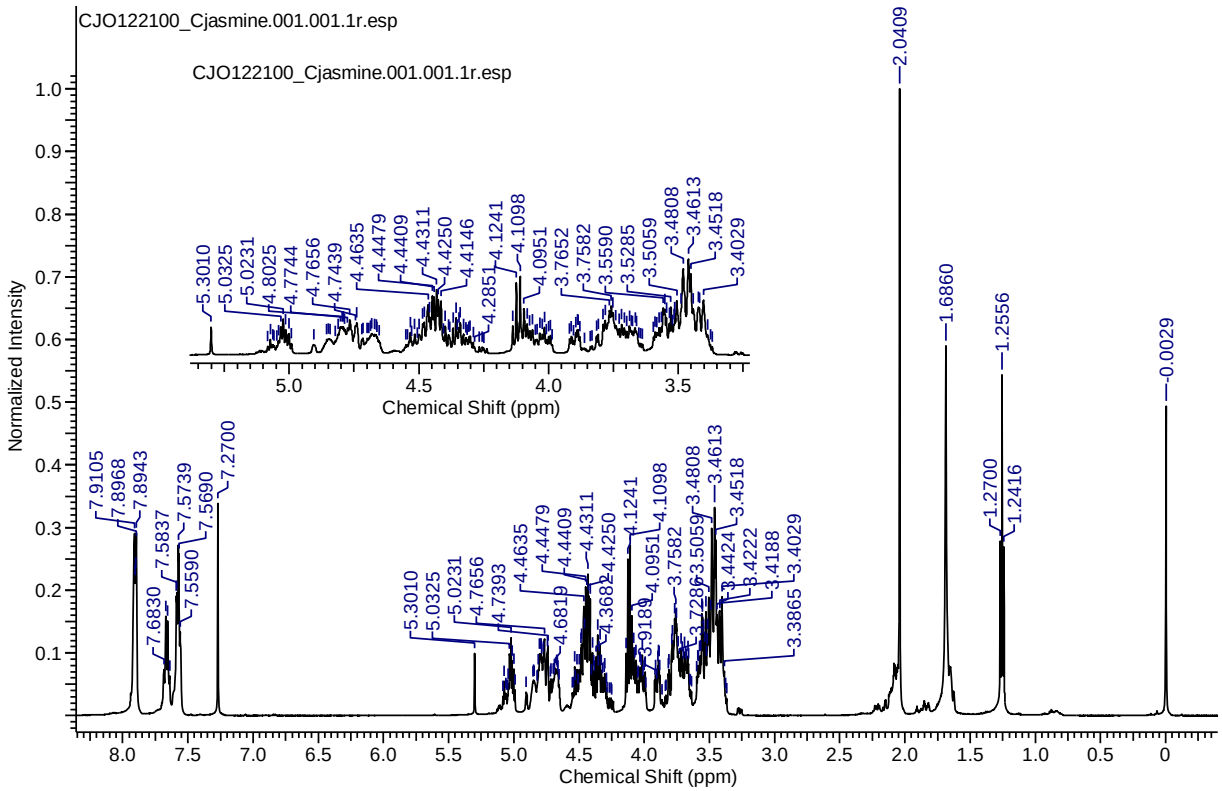

Source: The author (2024).

In the aromatic region between δ 8.0 and δ 7.5 ppm, was observed the characteristic signals H-*o*, H-*m*, and H-*p* of the PSE protector group. At δ 5.05 ppm

was observed a triplet with J = 4.4 Hz referring to H-7, and at δ 4.88 ppm a duplet referring to H-1 with *J* = 3.5 Hz. A multiplet was found between δ 4.85-4.80 ppm referring to H-4' of the glycerol carbonate ring.

Figure 27 - ^{1}H NMR spectrum and expansions (500 MHz, $CDCl_3$) of compound **14b**.

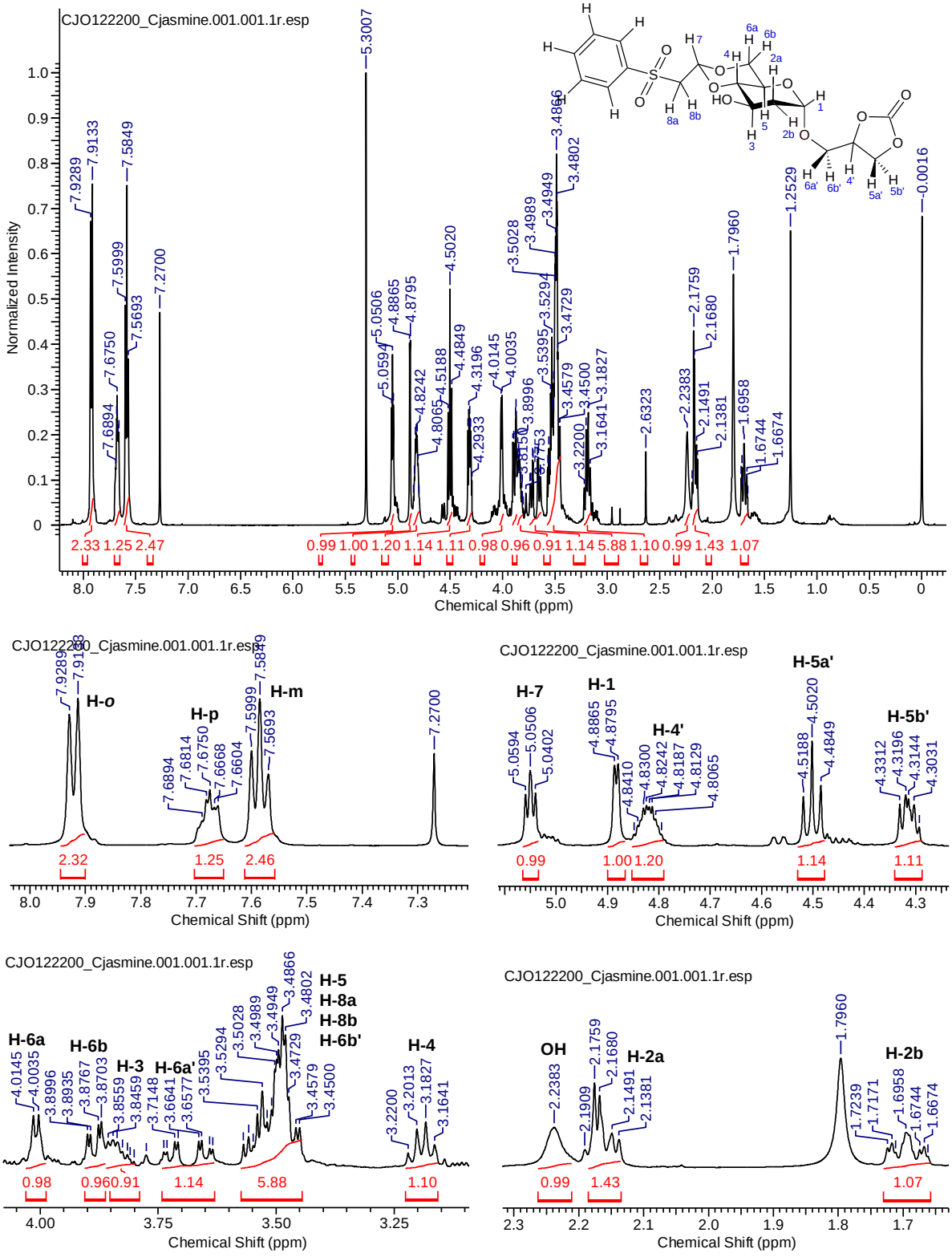

Source: The author (2024).

At δ 4.50 ppm was noticed a triplet referring to H-5a' with *J* = 8.4 Hz, and a multiplet between δ 4.33-4.29 ppm referring to H-5b'. A duplet was found at δ 4.01 ppm with *J* = 5.5 Hz referring to H-6a, and a double duplet at δ 3.88 ppm referring to H-6b with $J_{6b,6a}$ = 14.65 Hz and $J_{6b,5}$ = 3.05 Hz. Between δ 3.92-3.81 ppm was found a multiplet referring H-3, and a doublet of doublets of duplets referring to H-6a' with *J* = 15.1 Hz, $J_{6a',\,6b'}$ = 11.6 Hz, and $J_{6a',4'}$ = 3.35 Hz at δ 3.67 ppm. Another multiplet was observed between δ 3.53-3.47 ppm referring to H-5, H-8a, H-8b, and H-6b', and a double duplet at δ 3.19 ppm referring to H-4 with *J* = 18.65 Hz and *J* = 9.35 Hz. At δ 2.24 ppm was found a singlet referring to OH. Finally, was observed two multiplets between δ 2.18-2.14 ppm and δ 1.72-1.66 ppm referring to H-2a and H-2b, respectively. Similarly, to the ^{13}C NMR of *α*-mannopyranoside **13**, we also observed duplicate signals from the carbons in the ^{13}C NMR of 2-deoxy-*O*-glucoside **14b**, which indicates the presence of the R/S mixture.

4.4 ATTEMPTS OF SYNTHESIS OF *S*-GLYCOSIDES FROM TRI-*O*-ACETYL-*D*-GLUCAL

One of the methods for preparing *S*-glycosides is the reaction of glycals with thiols catalyzed by a Lewis acid through the Ferrier allylic rearrangement. The thiol chosen in this work was glycerol thio-carbonate **4**, prepared from glycerol. We used tri-*O*-acetyl-*D*-glucal **5** as a per-*O*-acetylated sugar with different Lewis acids such as montmorillonite K-10 doped with $FeCl_3$ and $BF_3.Et_2O$ in different stoichiometric quantities (Table 3). In the scheme 33 below we can see the reaction to prepare the 2,3-unsaturated *S*-glycoside.

Scheme 33 - Synthesis of 2,3-unsaturated *S*-glycosides.

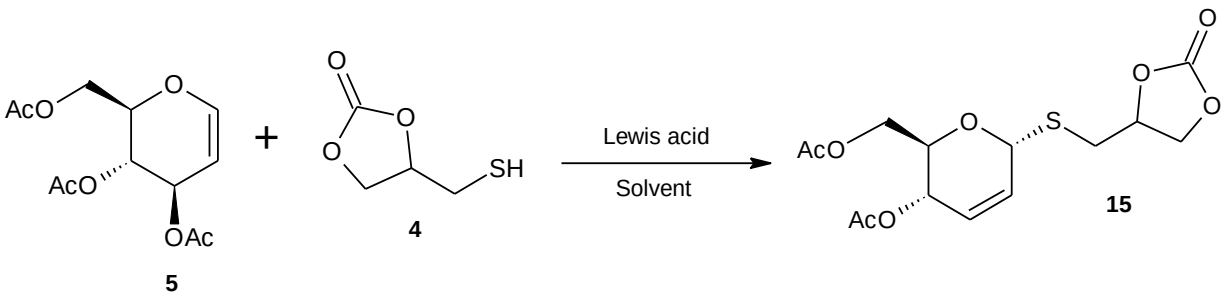

Source: The author (2024).

Thio-GC **4** have good solubility in more polar solvents such as acetone and DMF, and for this reason, we initially tested the combination of dichloromethane with these solvents. In the first entry, we used 20% K-10 doped with 5% $FeCl_3.6H_2O$ and dichloromethane as a solvent with a few drops of DMF, but after 3 hours no reaction was observed on TLC plate. Then, in the second entry, 200% K-10 doped with 10% $FeCl_3.6H_2O$ and dichloromethane with acetone was used as a binary solvent system, and even after 3 hours of reaction only the starting materials remains.

In the third and fourth entries, $BF_3.Et_2O$ and dichloromethane and acetone were used as solvents, respectively. After 24 hours, we observed the formation of a point at the origin that showed in 10% sulfuric acid/ethanol, below the standard of glycerol thio-carbonate (Figure 28). We suspected that this point might be the deprotected *D*-glucal, because after performing an acetylation reaction on the crude material, the tri-*O*-acetyl-*D*-glucal was recovered. We also observed the formation of another spot (below the *D*-glucal spot) which only showed up under ultraviolet light at 365 nm, and we supposed that this may be the dimeric disulfide of thio-GC **4**, since thio-GC **4** can undergo spontaneous and rapid oxidation. Unfortunately, the *S*-glycosylation attempts were unsuccessful.

Table 3 - Attempts to optimization of *S*-glycosylation reaction via Ferrier Rearrangement.

Entry	Lewis acid	Solvent	Time
1	20% (K-10/5% $FeCl_3.6H_2O$)	DCM (drops of DMF)	3h
2	200% (K-10/10% $FeCl_3.6H_2O$)	DCM (drops of acetone)	3h
3	$BF_3.Et_2O$ (1.2 eq.)	DCM	24h
4	$BF_3.Et_2O$ (1.2 eq.)	Acetone	24h

Source: The author (2024).

Figure 28 - TLC plate revealed in ultraviolet light at 365 nm (a) and in 5% (v/v) sulfuric acid/ethanol (b) for entry 4 in EtOAc/Hex (8:2).

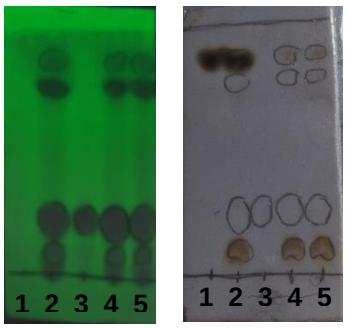

(a) b)

1- *D*-glucal **5**
2- *D*-glucal **5** + reaction
3- Thio-GC **4**
4- Thio-GC **4** + reaction
5- Reaction

Source: The author (2024).

4.5 SYNTHESIS OF THE THIO-DERIVATIVES OXAZOLIDINETHIONE, THIAZOLIDINETHIONE, AND OXAZOLE

Mishra, Agrahari, and Tiwari (2017) reported the exclusive synthesis of oxazolidine-2-thiones, when 1 equivalent of an azido-glucosyl alcohol was used in 1mL of toluene, 1.2 equivalents of PPh_3 and an excess of CS_2 (47 equivalents, 1mL) for 3 hours. We therefore decided to test the selectivity of our azido-alcohol **7a** (Scheme 34) using the same conditions as the authors. However, we observed the formation of three spots on the TLC plate (Figure 29), which indicates the formation of not only the 1,3-oxazolidine-2-thione ring (OZT), the 1,3-thiazolidine-2-thione ring (TZT), and another product.

Figure 29 - TLC plate revealed in ultraviolet light at 365 nm (a) and in 5% (v/v) sulfuric acid/ethanol (b) of the synthesis reaction of **16a**,**16b**, and **16c** in EtOAc/Hex (6:4).

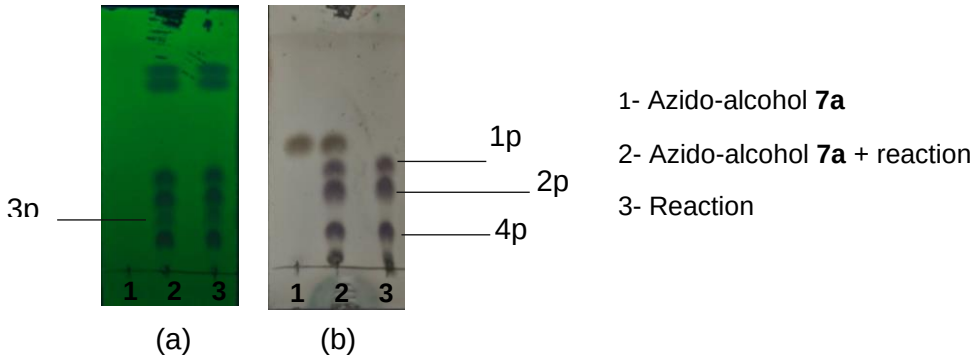

Source: The author (2024).

Scheme 34 - Synthesis of 1,3-oxazolidine-2-thione **16a** and 1,3-thiazolidine-2-thione **16b**.

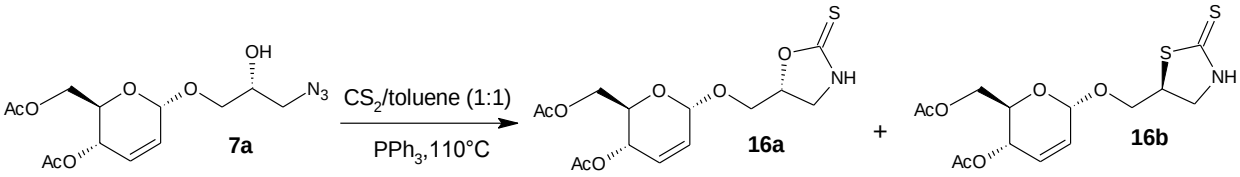

Source: The author (2024).

The ^{1}H and ^{13}C NMR spectral of 1p, 2p, 3p, and 4p were obtained. Figure 30 shows the ^{1}H NMR spectrum of 1p, which we believe to be the 1,3-oxazolidine-2-thione **16a**. At δ 7.88 ppm was found a broad singlet corresponding to the NH of the structure. A duplet referring to H-3 was observed at δ 5.93 ppm with $J_{3,2}$ = 10.2 Hz, while at δ 5.82 ppm was noticed another duplet referring to H-2 with $J_{2,3}$ = 10.25 Hz. A duplet

was noticed at δ 5.29 ppm for H-4 with $J_{4,5}$ = 10.84 Hz, and a singlet for H-1 at δ 5.07 ppm.

Figure 30 - ^{1}H NMR spectrum and expansions (500 MHz, $CDCl_3$) of 1,3-oxazolidine-2-thione **16a**.

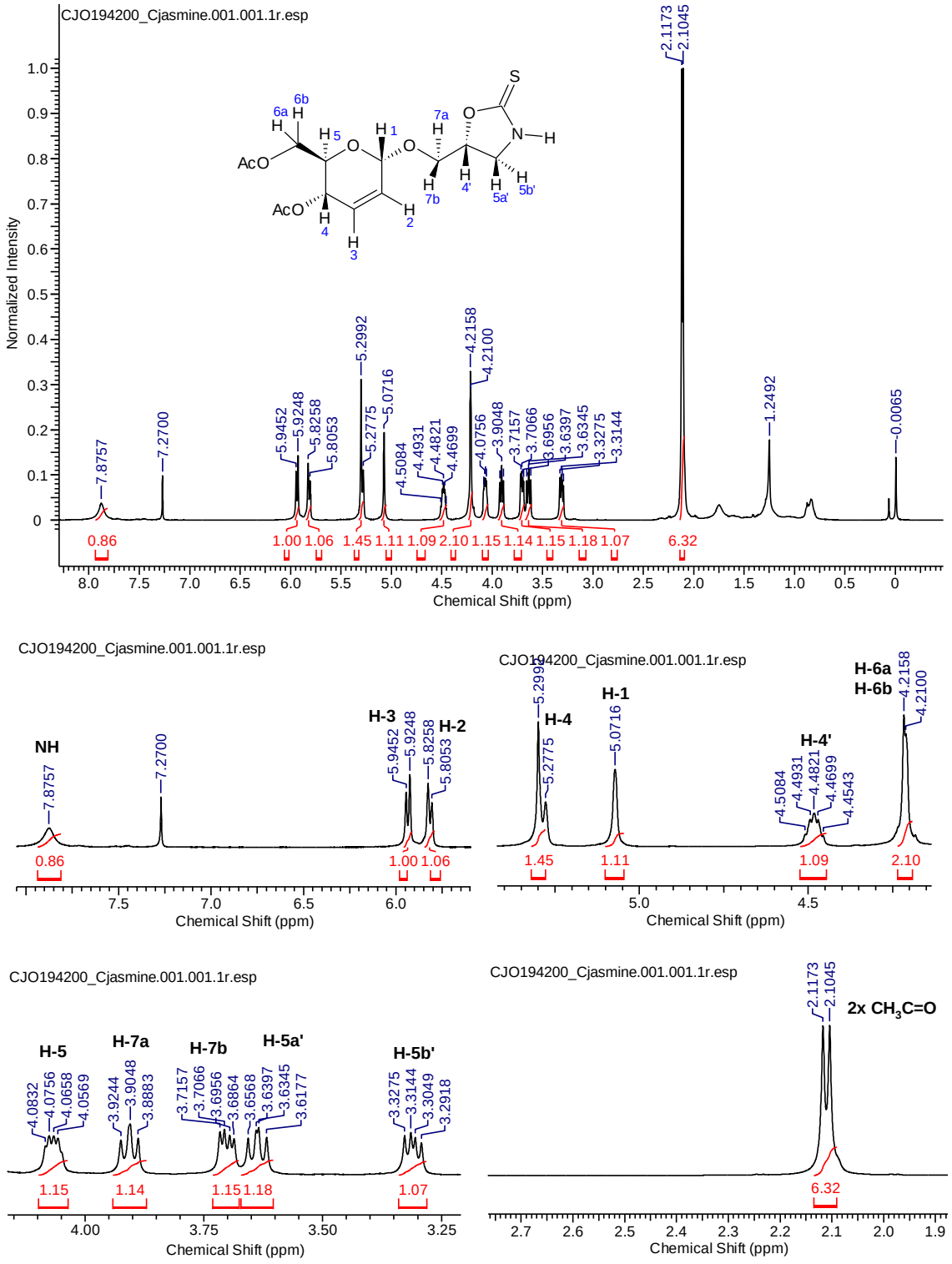

Source: The author (2024).

Between δ 4.51 and δ 4.45 ppm was observed a multiplet referring to H-4', an important observation is that this multiplet resembles the multiplet found in other structures that have the glycerol carbonate ring, which would be an indication that the carbon of H-4' is linked to an oxygen atom. At δ 4.22 ppm was found a duplet referring to H-6a and H-6b with J = 2.9 Hz, and between δ 4.08-4.06 ppm was observed a multiple referring to H-5. A triplet was found at δ 3.90 ppm for H-7a with $J_{7a,7b}$ = 9.8 Hz and a double duplet at δ 3.70 ppm for H-7b with $J_{7b,7a}$ = 10 Hz and $J_{7b,4'}$ = 4.55 Hz. A double duplet referring to H-5a' was noticed at δ 3.64 ppm with $J_{5a',5b'}$ = 11 Hz and $J_{5a',4'}$ = 8.55 Hz, and another double duplet at δ 3.31 ppm with $J_{5b',5a'}$ = 11.3 Hz and $J_{5b',4'}$ = 6.55 Hz referring to H-5b'. Finally, we noticed two singlets at 2.12 and 2.10 ppm referring to the two methyls from the acetyl groups.

Figure 31 - ^{13}C NMR spectrum (125 MHz, $CDCl_3$) of 1,3-oxazolidine-2-thione **16a**.

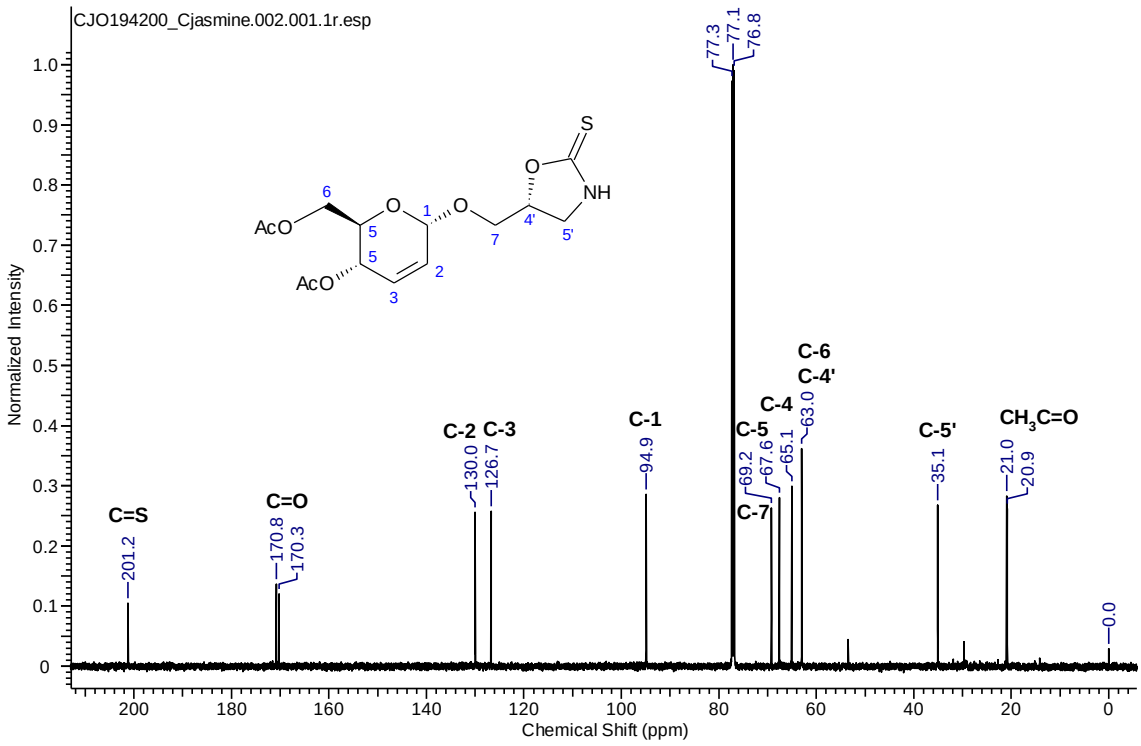

Source: The author (2024).

In the ^{13}C NMR spectrum of 1,3-oxazolidine-2-thione **16a** (Figure 31), at δ 201.2 ppm was noticed the thiocarbonyl signal, while at δ 170.8 and δ 170.3 ppm was observed the signals of the two carbonyls of the acetyl groups. At δ 130.0 ppm was found the C-2 signal, while at δ 126.7 ppm was noticed the C-3 signal. At δ 94.9 ppm was observed the C-1 signal, while at δ 69.2, δ 67.6, and δ 65.1 ppm was observed

the C-7, C-5, and C-4 signals. At δ 63.0 ppm was noticed C-6 and C-4' together. Finally, was observed C-5' at δ 35.1 ppm, and the two methyls from the acetyl groups at δ 21.0 and δ 20.9 ppm.

Figure 32 - ^{1}H NMR spectrum and expansions (500 MHz, $CDCl_3$) of 1,3-thiazolidine-2-thione **16b**.

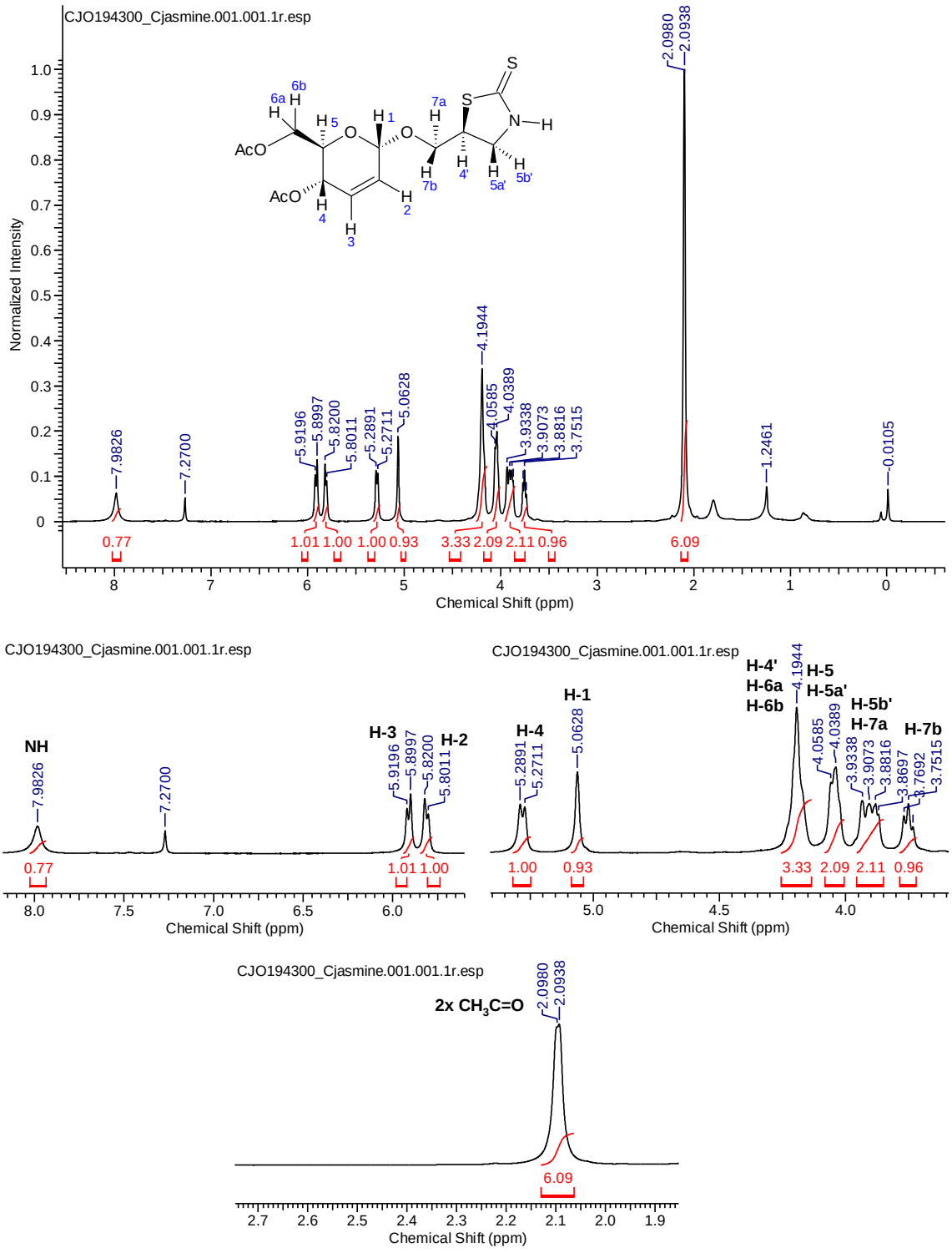

Source: The author (2024).

Figure 32 shows the ^{1}H NMR spectrum of the 2p point, which we believe to be the 1,3-thiazolidine-2-thione **16b**. It was possible to observe that the splitting of the signals was not satisfactory to determine the multiplicities; we believe that there was a shimming problem. A broad singlet corresponding to the NH of the structure was observed at δ 7.98 ppm. At δ 5.91 ppm was found a duplet corresponding to H-3 with $J_{3,2}$ = 9.95 Hz, while at δ 5.81 ppm another duplet corresponding to H-2 with $J_{2,3}$ = 9.45 Hz. We noticed a duplet at δ 5.29 ppm for H-4 with $J_{4,5}$ = 9.0 Hz, and a singlet at δ 5.06 ppm for H-1. At δ 4.19 ppm was observed an apparent singlet that looks like a signal that hasn't unfolded, we believe that this signal refers to H-4', H-6a, and H-6b. It is possible to see that the H-4' signal is displaced due to the carbon being linked to a sulfur atom. At δ 4.05 ppm was observed a duplet with J = 9.8 Hz for H-5 and H-5a'. Between δ 3.93-3.87 ppm was found a multiple for H-5b' and H-7a, while at δ 3.75 ppm a triplet for H-7b with J = 8.85 Hz. Finally, there are two singlets at δ 2.10 and δ 2.09 referring to the two methyls from the acetyl groups.

Figure 33 - ^{13}C NMR spectrum (125 MHz, $CDCl_3$) of 1,3-thiazolidine-2-thione **16b**.

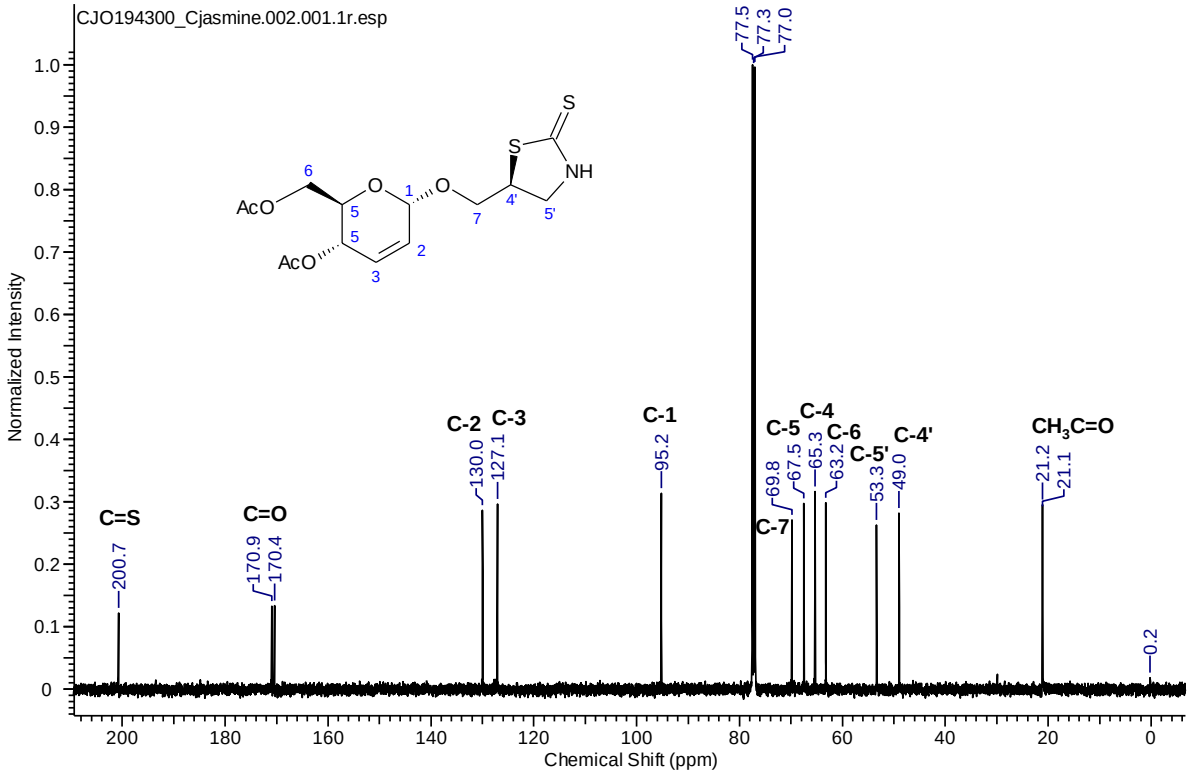

Source: The author (2024).

In the ^{13}C NMR spectrum of 1,3-thiazolidine-2-thione **16b** (Figure 33), at δ 200.7 ppm was found the thiocarbonyl signal, while at δ 170.9 and δ 170.4 ppm was observed

the signals from the two carbonyls of the acetyl groups. At δ 130.0 ppm was found the C-2 signal, while at δ 127.1 ppm was noticed the C-3 signal. At δ 95.2 ppm was observed the C-1 signal, while at δ 69.8, δ 67.5, δ 65.3, and δ 63.2 ppm was noticed the C-7, C-5, C-4, and C-6 signals. Finally, at δ 53.3 and δ 49.0 ppm, we found C-5' and C-4' respectively, and the two methyls from the acetyl groups at δ 21.2 and δ 21.1 ppm.

Scheme 35 - Mechanism for the formation of 1,3-oxazolidine-2-thione, 1,3-thiazolidine-2-thione.

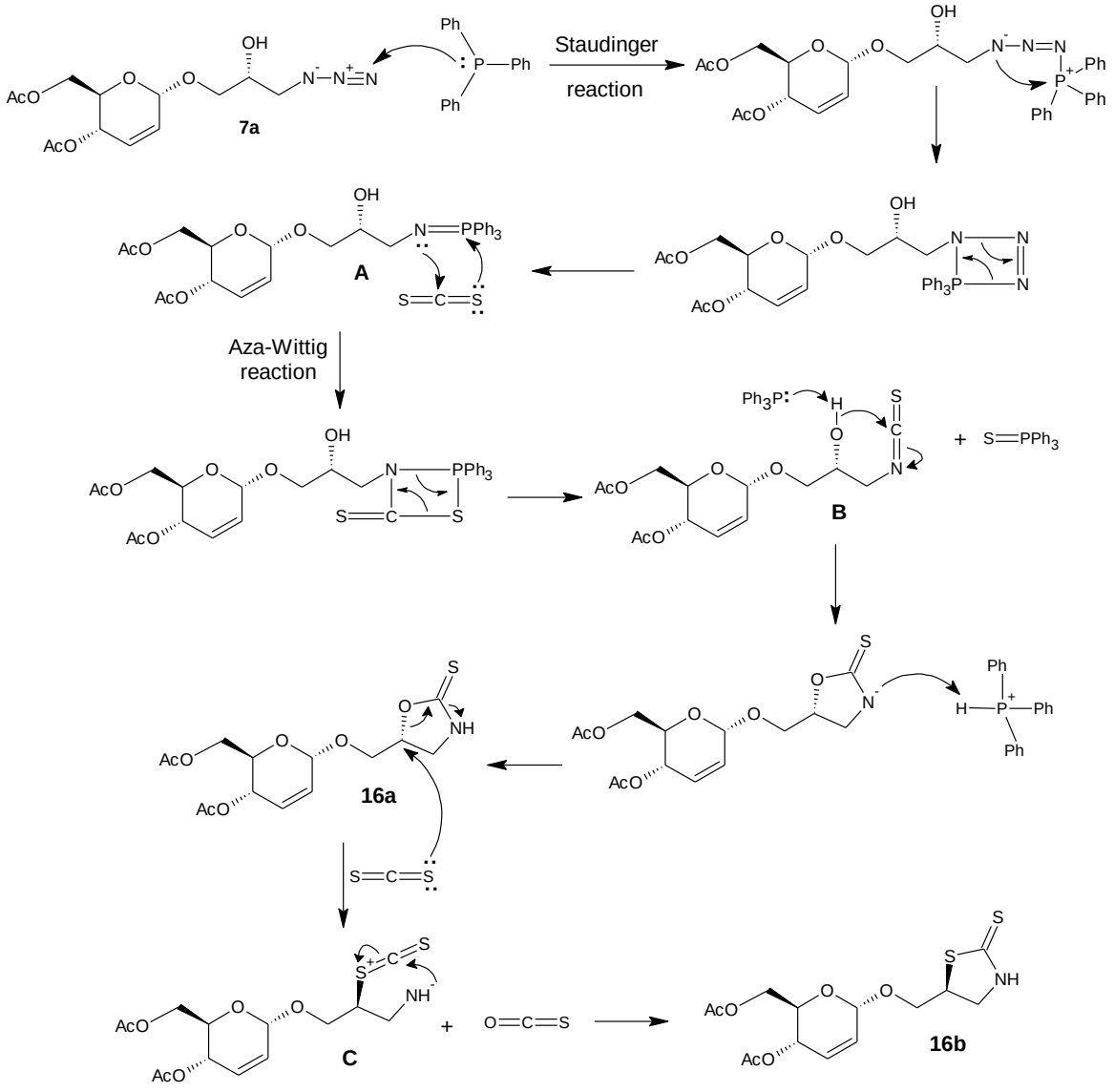

Source: The author (2024).

Following the mechanism already proposed in the literature (Mishra; Agrahari; Tiwari, 2017) and similar to the Staudinger reaction, the reaction starts with the formation of an iminophosphorane intermediate **A**, which reacts with CS_2 to generate

the isothiocyanate intermediate **B**, and then undergoes intramolecular attack of the vicinal hydroxyl group to generate oxazolidinethione **16a** (Scheme 35). With the excess of CS_2, the oxazolidinethione ring is attacked, and another intermediate **C** is formed to produce thiazolidinethione **16b**. It is important to note that during the formation of the isothiocyanate intermediate, triphenylphosphine sulfide is formed, which we believe is the 3p formed in our reaction. In our studies, was also observed the formation of 4p, which we wondered if it was the isothiocyanate intermediate **B**, and the NMR analysis confirmed that. The discussion of the structure will be presented next.

Figure 34 shows the ^{1}H NMR spectrum of 3p, and the signals found confirm that it's the triphenylphosphine sulfide. Between δ 7.69-7.65 ppm was found a multiplet referring to H-*o*, between δ 7.55-7.52 ppm there is another multiplet referring to H-*p*, and finally another multiplet between δ 7.48-7.44 ppm referring to H-*m*.

Figure 34 - ^{1}H NMR spectrum and expansion (500 MHz, $CDCl_3$) of 3p.

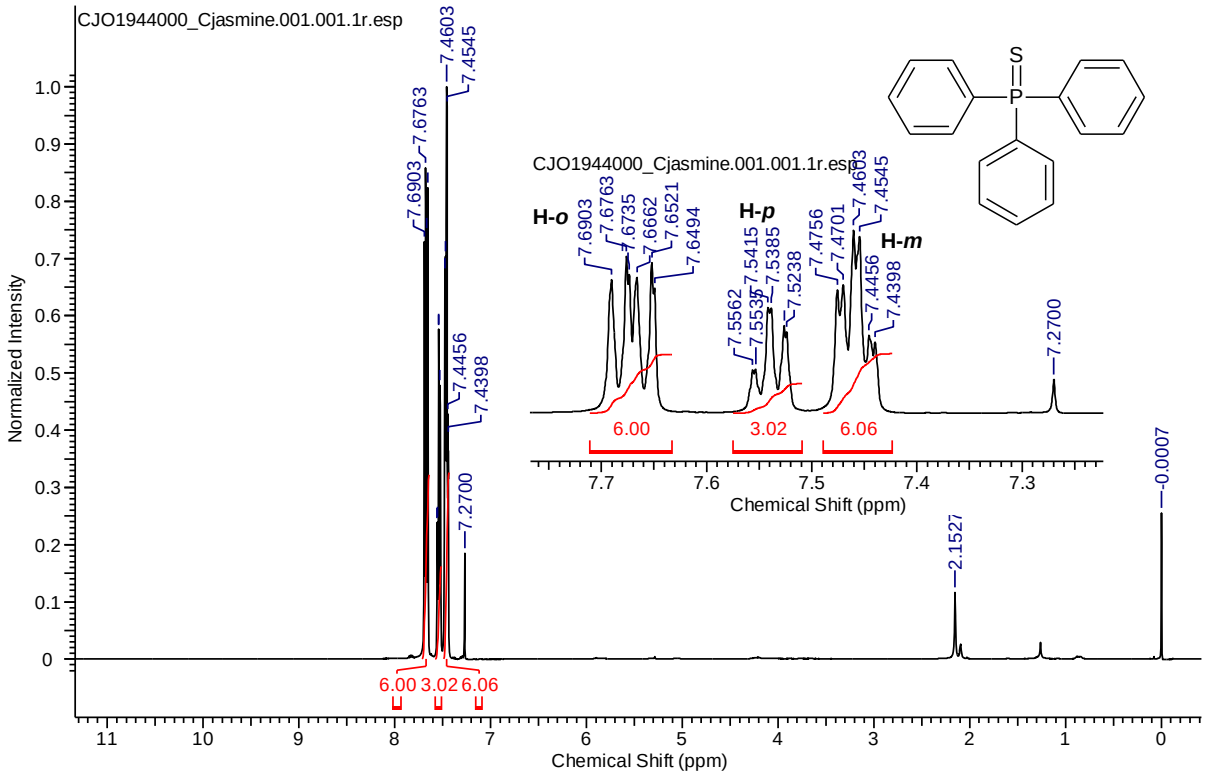

Source: The author (2024).

In the ^{1}H NMR spectrum of 4p in $CDCl_3$ (Figure 35), which we believe that is the isothiocyanate intermediate **16c**, was observed traces of the 3p, the triphenylphosphine sulfide, in the aromatic region (between 7-8 ppm). At δ 7.83 ppm was observed a singlet referring to the OH. At δ 5.92 ppm was found a duplet referring

to H-3 with $J_{3,2}$ = 10.25 Hz, while at δ 5.82 ppm was noticed a double triplet with $J_{2,3}$ = 10.2 Hz, $J_{2,1}$ = 4.55 Hz, and $J_{2,4}$ = 2.3 Hz referring to H-2.

Figure 35 - ^{1}H NMR spectrum and expansions (500 MHz, $CDCl_3$) of compound **16c**.

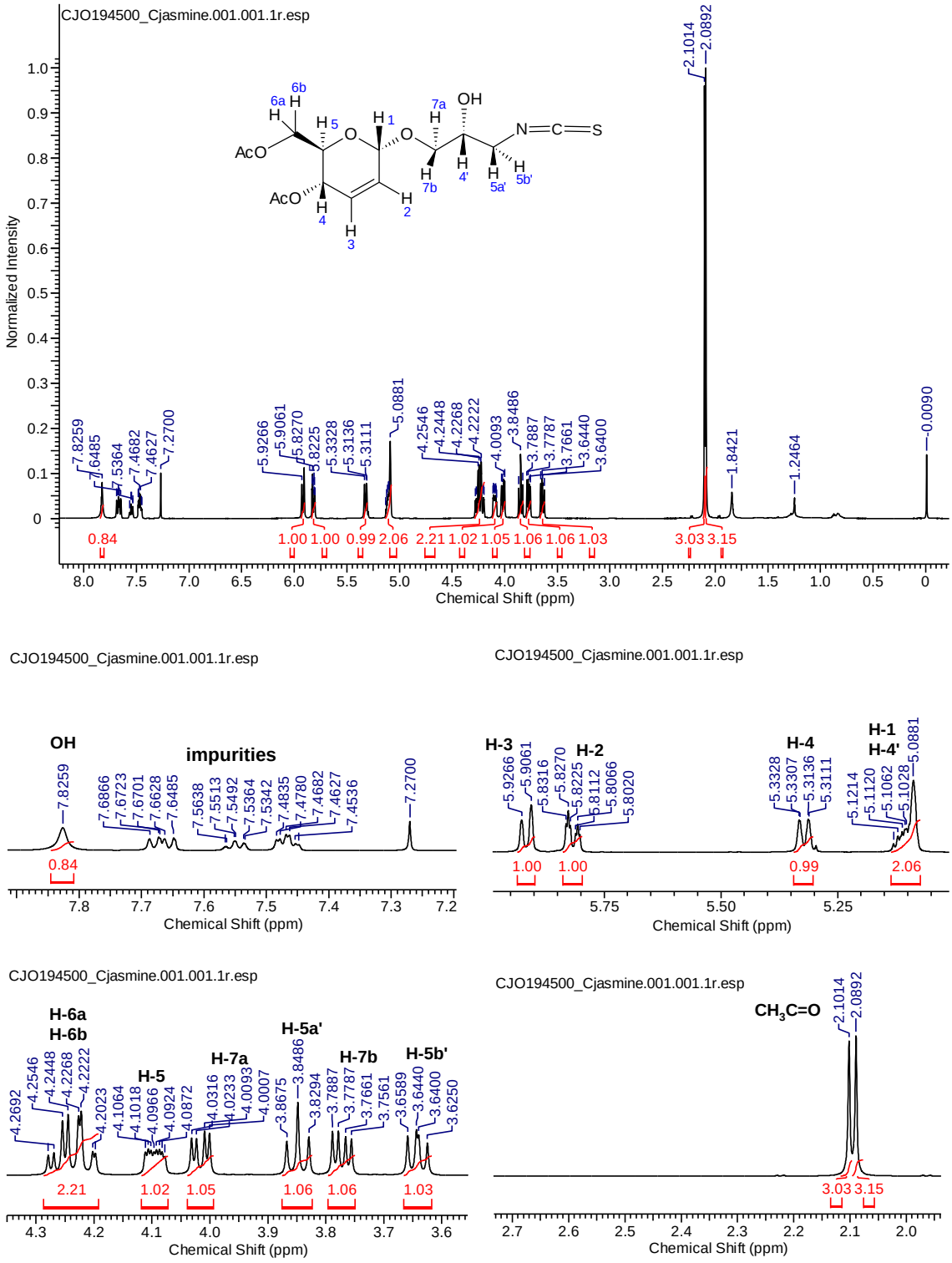

Source: The author (2024).

At δ 5.32 ppm was found a double duplet referring to H-4 with $J_{4,5}$ = 9.6 Hz and $J_{4,3}$ = 1.25 Hz, while between δ 5.13-5.09 ppm a multiplet referring to H-1 and H-4'. Between δ 4.28-4.20 ppm was found another multiplet referring to H-6a and H-6b, while between δ 4.11-4.08 ppm a multiplet referring to H-5. At δ 3.90 ppm was noticed a double duplet for H-5a' with $J_{5a',5b'}$ = 11.3 Hz and $J_{5a',4'}$ = 4.15 Hz, and a triplet at δ 3.85 ppm for H-7a with $J_{7a,7b}$ = 9.45 Hz. At δ 3.77 ppm was observed a double duplet referring to H-5b' with $J_{5b',5a'}$ = 11.3 Hz and $J_{5b',4'}$ = 5 Hz, and another double duplet at δ 3.64 ppm with $J_{7b,7a}$ = 9.45 HZ and $J_{7b,4'}$ = 7.15 Hz referring to H-7b. Finally, there are two singlets at δ 2.10 and δ 2.09 ppm from the methyls of the acetyl groups.

Figure 36 - ^{1}H NMR spectrum and expansions (500 MHz, DMSO-d_6) of compound **16c**.

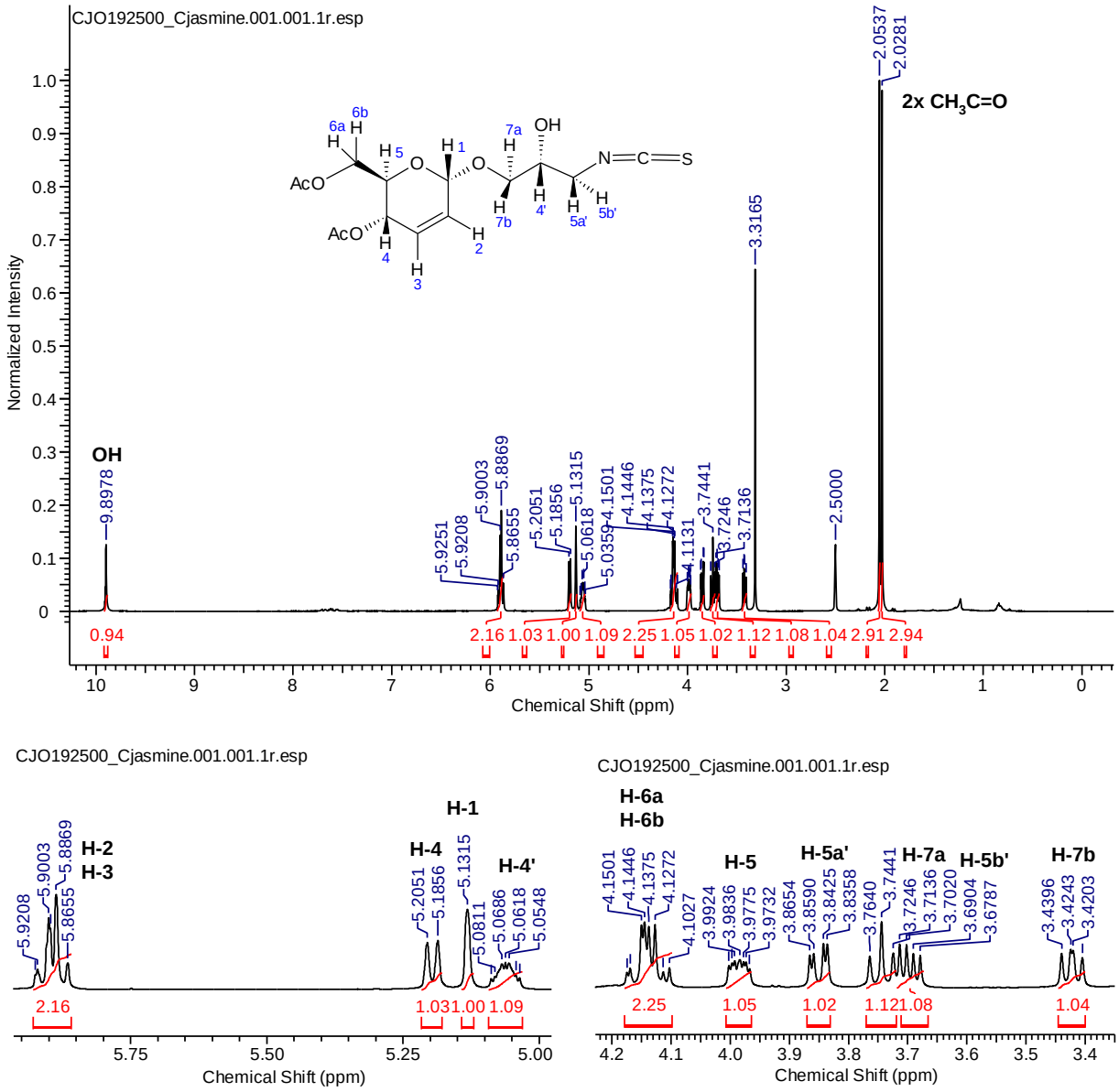

Source: The author (2024).

The sample was purified again and in the ^{1}H NMR spectrum was realized in DMSO-d_6 (Figure 36). At δ 9.90 ppm was observed a singlet referring to the OH, nothing was found in the aromatic region, and the other signs also confirm the structure. The presence of the OH signal in a high field, in the both spectrum $CDCl_3$ (δ 7.82 ppm) and DMSO-d_6 (δ 9.90 ppm), can be explained by the formation of a hydrogen bond. In a hydrogen bond, the H is receiving electron density from the donor atom, and the field created by the presence of the interaction causes deshielding. The hydrogen bond can be intramolecular between the OH and the nitrogen of the isothiocyanate group, or it can be intermolecular.

In the work carried out by Guimarães (2022, Thesis), the azido-alcohol reaction was carried out only with triphenylphosphine to form the iminophosphorane intermediate. In the ^{1}H NMR spectrum (Figure 37) presented in this work, the OH was found at δ 7.88 ppm and the H-1 and H-4' also came out together similarly to the spectrum of the isothiocyanate intermediate in $CDCl_3$ (Figure 35).

Figure 37 - 1H NMR spectrum (400 MHz, $CDCl_3$) of the iminophosphorane intermediate carried out by Guimarães (2022, Thesis).

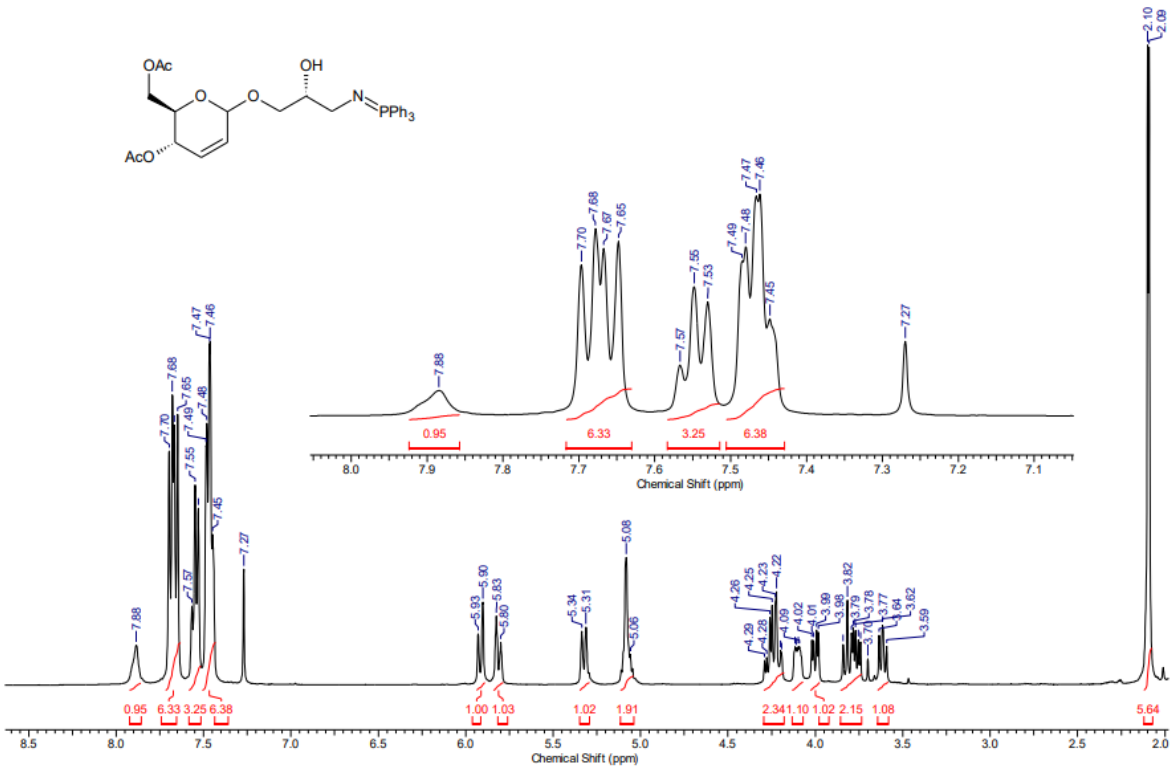

Source: Guimarães (2022, Thesis).

The ^{13}C NMR spectrum of 4p (Figure 38) shows a signal at δ 189.6 ppm, which refers to the carbon S=C=N, and the other signals correspond to the molecule.

Figure 38 - ^{13}C NMR spectrum (125 MHz, DMSO-d_6) of compound **16c**.

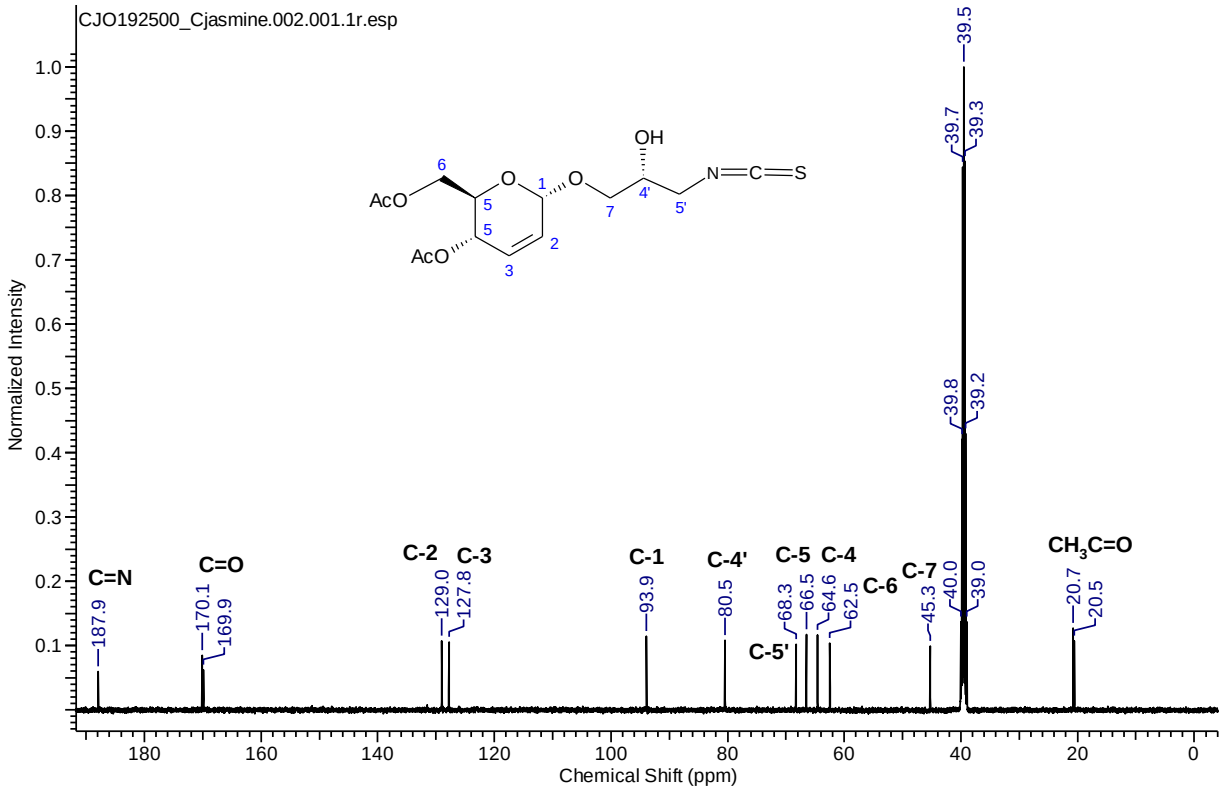

Source: The author (2024).

We decided to change reaction conditions such as CS_2 equivalence and time (Table 4) to see if the intermediate would be consumed. For the first entry, we carried out the reaction according to the methodology described by Mishra, Agrahari, and Tiwari (2017). In the second run, we left the reaction for longer, 6 hours, and there was no change in yield.

Table 4 - Optimizations carried out in the reaction to obtain 1,3-oxazolidine-2-thione **16a** and 1,3-thiazolidine-2-thione **16b** and isothiocyanate intermediate **16c**.

Entry	CS_2	Toluene	Time	Yield (16a)	Yield (16b)	Yield (16c)
1	1 mL (47 eq.)	1 mL	3h	22%	33%	18%
2	1 mL (47 eq.)	1 mL	6h	22%	33%	24%
3	2 mL (94 eq.)	2 mL	6h	22%	39%	25%

Source: The author (2024).

We then decided to double the equivalence of CS_2 (94 eq.) and leave the reaction for 6 hours and thus observed an increase in the yield of 1,3-thiazolidine-2-thione **14b**. However, in all the reactions we still observed the presence of 4p, which we consider to be the isothiocyanate intermediate, which indicates that the reaction is not being completed and may require a longer reaction time.

Oka, Yabuuchi, and Sekiguchi (2013) reported the synthesis of 2-mercapto-oxazoles by reacting 1 eq. of a *β*-ketoazide with 1.5 eq. of PPh_3 and 3 eq. of CS_2 in 1,4-dioxane for 4 hours. We decided to test the conditions proposed by the authors using our keto-azide **8** (Scheme 36).

Scheme 36 - Synthesis of 2-mercapto-oxazole **17**.

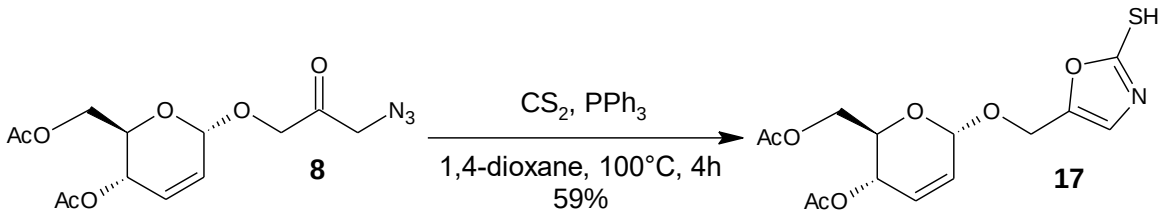

Source: The author (2024).

After 4 hours of reaction, the starting material was consumed and the formation of 2-mercapto-oxazole (OXT) **17** was observed in 59% yield. As with the previous reaction, during the mechanism of this reaction, the iminophosphorane intermediate was formed, which then reacted with CS_2 to generate the isothiocyanate intermediate and triphenylphosphine sulfide (Scheme 37). In the figure 39 we can see the TLC plate of the reaction and a spot under the product which could be triphenylphosphine sulfide.

Figure 39 - TLC plate revealed in ultraviolet light at 365 nm (a) and in 5% (v/v) sulfuric acid/ethanol (b) of the 2-mercapto-oxazole **17** formation reaction in EtOAc/Hex (6:4).

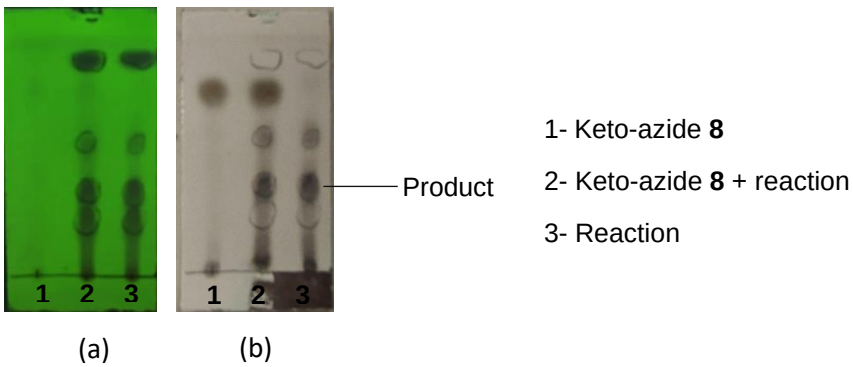

Source: The author (2024).

Scheme 37 - Mechanism for the formation of the 2-mercapto-oxazole **17** ring.

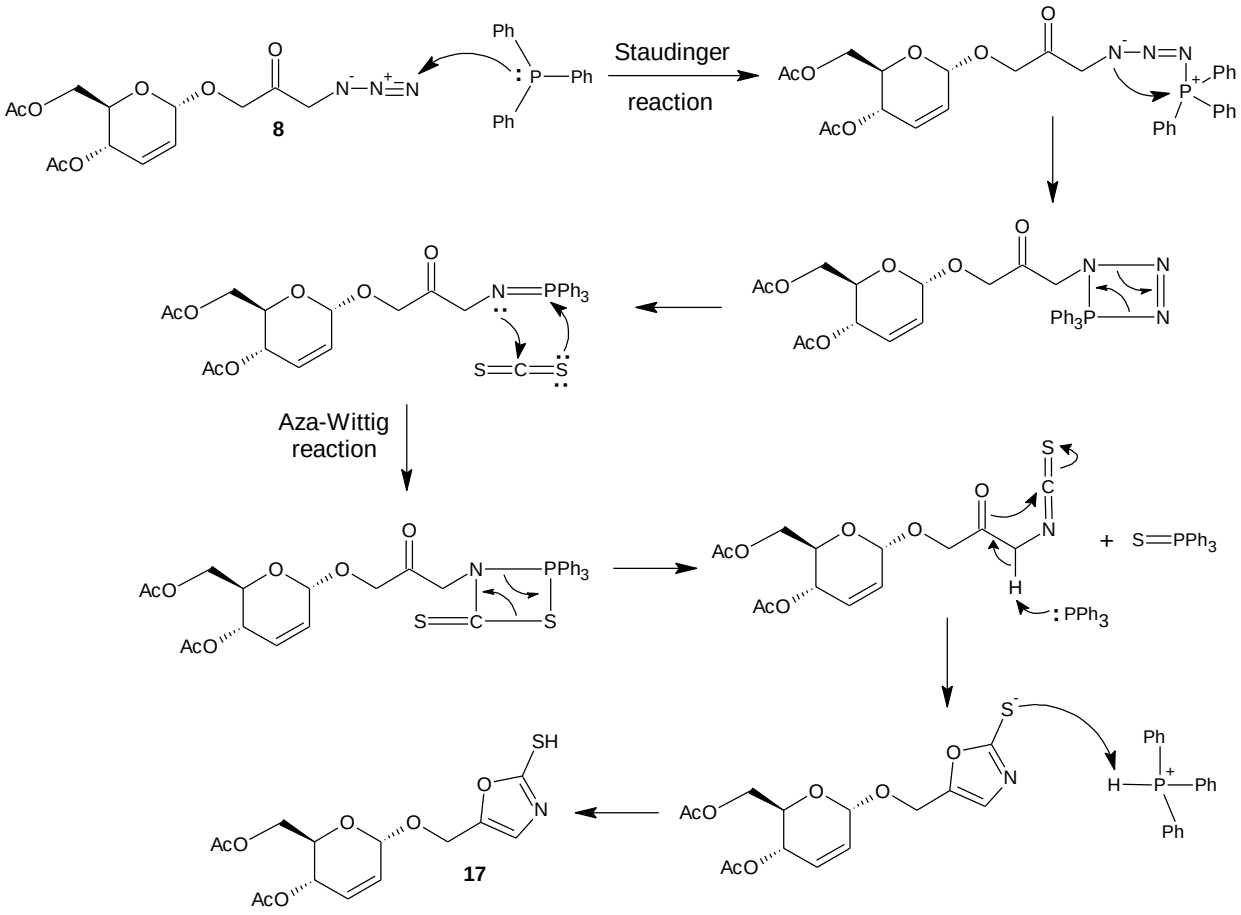

Source: The author (2024).

In the ^{1}H NMR spectrum of 2-mercapto-oxazole **17** (Figure 40), at δ 11.20 ppm was found a singlet referring to the SH of the 2-mercapto-oxazol structure. At δ 6.90 ppm was noticed a singlet referring to H-5', while at δ 5.95 ppm a duplet referring to H-3 with $J_{3,2}$ = 10.25 Hz. At δ 5.95 ppm was found a double triplet for H-2 with $J_{2,3}$ = 10.25 Hz, $J_{2,1}$ = 4.47 Hz, and $J_{2,4}$ = 2.3 Hz, while a double duplet for H-4 with $J_{4,5}$ = 9.65 Hz and $J_{4,2}$ = 1.1 Hz at δ 5.34 ppm. At δ 5.14 ppm was observed a singlet referring to H-1, a duplet with $J_{7a,7b}$ = 13.6 Hz referring to H-7a at δ 5.62 ppm, and another duplet referring to H-7b at δ 4.50 ppm with $J_{7b,7a}$ = 13.6 Hz. At δ 4.26 ppm was noticed a triplet referring to H-6a and H-6b with J = 4.75 Hz, and δ 4.13 from δ 4.10 ppm was observed multiplet referring to H-5. Finally, was found two singlets at δ 2.13 and δ 2.11 ppm referring to the two methyls from the acetyl groups.

Figure 40 - ^{1}H NMR spectrum and expansions (500 MHz, $CDCl_3$) of 2-mercapto-oxazole **17**.

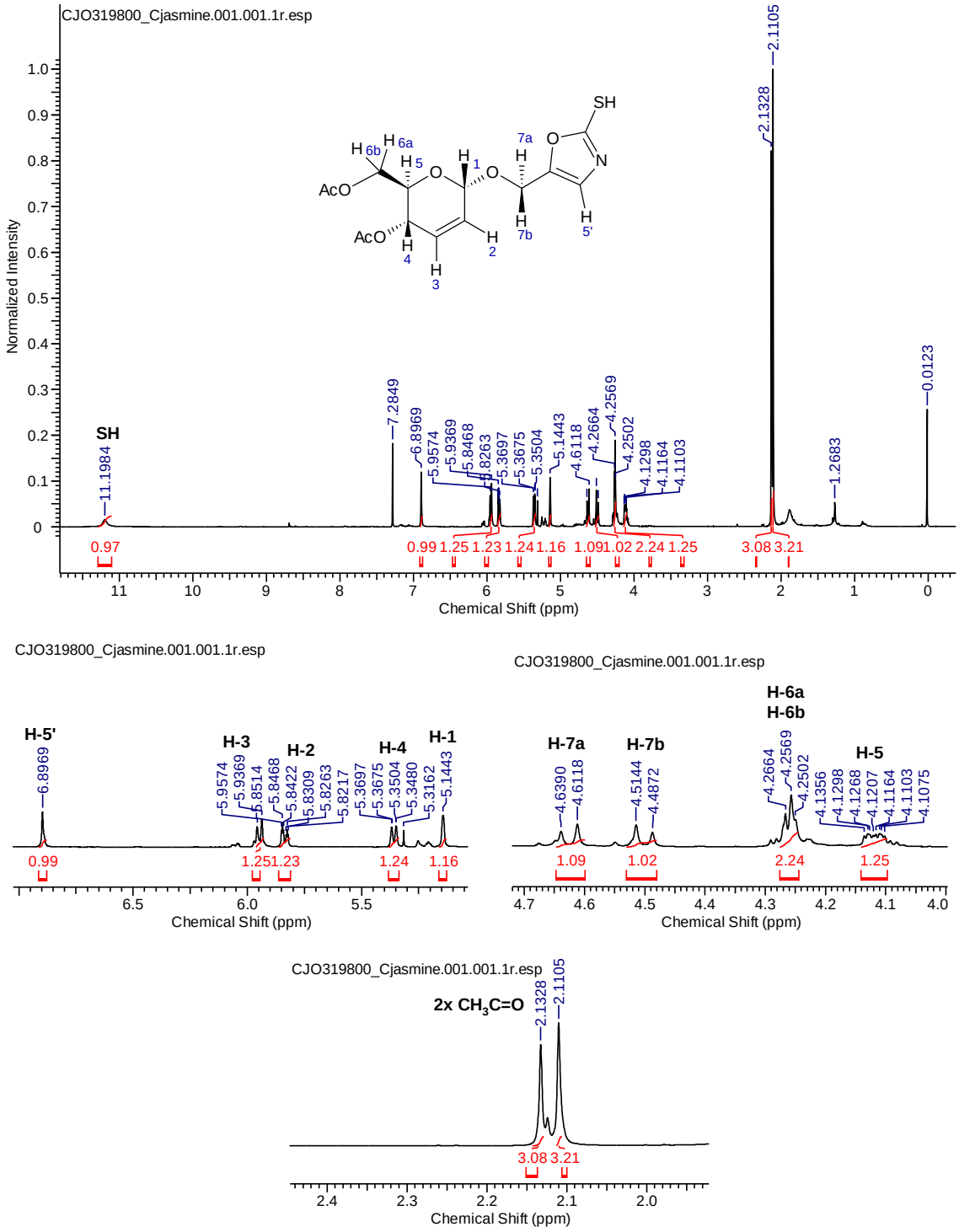

Source: The author (2024).

In the ^{13}C NMR spectrum of 2-mercapto-oxazole **17** (Figure 41), at δ 179.4 ppm was found the C-SH signal, while at δ 170.9 and δ 170.3 ppm was observed the signals from the two carbonyls of the acetyl groups. At δ 146.5 ppm was noticed the C-4' signal, while at δ 130.0 and δ 126.8 ppm the C-2 and C-3 signals. At δ 114.4 ppm was

observed C-5' and at δ 93.8 ppm the C-1 signal. At δ 67.3, δ 65.1, δ 62.8, and δ 59.3 ppm we found the C-5, C-4, C-6, and C-7 signals. Finally, we observed the methyls from the acetyl groups at δ 21.0 and δ 20.9 ppm.

Figure 41 - ^{13}C NMR spectrum (125 MHz, $CDCl_3$) of 2-mercapto-oxazole **17**.

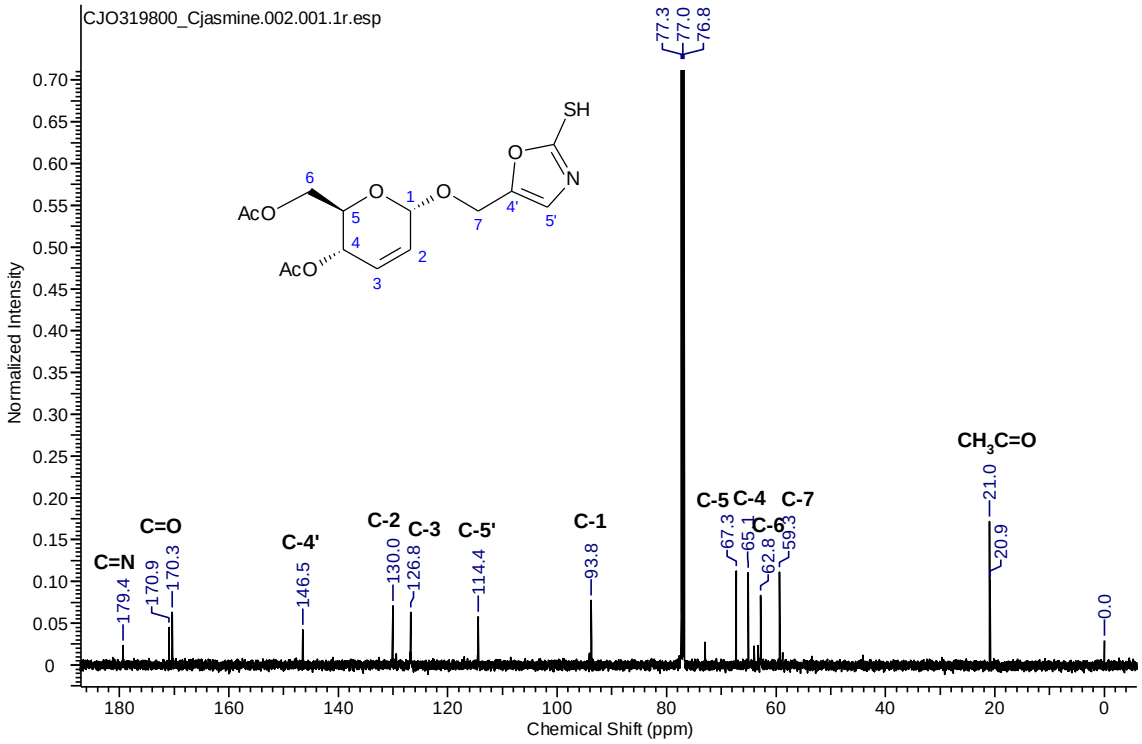

Source: The author (2024).

4.6 EVALUATION OF THE CYTOTOXIC AND ANTIMYCOBACTERIAL ACTIVITY

The compounds selected for evaluation against tuberculosis were the thio-derivatives oxazolidine-2-thione **16a**, thiazolidine-2-thione **16b**, and 2-mercapto-oxazole **17** (Figure 42). The cytotoxicity (CC_{50}) of thio-derivatives was carried out to assess the concentration capable of keeping more than 50% of the cells alive. The cells used were J774A.1, which corresponds to a murine macrophage, since the reproduction and dissemination cycle of *Mtb* occurs in host macrophages. Nine concentrations (128 to 0.5 µg/mL) of the compounds were used, as can be seen in figure 43, the compounds **16a** and 17 kept more than 50% of the cells alive from a concentration of 32 µg/mL, while compound **16b** kept more than 50% of the cells alive from a concentration of 8 µg/mL. Thus, compounds **16a** and **17** were the least toxic.

Figure 42 - Structures of the selected thio-derivatives.

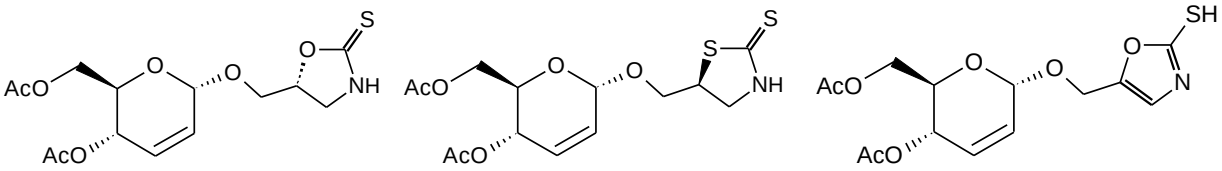

Oxazolidine-2-thione **16a** | Thiazolidine-2-thione **16b** | 2-mercapto-oxazole **17**

Source: The author (2024).

Figure 43 - Cytotoxicity graph of thio-derivatives **16a**, **16b** and **17**.

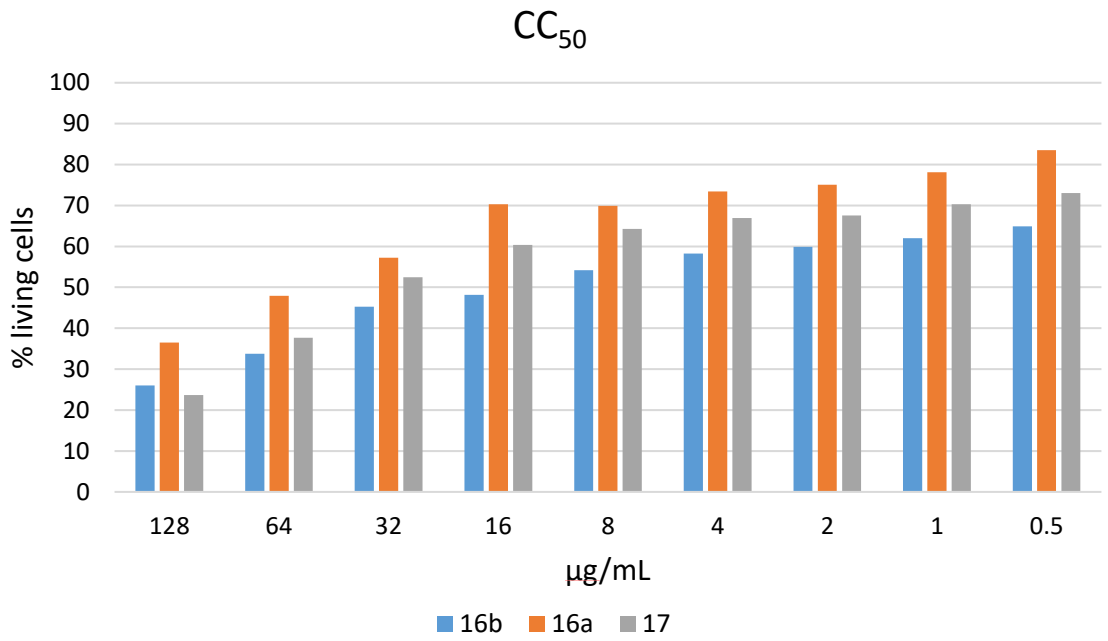

Source: The author (2024).

The antimycobacterial activity of compounds **16a**, **16b** and **17** was determined using the Minimum Inhibitory Concentration (MIC). *Mycobacterium tuberculosis* H37Ra was used as the reference strain, and rifampicin was used as the standard drug and its inhibitory concentration was 0.125 µg/mL (Table 5). The compounds did not inhibit the bacteria at the 9 concentrations (128 to 0.5 µg/mL), that were also used for cytotoxicity. In this way, they did not exhibit activity against tuberculosis, but they can be directed to another activity since they weren't toxic.

Table 5 - Antimycobacterial activity of compounds **16a**, **16b** and **17** against *Mtb* strain H37Ra expressed by Minimum Inhibitory Concentration (MIC).

Compound	J774A.1	H37Ra
	CC_{50} (µg/mL)	MIC (µg/mL)
16a	32	>128
16b	8	>128
17	32	>128
Rifampicin	-	0.125

Source: The author (2024).

5 CONCLUSION

Initially, the precursor materials were prepared: glycerol carbonate **1**, glycerol thio-carbonate **4** after three steps from GC, tri-*O*-acetyl-*D*-glucal **5**, and PSE-glucal **10** after two steps from *D*-glucal, with yields of 96, 85, 49, and 77%, respectively. It was possible to observe that the presence of the phenylsulfonylethylidene (PSE) protective group implies unusual behavior in the *O*-glycosylation reactions. In the epoxidation reaction of PSE-glucal **10** with m-CPBA was observed the stereoselective formation of the new *α*-mannopyranoside **11** with yield of 42% in conventional condition, and 52% in focused irradiation with a reduction in reaction time from 3 hours to 10 min. The acetylated *α*-mannopyranoside **12** was obtained after acetylation reaction under acidic conditions, with a yield of 77%. We take advantage of the m-chlorobenzoate moiety in the anomeric position to use the *α*-mannopyranoside **12** as a glycosyl donor in glycosylation with glycerol carbonate ring to form the unprecedented *β*-mannopyranoside **13** in 64% yield as a mixture of diastereoisomer. On the other hand, applying direct Ferrier reaction conditions, onto PSE-glucal **10** with glycerol carbonate lead to the addition reaction to form the diasteroisomeric mixture *R*/*S* of the *α*-2-deoxy-*O*-glycoside **14b** with yield 42% and an also an complex isomeric mixture **14a** with 33% yield. Attempts for *S*-glycosylation with glycerol thio-carbonate **4** onto tri-O-acetyl-*D*-glucal **5** using K-10 doped with 5% or 10% $FeCl_3.H_2O$ or $BF_3.Et_2O$ as Lewis acid were unsuccessful. Finally, from the (S) azido-alcohol **7a**, obtained by opening the cyclic carbonate ring of the 2,3-unsaturated O-glycoside **6a,** we carried out the cyclization with CS_2 to prepare the new oxazolidine-2-thione **16a** (22%) and thiazolidine-2-thione **16b** (39%) rings. The new 2-mercapto-oxazole **17** (59%) was also prepared from the keto-azide **8**, which was obtained after the oxidation reaction of the mixture of diastereoisomers **7a**/**7b** with an 88% yield. No biological activity against tuberculosis (H37Ra) was observed for the compounds **16a**, **16b** and **17**. Furthemore, these compounds showed low cytotoxicity in macrophage cells (J774A.1), and will be considered for further biological activities.

6 FUTURE SCOPE

We plan to synthesize of azido-alcohols and keto-azides from mannopyranosides and 2-deoxy-*O*-glucosides, and the synthesis of the oxazolidine-2-thione, thiazolidine-2-thione, and 2-mercapto-oxazole rings from this azido-alcohols and keto-azides. We also plan to carry out a carbon-carbon coupling reaction onto the oxazolidine-2-thione, thiazolidine-2-thione, and 2-mercapto-oxazole rings.

REFERENCES

AGNIHOTRI, G.; TIWARI, P.; MISRA, A. K. One-pot synthesis of per-O-acetylated thioglycosides from unprotected reducing sugars. **Carbohydrate research**, 2005, 340, 1393-1396. https://doi.org/10.1016/j.carres.2005.02.027.

AL-MULLA, A. A review: biological importance of heterocyclic compounds. **Der Pharma Chemica**, 2017, 9, 141-147. ISSN: 0975-413X.

ARBEX, M. A.; VARELLA, M. C. L.; SIQUEIRA, H. R.; MELLO, F. A. F. Drogas antituberculose: interações medicamentosas, efeitos adversos e utilização em situações especiais-parte 1: fármacos de primeira linha. **Jornal Brasileiro de Pneumologia**, 2010, 36, 626-640. https://doi.org/10.1590/S1806-37132010000500016.

ARORA, P.; ARORA, V.; LAMBA, H.S.; WADHWA, D. Importance of heterocyclic chemistry: a review. **International Journal of Pharmaceutical Sciences and Research**, 2012, 3, 2947. ISSN: 0975-8232

BANSAL, S.; HALVE, A. K. Oxazolines: Their synthesis and biological activity. **International Journal of Pharmaceutical Sciences and Research**, 2014, 5, 4601. https://doi.org/10.13040/IJPSR.0975-8232.

CHECA, M.; NOGALES-DELAGADO, S.; MONTES, V.; ENCINAR, J. M. Recent advances in glycerol catalytic valorization: A review. **Catalysts**, 2020, 10, 1279. https://doi.org/10.3390/catal10111279.

CHÉRY, F.; CABIANCA, E.; TATIBOUËT, A.; DE LUCCHI, O.; ROLLIN, P. Carbohydrate-derived PSE acetals: controlled base-induced ring cleavage. **Tetrahedron**, 2012, 68, 544-551. https://doi.org/10.1016/j.tet.2011.11.009.

CHÉRY, F.; ROLLIN, P.; DE LUCCHI, O.; COSSU, S. Phenylsulfonylethylidene (PSE) acetals as atypical carbohydrate-protective groups. **Tetrahedron Letters**, 2000, 41, 2357-2360. https://doi.org/10.1016/S0040-4039(00)00199-4.

CHÉRY, F.; ROLLIN, P.; DE LUCCHI, O.; COSSU, S. Phenylsulfonylethylidene (PSE) Acetals: A Novel Protective Group in Carbohydrate Chemistry. **Synthesis**, 2001, 2001, 0286-0292. https://doi.org/10.1055/s-2001-10817.

CODÉE, J. D.C.; ALI, A.; OVERKLEEFT, H.S.; VAN DER MAREL, G. A. Novel protecting groups in carbohydrate chemistry. **Comptes Rendus Chimie**, 2011, 14, 178-193. https://doi.org/10.1016/j.crci.2010.05.010.

DA COSTA, P. L. F.; MELO, V. N.; GUIMARÃES, B. M.; SCHULER, M.; PIMENTA, V.; ROLLIN, P.; TATIBOUËT, A.; DE OLIVEIRA, R. N. Glycerol carbonate in Ferrier reaction: Access to new enantiopure building blocks to develop glycoglycerolipid analogues. **Carbohydrate Research**, 2016, 436, 1-10. https://doi.org/10.1016/j.carres.2016.10.009.

DE LUCCHI, O.; LUCCHINI, V.; PASQUATO, L.; MODENA, G. The (Z)-and (E)-1, 2-bis (phenylsulfonyl) ethylenes as synthetic equivalents to acetylene as dienophile. **The Journal of Organic Chemistry**, 1984, 49, 596-604. https://doi.org/10.1021/jo00178a004.

DE LUCCHI, O.; PASQUATO, L.; ROLLIN, P.; TATIBOUËT, A. 1, 2-Bis (phenylsulfonyl) ethylene. **Encyclopedia of Reagents for Organic Synthesis**, 2005. https://doi.org/10.1002/047084289X.rb183.pub2.

DE OLIVEIRA, R. J.; GUIMARÃES, B. M.; SILVA, R. O.; RAMOS, C. S.; HOLANDA, L. E. G.; FREITAS, J. C. R.; FREITAS FILHO, J. R. Ocorrência, Biossíntese, Síntese e Aplicações de S-Glicosídeos: uma Visão Geral. **Revista Virtual de Química**, 2021, 13, 13-42. ISSN: 1984-6835.

DUA, R.; SHRIVASTAVA, S.; SONWANE, S. K.; SRIVASTAVA, S. K. Pharmacological significance of synthetic heterocycles scaffold: a review. **Advances in Biological Research**, 2011, 5, 120-144. ISSN: 1992-0067.

FERNANDES, A.; DELL'OLMO, M.; TATIBOUËT, A.; IMBERTY, A.; PHILOUZE, C.; ROLLIN, P. Dramatic effect of PSE clamping on the behaviour of d-glucal under Ferrier I conditions. **Tetrahedron Letters**, 2008, 49, 3484-3488. https://doi.org/10.1016/j.tetlet.2008.03.093.

FOTI, C.; PIPERNO, A.; SCALA, A.; GIUFFRÈ, O. Oxazolidinone antibiotics: chemical, biological and analytical aspects. **Molecules**, 2021, 26, 4280. https://doi.org/10.3390/molecules26144280.

GADE, S. M.; SAPTAL, V. B.; BHANAGE, B. M. Perception of glycerol carbonate as green chemical: Synthesis and applications. **Catalysis Communications**, 2022, 106542. https://doi.org/10.1016/j.catcom.2022.106542.

GANDHI, N.; SRIVASTAVA, B. K.; LOHRAY, V. B.; LOHRAY, B. B. Oxazolidine-2-thiones: a molecular modeling study. **Tetrahedron letters**, 2004, 45, 6269-6272. https://doi.org/10.1016/j.tetlet.2004.06.090.

GHOSH, B.; KULKARNI, S. S. Advances in protecting groups for oligosaccharide synthesis. **Chemistry–An Asian Journal**, 2020, 15, 450-462. https://doi.org/10.1002/asia.201901621.

GIARDI, C.; LAPINTE, V.; NIELLOUD, F.; DEVOISSELLE, J.M.; ROBIN, J.J. Synthesis of polyoxazolines using glycerol carbonate derivative and end chains functionalization via carbonate and isocyanate routes. **Journal of Polymer Science Part A: Polymer Chemistry**, 2010, 48, 4027-4035. https://doi.org/10.1002/pola.24188.

GONÇALVES, R. S. B.; KAISER, C. R.; LORENÇO, M. C. S.; BEZERRA, F. A. F. M.; DE SOUZA, M. V. N.; WARDELL, J. L.; WARDELL, S. M. S. V.; HENRIQUES, M. G. M. O.; COSTA, T. Mefloquine–oxazolidine derivatives, derived from mefloquine and arenecarbaldehydes: In vitro activity including against the multidrug-resistant

tuberculosis strain T113. **Bioorganic & medicinal chemistry**, 2012, 20, 243-248. https://doi.org/10.1016/j.bmc.2011.11.006.

GUIMARÃES, B. M. **PLANEJAMENTO SINTÉTICO, ELUCIDAÇÃO ESTRUTURAL E AVALIAÇÃO BIOLÓGICA DE INÉDITOS O-GLICOSÍDEOS 2,3-INSATURADOS CANDIDATOS A DROGAS COM PROPRIEDADES BIOATIVAS**. 2022. Thesis (Doctorate in chemistry) - Universidade Federal Rural de Pernambuco, Recife, 2022.

GUO, J.; YE, X. Protecting groups in carbohydrate chemistry: influence on stereoselectivity of glycosylations. **Molecules**, 2010, 15, 7235-7265. https://doi.org/10.3390/molecules15107235.

HOUACHE, M. S.; HUGHES, K.; BARANOVA, E. A. Study on catalyst selection for electrochemical valorization of glycerol. **Sustainable Energy & Fuels**, 2019, 3, 1892-1915. https://doi.org/10.1039/C9SE00108E.

HUNG, S.; WANG, C. Protecting group strategies in carbohydrate synthesis. **Glycochemical Synthesis: Strategies and Applications**, 2016, 35-68. https://doi.org/10.1002/9781119006435.ch2.

KABIR, E.; UZZAMAN, M. A review on biological and medicinal impact of heterocyclic compounds. **Results in Chemistry**, 2022, 100606. https://doi.org/10.1016/j.rechem.2022.100606.

KAFLE, A.; LIU, J.; CUI, L. Controlling the stereoselectivity of glycosylation via solvent effects. **Canadian Journal of Chemistry**, 2016, 94, 894-901. https://doi.org/10.1139/cjc-2016-0417.

KAUR, J.; SARMA, A. K.; JHA, M. K.; GERA, P. Valorisation of crude glycerol to value-added products: Perspectives of process technology, economics and environmental issues. **Biotechnology Reports**, 2020, 27, 00487. https://doi.org/10.1016/j.btre.2020.e00487.

KEDERIENĖ, V.; ROUSSEAU, J.; SCHULER, M.; SACKUS, A., TATIBUOËT, A. Copper-catalyzed S-arylation of Furanose-Fused Oxazolidine-2-thiones. **Molecules**, 2022, 27, 5597. https://doi.org/10.3390/molecules27175597.

KOMAROVA, B. S.; USTYUZHANINA, N. E., TSVETKOV, Y. E., NIFANTIEV, N. E. Stereocontrol of 1, 2--Glycosylation by Remote O-Acyl Protecting Groups. **Modern Synthetic Methods in Carbohydrate Chemistry: From Monosaccharides to Complex Glycoconjugates**, 2013, 125-159. https://doi.org/10.1002/9783527658947.ch5.

KOZAKEVICH, G. V.; SILVA, R. M. TUBERCULOSE: REVISÃO DE LITERATURA. **Arquivos Catarinenses De Medicina**, 2015, 44, 34–47.

LECONTE, N., SILVA, S.; TATIBOUËT, A.; RAUTER, A. P.; ROLLIN, P. Aromatic or chiral heterocycle-Balance between 1, 3-oxazoline-2-thione and 1, 3-oxazolidine-2-thione. **Synlett**, 2006, 2006, 301-305. https://doi.org/10.1055/s-2005-923583.

LIAN, G.; ZHANG, X.; YU, B. Thioglycosides in carbohydrate research. **Carbohydrate research**, 2015, 13-22. https://doi.org/10.1016/j.carres.2014.06.009.

LIMA, P. J. M.; DA SILVA, R. M.; GIRÃO NETO, C. A. C.; SILVA, N. C. G.; SOUZA, J. E. S.; NUNES, Y. L.; DOS SANTOS, J. C. S. An overview on the conversion of glycerol to value-added industrial products via chemical and biochemical routes. **Biotechnology and Applied Biochemistry**, 2022, 69, 2794-2818. https://doi.org/10.1002/bab.2098.

MARÍN, I.; CASTILHA, J.; MATHEU, M. I.; DÍAZ, Y.; CASTIILLÓN, S. Sequential Directed Epoxydation-Acidolysis from Glycals with MCPBA. A Flexible Approach to Protected Glycosyl Donors. **The Journal of Organic Chemistry**, 2011, 76, 9622-9629. https://doi.org/10.1021/jo201165v.

MASSABNI, A. C.; BONINI, E. H. Tuberculose: história e evolução dos tratamentos da doença. **Revista Brasileira Multidisciplinar**, 2019, 22, 6-34. https://doi.org/10.25061/2527-2675/ReBraM/2019.v22i2.678.

MELO, V. N.; DANTAS, W. M.; CAMARA, C. A.; DE OLIVEIRA, R. N. Synthesis of 2, 3-unsaturated alkynyl O-glucosides from tri-O-acetyl-d-glucal by using montmorillonite K-10/iron (III) chloride hexahydrate with subsequent copper (I)-catalyzed 1, 3-dipolar cycloaddition. **Synthesis**, 2015, 47, 3529-3541. https://doi.org/10.1055/s-0034-1378829.

MICHALSKA, K.; KARPIUK, I.; KRÓL, M.; TYSKI, S. Recent development of potent analogues of oxazolidinone antibacterial agents. **Bioorganic & medicinal chemistry**, 2013, 21, 577-591. https://doi.org/10.1016/j.bmc.2012.11.036.

MISHRA, K. B.; AGRAHARI, A. K.; TIWARI, V. K. One-pot synthesis of oxazolidine-2-thione and thiozolidine-2-thione from sugar azido-alcohols. **Carbohydrate research**, 2017, 450, 1-9. https://doi.org/10.1016/j.carres.2017.08.002.

MORALES-NAVA, R.; FERNÁNDEZ-ZERTUCHE, M.; ORDÓÑEZ, M. Microwave-assisted improved synthesis of oxazolidin-2-ones, oxazolidine-2-thiones and thiazolidine-2-thione chiral auxiliaries. **Molecules**, 2011, 16, 8803-8814. https://doi.org/10.3390/molecules16108803.

MORASKI, G. C.; FRANZBLAU, S. G.; MILLER, M. J. Utiliztion of the suzuki coupling to enhance the antituberculosis activity of aryl oxazoles. **Heterocycles**, 2010a, 80, 977. https://doi.org/10.3987%2FCOM-09-S(S)69.

MORASKI, G. C.; CHANG, M.; VILLEGAS-ESTRADA, A.; FRANZBLAU, S. G.; MÖLLMANN, U.; MILLER, M. J. Structure–activity relationship of new anti-tuberculosis agents derived from oxazoline and oxazole benzyl esters. **European Journal of Medicinal Chemistry**, 2010b, 45, 1703-1716. https://doi.org/10.1016/j.ejmech.2009.12.074.

MOURA, A. L.; LIMA, L. M. A.; BEZERRA, G. B.; FREITAS, J. J. R.; BELIAN; M. F.; RAMOS, C. S.; AVELINO, R. A.; FREITAS FILHO, J. R. O-glicosídeos 2, 3-

insaturados: aplicações, rearranjo de ferrier e reações. **Química Nova**, 2018, 41, 550-566. https://doi.org/10.21577/0100-4042.20170209.

MUKHERJEE, M. M.; GHOSH, R.; HANOVER, J. A. Recent advances in stereoselective chemical O-glycosylation reactions. **Frontiers in Molecular Biosciences**, 2022, 9, 896187. https://doi.org/10.3389/fmolb.2022.896187.

OKA, Y.; YABUUCHI, T.; SEKIGUCHI, Y. A CONVENIENT SYNTHESIS OF 2-MERCAPTO-OXAZOLES VIA β-KETOAZIDE AND ITS APPLICATION TO A KEY INTERMEDIATE OF PI3Kγ INHIBITORS. **Heterocycles**, 2013, 87, 1881-1887. ISSN：0385-5414.

OLIVEIRA, V. N. **Síntese e atividade biológica de glicoglicero-heterociclos funcionalizados com 1, 2, 3-triazol/1, 2, 4-oxadiazol**. 2020. Thesis (Doctorate in chemistry) - Universidade Federal de Pernambuco, Recife, 2020.

OSCARSON, S. S-Glycosylation. **Glycoscience: Chemistry and Chemical Biology I–III**, 2001, 643-671.

PANDIT, N.; SINGLA, R. K.; SHRIVASTAVA, B. Current updates on oxazolidinone and its significance. **International Journal of Medicinal Chemistry**, 2012. https://doi.org/10.1155/2012/159285

PARHAM, W. E.; HEBERLING, J. Heterocyclic Vinyl Ethers. IX. 1 Substitution Reactions of cis-and trans-Bis-(phenylmercapto)-ethylene. **Journal of the American Chemical Society**, 1955, 77, 1175-1177. https://doi.org/10.1021/ja01610a027.

PÉTURSSON, S. Protecting groups in carbohydrate chemistry. **Journal of Chemical Education**, 1997, 74, 1297. https://doi.org/10.1021/ed074p1297.

PROCOPIO, A.; DALPOZZO, R.; DE NINO, A.; MAIUOLO, L., NARDI, M., OLIVERIO, M.; RUSSO, B. A facile Er (OTf) 3-catalyzed synthesis of 2, 3-unsaturated O-and S-glycosides. **Carbohydrate Research**, 2007, 342, 2125-2131. https://doi.org/10.1016/j.carres.2007.05.034.

REDDY, R. B.; SURENDER, E.; MOULI, G. V. P. C.; REDDY, Y. D. Synthesis and antimicrobial activity of 2-substituted mercapto (4: 5)-phenazino oxazole derivatives. **Phosphorus and Sulfur and the Related Elements**, 1984, 20, 49-53. https://doi.org/10.1080/03086648408077610.

ROKICKI, G.; RAKOCZY, P.; PARZUCHOWSKI, P.; SOBIECKI, M. Hyperbranched aliphatic polyethers obtained from environmentally benign monomer: glycerol carbonate. **Green Chemistry**, 2005, 7, 529-539. https://doi.org/10.1039/B501597A.

ROUSSEAU, J.; ROUSSEAU, C.; LYNIKAITÈ, B.; SACKUS, A.; DE LEON, C.; ROLLIN, P.; TATIBOUËT, A. Tosylated glycerol carbonate, a versatile bis-electrophile to access new functionalized glycidol derivatives. **Tetrahedron**, 2009, 65, 8571-8581. https://doi.org/10.1016/j.tet.2009.07.095.

SANSINENEA, E.; ORTIZ, A.; ROLLIN, P.; SILVA, S. Oxazolidine-and oxazoline-2-thiones: an update. **Current Organic Synthesis**, 2017, 14, 1109-1131. https://doi.org/10.2174/1570179414666170503165413.

SAYGILI, N.; ÖZALP, M.; YILDIRIM, L. T. Synthesis, X-ray Analysis, and Biological Activities of Novel Oxazolidinethiones. **Journal of Heterocyclic Chemistry**, 2014, 51, 1264-1269. https://doi.org/10.1002/jhet.1863.

SHAMSZAD, M.; CRIMMINS, M. T. **Amino acid derived heterocyclic chiral auxiliaries**: the use of oxazolidinones, oxazolidinethiones, thiazolidinethiones, and imidazolidinones. 1° edition, Volume 3. Elsevier Science, 2012. https://doi.org/10.1016/b978-0-08-095167-6.00302-5.

SHULL, B. K.; WU, Z.; KOREEDA, M. A convenient, highly efficient one-pot preparation of peracetylated glycals from reducing sugars. **Journal of carbohydrate chemistry**, 1996, 15, 955-964. https://doi.org/10.1080/07328309608005701.

SILVA, S.; SYLLA, B.; SUZENET, F.; TATIBOUËT, A.; RAUTER, A. P.; ROLLIN, P. Oxazolinethiones and oxazolidinethiones for the first copper-catalyzed desulfurative cross-coupling reaction and first Sonogashira applications. **Organic Letters**, 2008a, 10, 853-856. https://doi.org/10.1021/ol703003e.

SILVA, S.; TARDY, S.; ROUTIER, S.; SUZENET, F.; TATIBOUËT, A.; RAUTER, A. P.; ROLLIN, P. 1, 3-Oxazoline-and 1, 3-oxazolidine-2-thiones as substrates in direct modified Stille and Suzuki cross-coupling. **Tetrahedron Letters**, 2008b, 49, 5583-5586. https://doi.org/10.1016/j.tetlet.2008.07.023.

SIMAO, A.C.; LYNIKAITE-PUKLEVICIENEA, B.; ROUSSEAU, C.; TATIBUOËT, A.; CASSEL, S.; SACKUS, A.; RAUTER, A. P., ROLLIN, P. 1, 2-Glycerol carbonate: a versatile renewable synthon. **Letters in Organic Chemistry**, 2006, 3, 744-748. http://dx.doi.org/10.2174/157017806779025960.

SINGH, G.; PRADHAN, G.; PRADHAN, S.; SHARMA, Y. C. Transformation of biodiesel waste glycerol to value added glycerol carbonate. **Chemical Science Review and Letters**, 2020, 9, 1003-1013. https://doi.org/10.37273/chesci.CS205107179.

SOUZA NETO, P. R.; GUIMARÃES, B. M.; FREITAS, J. J. R.; DE OLIVEIRA, R. N.; FREITAS FILHO, J. R. DESENVOLVIMENTO NOS MÉTODOS DE GLICOSILAÇÃO: UMA CHAVE PARA ACESSAR SUAS APLICAÇÕES NA SÍNTESE DE MOLÉCULAS BIOATIVAS. **Química Nova**, 2021, 44, 432-459. http://dx.doi.org/10.21577/0100-4042.20170676.

TRUCE, W. E.; MCMANIMIE, R. J. Stereoisomeric 1, 2-Bis-(arylmercapto)-ethenes and Corresponding Sulfones1. **Journal of the American Chemical Society**, 1954, 76, 5745-5747. https://doi.org/10.1021/ja01651a036.

VAN DER VORM, S.; HANSEN, T.; OVERKLEEFT, H. S.; VAN DER MAREL, G. A.; CODÉE, J. D. C. The influence of acceptor nucleophilicity on the glycosylation reaction

mechanism. **Chemical Science**, 2017, 8, 1867-1875. https://doi.org/10.1039/C6SC04638J.

VILKAUSKAITĖ, G.; KRIKSTOLAITYTE, S.; PALIULIS, O.; ROLLIN, P.; TATIBOUËT, A.; SACKUS, A. Use of tosylated glycerol carbonate to access N-glycerylated aza-aromatic species. **Tetrahedron**, 2013, 69, 3721-3727. https://doi.org/10.1016/j.tet.2013.03.002.

VOLBEDA, A. G.; VAN DER MAREL, G. A.; CODÉE, J. D. C. Protecting group strategies in carbohydrate chemistry. **Protecting Groups: Strategies and Applications in Carbohydrate Chemistry**, 2019, 1-27. https://doi.org/10.1002/9783527697014.ch1.

WHO. **WHO consolidated guidelines on tuberculosis. Module 4: treatment-drug-susceptible tuberculosis treatment**. World Health Organization, 2022.

WHO. **World Health Organization**, 2023. Tuberculosis. Disponível em: <https://www.who.int/news-room/fact-sheets/detail/tuberculosis>. Acessado em: 25, mai. 2023.

WILLEMS, J. F.; VANDENBERGHE, A. A New Method for the Preparation of 4, 5-Substituted 4-Oxazoline-2-Thiones. **Bulletin des Sociétés Chimiques Belges**, 1961, 70, 745-757. https://doi.org/10.1002/bscb.19610701108.

XIANG, S.; HOANG, K. L. M.; HE, J.; TAN, Y. J.; LIU, X. W. Reversing the Stereoselectivity of a Palladium-Catalyzed O-Glycosylation through an Inner-Sphere or Outer-Sphere Pathway. **Angewandte Chemie**, 2015, 127, 614-617. https://doi.org/10.1002/ange.201408739.

XIONG, T.; XIE, R.; HUANG, C.; LAN, X.; HUANG, N.; YAO, H. Recent advances in the synthesis of thiosugars using glycal donors. **Journal of Carbohydrate Chemistry**, 2021, 40, 401-439. https://doi.org/10.1080/07328303.2022.2027433.

YUAN, S.; SHEN, D. D.; BAI, Y. R.; ZHANG, M.; ZHOU, T.; SUN, C.; ZHOU, L.; WANG, S.Q.; LIU, H.M. Oxazolidinone: A promising scaffold for the development of antibacterial drugs. **European Journal of Medicinal Chemistry**, 2023, 250, 115239. https://doi.org/10.1016/j.ejmech.2023.115239.

ZHANG, G.; LIU, Q. Ferric Sulphate Hydrate–Catalyzed, Microwave-Assisted Synthesis of 2, 3-Unsaturated O-Glycosides via the Ferrier Reaction. **Synthetic Communications**, 2007, 37, 3485-3492. https://doi.org/10.1080/00397910701555402.

ZHAO, J.; WEI, S.; MA, Z.; SHAO, H. A simple and convenient method for the synthesis of pyranoid glycals. **Carbohydrate Research**, v. 345, n. 1, p. 168-171, 2010. https://doi.org/10.1016/j.carres.2009.10.003.

APPENDIX A - NOTA DE IMPRENSA

A tuberculose pode parecer uma doença que não traz mais preocupação para a população, no entanto, segundo a Organização Mundial de Saúde ela é a segunda doença infecciosa que mais mata no mundo, atrás apenas da Covid-19, atingindo principalmente as pessoas mais vulneráveis. De acordo com o boletim epidemiológico da Secretaria de Vigilância em Saúde e Ambiente, o estado de Pernambuco registrou uma média de casos superior à média nacional no ano de 2022. Por essa razão, o surgimento de novos tratamentos é de extrema importância.

Neste trabalho, produzimos e caracterizamos novas substâncias orgânicas, desde o material de partida até a substância final, com o objetivo de avaliar se as mesmas poderão ser utilizadas como futuros fármacos contra a tuberculose. Os dados apresentados são resultados de uma dissertação de mestrado do Programa de Pós-Graduação em Química da Universidade Federal de Pernambuco. O trabalho foi realizado pela mestranda Carla Jasmine Oliveira e Silva, orientada pelos professores Dr. Ronaldo Nascimento de Oliveira e Dr. Arnaud Tatibouët em colaboração internacional, com uma bolsa de mestrado acadêmico financiada pela Fundação de Amparo à Ciência e Tecnologia do Estado de Pernambuco (FACEPE).

APPENDIX B - GRAPHICAL ABSTRACT

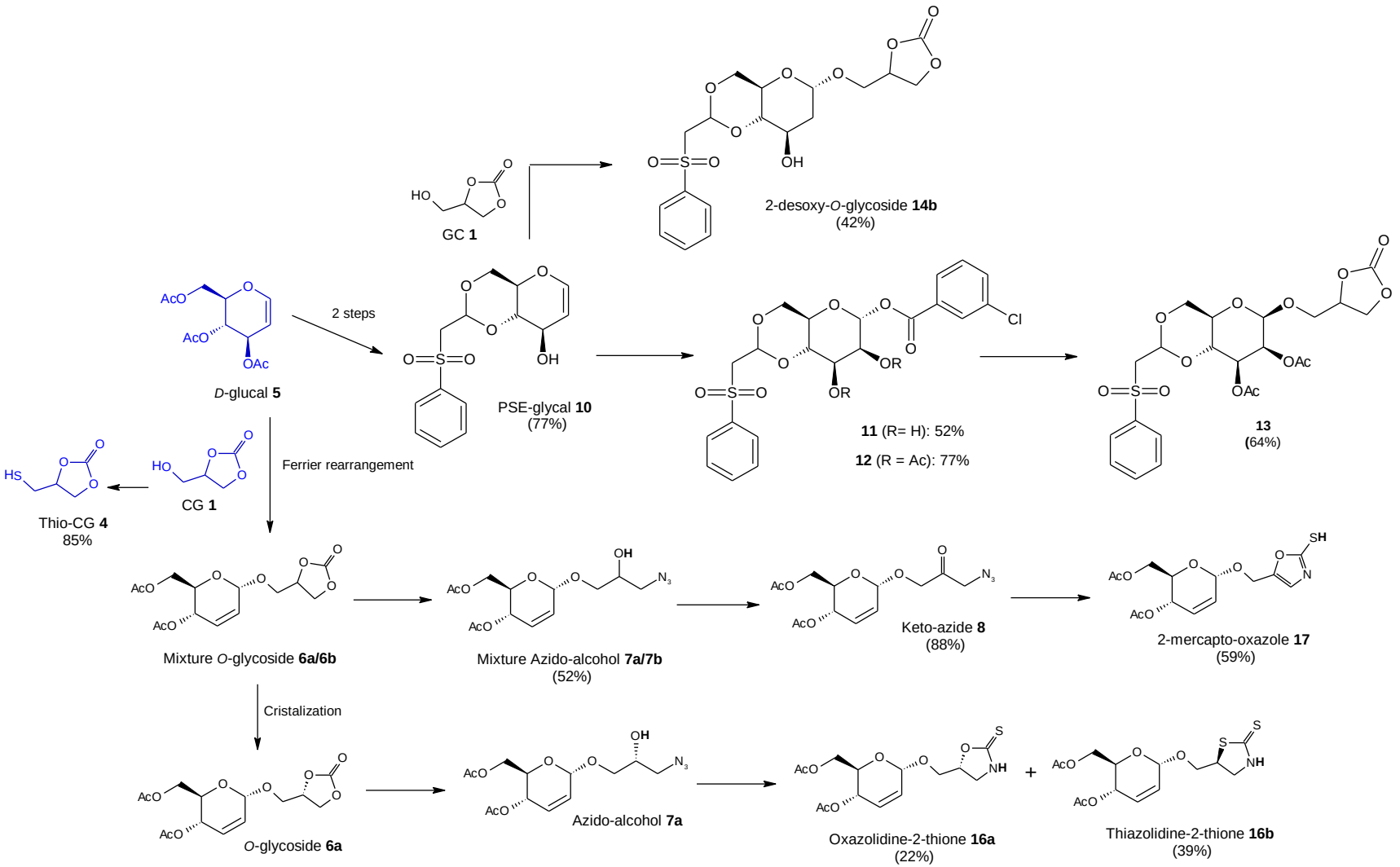

ANNEX A - SPECTRAL DATA

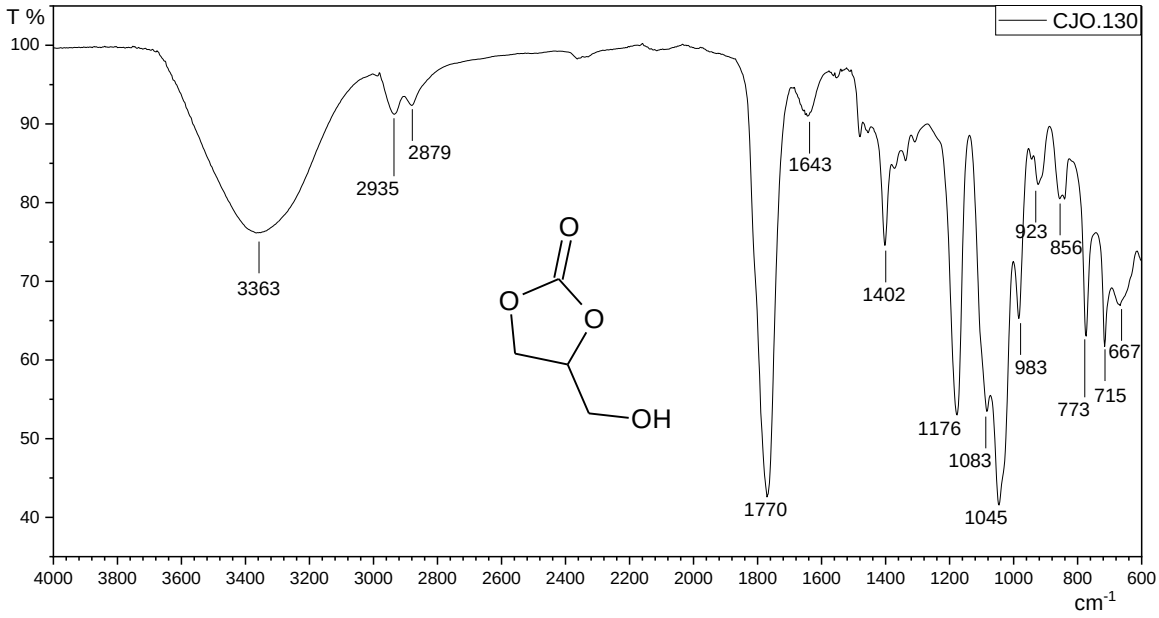

Infrared of compound **1**

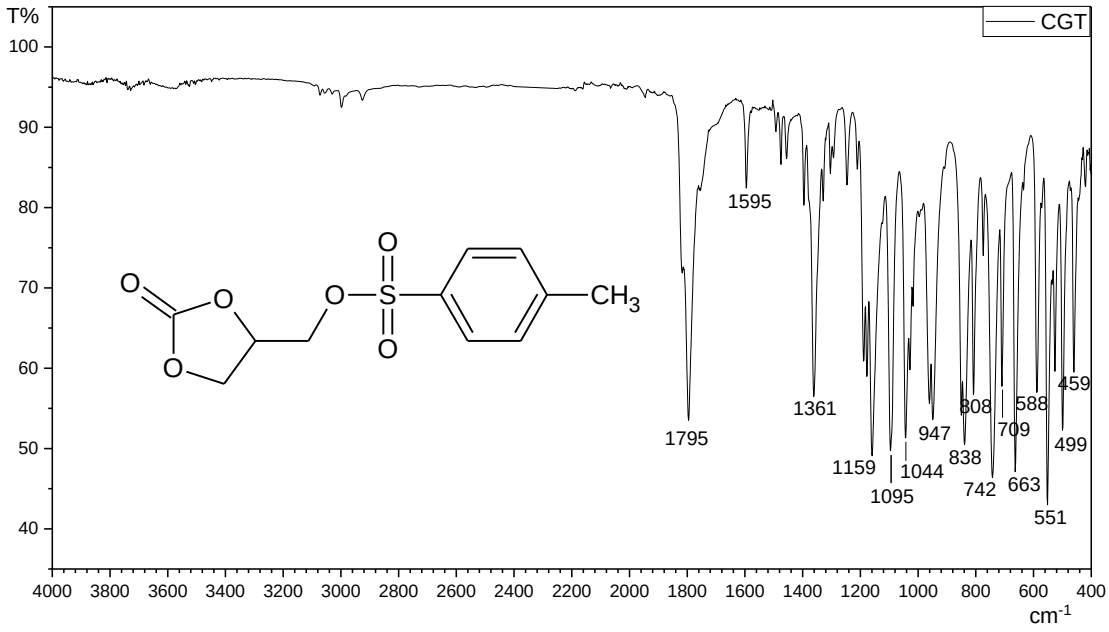

Infrared of compound **2**

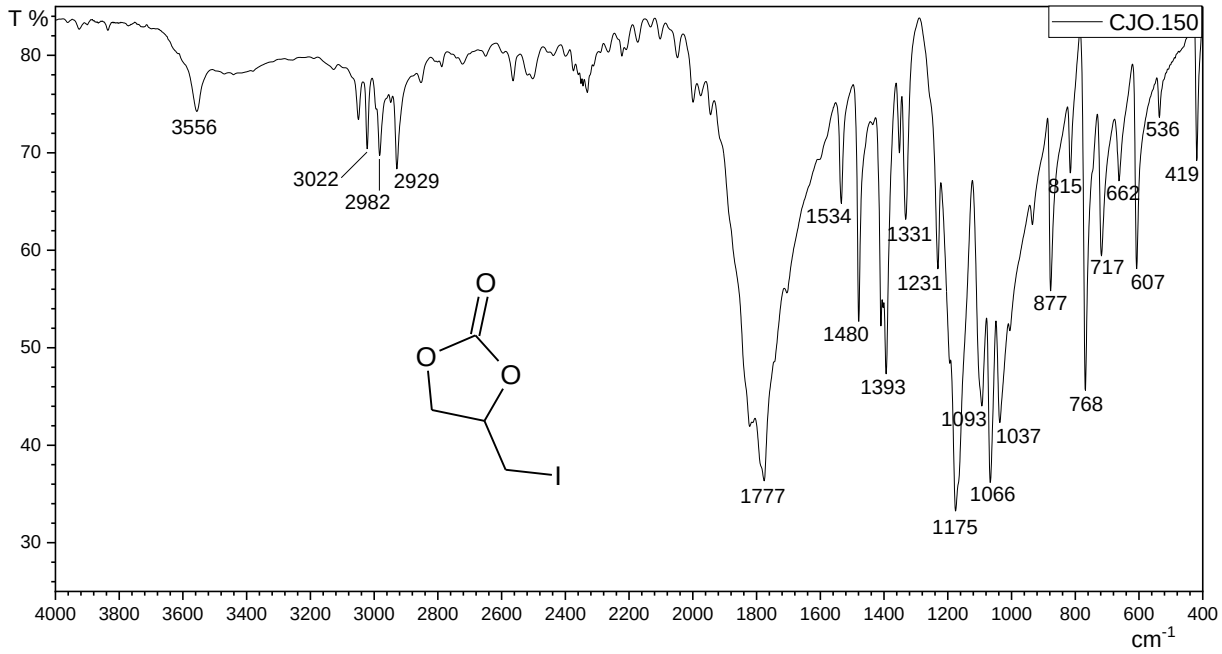

Infrared of compound **3**

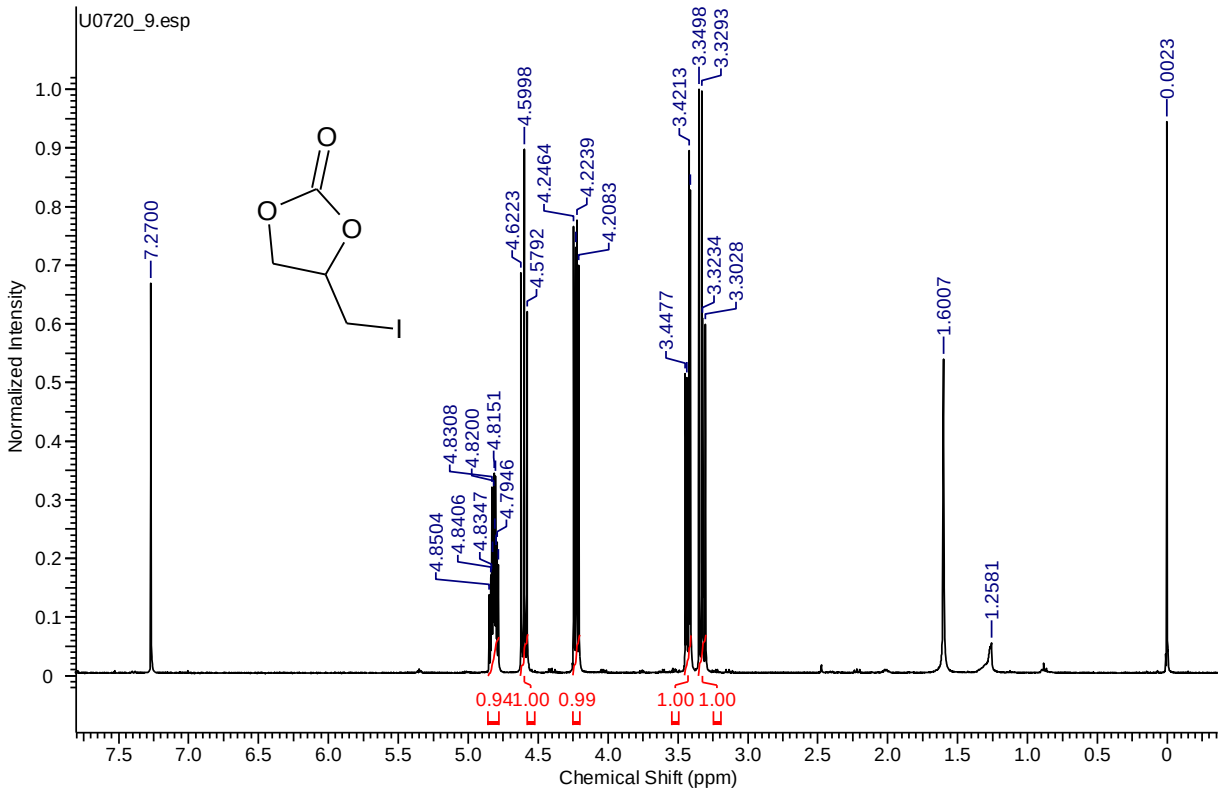

^{1}H NMR ($CDCl_3$, 400 MHz) of compound **3**

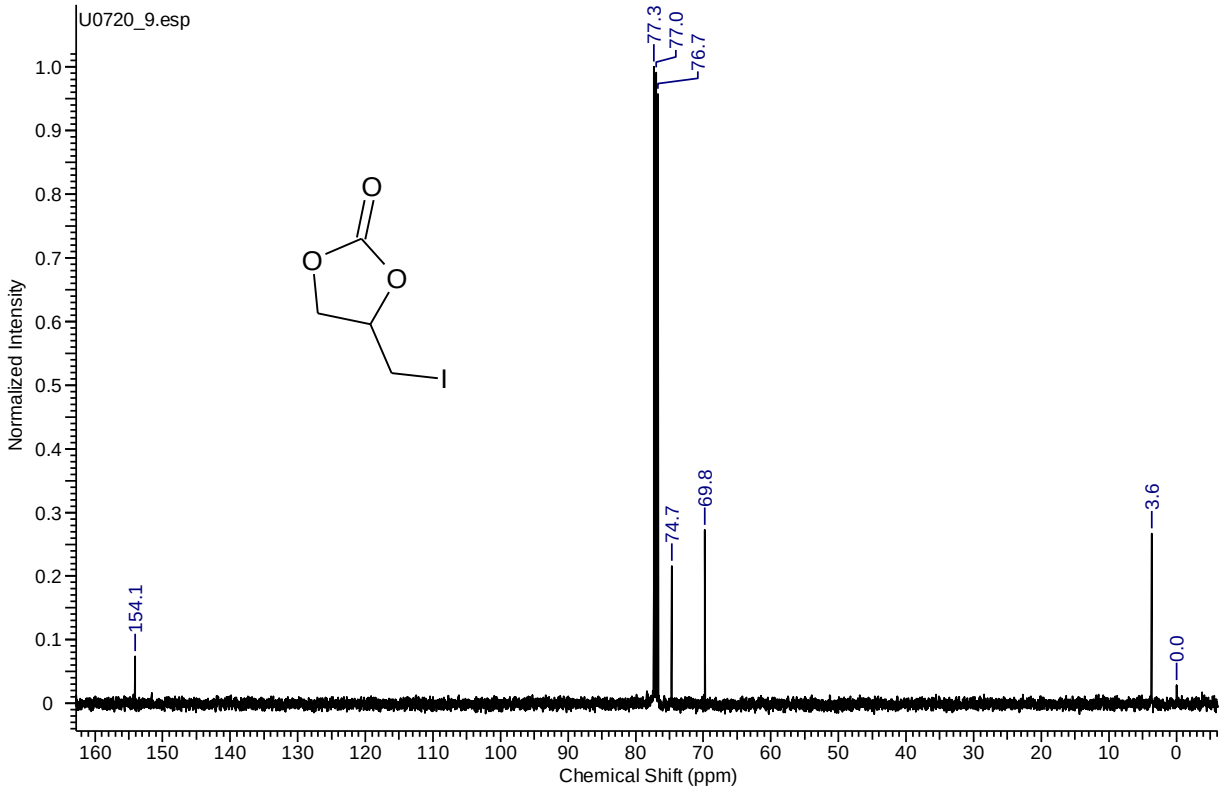

^{13}C NMR ($CDCl_3$, 100 MHz) of compound **3**

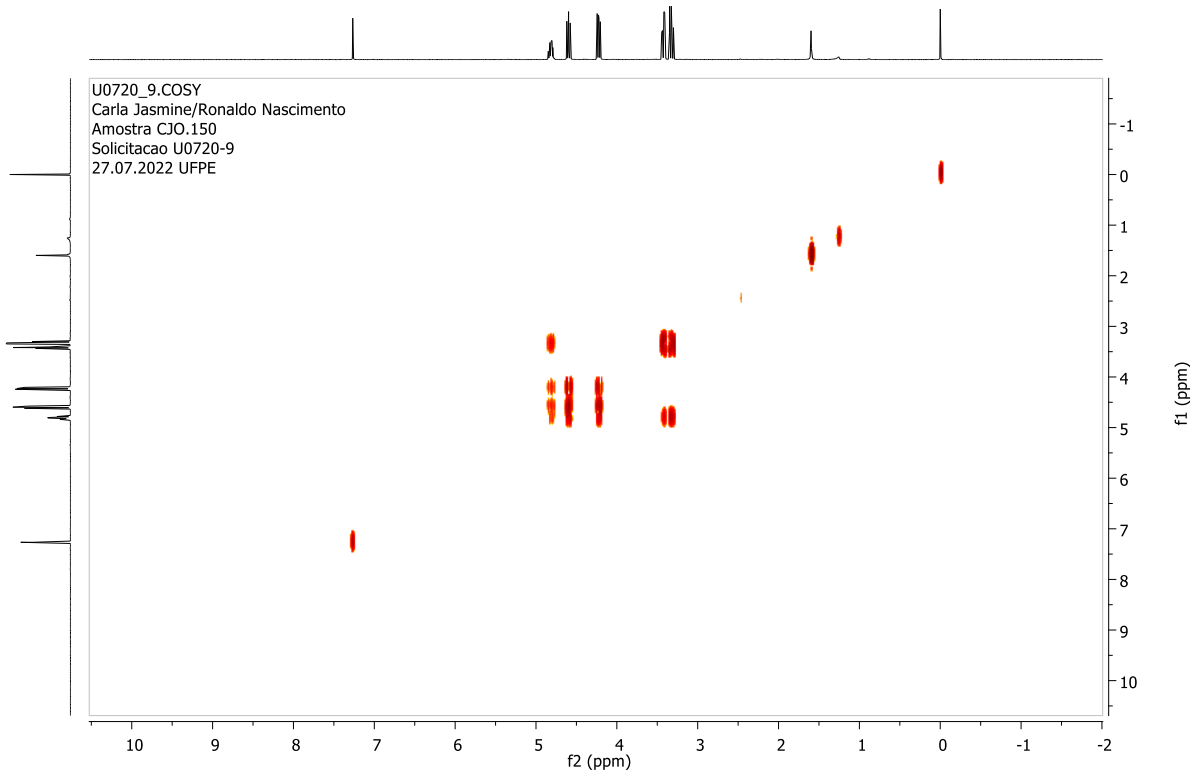

2D COSY NMR of compound **3**

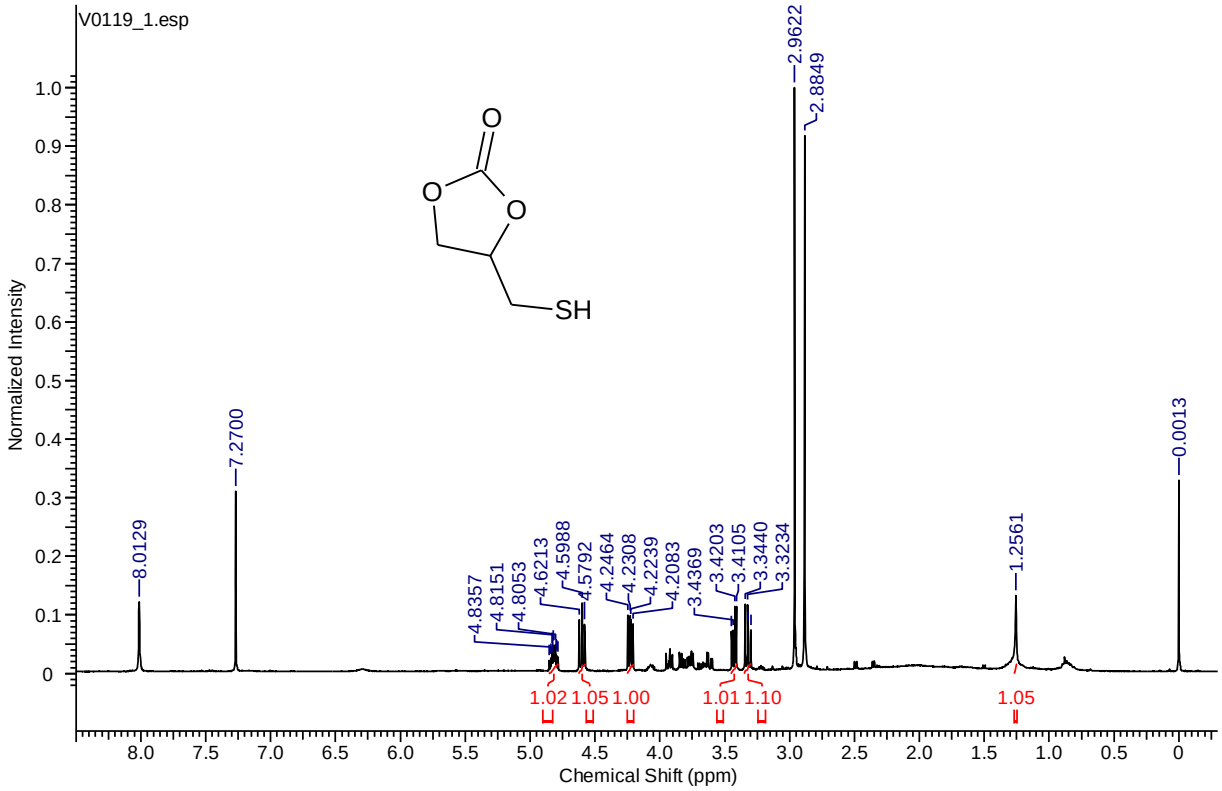

^{1}H NMR ($CDCl_3$, 400 MHz) of compound **4**

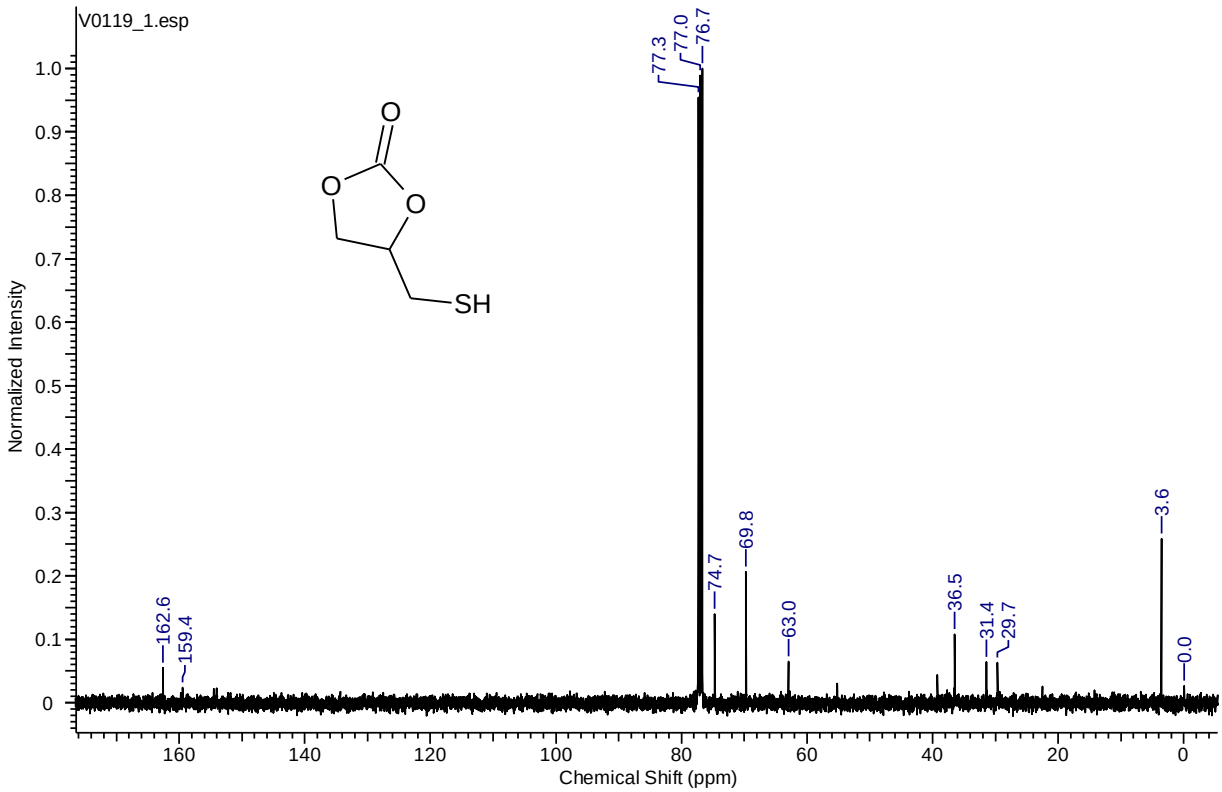

^{13}C NMR ($CDCl_3$, 100 MHz) of compound **4**

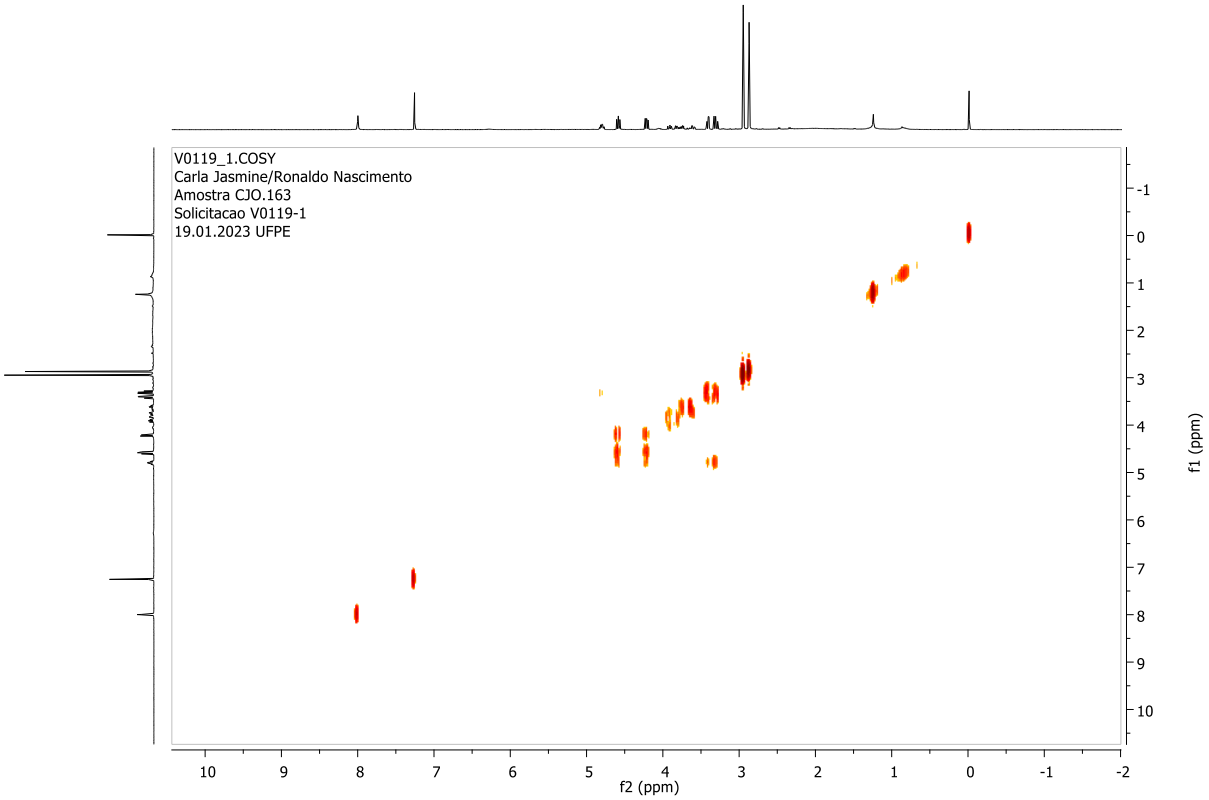

2D COSY NMR of compound **4**

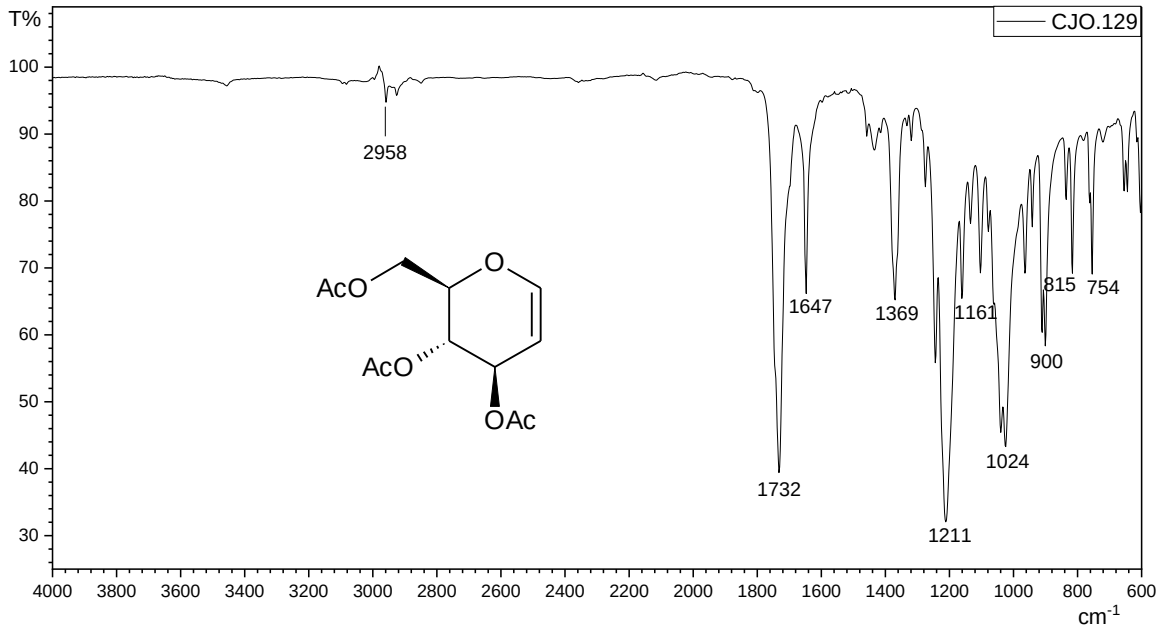

Infrared of compound **5**

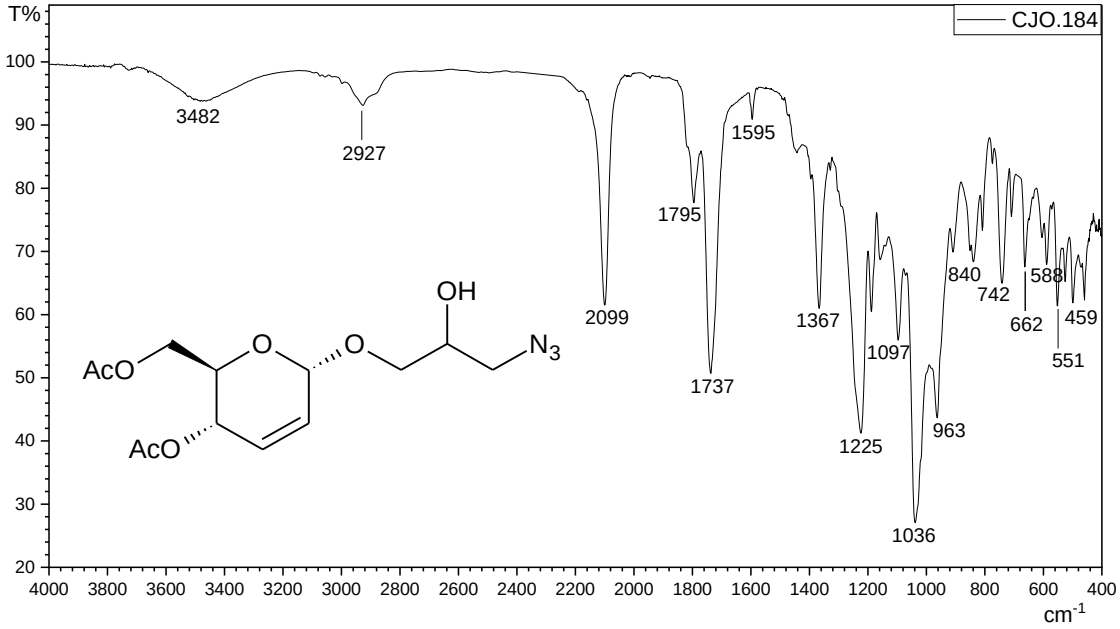

Infrared of compound **7a/7b**

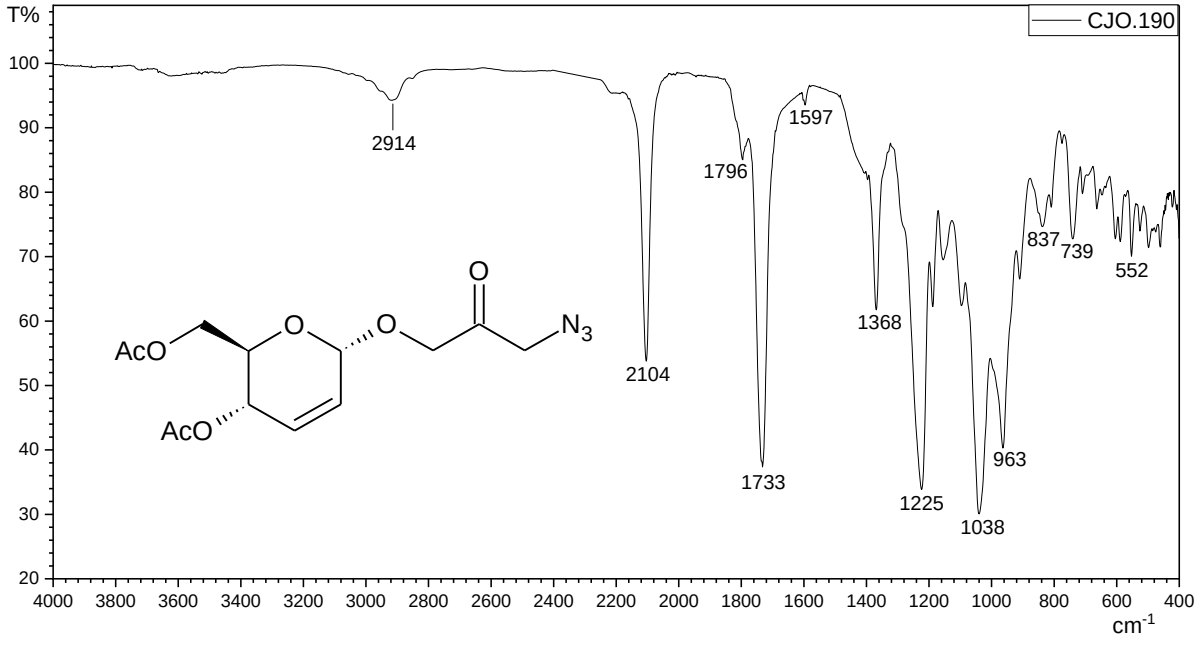

Infrared of compound **8**

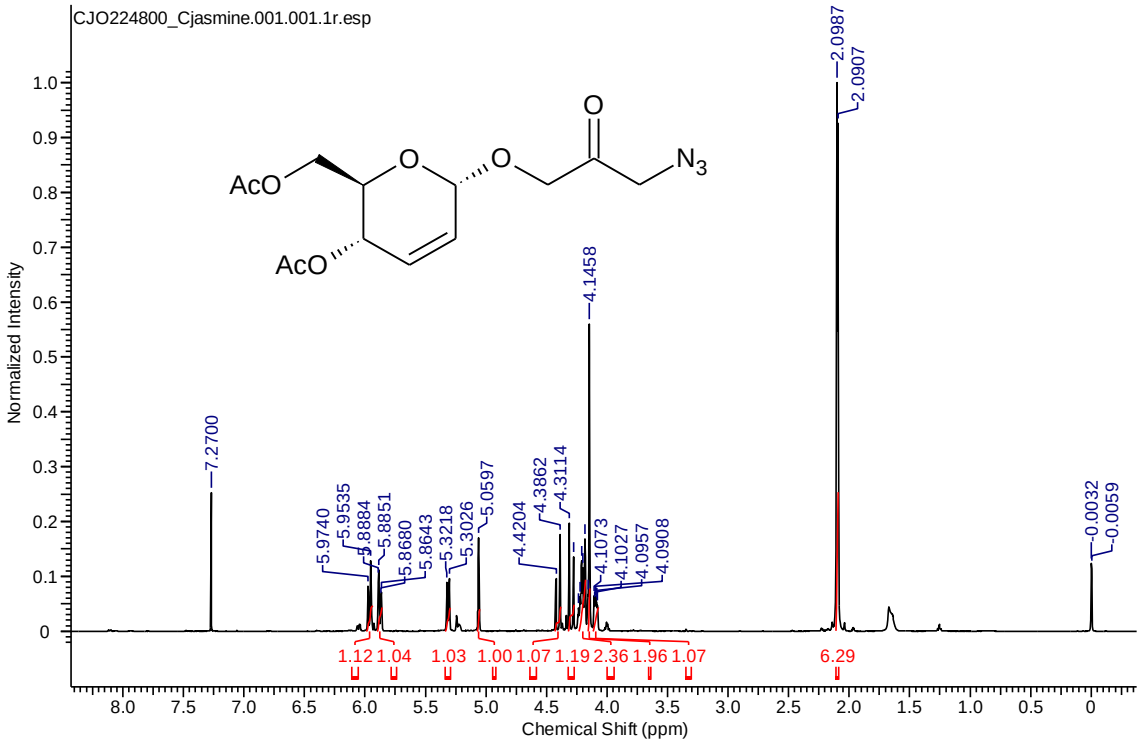

^{1}H NMR ($CDCl_3$, 500 MHz) of compound **8**

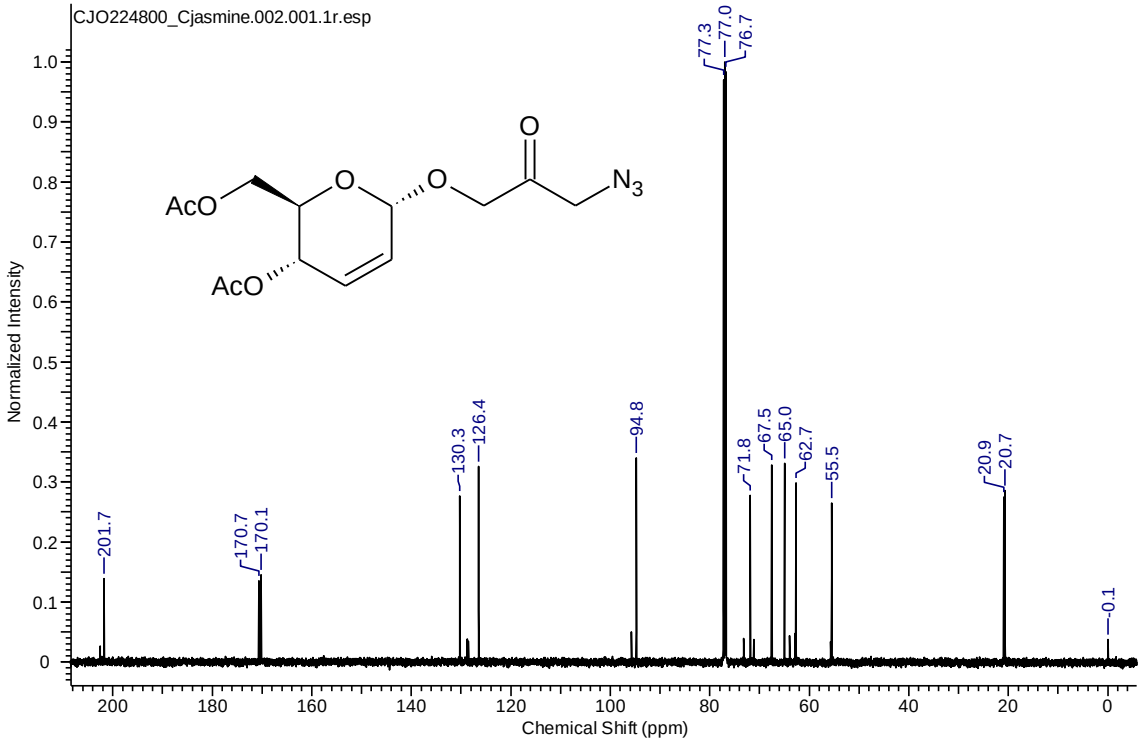

^{13}C NMR ($CDCl_3$, 125 MHz) of compound **8**

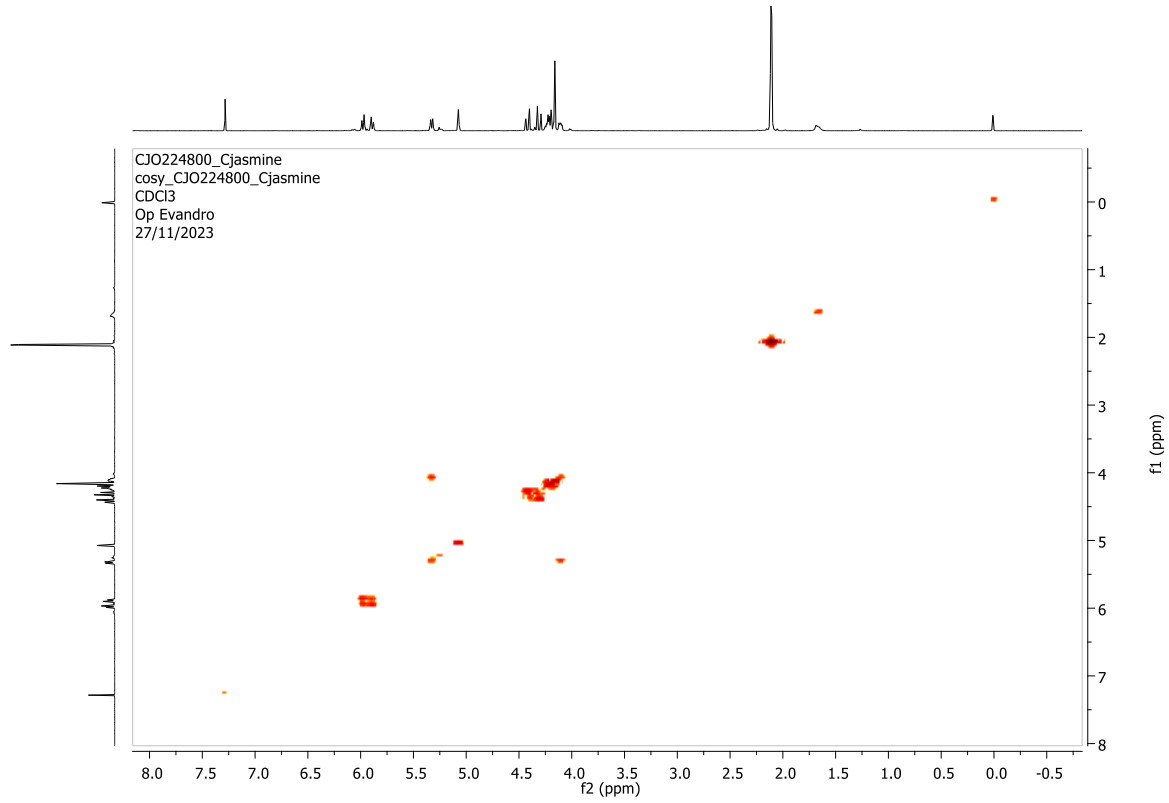

2D COSY NMR of compound **8**

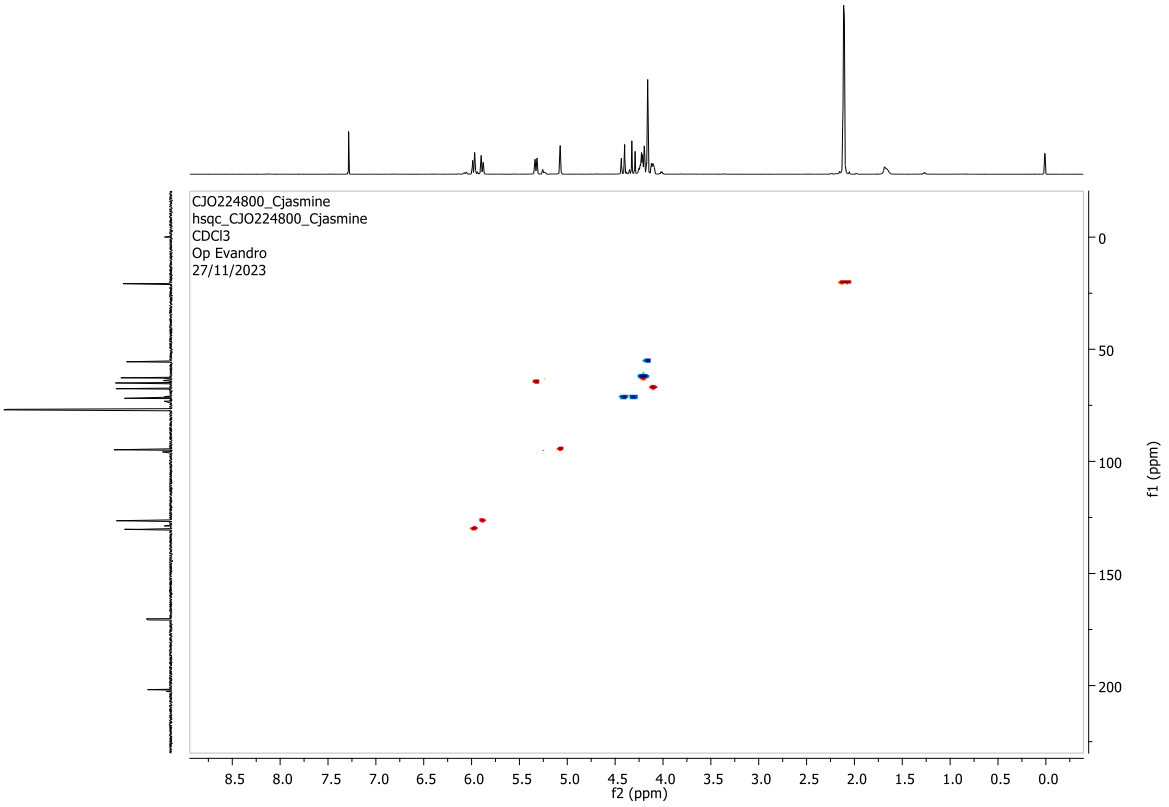

2D HSQC NMR of compound **8**

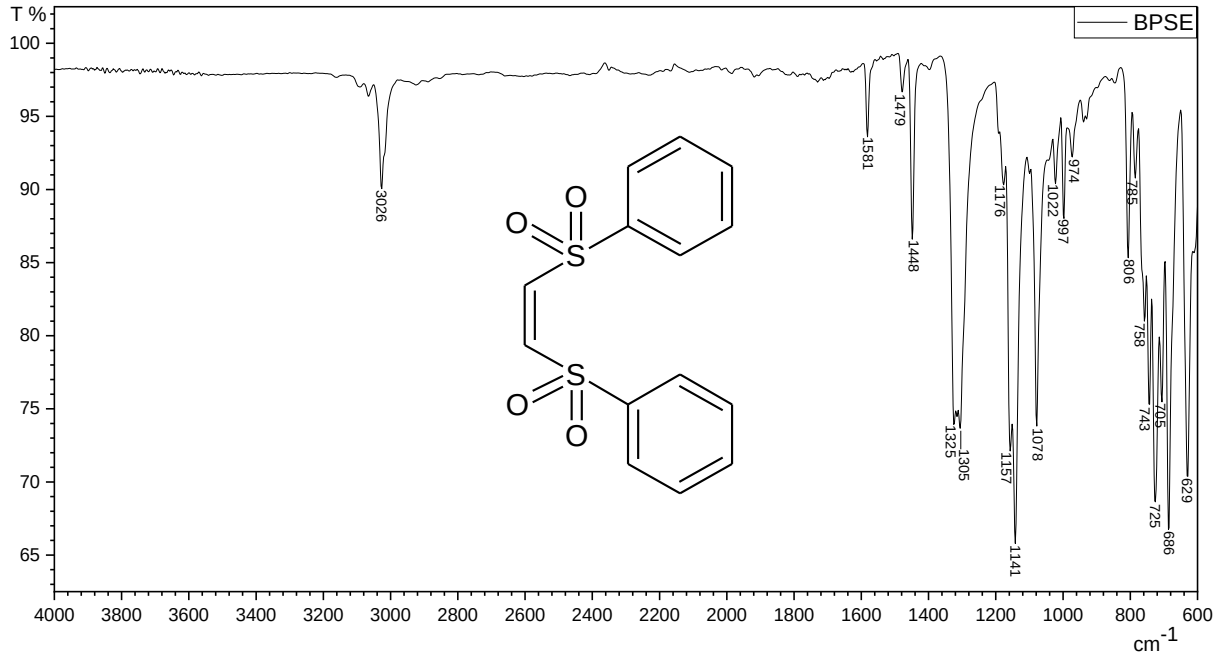

Infrared of compound **9**

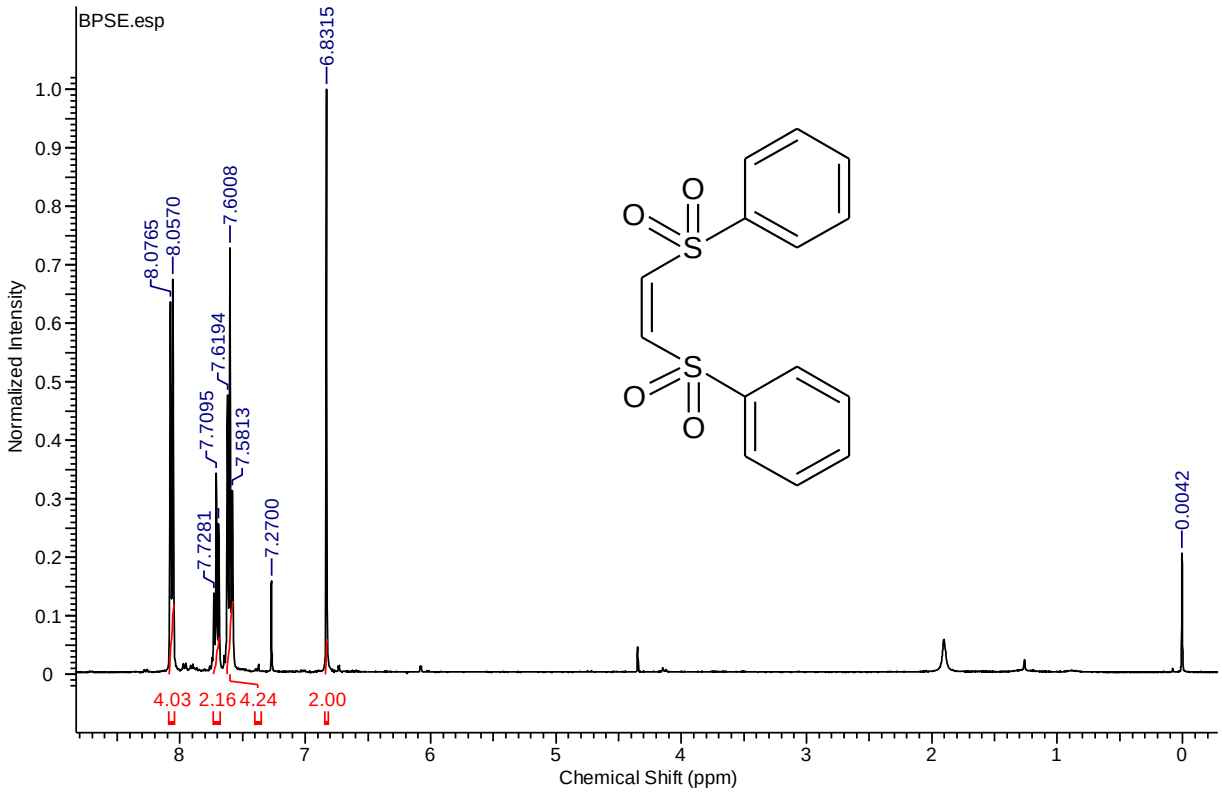

^{1}H NMR ($CDCl_3$, 400 MHz) of compound **9**

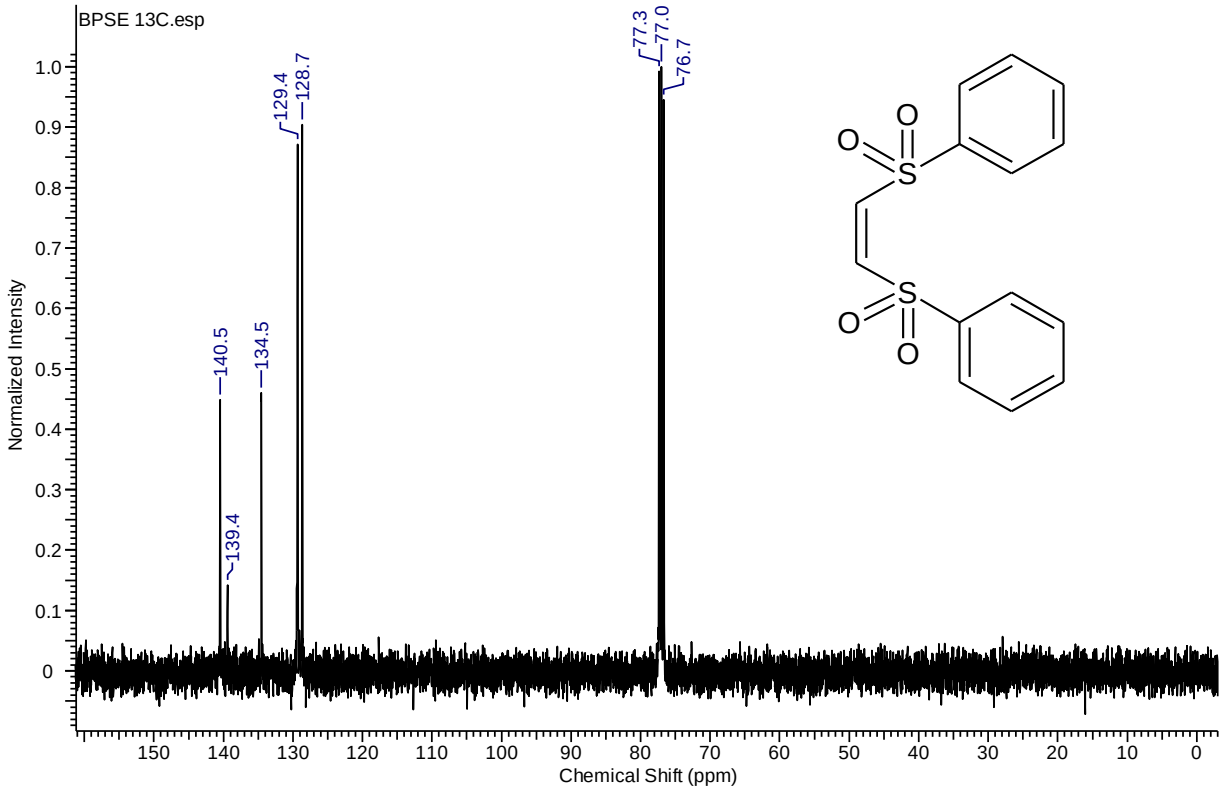

^{13}C NMR ($CDCl_3$, 100 MHz) of compound **9**

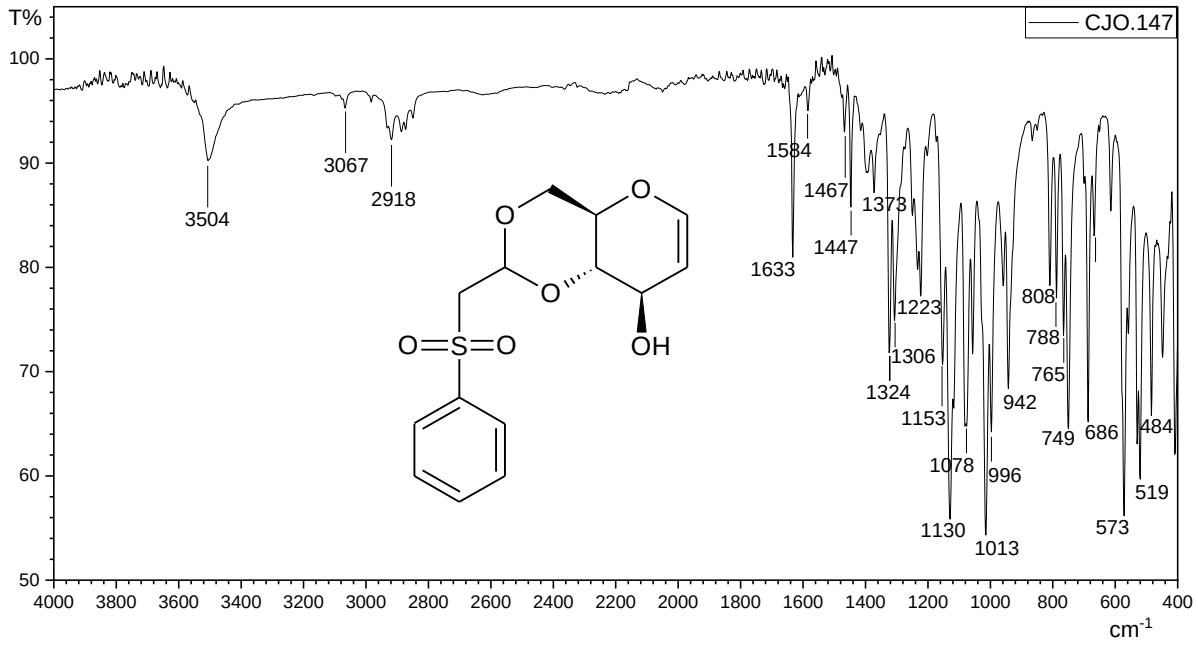

Infrared of compound **10**

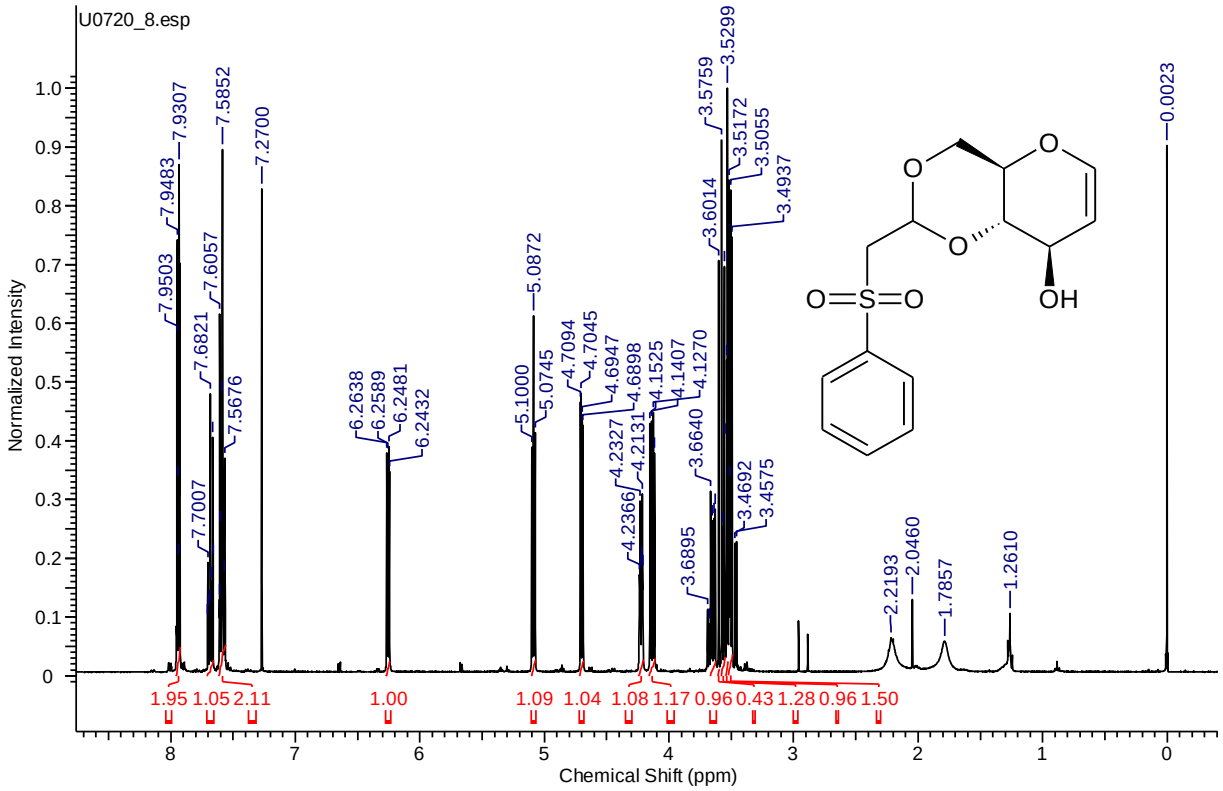

^{1}H NMR ($CDCl_3$, 400 MHz) of compound **10**

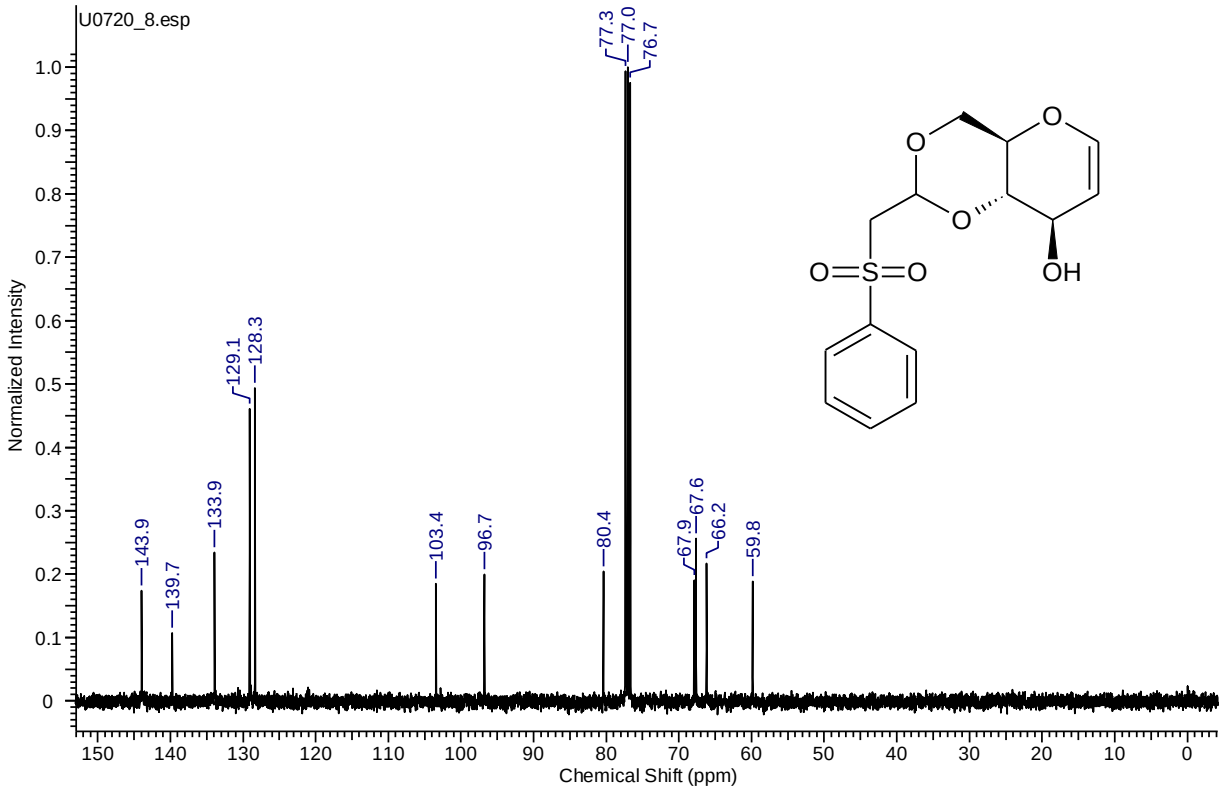

^{13}C NMR ($CDCl_3$, 100 MHz) of compound **10**

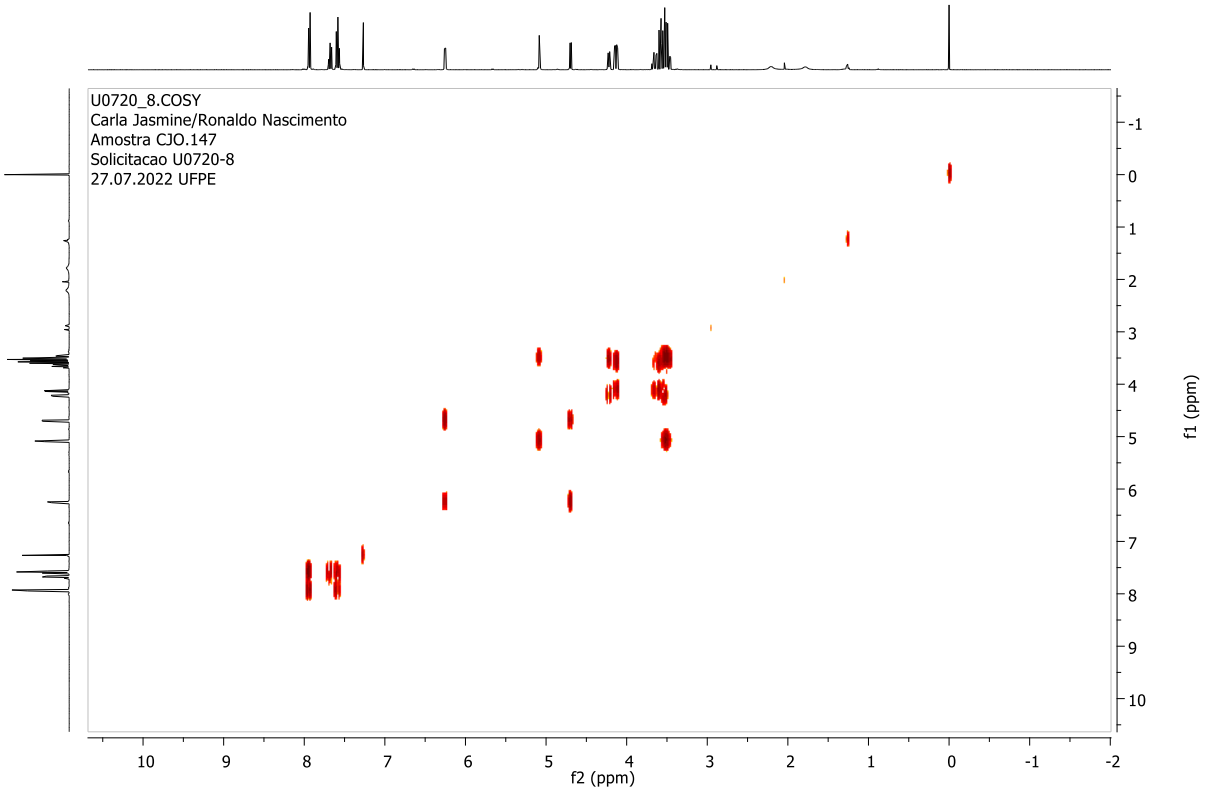

2D COSY NMR of compound **10**

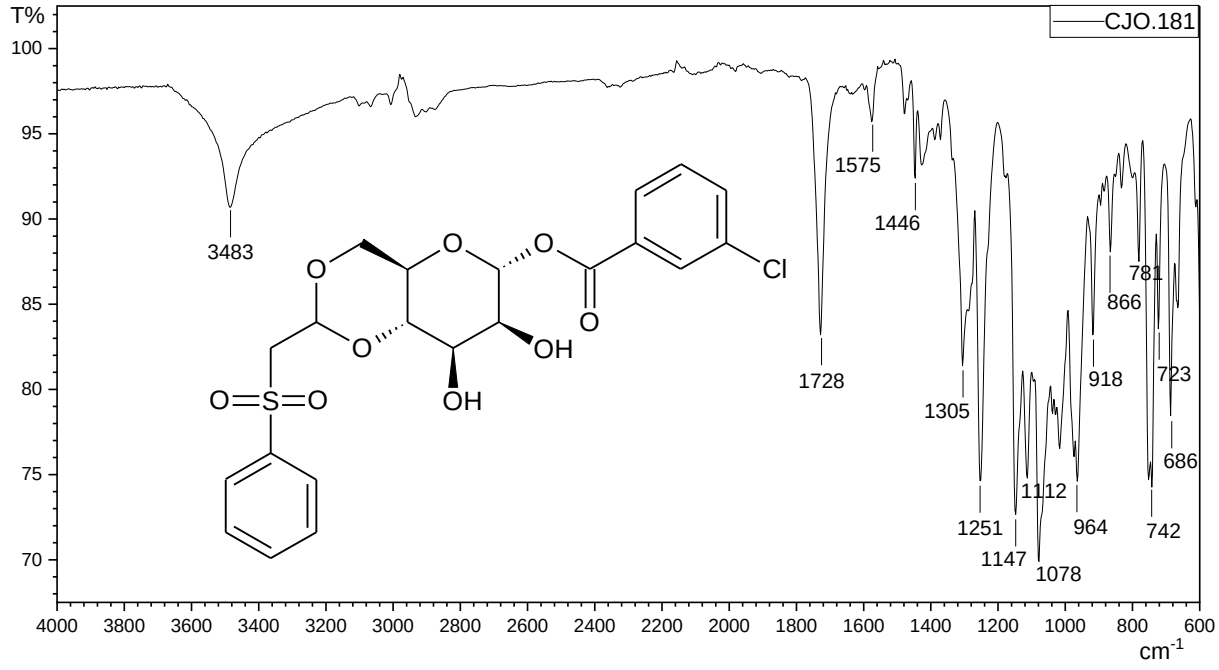

Infrared of compound **11**

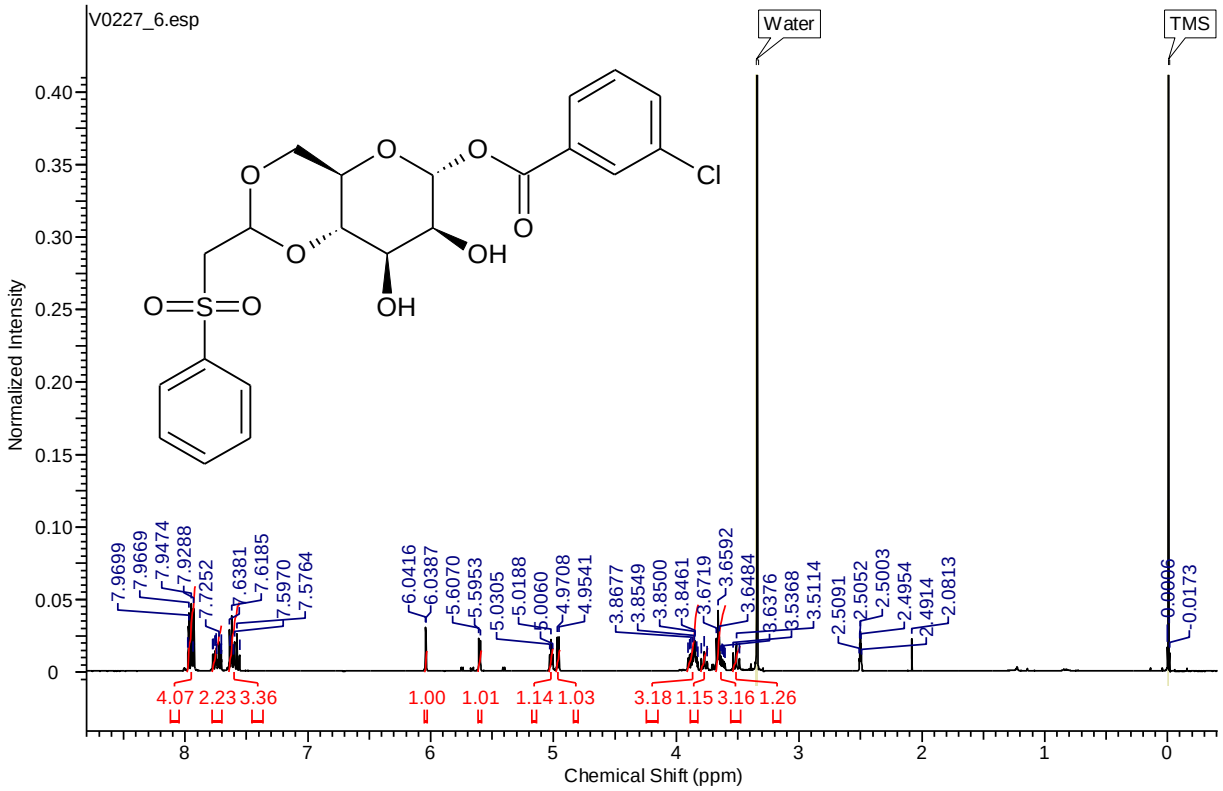

^{1}H NMR (DMSO-d_6, 400 MHz) of compound **11**

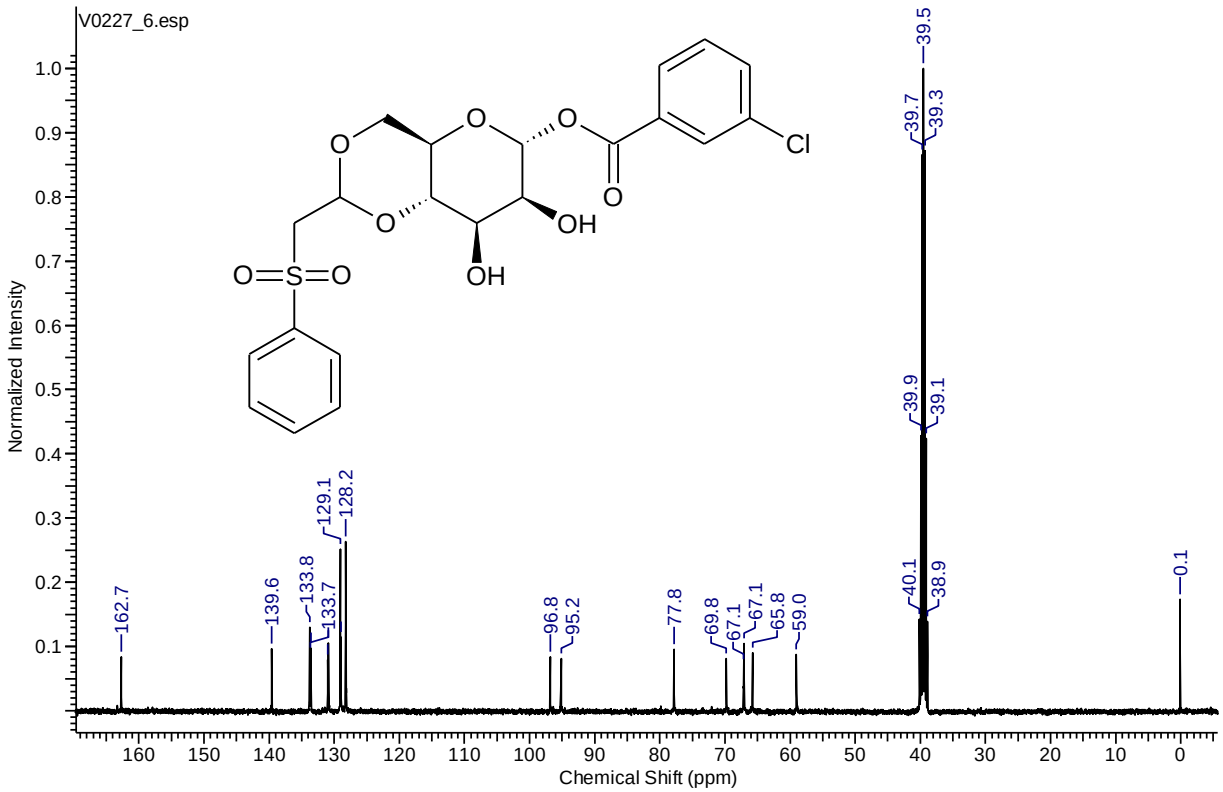

^{13}C NMR (DMSO-d_6, 100 MHz) of compound **11**

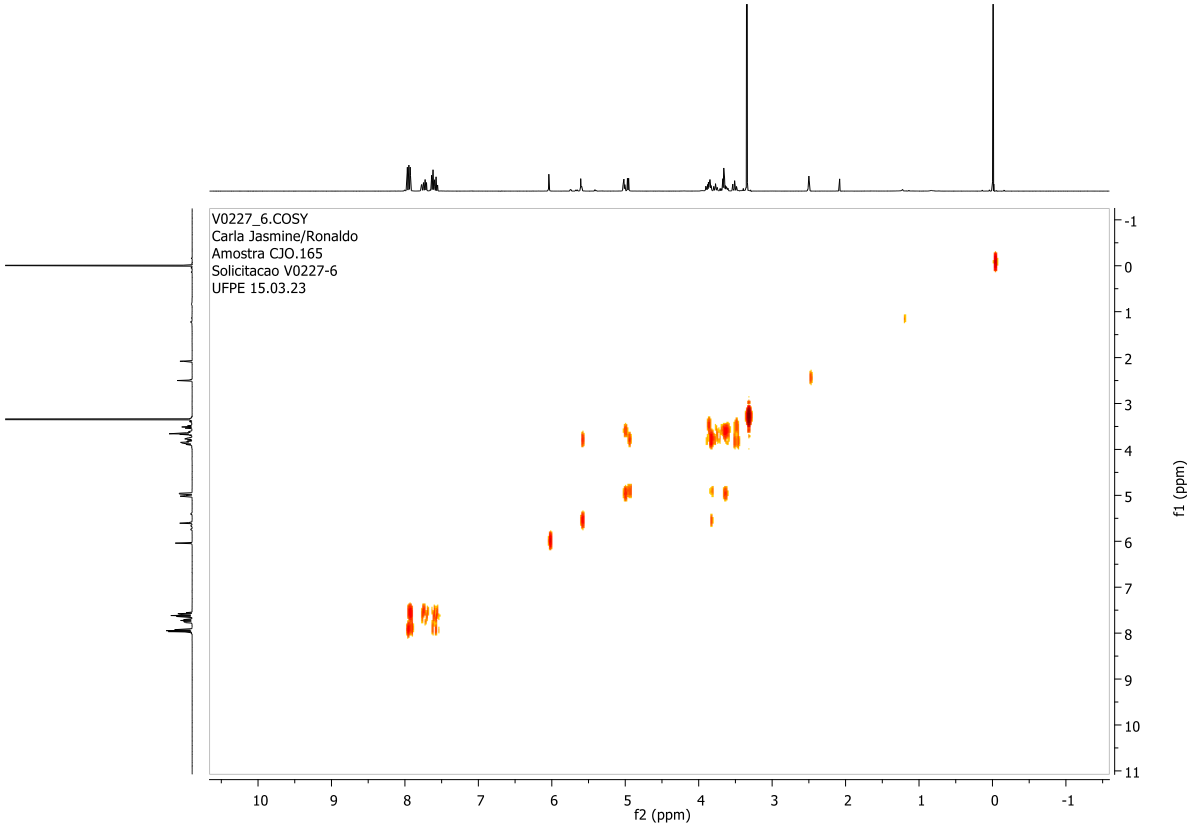

2D COSY NMR of compound **11**

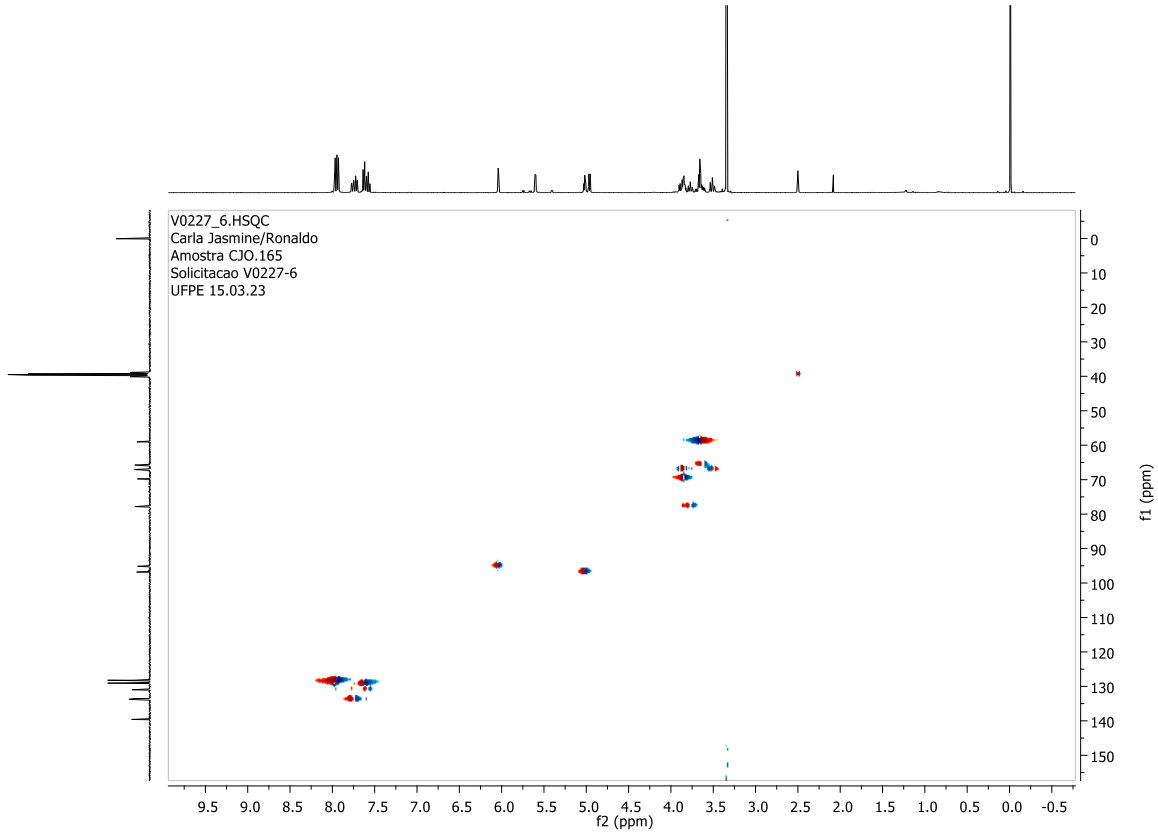

2D HSQC NMR of compound **11**

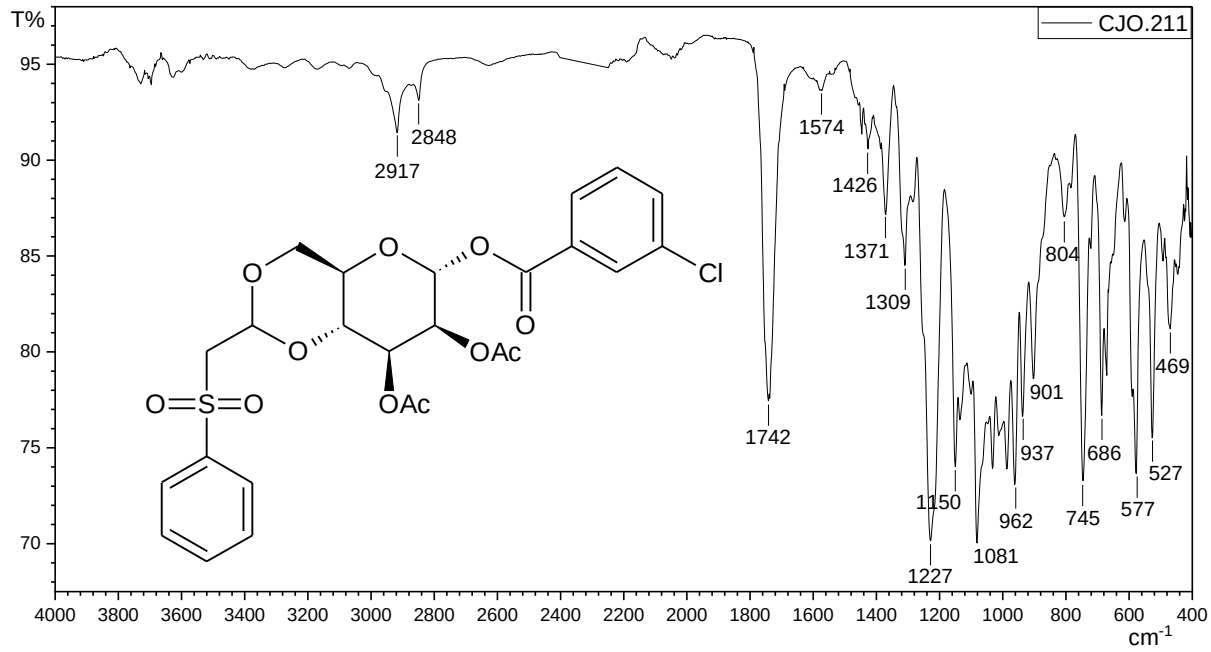

Infrared of compound **12**

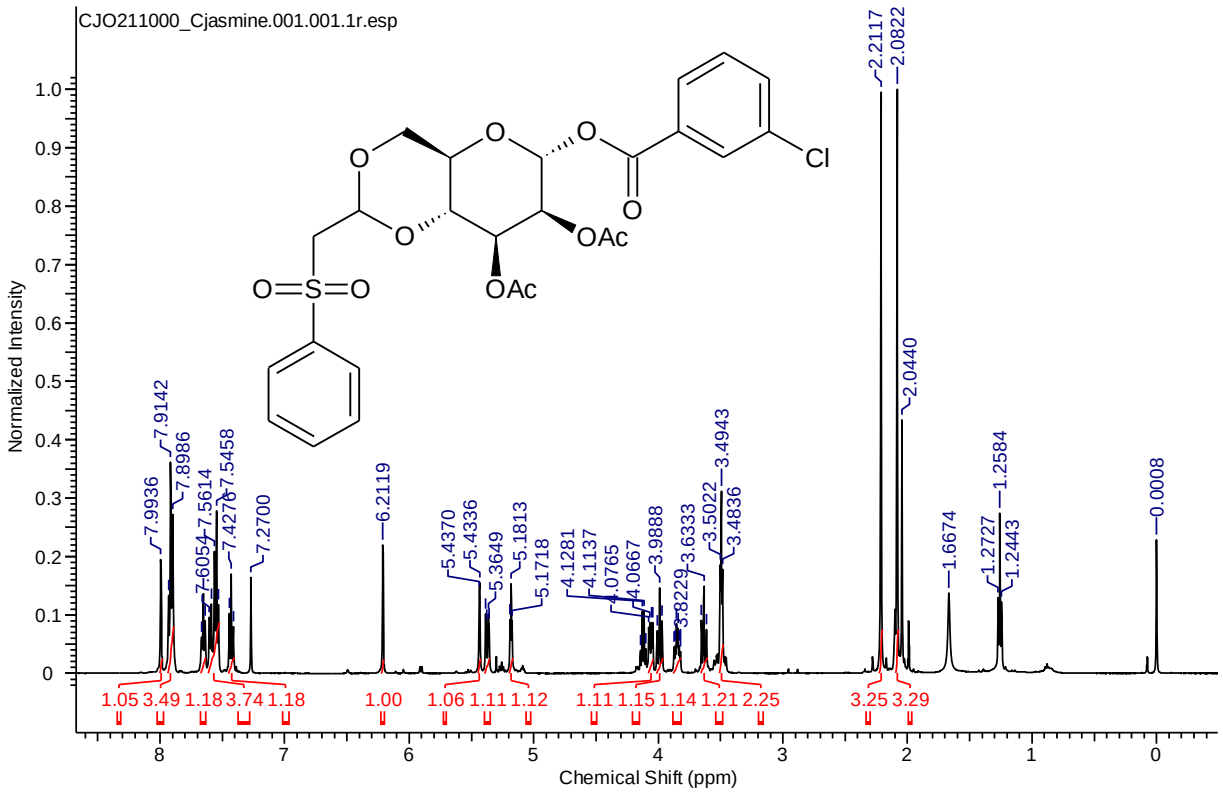

^{1}H NMR ($CDCl_3$, 500 MHz) of compound **12**

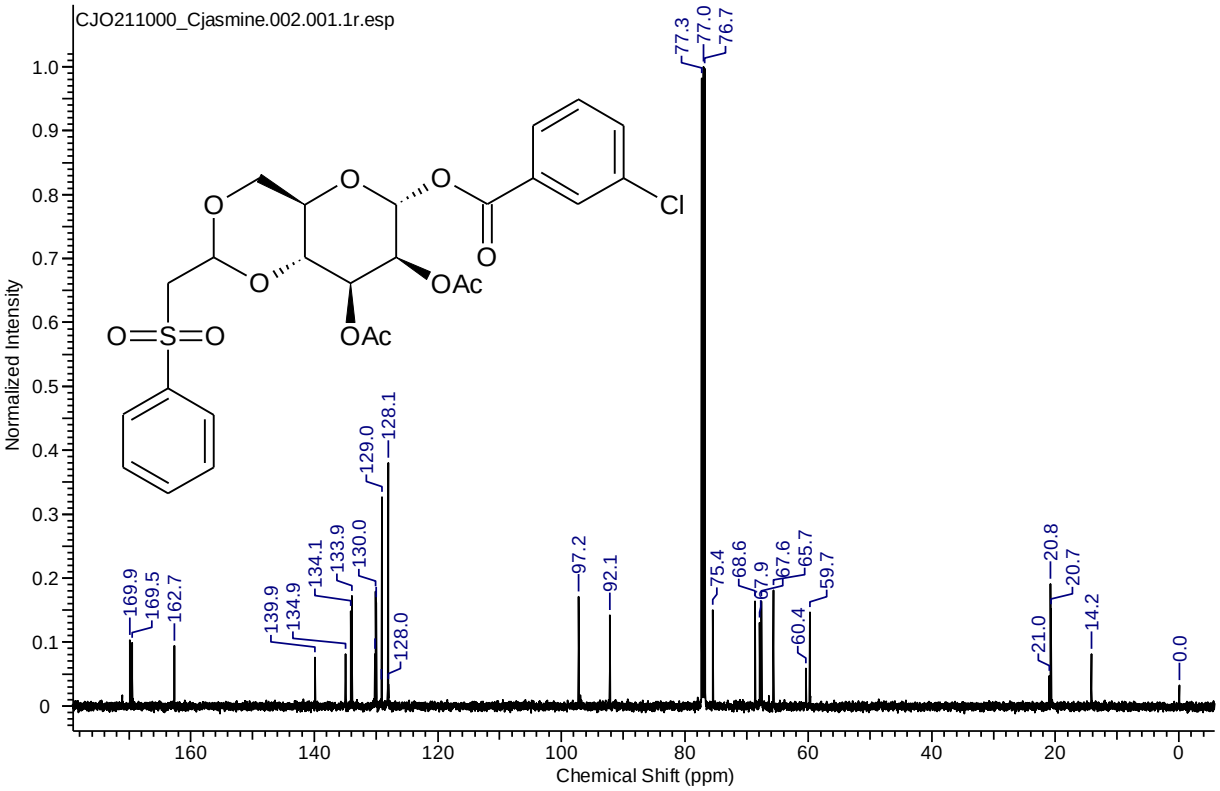

^{13}C NMR ($CDCl_3$, 125 MHz) of compound **12**

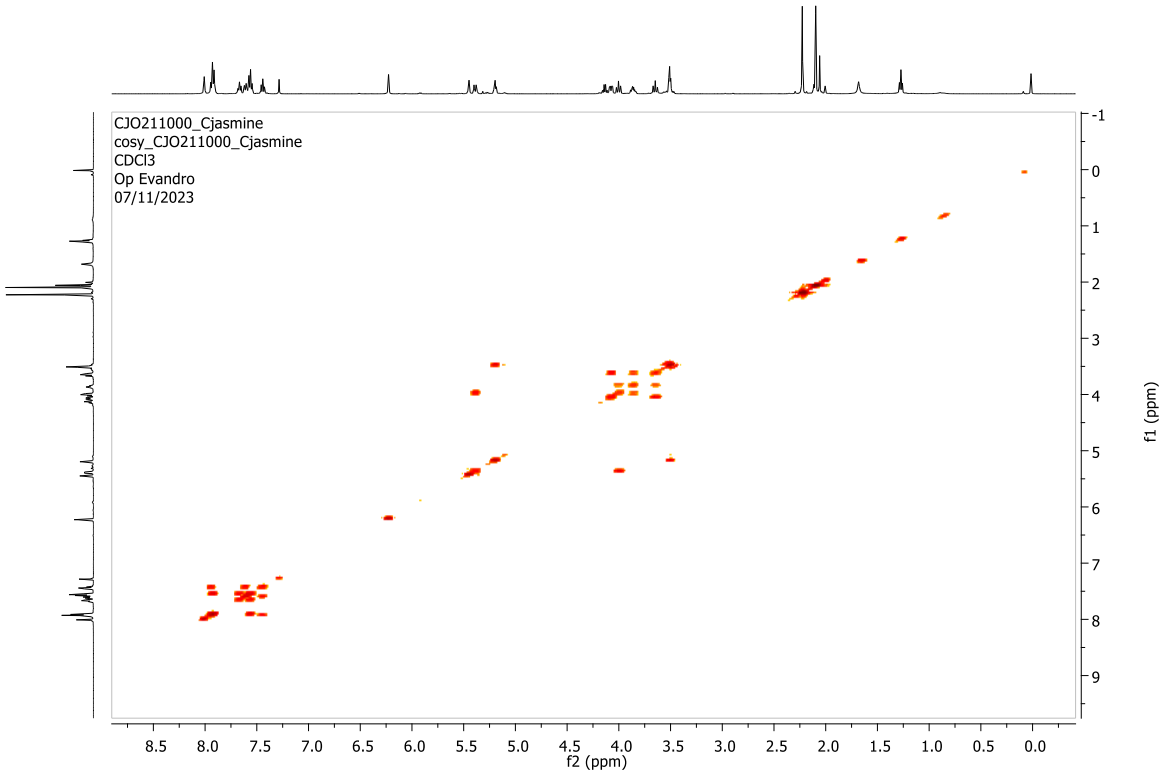

2D COSY NMR of compound **12**

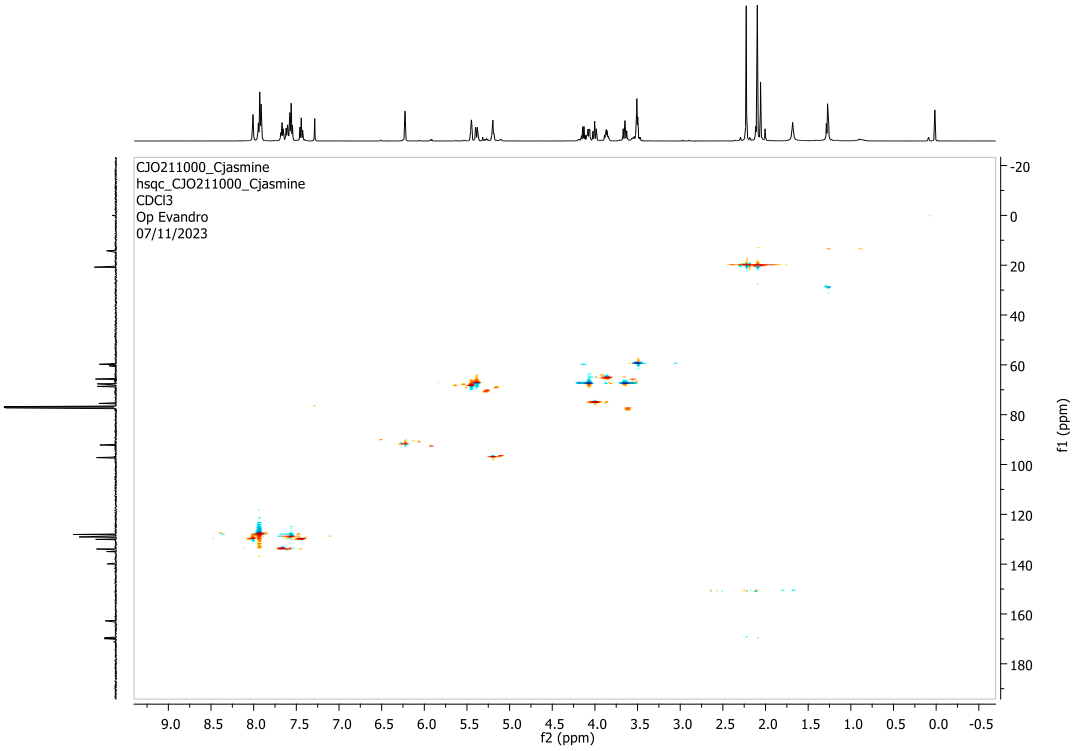

2D HSQC NMR of compound **12**

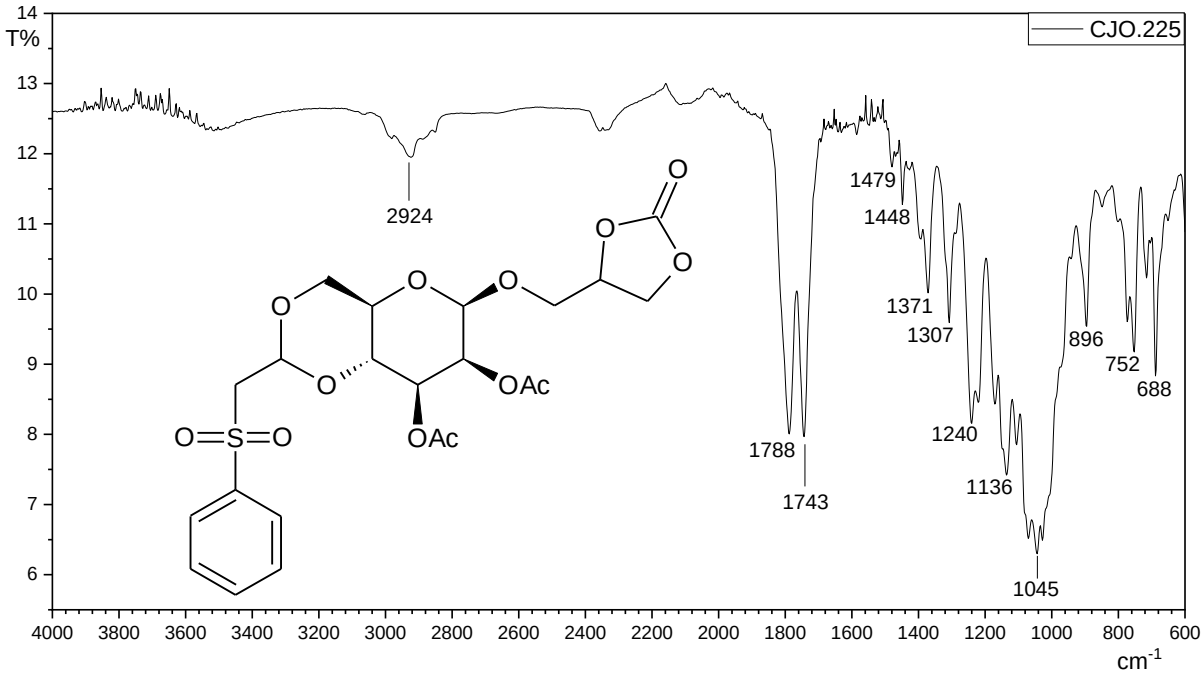

Infrared of compound **13**

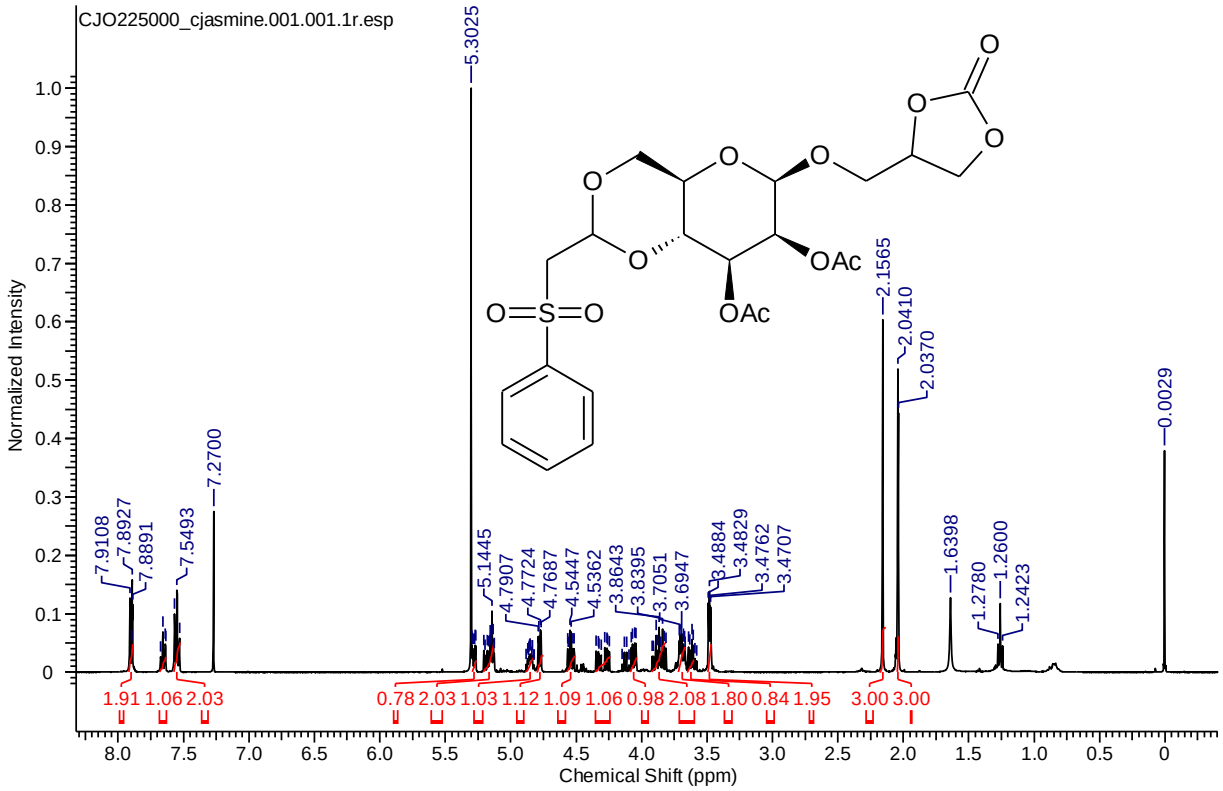

^{1}H NMR ($CDCl_3$, 400 MHz) of compound **1**

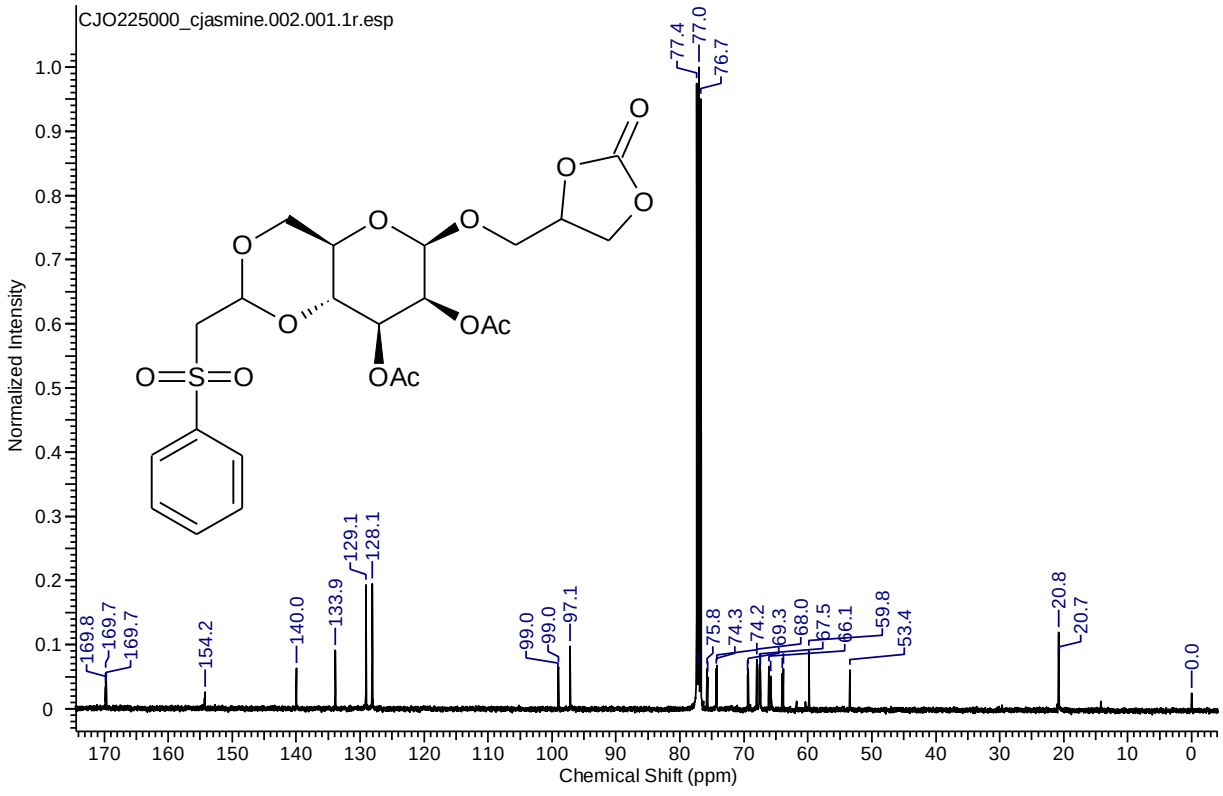

^{13}C NMR ($CDCl_3$, 100 MHz) of compound **13**

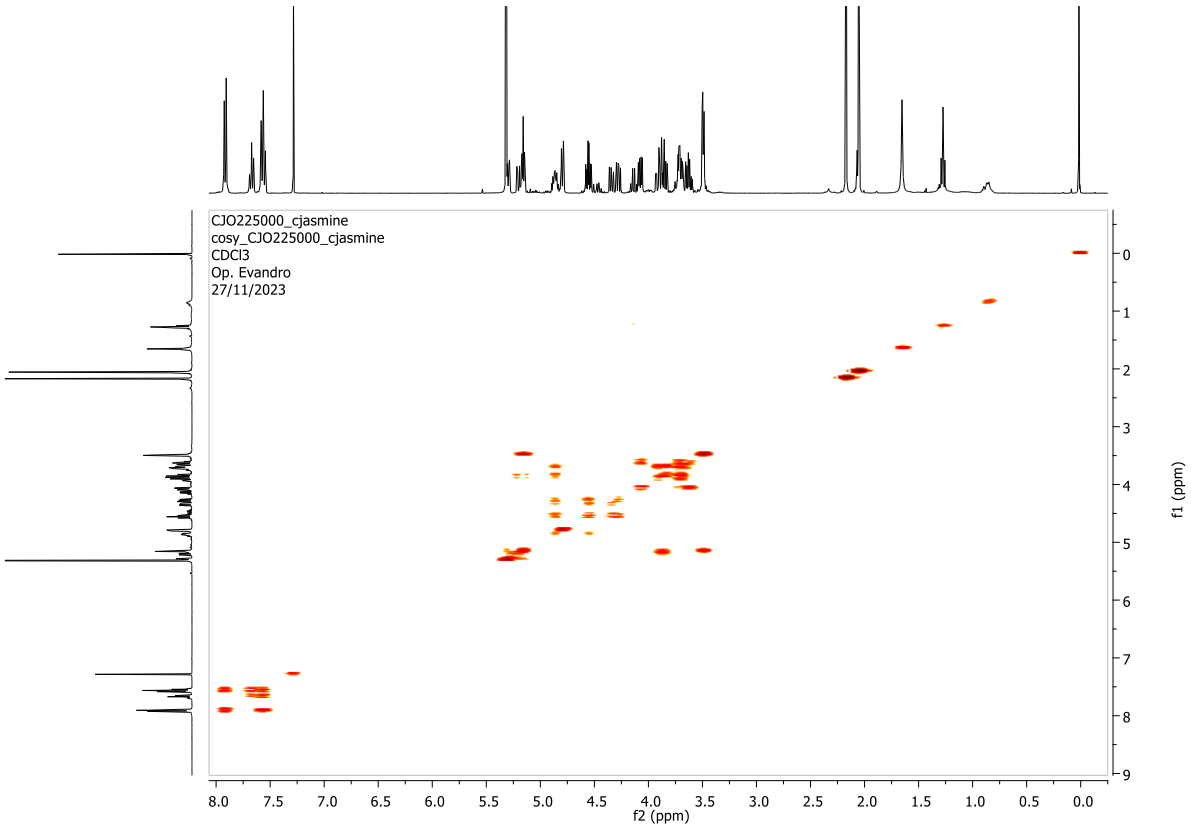

2D COSY NMR of compound **13**

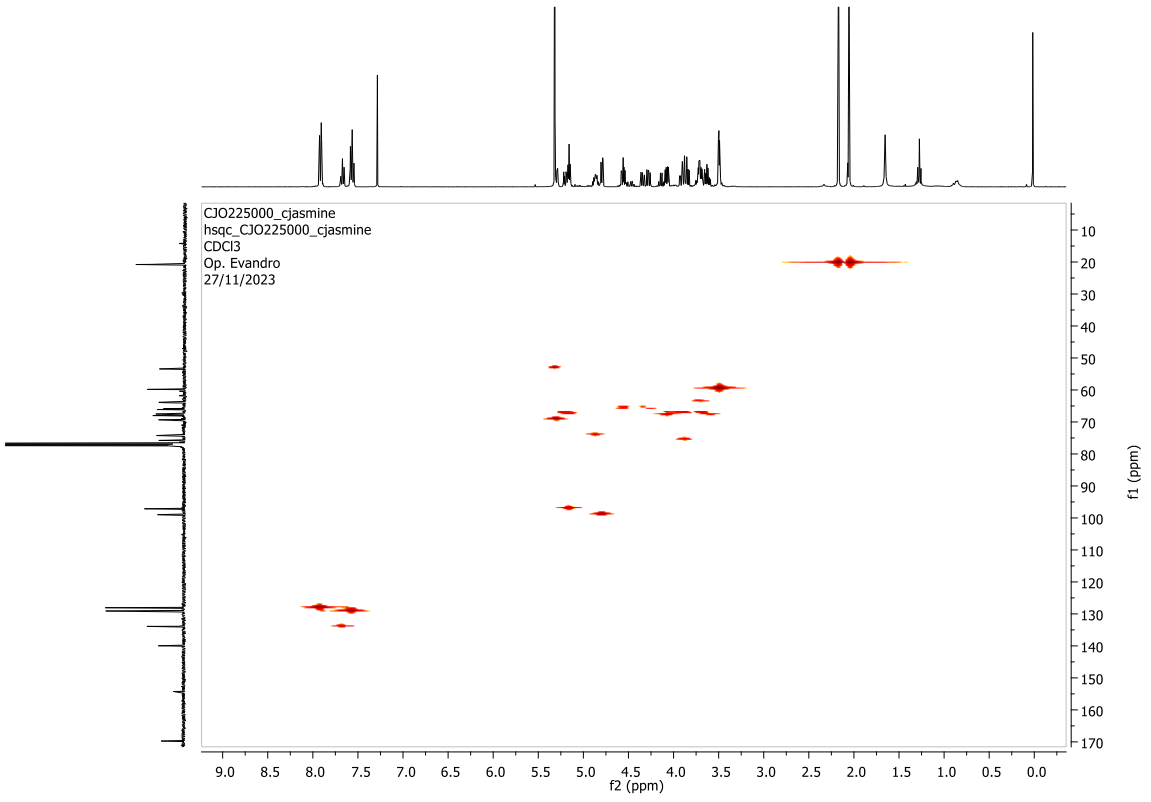

2D HSQC NMR of compound **13**

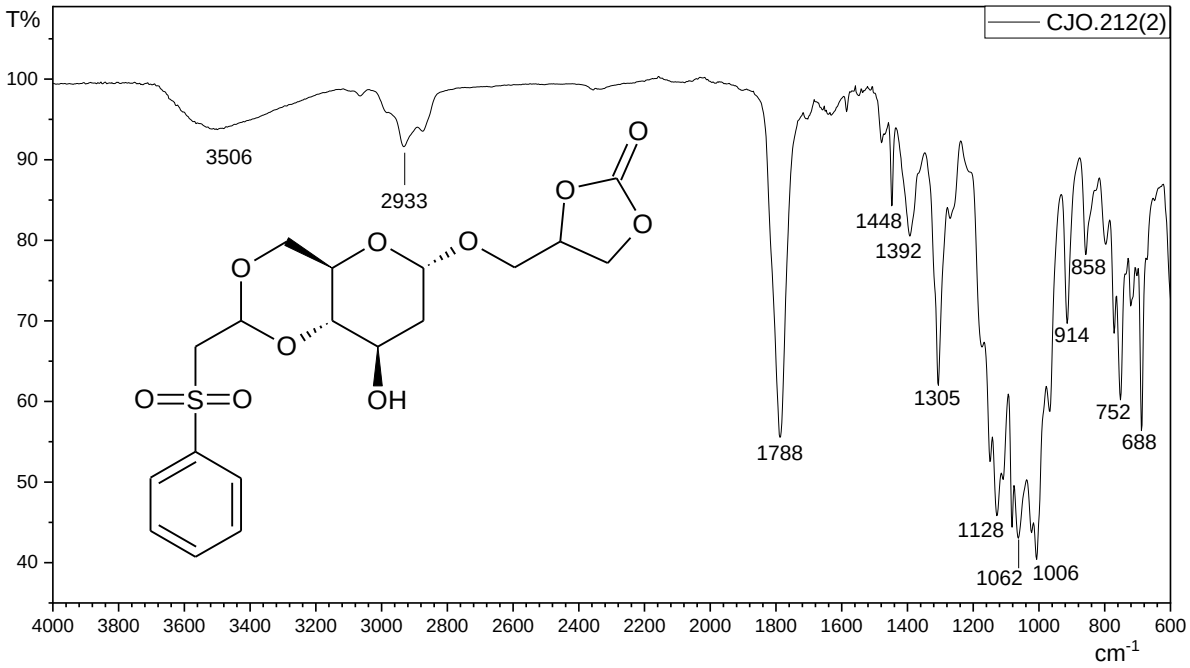

Infrared of compound **14b**

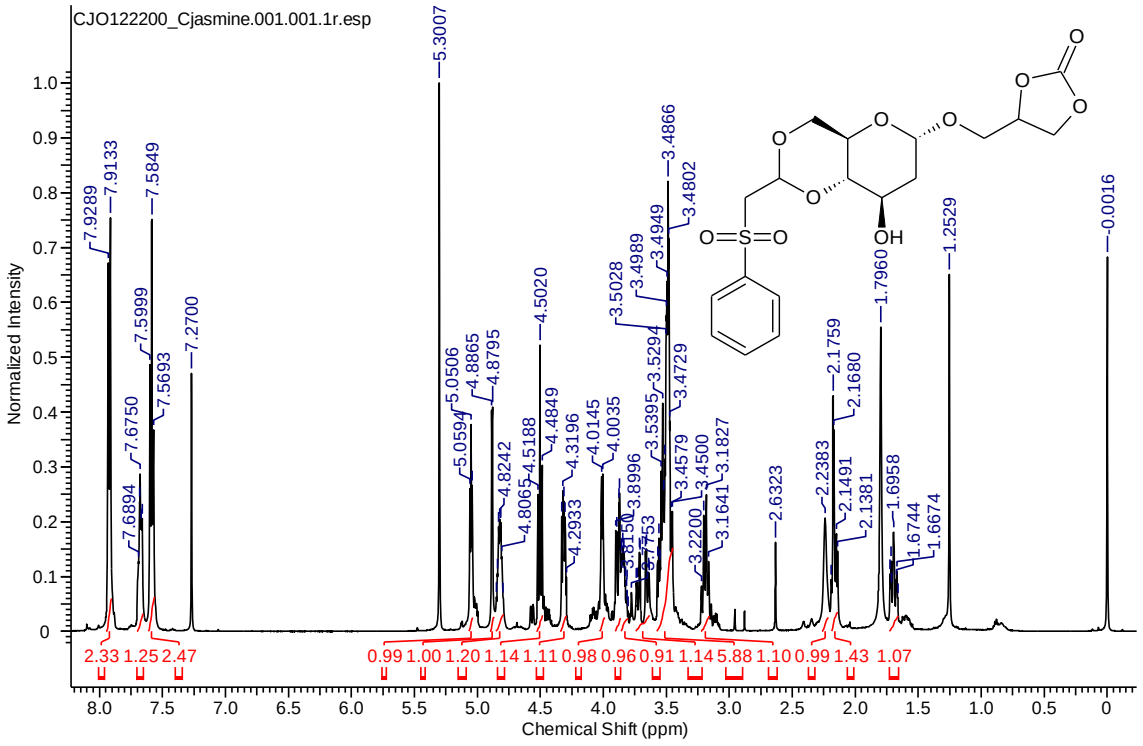

^{1}H NMR ($CDCl_3$, 500 MHz) of compound **14b**

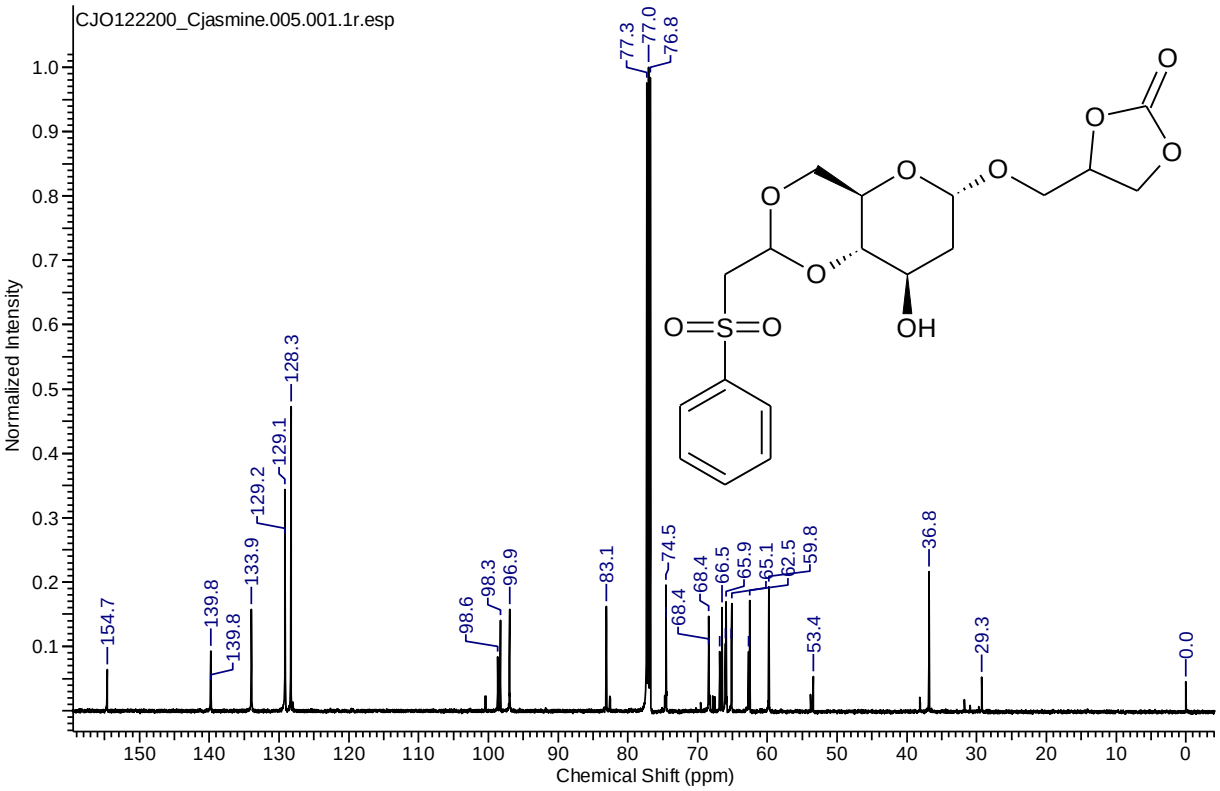

^{13}C NMR ($CDCl_3$, 125 MHz) of compound **14b**

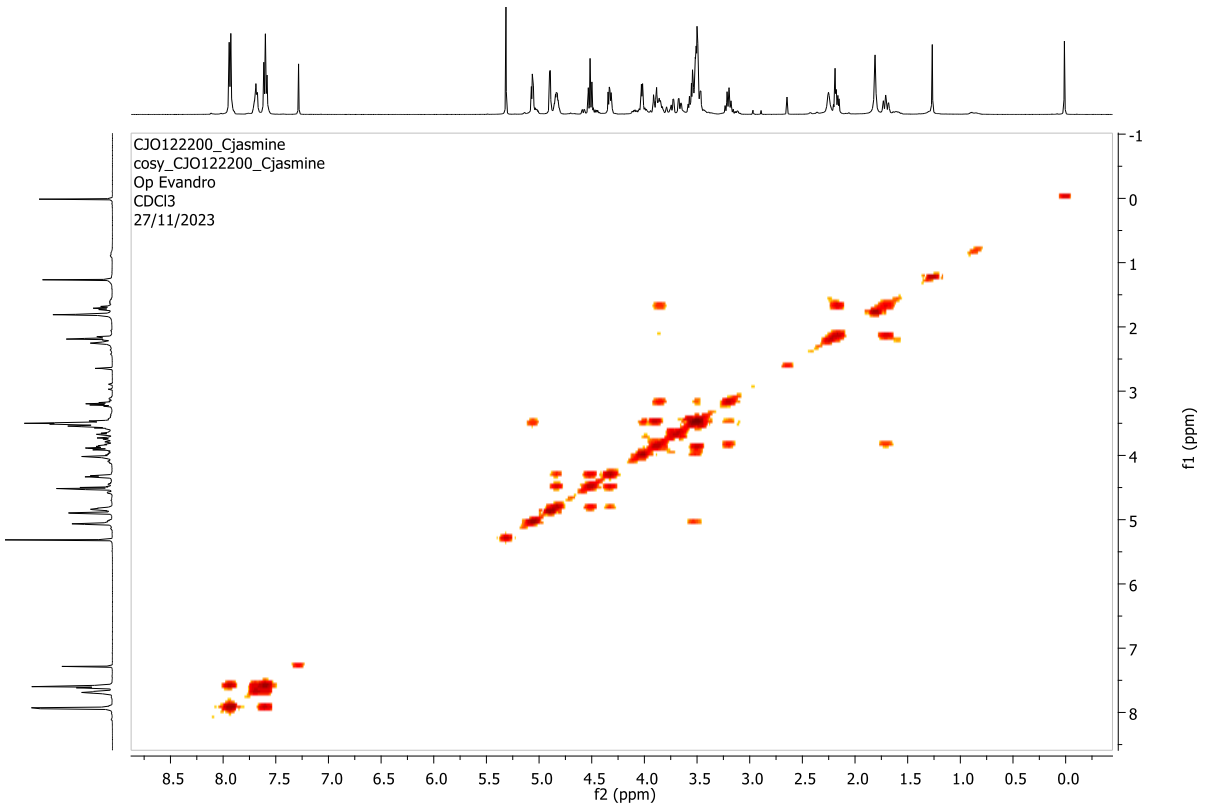

2D COSY NMR of compound **14b**

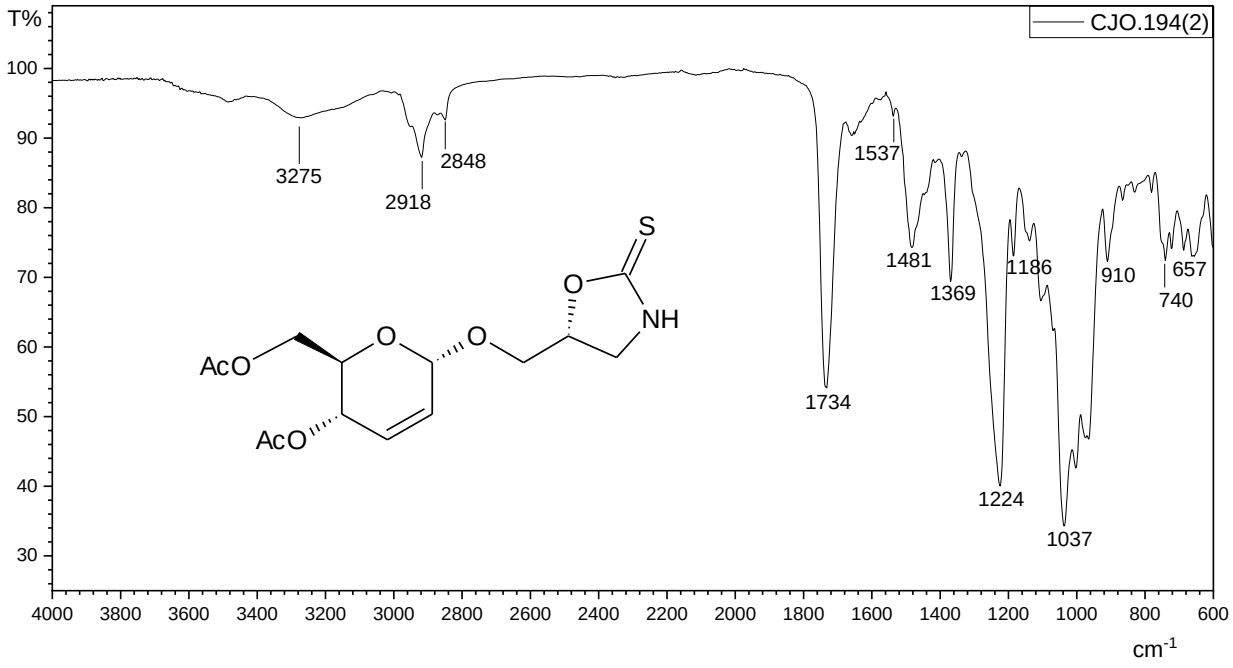

Infrared of compound **16a**

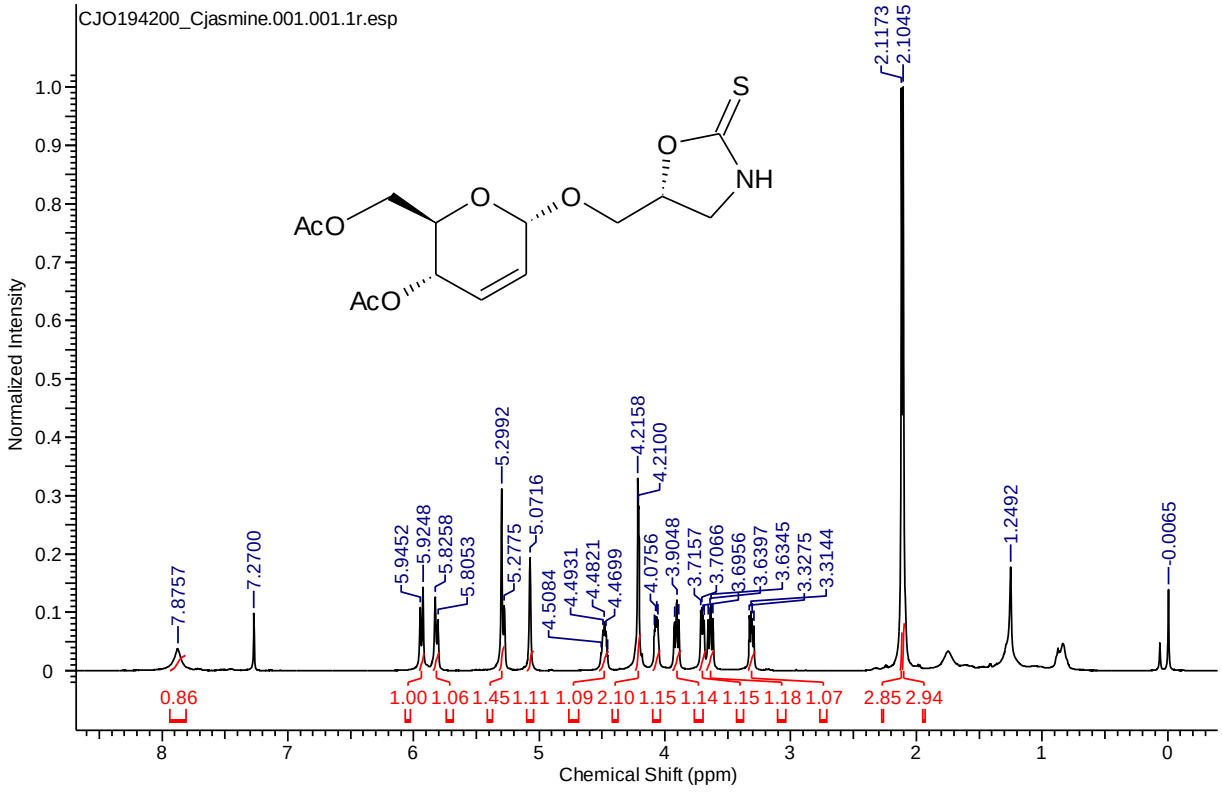

^{1}H NMR ($CDCl_3$, 500 MHz) of compound **16a**

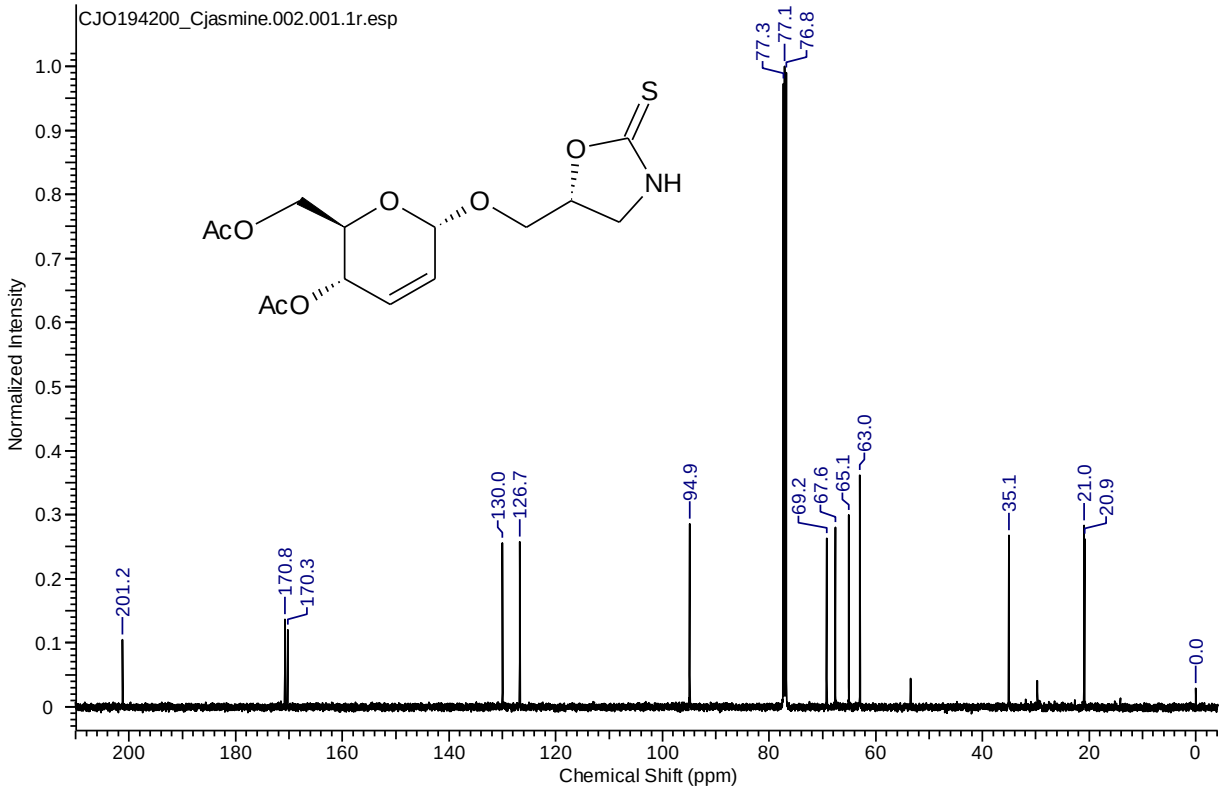

^{13}C NMR ($CDCl_3$, 125 MHz) of compound **16a**

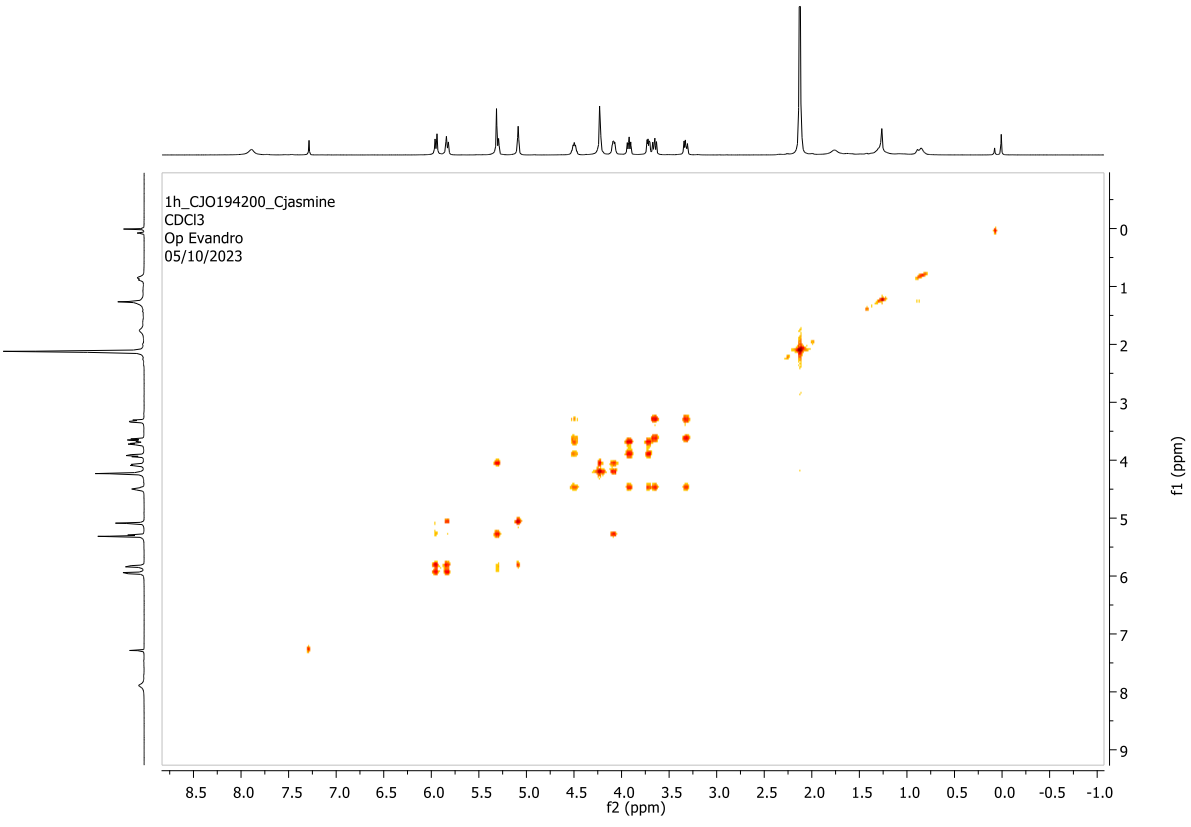

2D COSY NMR of compound **16a**

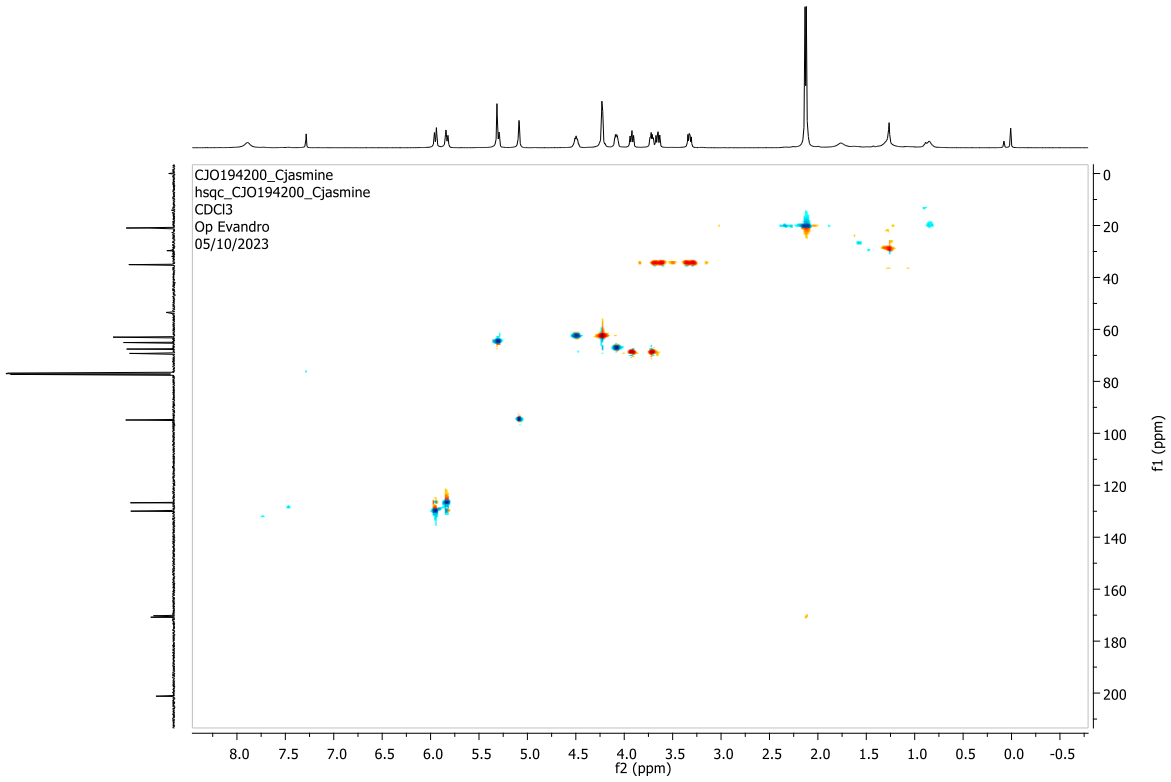

2D HSQC NMR of compound **16a**

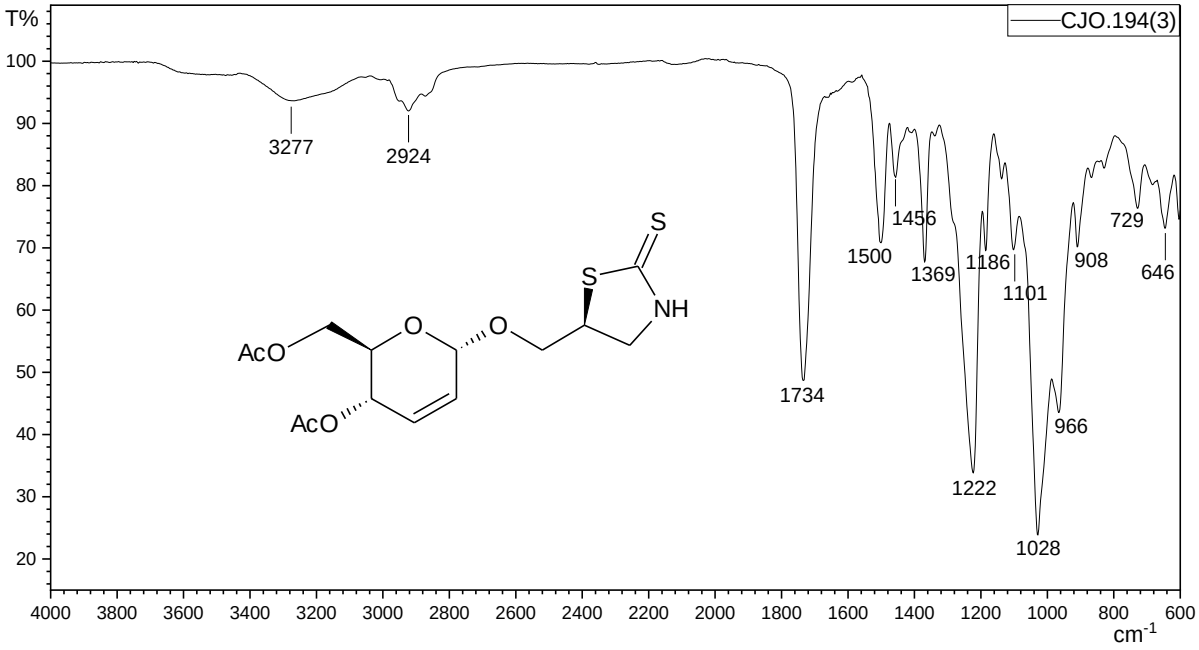

Infrared of compound **16b**

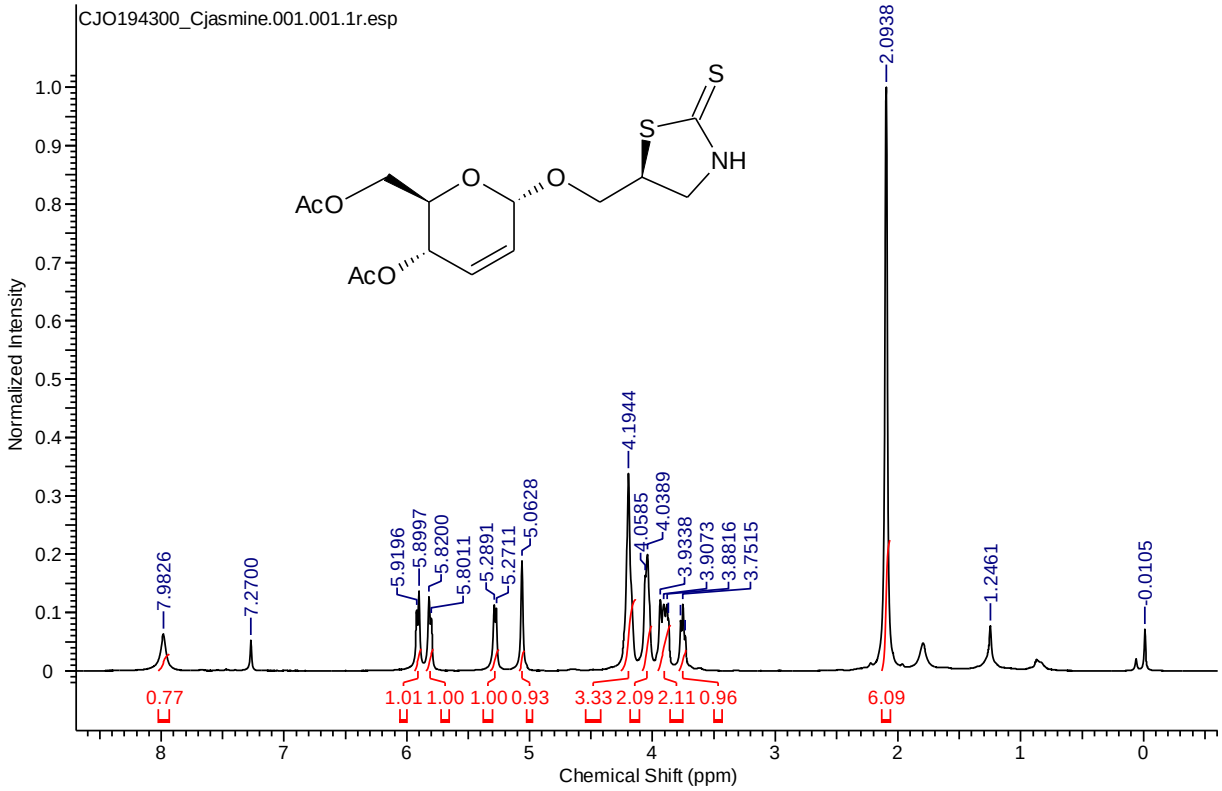

^{1}H NMR ($CDCl_3$, 500 MHz) of compound **16b**

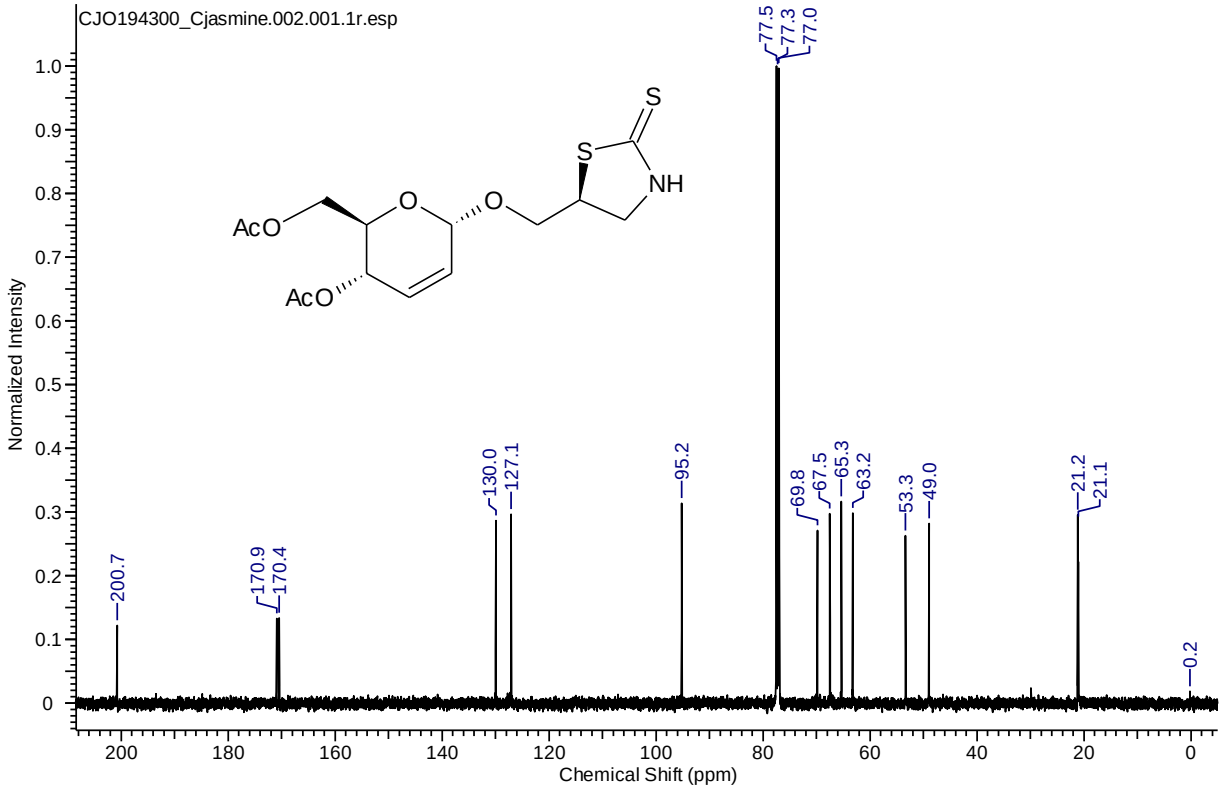

^{13}C NMR ($CDCl_3$, 125 MHz) of compound **16b**

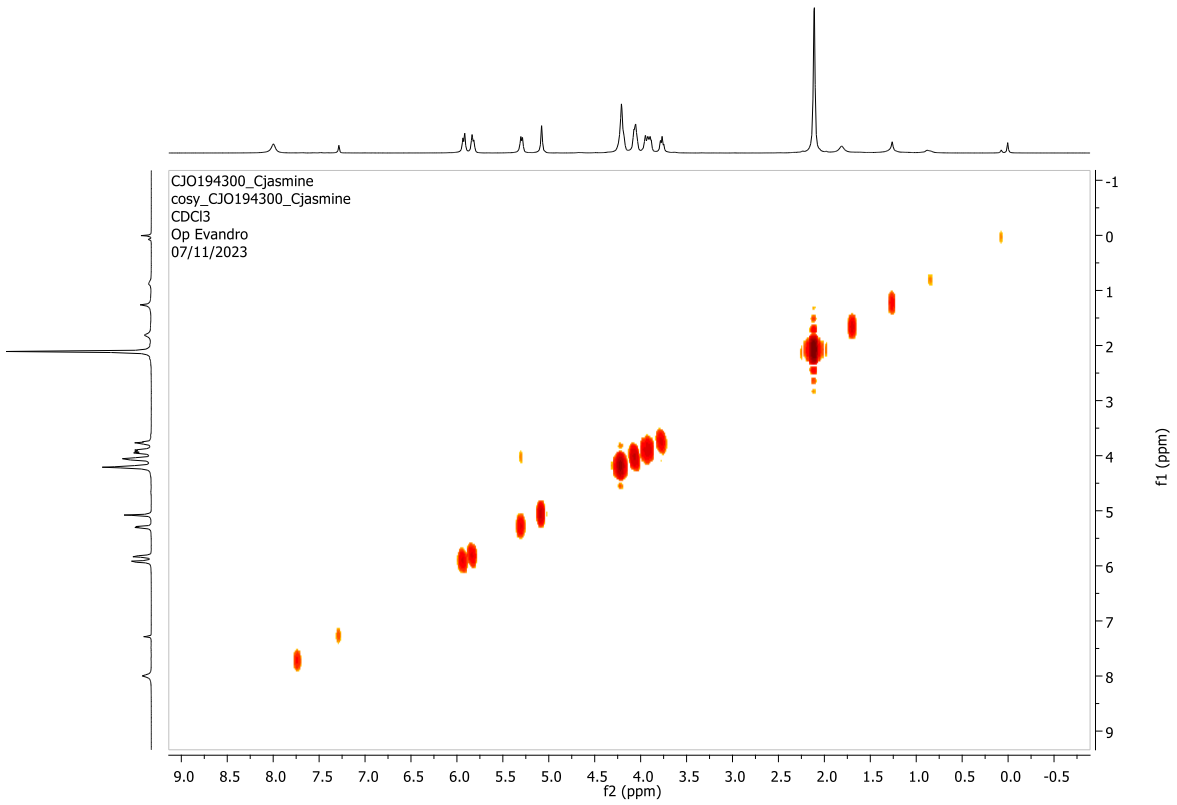

2D COSY NMR of compound **16b**

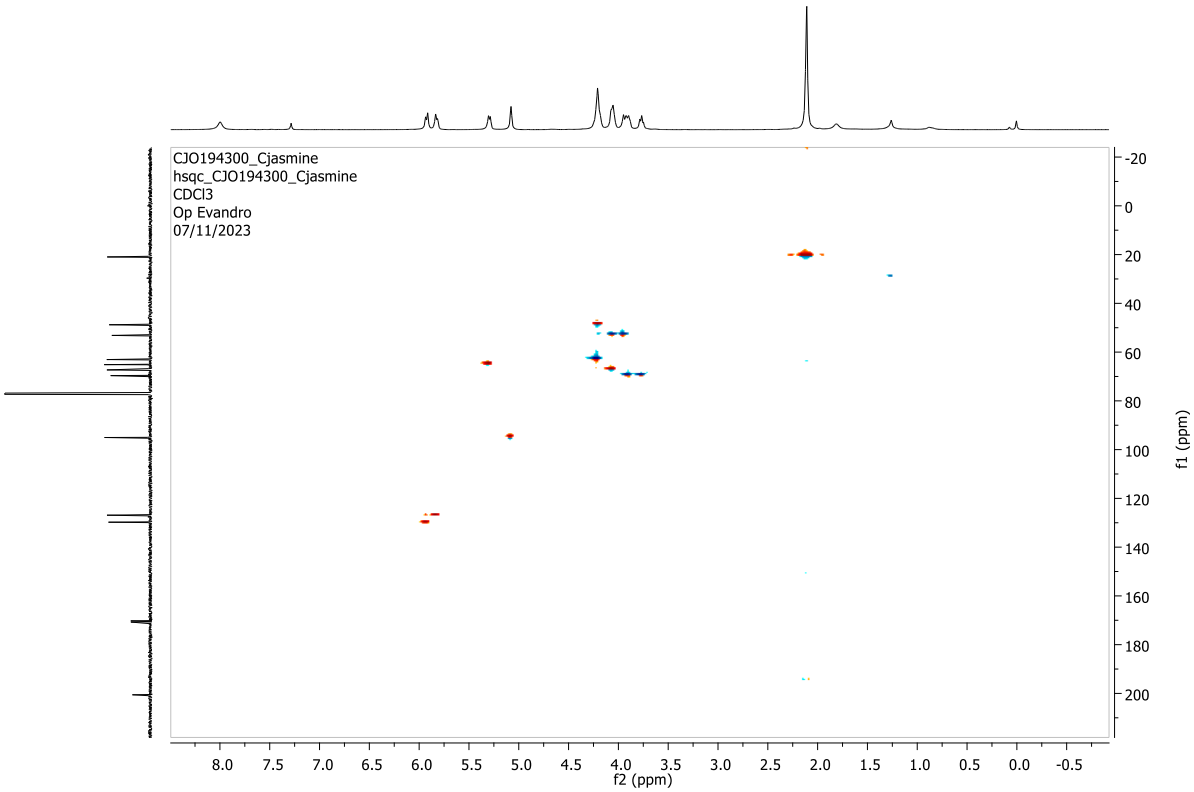

2D HSQC NMR of compound **16b**

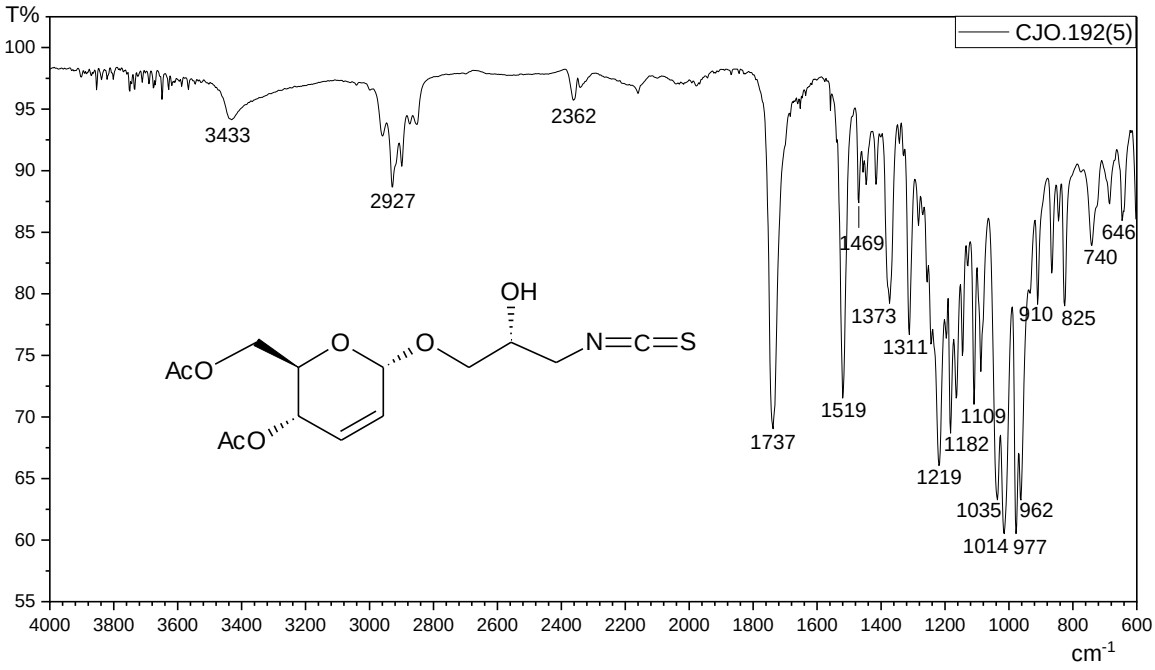

Infrared of compound **16c**

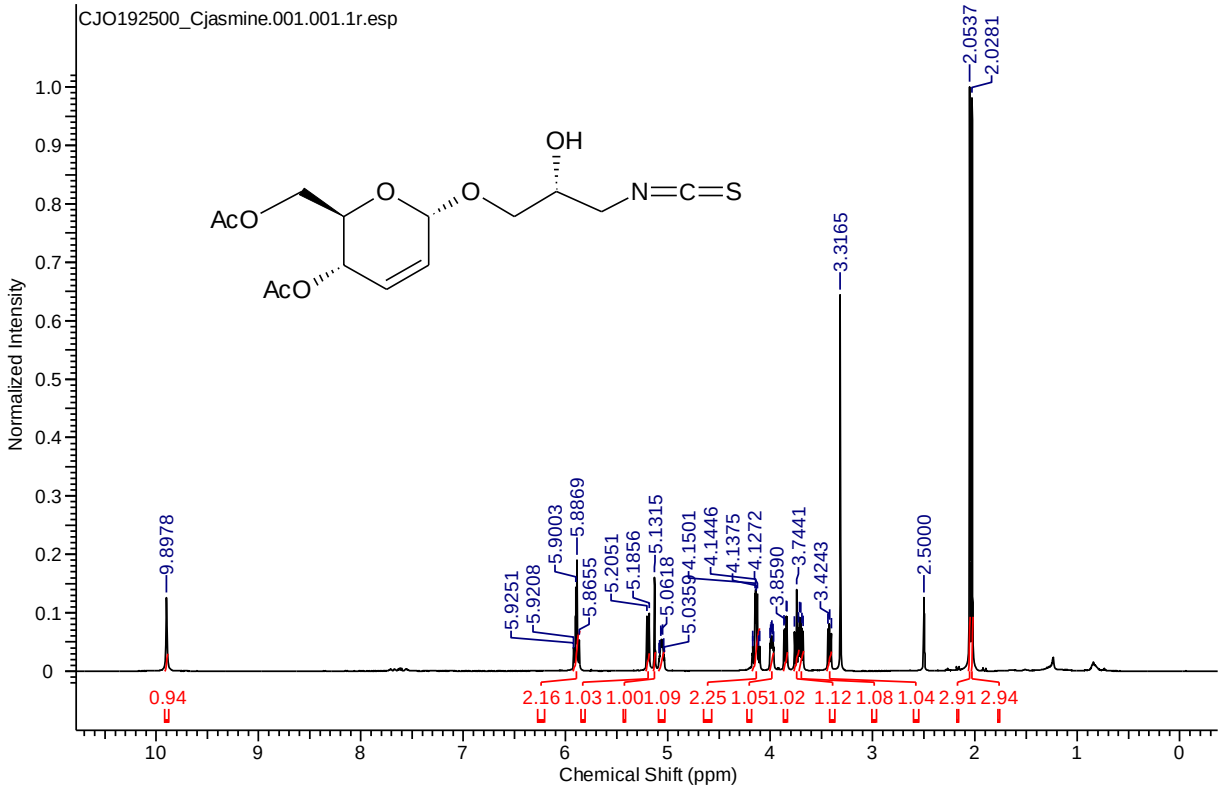

^{1}H NMR (DMSO-d_6, 500 MHz) of compound **16c**

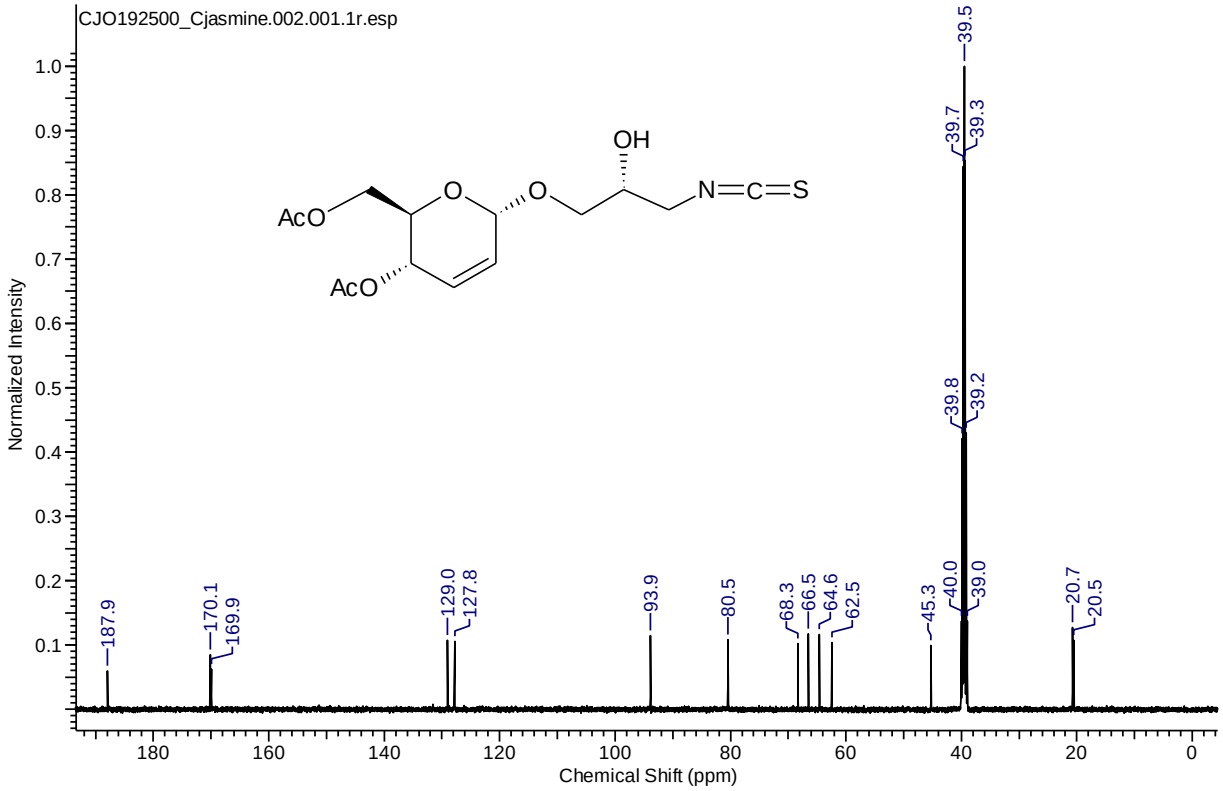

^{13}C NMR (DMSO-d_6, 125 MHz) of compound **16c**

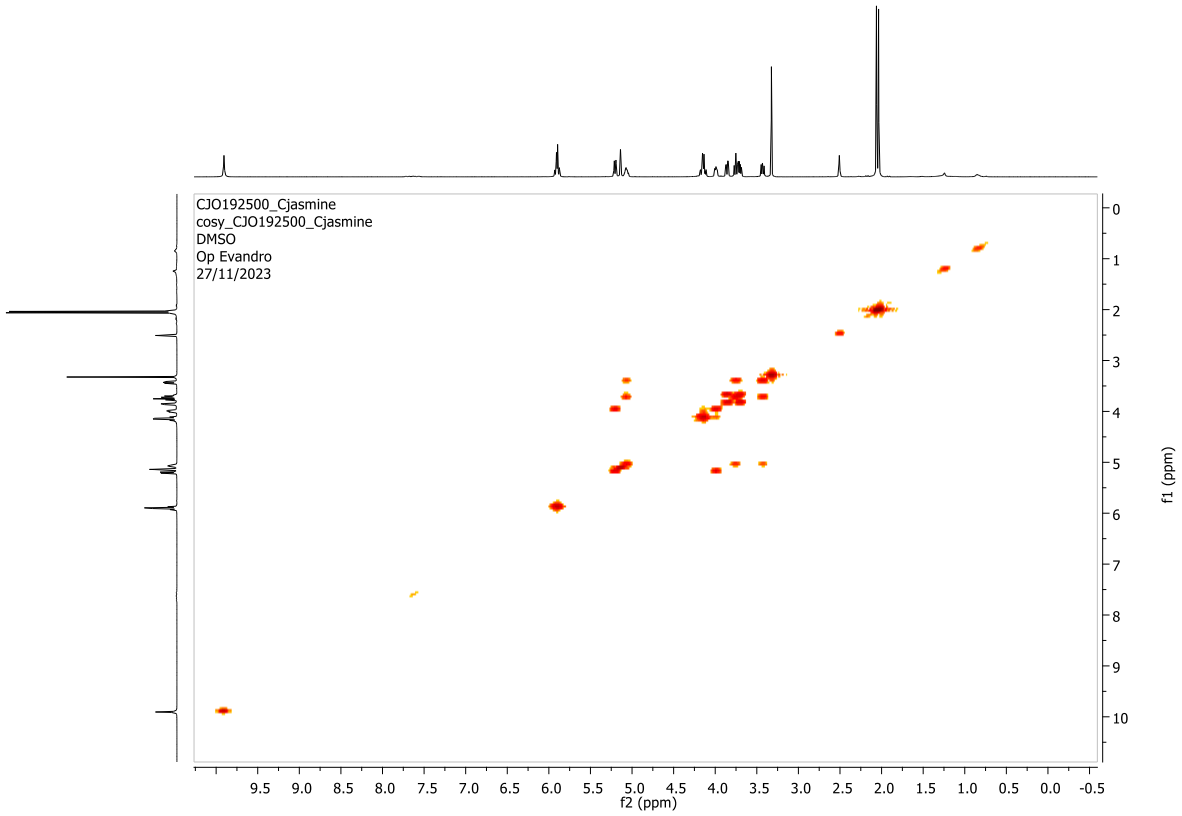

2D COSY NMR of compound **16c**

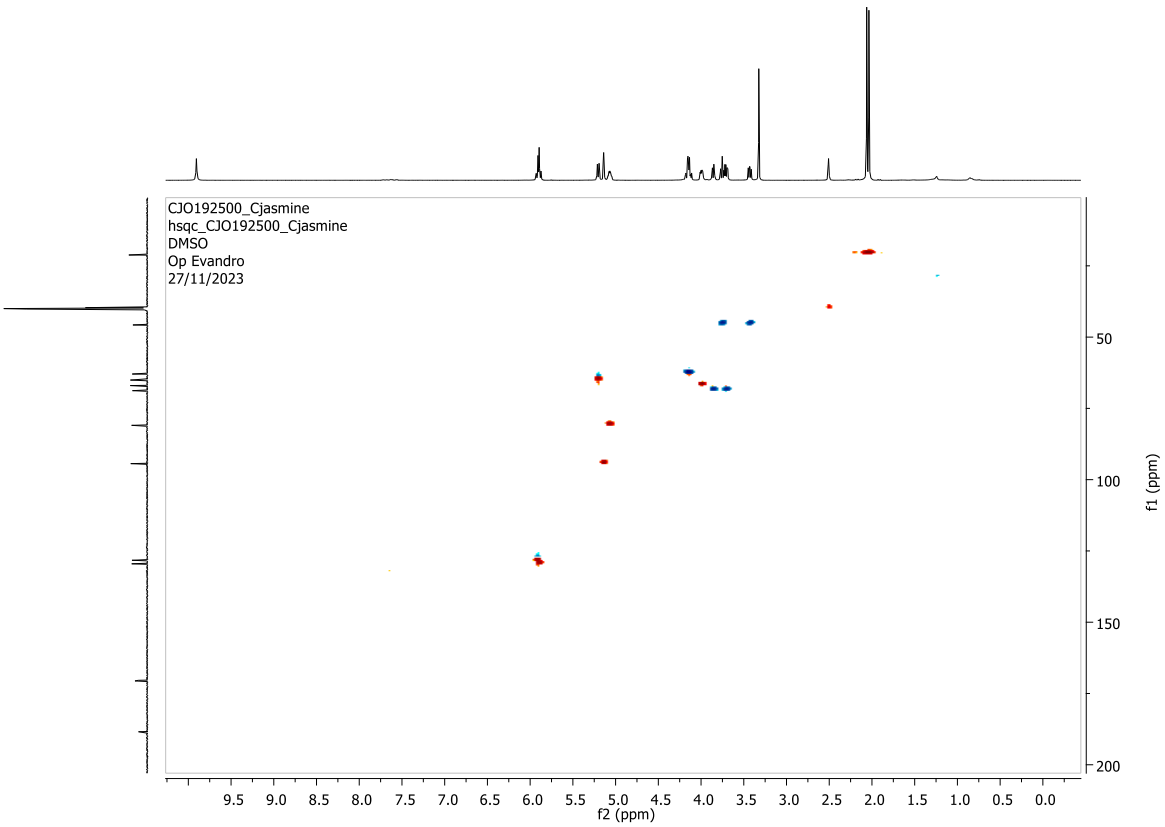

2D HSQC NMR of compound **16c**

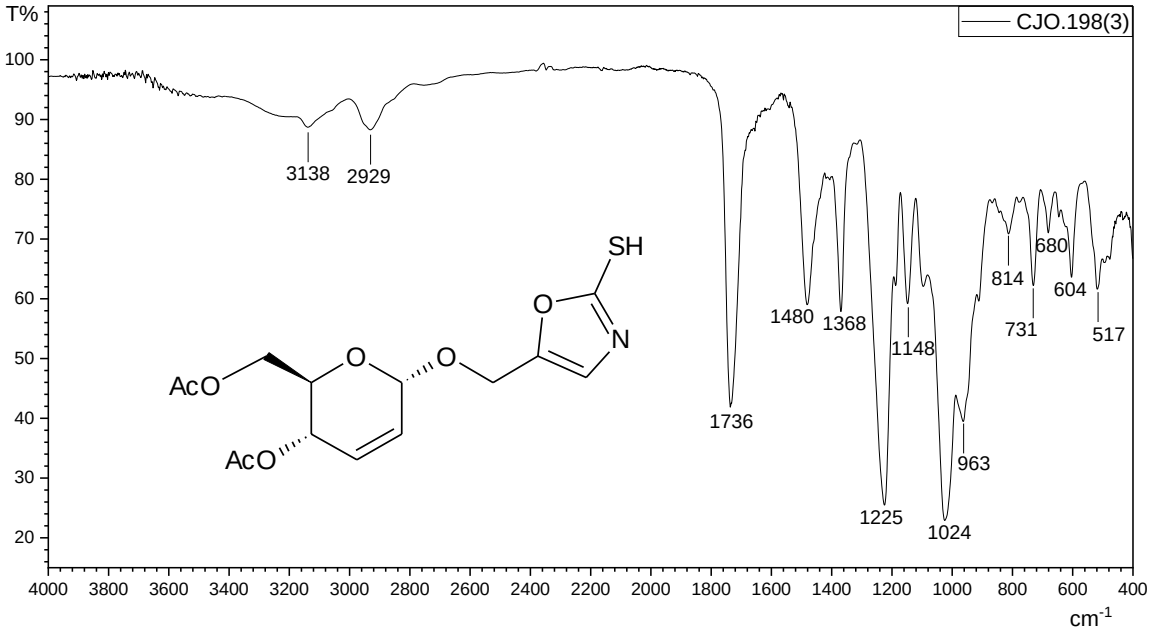

Infrared of compound **17**

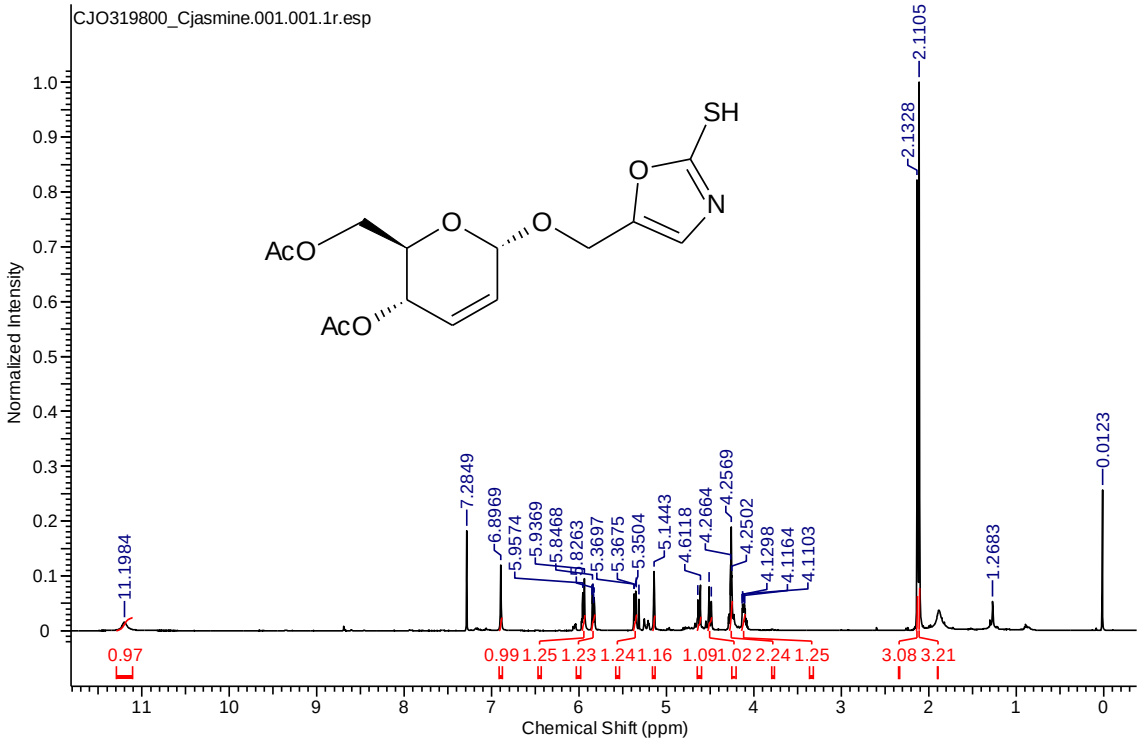

^{1}H NMR ($CDCl_3$, 500 MHz) of compound **17**

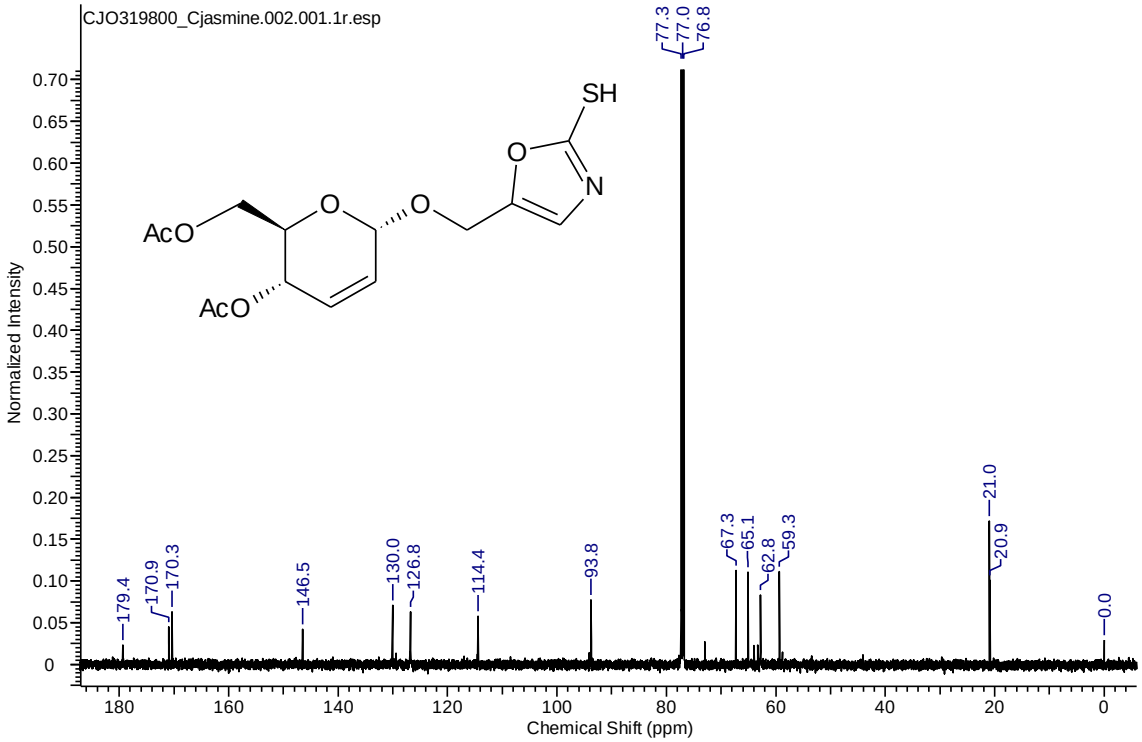

^{13}C NMR ($CDCl_3$, 125 MHz) of compound **17**

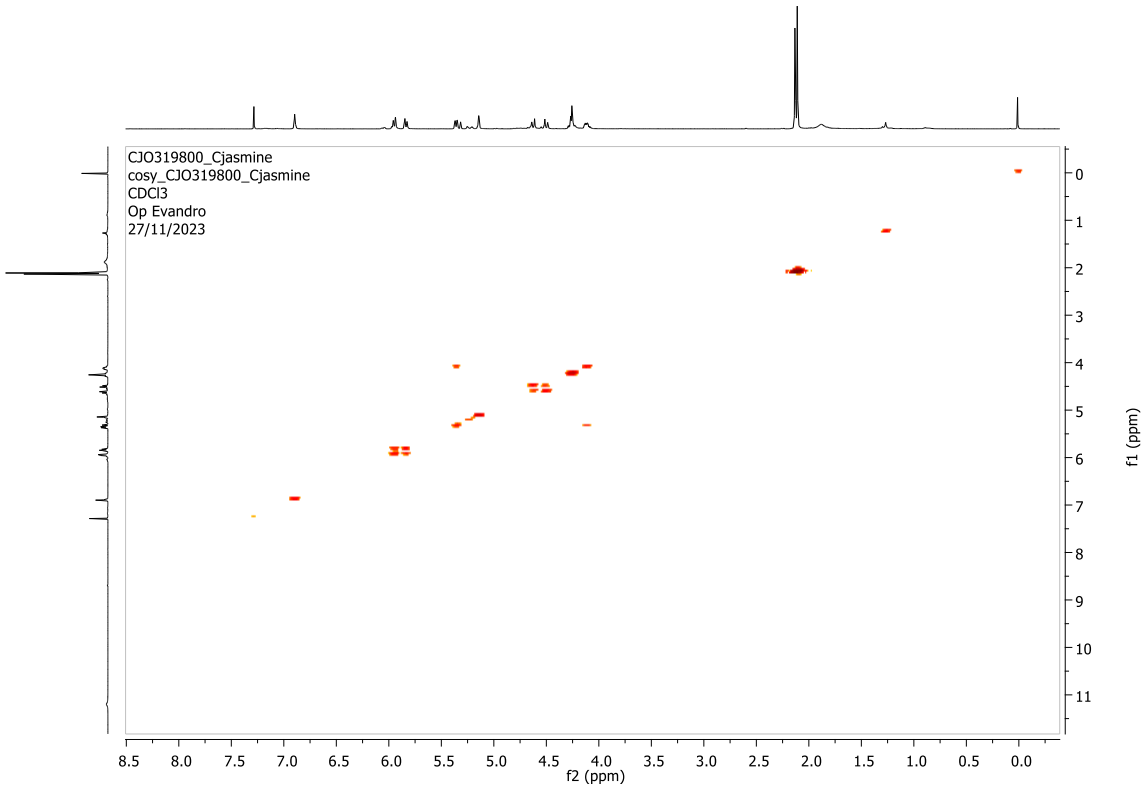

2D COSY NMR of compound **17**

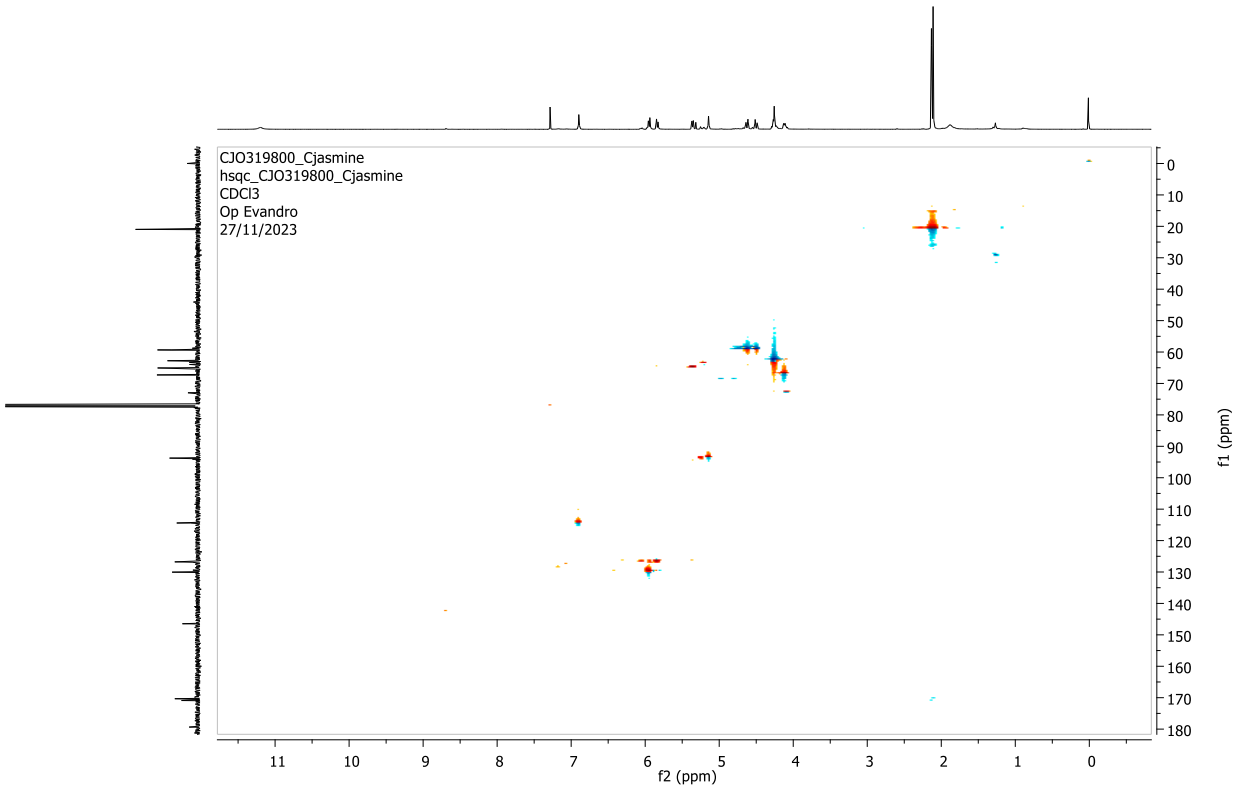

2D HSQC NMR of compound **17**